

DETERMINING THE OPTIMUM COMPACTION LEVEL FOR DESIGNING
STONE MATRIX ASPHALT MIXTURES

Except where reference is made to the work of others, the work described in this dissertation is my own or was done in collaboration with my advisory committee. This dissertation does not include proprietary or classified information.

Hongbin Xie

Certificate of Approval:

Mary Stroup-Gardiner
Associate Professor
Civil Engineering

E. Ray Brown, Chairman
Professor
Civil Engineering

David Timm
Assistant Professor
Civil Engineering

Stephen L. McFarland
Acting Dean
Graduate School

DETERMINING THE OPTIMUM COMPACTION LEVEL FOR DESIGNING
STONE MATRIX ASPHALT MIXTURES

Hongbin Xie

A Dissertation

Submitted to

the Graduate Faculty of

Auburn University

in Partial Fulfillment of the

Requirements for the

Degree of

Doctorate of Philosophy

Auburn, Alabama

May 11, 2006

DETERMINING THE OPTIMUM COMPACTION LEVEL FOR DESIGNING
STONE MATRIX ASPHALT MIXTURES

Hongbin Xie

Permission is granted to Auburn University to make copies of this dissertation at its discretion, upon request of individuals or institutions and at their expense. The author reserves all publication rights.

Signature of Author

Date of Graduation

VITA

Hongbin Xie, was born on June 7, 1976, in China. He entered Tongji University in September 1993 and gained his Bachelor of Science and Master of Science, both in Civil Engineering, in July 1997 and March 2000, respectively. He entered Royal institute of Technology, Sweden, in May 2000 to pursue his Ph.D. degree, also in Civil Engineering, and transferred to Auburn University in February 2002. He was employed as a part-time on-site quality control engineer during his senior undergraduate year for a new constructed freeway project following the summer intern in the same project. His Bachelor thesis was on polymer-modified asphalt, including lab comparison of several polymer additives and field verification tests. During his graduate study in China, he participated in two SMA research projects in Shanghai and Shenzhen, and was employed as on-site asphalt plant quality control engineer and did the major work on SMA mix designs for the Shenzhen project. His Master thesis was on mix design of Asphalt Treated Permeable Base (ATPB). The thesis work included developing a design method for ATPB mixes and construction of two test roads. His Ph.D. program in Sweden was on unbound granular base materials, he finished the literature review report and some course work before he transferred to Auburn University. Hongbin married Jingna Zhang, on May 16, 2000. They are the parents of one cute boy, Edwin Anthony Xie.

DISSERTATION ABSTRACT
DETERMINING THE OPTIMUM COMPACTION LEVEL FOR DESIGNING
STONE MATRIX ASPHALT MIXTURES

Hongbin Xie

Doctor of Philosophy, May 11, 2006
(M.S., Tongji University, 2000)
(B.S., Tongji University, 1997)

348 Typed Pages

Directed by E. Ray Brown

As Stone matrix asphalt (SMA) becomes more widely used in the United States, there is a need to further refine its mix design procedure. Some states have found that 100 gyrations with the Superpave Gyratory Compactor (SGC) suggested in current design guides are excessive for their materials and have specified the use of lower compaction levels. However, the use of these low compaction levels had little research support.

The objective of this study was to determine the optimum compaction level for SMA mixtures that will provide increased durability and acceptable rutting resistance. The study is also needed to determine if the same compaction effort is applicable for SMA mixes of various nominal maximum aggregate sizes (NMAS).

The study was carried out by conducting SMA mixture designs using different compaction levels, and comparing these different compaction levels in terms of volumetric properties and rutting performance. Five aggregates with a wide range of Los

angles (L.A.) abrasion values were selected. For each aggregate, three NMAS (19 mm, 12.5 mm, and 9.5 mm) mixtures were designed by at least three compaction efforts (50 blows Marshall, 65 and 100 gyrations with the SGC. A further lower gyration level (40 gyrations) was also used to design two mixtures, to show the effect of further reduction in number of gyrations. A total of 47 mixture designs were conducted in this study. Both vacuum seal (CoreLok) and saturated surface dry (SSD) methods were used for measurement of air voids. Aggregate breakdown was evaluated for all compaction efforts. Permeability, wheel load tracking (Asphalt pavement analyzer, APA), dynamic modulus, static creep, and repeated load tests were conducted on all mixtures designed with the different gyration levels.

The CoreLok and SSD method provided a significant difference in air void results for lab compacted SMA mixtures. The correction factor embedded in the CoreGravity™ software is not acceptable for determining the bulk specific gravity of SMA mixtures. The error potentials for both methods were analyzed and suggestions were made to properly use these two methods for determining air voids of SMA mixtures.

SMA mixtures designed with 65 gyrations should provide improved durability than those designed with 100 gyrations due to the increased optimum asphalt content. SMA mixtures designed with 65 gyrations were generally had similar or lower permeability than those designed with 100 gyrations at similar air voids. Marshall compaction resulted in significant higher aggregate breakdown than gyratory compaction. The aggregate breakdowns for both 65 and 100 gyrations were very similar to that observed in the field. All designed SMA mixtures achieved stone-on-stone contact as indicated by the VCA ratio, and had acceptable asphalt draindown.

For the APA rutting test, 13 of 15 SMA mixtures designed with 65 gyrations performed well when 5.0 mm was used as the maximum allowable rut depth. The dynamic modulus test results indicated that reducing the compaction level from 100 gyrations to 65 gyrations only resulted in a small difference, and the ability to use $E^*/\sin\phi$ term for predicting rutting resistance is questionable at high temperature for SMA mixtures due to the erroneous trend shown. Due to high test variability and long testing time, static creep test was not recommended to be used for evaluating SMA rutting resistance. Most (14 of 15) mixtures designed with 65 gyrations met the suggested 5 percent cumulative strain criterion after 10,000 cycles in the repeated load test. The rutting resistance indicated by the APA rut depth and cumulative strain from repeated load test becomes marginal when the gyration level reduced to 40 gyrations.

The findings of this study indicated that 65 gyrations (the SGC used had an internal gyration angle of 1.23 degrees) can be used to design a more durable SMA mixture, while still maintaining the good rutting resistance that SMA mixtures are noted for. The successful design with 65 gyrations for all five aggregates in this study indicates that a lower design compaction level may allow the use of more aggregate sources for SMA mixtures without adversely affecting the performance. The current requirements for L.A abrasion and F&E content may be too stringent and these two aggregate properties within the range of this study appear not detrimental for the rutting performance. The NMAS did not show as a significant factor for many of the test results, therefore, no difference in compaction level was suggested for different NMAS mixtures.

ACKNOWLEDGEMENTS

The work presented in this document was accomplished as part of the Federal Highway Administration Project AU-334, *determining the optimum compaction level for SMA mixtures*. The author wishes to thank everyone associated with the project for his or her efforts. Special thanks go to Dr. E. Ray Brown, for his direction for my whole Ph.D. study and research. Special thanks also go to Mr. Donald E. Watson, for his detailed guidance and valuable discussion in the whole research period. Thanks to Tim Vollar and the entire laboratory staff at the National Center for Asphalt Technology, for their consistent support on my laboratory work. The author also extends his appreciation to Dr. Mary-Stroup Gardiner and Dr. David Timm, for their inspiring discussion on data analysis and review of the dissertation. Very special thanks are given to Jingna Zhang, and Edwin Anthony Xie, for their support and understanding during the completion of this research and dissertation.

Style manual or journal used Transportation Research Board, National Academy of Sciences

Computer software used Microsoft Office XP, Minitab version 14.1

TABLE OF CONTENTS

CHAPTER 1 INTRODUCTION	1
1.1 BACKGROUND	1
1.2 OBJECTIVES	2
1.3 SCOPE OF STUDY	3
CHAPTER 2 LITERATURE REVIEW	6
2.1 DEVELOPMENT AND EVALUATION OF THE SUPERPAVE GYRATORY COMPACTOR.....	6
2.1.1 Individual Literature	6
2.1.2 Summary of Literature.....	37
2.2 THE DEVELOPMENT OF SMA MIX DESIGN	39
2.2.1 Individual Literature	39
2.2.2 Summary of Literature.....	74
2.3 FINDINGS ON COMPACTION EFFORT FOR DESIGNING SMA MIXTURES	76
2.4 OTHER RELEVANT TESTS RELATED TO TOPICS	78
2.4.1 Vacuum Seal Method (CoreLok).....	78
2.4.2 Permeability	80
2.4.3 Aggregate Breakdown	81
2.4.4 Locking Point.....	83
2.4.5 Asphalt Pavement Analyzer Rutting Test.....	85
2.4.6 Triaxial Tests	90
CHAPTER 3 EXPERIMENTAL PROCEDURES.....	98
3.1 RESEARCH PLAN	98

3.1.1 Materials Selection.....	98
3.1.2 Mixture Design and Volumetric Properties	101
3.1.3 Performance Testing	105
3.2 MATERIALS SELECTION.....	106
3.2.1 Aggregate Tests	106
3.2.1.1 Specific gravity test.....	106
3.2.1.2 L.A abrasion test	106
3.2.1.3 Flat and elongated content test.....	107
3.2.1.4 Fine aggregate angularity.....	107
3.2.1.5 Uncompacted air voids of coarse aggregate	108
3.2.1.6 Voids in coarse aggregates.....	109
3.2.2 Fine Mortar Tests.....	109
3.2.2.1 Dynamic shear rheometer test.....	109
3.2.2.2 Bending beam rheometer test.....	111
3.3 MIXTURE DESIGN PROCEDURES.....	112
3.3.1 Mixture Design by Marshall Hammer	112
3.3.2 Mixture Design by Superpave Gyratory Compactor	114
3.3.3 Draindown Test.....	114
3.4 TESTS CONDUCTED ON MIX DESIGN SAMPLES.....	115
3.4.1 Air Void Content Determination	115
3.4.2 Flexible Wall Falling Head Permeability	117
3.4.3 Ignition Oven Test	118
3.5 PERFORMANCE TESTING EQUIPMENT AND METHODS	119
3.5.1 Asphalt Pavement Analyzer (APA) Wheel Tracking	119
3.5.2 Dynamic Modulus.....	120
3.5.2.1 Testing setup	120
3.5.2.2 Method of analysis.....	122
3.5.3 Static Creep.....	124
3.5.3.1 Background of Creep Behavior	124
3.5.3.2 Testing Setup	127

3.5.3.3 Method of analysis.....	127
3.5.4 Repeated Load Confined Creep.....	130
3.5.4.1 Testing setup.....	130
3.5.4.2 Method of analysis.....	131
3.6 PERFORMANCE TEST SPECIMEN PRODUCTION.....	132
3.6.1 APA Specimen Production.....	132
3.6.2 Triaxial Test Specimen Production.....	133
CHAPTER 4 TEST RESULTS, ANALYSIS AND DISCUSSION ON MIX DESIGN	
PROPERTIES.....	136
4.1 MATERIAL PROPERTIES.....	136
4.1.1 Coarse Aggregate Properties.....	136
4.1.2 Fine Aggregate Angularity.....	138
4.1.3 Mineral Filler Properties.....	138
4.1.4 Asphalt Binder Properties.....	138
4.1.5 Fiber Properties.....	139
4.1.6 Fine Mortar Properties.....	139
4.2 MIXTURE DESIGN PROPERTIES.....	141
4.2.1 Marshall Mix Design.....	141
4.2.2 Gyratory Mix Design.....	142
4.2.2.1 Locking points.....	142
4.2.2.2 Gyratory mix design results.....	148
4.2.3 Effects of Compaction on Volumetric Properties.....	150
4.2.4 Draindown Test Results.....	154
4.3 AIR VOID CONTENT MEASUREMENT.....	155
4.3.1 Concepts of Air Voids.....	157
4.3.2 Comparison of Two Test Methods.....	160
4.3.3 Effect on Mix Design Volumetric Properties.....	170
4.3.4 Triaxial Test Sample Preparation.....	173
4.3.5 Vacuum Seal Method Manual Calculation.....	178

4.4 PERMEABILITY TEST.....	184
4.4.1 The Relationship between Permeability and Air Voids.....	184
4.4.2 Effect of Compaction level on Permeability.....	188
4.5 AGGREGATE DEGRADATIONS.....	193
4.6 SUMMARY	208
CHAPTER 5 TEST RESULTS, ANALYSIS AND DISCUSSION ON PERFORMANCE TESTS	211
5.1 APA RUTTING TEST	211
5.1.1 APA Test Results and Analysis.....	211
5.1.2 Discussion on APA Rut Depth versus Gyration Level.....	218
5.2 DYNAMIC MODULUS.....	222
5.3 STATIC CREEP	245
5.4 REPEATED LOAD TEST	255
5.4.1 Repeated Load Test Results and Analysis.....	255
5.4.2 Discussion on Cumulative Strain Criteria.....	268
5.5 SUMMARY	275
CHAPTER 6 CONCLUSIONS AND RECOMMENDATIONS.....	278
6.1 CONCLUSIONS.....	278
6.2 RECOMMENDATIONS.....	281
REFERENCES	283
APPENDIX A AIR VOID CONTENT AND PERMEABILITY TEST RESULTS	293
APPENDIX B COREGRAVITY™ PROGRAM CORRECTION FACTOR	303
APPENDIX C AGGREGATE BREAKDOWN FOR DIFFERENT COMPACTION EFFORTS	305
APPENDIX D TRIAXIAL PERFORMANCE TEST RESULTS	314

LIST OF TABLES

TABLE 2.1	Summary of Average Differences between Field Cores and Lab-Compacted Specimens (6).....	10
TABLE 2.2	Mean Squared Error (MSE) Comparison of Compaction Data (6)	11
TABLE 2.3	Evolution of Gyratory Compaction (23).....	35
TABLE 2.4	Aggregate Gradations of Mixtures Tested (33)	51
TABLE 2.5	Volumetric Properties of SMA Mixtures Compacted by the Marshall Hammer (36).....	59
TABLE 2.6	Volumetric Properties of SMA Mixtures Compacted by the SGC (36)	59
TABLE 2.7	APA Testing Specifications Used by Various State Agencies	87
TABLE 2.8	APA Rut Depth Criteria (70-71, 79, 82).....	89
TABLE 2.9	Criteria for Static Creep Test Results (95).....	93
TABLE 3.1	Trial Gradations Used in Preliminary Mix Designs	100
TABLE 3.2	Preliminary Mix Design Results.....	101
TABLE 3.3	Gradations Used in This Study	103
TABLE 3.4	SMA Mortar Quality Requirements (43).....	111
TABLE 3.5	Automatic Marshall Hammer Calibration Data.....	112
TABLE 3.6	Geometric Requirements for Triaxial Samples (84, 86).....	133
TABLE 4.1	Aggregate Properties.....	137
TABLE 4.2	Mineral Filler Properties	138
TABLE 4.3	PG 76-22 Asphalt Binder Properties.....	139
TABLE 4.4	Cellulose Fiber Properties.....	139
TABLE 4.5	Mortar Test Results.....	140
TABLE 4.6	Marshall Mix Design Volumetric Properties ¹ Summary	142

TABLE 4.7 Locking Point Results Summary	143
TABLE 4.8 Forward Stepwise Regression Results for Locking Point.....	145
TABLE 4.9 100 Gyration Mix Design Volumetric Properties ¹	149
TABLE 4.1065 Gyration Mix Design Volumetric Properties ¹	149
TABLE 4.1140 Gyration Mix Design Volumetric Properties ¹	150
TABLE 4.12Draindown Test Results Summary	155
TABLE 4.13Paired T-Test for CoreLok and SSD air voids.....	161
TABLE 4.14GLM for Influencing Factors on VTM Ratio	162
TABLE 4.15GLM for Influencing Factors on Water Absorption	168
TABLE 4.16Mix Design Volumetric Properties ¹ Summary	171
TABLE 4.17Targeting Whole Samples VTM ¹ for Triaxial Samples.....	177
TABLE 4.18Critical Air Void Content for Permeable SMA Mixtures.....	187
TABLE 4.19Critical Air Void Content for Permeable SMA Mixtures.....	191
TABLE 4.20F-tests for permeability regressions of two compaction levels.....	192
TABLE 4.21Marshall Compaction Aggregate Breakdown Results.....	195
TABLE 4.22100 Gyration Aggregate Breakdown Results.....	196
TABLE 4.2365 Gyration Aggregate Breakdown Results.....	197
TABLE 4.24Paired-T Test on Degradation for Two gradations	198
TABLE 4.25ANOVA on Aggregate Breakdown at Critical Sieve Size	200
TABLE 4.26Paired T Test on Degradation for 100 Gyration and Marshall Compaction	204
TABLE 4.27Paired T Test on Degradation for 65 and 100 Gyration	204
TABLE 4.28Average Percent Passing Changes at Three Sieve Sizes	205
TABLE 4.29Average Test Results for Different Compaction Levels.....	208
TABLE 5.1 APA Rutting Results.....	212
TABLE 5.2 ANOVA for APA Rutting Results.....	215

TABLE 5.3 ANOVA for Dynamic Modulus.....	224
TABLE 5.4 ANOVA for Phase Angle	224
TABLE 5.5 Dynamic Modulus Test Results at Load Frequency of 10 Hz.....	230
TABLE 5.6 Dynamic Modulus Test Results at Load Frequency of 0.1 Hz.....	231
TABLE 5.7 Dynamic Modulus Test Results at Load Frequency of 10 Hz (Without 6 Outlier Samples)	233
TABLE 5.8 Dynamic Modulus Test Results at Load Frequency of 0.1 Hz (Without 6 Outlier Samples)	234
TABLE 5.9 GLM Results on $E^*/\sin\phi$ at Load Frequency of 10 Hz.....	235
TABLE 5.10 Pair T-Test Results on $E^*/\sin\phi$ Value of Two Compaction Levels.....	237
TABLE 5.11 GLM Results on $E^*/\sin\phi$ at Load Frequency of 0.1 Hz.....	238
TABLE 5.12 Static Creep Test Results Summary.....	248
TABLE 5.13 ANOVA for Slope of Strain in Secondary Phase of Static Creep Test	249
TABLE 5.14 ANOVA for Log Test Time when 4 Percent Strain Occurred.....	251
TABLE 5.15 Summary of Repeated Load Test Results.....	257
TABLE 5.16 ANOVA for Strain at 10,000 Cycles	260
TABLE 5.17 Paired-T Test Results on Strain at 10,000 Cycles.....	263
TABLE 5.18 ANOVA for Strain Slope at Secondary Phase of Repeated Load Test	265
TABLE 5.19 Average Test Results for Different Compaction Levels.....	275
TABLE A1 Air Voids and Permeability Test Results.....	294
TABLE B1 CoreGravity TM Program Correction Factors (<i>110</i>)	304
TABLE D1 Dynamic Modulus Test Results.....	315
TABLE D2 Static Creep Test Results	319
TABLE D3 Repeated Load Confining Creep Test Results.....	323

LIST OF FIGURES

FIGURE 2.1	Effect of increase in compaction effort on limestone SMA mixture (31).	48
FIGURE 2.2	Optimum asphalt content from two compaction efforts (36).	58
FIGURE 2.3	Gmb ratio as a function of gyratory level and L.A. abrasion loss (42).	71
FIGURE 2.4	Correlation of L.A Abrasion values and aggregate breakdown for field compacted samples (64).	83
FIGURE 2.5	Permanent strains of core samples by triaxial repeated load test (89).	96
FIGURE 2.6	Field rut depth versus the lab strain from repeated load test (96).	96
FIGURE 3.1	Work plan for phase I: material selection and preliminary test.	99
FIGURE 3.2	Work plan for phase II: SMA mix designs.	102
FIGURE 3.3	Gradations used in this study.	103
FIGURE 3.4	Work plan for phase III: performance tests.	104
FIGURE 3.5	Components of complex modulus G^* .	110
FIGURE 3.6	Automatic Marshall hammer calibration.	113
FIGURE 3.7	Flexible wall falling head permeameter.	117
FIGURE 3.8	Asphalt Pavement Analyzer.	119
FIGURE 3.9	Haversine loading pattern or stress pulse for the dynamic modulus test.	120
FIGURE 3.10	The MTS and environmental chamber used for triaxial testing.	121
FIGURE 3.11	A sample prepared for triaxial testing.	122
FIGURE 3.12	HMA creep behavior in static creep test.	125
FIGURE 3.13	Krass's model for creep behavior (107).	126
FIGURE 3.14	Typical test results between compliance and loading time.	128

FIGURE 3.15 Regression constants a and m obtained from the secondary zone of the log compliance–log time plot.....	129
FIGURE 3.16 Repeated load test schematic graph.	130
FIGURE 3.17 Typical relationship between total cumulative plastic strain and loading cycles.....	131
FIGURE 3.18 Regression constants a and b when plotted on a log–log scale.....	132
FIGURE 3.19 Whole and cored sample prepared for triaxial testing.	134
FIGURE 4.1 Histogram of locking point results.....	144
FIGURE 4.2 Average locking point results.	146
FIGURE 4.3 Average locking point values versus asphalt content.	148
FIGURE 4.4 Comparison of optimum asphalt content.	150
FIGURE 4.5 Comparison of VMA for various compaction levels.....	152
FIGURE 4.6 Comparison of VCA ratio for various compaction levels.	153
FIGURE 4.7 Volumes associated with compacted HMA (49).	157
FIGURE 4.8 Comparison of the CoreLok and SSD air voids.....	161
FIGURE 4.9 Surface textures for different NMAS mixtures.....	163
FIGURE 4.10 Relationships between the CoreLok and SSD air voids for three NMAS.	164
FIGURE 4.11 Air voids difference between the CoreLok and SSD method versus the SSD air voids.	165
FIGURE 4.12 Relationships between absorbed water and air void content.	168
FIGURE 4.13 The difference between the CoreLok and SSD air voids versus absorbed water content.	169
FIGURE 4.14 Effect of CoreLok and SSD methods on optimum asphalt content.	170
FIGURE 4.15 Effect of CoreLok and SSD methods on voids in mineral aggregate.	172
FIGURE 4.16 Corrected CoreLok and SSD Air Voids for Whole Samples.....	174
FIGURE 4.17 CoreLok and SSD air voids for core samples.....	175

FIGURE 4.18 Air voids relationships between the whole and core samples by the SSD method.....	176
FIGURE 4.19 CoreLok air voids by program versus uncorrected air voids.....	181
FIGURE 4.20 Air voids difference between program and uncorrected calculation.	182
FIGURE 4.21 Relationship between permeability and VTM for 19 mm NMAAS.....	185
FIGURE 4.22 Relationship between permeability and VTM for 12.5 mm NMAAS.....	185
FIGURE 4.23 Relationship between permeability and VTM for 9.5 mm NMAAS.....	186
FIGURE 4.24 Permeability results for 65 and 100 gyration levels for 19 mm NMAAS.	189
FIGURE 4.25 Permeability results for 65 and 100 gyration levels for 12.5 mm NMAAS.	189
FIGURE 4.26 Permeability results for 65 and 100 gyration levels for 9.5 mm NMAAS.	190
FIGURE 4.27 Typical aggregate breakdown results for different compaction efforts (C.GVL 12.5 mm NMAAS).	193
FIGURE 4.28 Comparison of N and F gradation on aggregate breakdown.	198
FIGURE 4.29 Critical sieve changes due to compaction.	199
FIGURE 4.30 Average aggregate breakdown for all main factors.	201
FIGURE 4.31 Relationship between aggregate breakdown and L.A abrasion value. ...	202
FIGURE 4.32 Relationship between aggregate breakdown and F&E content.	203
FIGURE 4.33 Interaction between aggregate type and compaction level on aggregate breakdown.....	206
FIGURE 4.34 Interaction between aggregate type and NMAAS on aggregate breakdown... ..	206
FIGURE 4.35 Interaction between compaction level and NMAAS on aggregate breakdown.....	207
FIGURE 5.1 Comparison of APA rutting for three compaction levels.	213
FIGURE 5.2 Comparison of average APA rut depth.....	215

FIGURE 5.3	Interaction between aggregate type and NMAS on APA rut depth.....	217
FIGURE 5.4	Interaction between NMAS and compaction level on APA rut depth....	218
FIGURE 5.5	The relationship between APA rut depth and compaction level.....	219
FIGURE 5.6	Correlation between field and APA rut depth from NCHRP 9-17 project (80).....	220
FIGURE 5.7	Effects of air voids on APA rut depths (80).	221
FIGURE 5.8	Average dynamic modulus versus load frequency.	226
FIGURE 5.9	Average phase angle versus load frequency.	227
FIGURE 5.10	Average storage and loss modulus at different frequencies.....	228
FIGURE 5.11	Average $E^*/\sin\phi$ results at frequency of 10 Hz.	236
FIGURE 5.12	Interaction between aggregate type and NMAS on $E^*/\sin\phi$ results at frequency of 10 Hz.....	237
FIGURE 5.13	Average $E^*/\sin\phi$ results at frequency of 0.1 Hz.	239
FIGURE 5.14	Interaction between aggregate type and NMAS on $E^*/\sin\phi$ results at frequency of 0.1 Hz.....	239
FIGURE 5.15	The comparison of $E^*/\sin\phi$ between 10 Hz and 0.1 Hz.....	240
FIGURE 5.16	The correlations between field rut depths and $E^*/\sin\phi$ values (84).....	242
FIGURE 5.17	The relationships between $E^*/\sin\phi$ and APA rut depths.....	244
FIGURE 5.18	A typical static creep test result with tertiary flow.	245
FIGURE 5.19	A typical static creep test result without tertiary flow.	246
FIGURE 5.20	Average slopes for two gyration levels.....	250
FIGURE 5.21	Interaction between aggregate type and NMAS on slope of strain in static creep test.	251
FIGURE 5.22	Average log time to reach 4 percent strain in static creep test.....	252
FIGURE 5.23	Interaction between aggregate type and NMAS on average log time to reach 4 percent strain.	253

FIGURE 5.24	The Correlations between flow time and field rut depths (84).	254
FIGURE 5.25	A typical repeated load test result with tertiary flow.	258
FIGURE 5.26	A typical repeated load test result without tertiary flow.	259
FIGURE 5.27	Strain level at 10,000 cycles for three gyration levels.	260
FIGURE 5.28	Average strains at 10,000 cycles for two main factors.	261
FIGURE 5.29	Interaction between aggregate type and compaction level on strain at 10,000 cycles.	263
FIGURE 5.30	Strain slope at secondary phase for three compaction levels.	264
FIGURE 5.31	Average strain slopes for different aggregate types.	265
FIGURE 5.32	Relationship between strain slope and uncompacted voids of coarse aggregate.	266
FIGURE 5.33	Interaction between aggregate type and compaction level on strain slope.	267
FIGURE 5.34	The relationship between ram strain and LVDT strain reading.	269
FIGURE 5.35	The relationship between strain at 3600 and 10,000 cycles.	269
FIGURE 5.36	The relationship between strain level and compaction level.	271
FIGURE 5.37	Relationship between repeated load cumulative strain and APA rut depth.	272
FIGURE 5.38	The Correlations between flow number and field rut depths (84).	273
FIGURE 5.39	Field rut depth versus the lab strain from repeated load test (96).	274
FIGURE C1	Aggregate breakdown for crushed gravel 19 mm NMAS mixture.	306
FIGURE C2	Aggregate breakdown for crushed gravel 12.5 mm NMAS mixture.	306
FIGURE C3	Aggregate breakdown for crushed gravel 9.5 mm NMAS mixture.	307
FIGURE C4	Aggregate breakdown for lab granite 19 mm NMAS mixture.	307
FIGURE C5	Aggregate breakdown for lab granite 12.5 mm NMAS mixture.	308
FIGURE C6	Aggregate breakdown for lab granite 9.5 mm NMAS mixture.	308

FIGURE C7	Aggregate breakdown for limestone 19 mm NMAS mixture.....	309
FIGURE C8	Aggregate breakdown for limestone 12.5 mm NMAS mixture.....	309
FIGURE C9	Aggregate breakdown for limestone 9.5 mm NMAS mixture.....	310
FIGURE C10	Aggregate breakdown for ruby granite 19 mm NMAS mixture.....	310
FIGURE C11	Aggregate breakdown for ruby granite 12.5 mm NMAS mixture.....	311
FIGURE C12	Aggregate breakdown for ruby granite 9.5 mm NMAS mixture.....	311
FIGURE C13	Aggregate breakdown for traprock 19 mm NMAS mixture.....	312
FIGURE C14	Aggregate breakdown for traprock 12.5 mm NMAS mixture.....	312
FIGURE C15	Aggregate breakdown for traprock 9.5 mm NMAS mixture.....	313

CHAPTER 1 INTRODUCTION

1.1 BACKGROUND

Stone Matrix Asphalt (SMA) was first introduced into the United States as a result of the European Asphalt Study Tour of 1990 (1). European experience with SMA showed that this mix technology resulted in improved resistance to rutting of hot mix asphalt pavements. As a result of information and recommendations from the tour, several states became interested in the SMA technology and placed test sections or test projects beginning in 1991 to evaluate this mix. A Technical Working Group (TWG) was sponsored by the FHWA to develop guidelines for materials and mix design requirements, and to assist state Departments of Transportation (DOTs) as needed in providing information in regards to mix design, production, and placement of SMA mixtures.

The TWG, in a cooperative effort with state and federal agencies and the asphalt paving industry, published “Guidelines for Materials, Production, and Placement of Stone Matrix Asphalt (SMA)” in 1994 (2). Based on European experience and limited experience in this country, the guidelines recommended a mix design compactive effort of 50 blows for each face of the test specimens using a Marshall hammer. The guidelines were updated in 1999 with a National Asphalt Pavement Association (NAPA) publication, “Designing and Constructing SMA Mixtures – State-of-the-Practice,” which described laboratory samples being compacted with either the 50 blow Marshall method or by using

100 gyrations of the Superpave gyratory compactor (SGC). However, some states such as Georgia and Texas have found that 100 gyrations with the SGC is excessive for their materials and results in mixtures with lower than desired optimum asphalt contents. The high level of density obtained in the laboratory is also difficult to obtain in the field without excessive fracturing of aggregate particles. Experience from Georgia and Texas indicates that for their materials the optimum SGC compactive effort should be between 50 and 75 gyrations. Georgia, for example, has required 50 gyrations as the standard gyratory compaction level for these mixes.

Since there is a renewed interest in SMA technology by state agencies around the country in their search for a more durable, rut-resistant pavement, there is a need to identify a standard compaction effort with the SGC that will provide optimum density and overall good performance.

1.2 OBJECTIVES

As states renew their interest in SMA mixture technology, some are finding that previous guidelines of 100 gyrations with the SGC may not be satisfactory for their materials, and may result in lower optimum asphalt contents than needed or desired. The objective of this research study is to evaluate a lower compaction level for SMA mixtures that will provide more durability and satisfactory rutting resistance through stone-on-stone contact without fracturing aggregates due to excessive compactive force. Another objective is to determine if the same compaction effort is applicable for SMA mixes of various nominal maximum aggregate sizes (NMAS).

1.3 SCOPE OF STUDY

The objectives will be accomplished by executing the following tasks:

Task 1: Select aggregates which will be representative of those used in typical SMA mixes, such as granite, limestone, crushed gravel, and traprock etc. Select aggregate from sources that represent a range in Los Angeles (L.A.) abrasion values. Aggregates with L.A. abrasion values ranging from approximately 20 to near 40 (based on the B grading in ASTM C131 (3)) will be used to determine if the compactive effort results in significant aggregate breakdown. Three nominal maximum aggregate sizes (19 mm, 12.5 mm and 9.5 mm) will be used to determine if the same compaction level can be used regardless of nominal maximum aggregate size.

Task 2: Conduct SMA mixture designs with Marshall compaction and Superpave gyratory compaction. Marshall compaction uses the compaction effort that is equivalent to 50 blows with the manual hammer. Conduct trial SMA mix designs by the SGC with different gyration levels. For this study two gyration levels will be used: (1) 100 gyrations, (2) the lowest level of gyrations that approach the locking point. Locking point is defined as a gyration level at which sample height remains the same or less than 0.1 mm in difference for two successive gyrations in this study. Locking point is a point in the compaction process where additional gyrations provide very little increase in density (4). A third compaction level will be used to show the effect of further reduction in compaction level. This will result in

45 mix designs (5 aggregates x 3 compaction efforts x 3 mix types), plus some extra mix design work for the third gyratory compaction level.

Task 3: Determine the air void content by using two methods: the vacuum seal (CoreLok) method and the saturated surface dry (SSD) method. Compare the effects of test method on determining SMA volumetric properties.

Task 4: Use the two gyratory compaction levels indicated from Task 3 to prepare SGC specimens for performance testing. Some additional testing will be done at a third gyration level. Laboratory permeability tests will be conducted for all mix design samples to help determine at what point SMA mixtures become permeable, and the effects of compaction level on permeability.

The APA will be used to test specimens at 64 °C for 8,000 cycles after which the amount of rutting will be measured. APA tests will be conducted for all mixtures designed using different gyration levels, to evaluate how sensitive SMA mixtures are to variations in asphalt content and the effect of such variation on rutting resistance.

Triaxial performance tests (dynamic modulus test, static creep test, and repeated load creep test) based on research by Arizona State University will be performed for all mixtures designed with different compaction levels. Triaxial samples will be cored and sawn from a SGC specimen with 150 mm in diameter and 170 mm in height to provide a specimen with 100 mm in diameter and 150 mm in height for testing. All the triaxial tests will be conducted at a high temperature of 60°C to

evaluate the rutting performance of designed SMA mixtures. A 20 psi confining pressure will be applied for all triaxial tests to simulate a typical in-place confining pressure. The dynamic modulus samples will be tested at a set of frequencies from 25 Hz to 0.1 Hz to simulate different traffic conditions. The load amplitude will be selected to produce a microstrain between 50 and 150 for each mixture. The static creep test will use a deviatoric stress of 100 psi and maintain the load till tertiary flow happens or after 5 hours loading, whichever comes first. Repeated load creep tests will use a peak deviatoric stress of 100 psi and will be conducted up to 10,000 cycles or until tertiary flow happens. A haversine loading of 0.1 second load time and 0.9 second rest will be used for the repeated load test.

Task 5: Summarize and analyze all test results, refine current compaction level if needed, to ensure the design compaction level provides stone-on-stone contact and the most rutting resistance possible. Determine if the same gyration level can be used for each NMAAS and, if not, establish the gyration levels needed for each NMAAS.

CHAPTER 2 LITERATURE REVIEW

This chapter presents an extensive literature review pertaining to the development and evaluation of the Superpave gyratory compactor (SGC), the development of stone matrix asphalt (SMA) mixture design, and other relevant literature related to topics of this study. The individual literature reviews are conducted for the background of the SGC development and SMA mixture design as two separate sections, and are in chronological sequence in each section. A section summary is given following each section, and a summary on SMA mixture design using different compaction levels is given at the end of this Chapter.

In the individual reviews, comments by the author are generally designated by text in square brackets with italic font. Those comments are intended to clarify the original text, sometimes to draw the reader's attention to the background of study or the premise of conclusions, occasionally to add information that was not contained in the original text but might be of advantage to the reader, or to correlate several papers having similar results or conflicting information.

2.1 DEVELOPMENT AND EVALUATION OF THE SUPERPAVE GYRATORY COMPACTOR

2.1.1 Individual Literature

The literature reviews in this section are conducted to specifically answer the following questions:

- How does the gyratory compactor compare to field compaction and other compactive efforts?
- What are the key parameters for gyratory compaction?

Ortolani, L. and H.A. Sandberg, Jr. “The Gyratory-Shear Method of Molding Asphaltic Concrete Test Specimens; Its Development and Correlation with Field Compaction Methods. A Texas Highway Department Standard Procedure”, Journal of Association of Asphalt Paving Technologists, Vol: 21, 1952.

Ortolani et al (5) presented the development of a gyratory compaction procedure, and showed how the specimen compacted with the gyratory compactor correlated with field compaction.

It is believed that simulating the final pavement density or ultimate density is the goal of any compaction method used in mix design. Several criteria were set up to determine a good compaction procedure:

1. A good laboratory compaction method should be able to be used for field quality control;
2. The compactor should yield essentially the same density as the pavement density after some years of traffic;
3. The compactor should have similar aggregate degradation as under the field condition.

Several compaction devices were investigated, including two hydraulic compression test machines with different loading speeds, a standard Proctor Soil Compaction Machine, Public Roads Administration Vibratory Machine, a pneumatic roller-type molding machine, and a compaction device utilizing a conical roller or

compaction ram. However, after being tested in the laboratory, all of them were rejected for various reasons. The Gyrotory Molding machine was another compactor to be investigated. It had been incorporated in a standard procedure by the Texas Highway Department.

It is reported in this paper that the Gyrotory Molding machine served its purpose well. The procedure was as fast or faster than most commonly accepted compaction techniques. It only required one operator and this person could easily compact thirty specimens a day by using the Gyrotory Molding machine.

It was also found that the gyrotory compactor, which produced proper orientation of aggregate at low initial pressures, closely simulated the degradation found in field compaction.

To correlate the field compaction with gyrotory compaction, more than 400 field cores were collected from widely separated asphalt pavement sections in the state of Texas. These pavements comprised many different designs using different aggregates and types of asphalt. In addition, these pavements had been in service from a minimum of one year to twelve years under varied weather conditions. The road densities were also recorded at the time of construction. Results indicated that newly constructed surface courses had an average density 3.8 percent less than laboratory design density, and field cores after several years in service had an average density of only 0.8 percent less than the laboratory design density.

It is also reported in this paper that samples prepared with gyrotory compaction had good reproducibility in density. Some mixes were prepared with original asphalt and extracted aggregate from cores that were known to contain sound aggregate and were

expected to have litter degradation. Results showed that re-compacted samples had a density average of only 0.3 percent less than the density of the cores.

Consuegra, A., D.H. Little, H.V. Quintus, and J. Burati, “Comparative Evaluation of Laboratory Compaction Devices Based on Their Ability to Produce Mixtures with Engineering Properties Similar to Those Produced in the Field”, Transportation Research Record 1228, TRB, National Research Council, Washington, D.C., 1989.

Consuegra et al (6) reported a field and laboratory study that evaluated the ability of five compaction devices to simulate field compaction in engineering properties. The compaction devices evaluated in this study included the mobile steel wheel simulator, the Texas gyratory compactor (gyration angle is fixed at 3 degrees), the California kneading compactor, the Marshall impact hammer, and the Arizona vibratory-kneading compactor. The engineering properties used for evaluation included resilient modulus, indirect tensile strength and strain at failure, and tensile creep data.

Five projects were selected for this study. These projects were located in Texas, Virginia, Wyoming, Colorado, and Michigan. Field cores from each project were drilled one day after compaction. The sampling of asphalt mixtures for laboratory specimen preparation was performed with great care to ensure the random selection of trucks and to prevent segregation of mixtures. The loose field mix was properly sealed and transported to the laboratory, then reheated to the same compaction temperature as was used in the field. A trial and error method was used to determine the compactive effort to produce similar air void contents to that for field cores.

The repeated load indirect tensile test (resilient modulus) was performed in accordance with ASTM D4123-82 on samples from all five field projects. Indirect tensile strength tests were performed for three of five projects in accordance with test methods TEX-226-F of the Texas State Department of Highways and Public Transportation at 41°F, 77°F, and 104°F and at a loading rate of 2.0 in./min. The indirect tensile creep was performed for all five projects in the same way as the resilient modulus except that a static load, instead of a repeated load, was continuously applied for 60 min and then removed.

Simple comparison of test results for the field cores and laboratory compacted specimens indicated the Texas gyratory compactor, on the average, simulated the field compaction most closely. The average differences for each of these properties are calculated by absolute difference between test value of field cores and laboratory compacted samples over test value of field cores. The summary of average differences is presented in Table 2.1.

TABLE 2.1 Summary of Average Differences between Field Cores and Lab-Compacted Specimens (6)

Compaction Device	Creep Compliance at 77°F	Indirect Tensile Strength	Tensile Strain at Failure	Resilient Modulus
Arizona Compactor	0.77	0.51	0.47	0.41
Marshall Hammer	0.80	0.35	0.45	0.55
California Kneading	0.59	0.21	0.27	0.42
Steel Wheel Simulator	0.51	0.31	0.11	0.26
Texas Gyratory Compactor	0.44	0.14	0.16	0.37

The mean squared error (MSE) using the mean test value from field cores as a target value, was also employed to analyze the difference between the engineering

properties of field- and laboratory-compacted specimens. All test results were sorted and analyzed in terms of project, test, and temperature. The MSE ranking results are summarized in Table 2.2. A lower MSE value indicates a smaller difference, therefore a better compaction device to simulate laboratory-compacted specimens to field cores.

TABLE 2.2 Mean Squared Error (MSE) Comparison of Compaction Data (6)

Compaction Device	Average MSE Rankings by Mixture		
	<i>Project</i>	<i>Property</i>	<i>Temperature</i>
Arizona Compactor	5.0	4.8	4.7
Marshall Hammer	4.0	3.5	3.3
California Kneading	2.0	2.0	2.0
Steel Wheel Simulator	1.7	2.8	2.0
Texas Gyrotory Compactor	2.0	1.5	1.3

The Texas gyratory method had generally better MSE ranking than the other methods in most of the tests. The evaluation on MSE of all laboratory compaction devices indicated that the engineering properties of asphalt mixture depended on the type of compaction device used.

Overall, the Texas gyratory compactor demonstrated the best ability to produce mixtures with similar engineering properties to those determined from field cores. The California kneading compactor and the mobile steel wheel simulator ranked second and third, respectively, but with little difference between the two. The Arizona vibratory-kneading compactor and the Marshall hammer ranked as the least effective in terms of their ability to produce mixtures with engineering properties similar to those from field cores.

Button, J.W., D.N. Little, V. Jagadam, and O.J. Pendleton. “Correlation of Selected Laboratory Compaction Methods with Field Compaction”, In Transportation Research Record 1454, TRB, National Research Council, Washington, D.C., 1994.

This study (7) compared the four laboratory compaction methods (Exxon rolling wheel, Texas gyratory, rotating base Marshall hammer, and the Elf linear kneading compactor) with the field compaction. The objective of this study was to recommend a best laboratory compaction method that can simulate the field compaction well and be convenient to use.

Six laboratory tests were selected to evaluate samples compacted using the four lab compaction procedures and core samples. The tests were indirect tension at 25°C, resilient modulus at 0°C and 25°C, Marshall stability, Hveem stability, and uniaxial repetitive compressive creep followed by compression to failure. These tests were selected because they can be performed on 100 mm core samples from thin pavement layers.

Based on the statistical analysis of the test data, the Texas gyratory compactor simulated pavement cores most often (73 percent of the tests performed). The Exxon rolling wheel and Elf compactor simulated pavement cores with equal frequency (64 percent of the tests performed). The rotating base Marshall hammer simulated pavement cores least often (50 percent of the tests performed). These differences are not statistically significant (at $\alpha=0.05$).

When compared with the Exxon rolling wheel compactor, the Texas gyratory compactor is more convenient for preparing lab specimens for routine mixture design testing of asphalt concrete. Air voids distribution of gyratory compacted specimens may

be less similar to pavement cores than rolling wheel compacted specimens, however, this difference did not adversely affect the mixture properties measured for this study. Based solely on the findings of this study, the Texas gyratory compactor was recommended to SHRP for use in preparing routine lab test specimens.

[Testing in this study was limited to dense graded mixtures, SMA was not evaluated.]

Blankenship, R.B., K.C. Mahboub, and G.A. Huber. “Rational Method for Laboratory Compaction of Hot-Mix Asphalt”, In Transportation Research Record 1454, TRB, National Research Council, Washington, D.C., 1994.

Blankenship et al (8) commented that the purpose of the N_{design} experiment was to determine the number of gyrations (N_{design}) required to represent mixture densification in the actual pavement. Gyrations must relate to traffic levels and different high-temperature climates. This relationship is proven to exist and provides a method of choosing a mix design to have the blended aggregate gradation and percent asphalt binder matched to a desired traffic level in a specific climate. *[For SMA mixture applications, the traffic levels are always considered to be high and asphalt binder used is usually 1 or 2 grades stiffer than that required for conventional mixes]*

The objective of this study was to determine the N_{design} required to represent the various traffic levels in different geographical locations and climates. To achieve this objective, two gyration levels were evaluated: one was $N_{\text{construction}}$ which represents the initial laydown compaction level, $C_{\text{construction}}$, and the other was N_{design} which represents the compaction in the wheel path of pavement under traffic, C_{design} . The value of $C_{\text{construction}}$ was assumed to be 92 percent of G_{mm} due to the lack of information.

Eighteen pavements were evaluated, with fifteen being available for final evaluation. It was assumed that all the mixtures were designed to have about 3 to 5 percent air voids in the laboratory and 7 to 9 percent after construction. The field cores from the various pavements were first extracted and then remixed with an unaged AC-20 asphalt cement. The mixed materials were then aged for 4 hours at 135°C and compacted to 230 gyrations using the SHRP gyratory compactor. All mixtures used in this study were fine-graded mixtures. Mixtures with NMAAS equal to or less than 19 mm were compacted using 100 mm compaction molds while mixtures with NMAAS larger than 19 mm used 150 mm molds.

Some reasonable relationship trends between gyrations and climate and traffic were made in this study, generally at the high temperature climate and higher traffic level, one should use a higher N_{design} .

Analysis of the testing results provided a method of choosing N_{design} for a desired traffic level and an average 7-day high temperature. The authors suggested that the results and conclusions from the experiment were acceptable but more research needed to be completed to increase the precision of N_{design} .

Harvey, J., C.L. Monismith, and J. Sousa. "A Investigation of Field- and Laboratory-Compacted Asphalt – Rubber, SMA Recycled and Conventional Asphalt – Concrete Mixes Using SHRP A-003A Equipment", Journal of Association of Asphalt Paving Technologists, Vol: 63, 1994.

Harvey et al (9) evaluated several laboratory compaction methods and field compaction in terms of the permanent deformation resistance of compacted samples. It is believed that different lab compaction methods can produce specimens with different degrees of

resistance to permanent deformation as measured in lab testing. The objective of this paper was to compare the performance of lab-compacted specimens to field-compacted specimens, and estimate which lab compaction method produces specimens most similar to those produced by field compaction. The lab methods evaluated include Texas gyratory (7-inch diameter molds), University of California at Berkeley (UCB) rolling wheel, ASTM kneading (7.5-inch diameter molds), SHRP gyratory (6-inch diameter molds), and Marshall hammer (6-inch molds) compaction.

Field samples were cored from three sites, with 13 test sections total, and mixtures were collected in the field at about the same locations (with one exception) for laboratory compaction. The mixtures used in the sections included conventional dense-graded mixtures, SMA mixtures, and mixtures with 30 percent of reclaimed asphalt pavement (RAP) material. The laboratory samples were compacted at the same temperatures as the field cores, except the SHRP gyratory and Marshall hammer samples were all cut and cored from larger compacted masses to the same 150-mm diameter, 50-mm high, cylindrical shape as the field cores.

All specimens were tested with the Universal Testing System (UTS) and the constant height repetitive shear test for permanent deformation developed as part of SHRP Project A-003A (10).

Based on the test results, it was concluded that the ranking of the methods in order of resistance to permanent shear deformation was: samples by SHRP gyratory > samples by Kneading compaction = core samples subject to some age hardening and trafficking > core samples subject to no or little age hardening and trafficking = samples by rolling wheel compaction > samples by Texas gyratory. The authors indicated that the significant

difference between the SHRP gyratory and the Texas gyratory was due to the different speed of rotation and gyration angle used in the two gyratory compactors. The Texas gyratory had a slower rotation and larger angle. The Marshall samples were not included in the comparison because the Marshall hammer could not achieve the air void contents obtained in the field no matter the number of blows. But even at the higher air void contents, the Marshall samples had much higher permanent shear deformation resistance than the field cores.

It was also concluded that specimens produced by rolling wheel compaction best duplicated the properties of specimens compacted in the field. The rolling wheel compaction is competitive in terms of labor and materials efficiency with the SHRP and Texas gyratory compactors.

Cominsky, R., Leahy, R.B., and Harrigan, E.T., “Level One Mix Design: Materials Selection, Compaction, and Conditioning.” Strategic Highway Research Program Report No. A-408, National Research Council, Washington D.C., 1994.

Cominsky et al (11) presented this SHRP report that provided the detailed background of the development of the Superpave mix design system. Specifically, this report provides a detailed description of how the Superpave gyratory compactor was selected for use in mix design and field control in the Superpave system. The major reasons that a gyratory compactor was selected for Superpave system were because gyratory compaction reasonably simulated field compaction and provided quick and economical means for a laboratory compaction procedure. After considerable research and effort, SHRP researchers selected a gyratory compactor operating with a similar protocol as the French

LCPC compactor for Superpave mix design system. Summaries of the development of Superpave compaction parameters are provided as following.

Revolutions per Minute

The French gyratory compactor operates at a speed of 6 revolutions per minute (rpm). SHRP researchers wanted to reduce the compaction time as long as the high speed didn't adversely affect the volumetric properties of mixtures. An experiment was conducted using crushed granite (SHRP code: RB) aggregate and a PG 64-22 (SHRP code: AAK-1) asphalt from SHRP's Material Reference Library, to compare the volumetric properties (optimum asphalt content, air void content, VMA, VFA, and density) based on the speed of 6, 15, and 30 rpm. The results showed no statistical difference between these three compaction speeds, therefore, a speed of 30 rpm was selected to reduce the laboratory compaction time.

Comparisons of Gyratory Compactors

An experiment was conducted to determine if it was sufficient to specify the angle of gyration, speed of rotation (30rpm), and vertical pressure (0.6 Mpa) in order to standardize requirements for the manufactories of gyratory compactors. The experiment compared the SHRP gyratory compactor (manufactured by the Rainhart Company), the modified Texas gyratory compactor, and Corps of Engineering (COE) Gyratory Testing Machine (GTM).

Four aggregate blends with nominal maximum aggregate sizes ranging from 9.5 to 25 mm were selected. Two specimen sizes were evaluated: 150 mm and 100 mm. Three asphalt contents were used with one asphalt binder. All specimens were short term aged at 135°C for four hours. Compaction parameters were selected: angle of gyration (1

degree), vertical pressure (600 kPa), and rotational speed (30 rpm), except for the compaction angle of the GTM, which changed during the compaction. Conclusions of the experiment are shown below.

1. The modified Texas gyratory compactor and the SHRP gyratory compactor did not compact mixtures similarly. A verification of the compaction parameters indicated that the two devices were not compacting at the same angle. The modified Texas gyratory compactor had an angle of 0.97 degrees while the SHRP gyratory compactor had angles of 1.14 and 1.30 degrees for the 150 mm and 100 mm specimens, respectively.
2. A change in the angle of compaction of 0.02 degree resulted in an air voids change of 0.22 percent at 100 gyrations. This resulted in a 0.15 percent change in the optimum asphalt content for the 19 mm NMAS mixture.
3. Specifying the angle of gyration, speed of rotation, and vertical pressure alone is not sufficient to produce similar compactors. [*We now know that the internal angle may be significantly different for different compactors even when the external angle is the same.*]
4. Based on limited information, the COE GTM did not produce similar results to the SHRP gyratory compactor. This is mainly due to the difference in the method of applying the angle for the two compaction devices.

Sousa, J.B., G. Way, J.T. Harvey and M. Hines. "Comparison of Mix Design Concepts". In Transportation Research Record 1492, TRB, National Research Council, Washington, D.C., 1995.

The goal of a mix design procedure is to combine aggregates and binder into a mix that is able to satisfy desired levels of performance. Sousa et al (12) summarized a set of mix design concepts, based on the level of complexity and ability to predict performance:

- Level 1: under a given set of conditions, mix design specimens are compacted to determine their volumetric characteristics. Aggregate and binder requirements are based on prior experience. Asphalt content is determined by volumetric information. This is basically the approach followed by Superpave Level I.
- Level 2: mix design specimens are compacted under a given set of conditions, and a reduced set of tests are conducted. Limits of those properties are based on prior experience. Asphalt content is based on limits, ranges, or extreme values of the properties evaluated. This is basically the concept followed by the Marshall method.
- Level 3: some fundamental properties of specimens are determined with some specific preconditioning. Performance is predicted on the basis of statistical correlations between laboratory results and field observations. Asphalt content can be selected based on desired pavement performance, such as fatigue and permanent deformation. This is achievable with current state of knowledge and is basically proposed by some other researchers and used by Superpave Level III.
- Level 4: fundamental properties of the mix (and/or components) and evolution of those properties with time, aging, strain and stress levels, and moisture are determined. Prediction of behavior is made through an elaborate set of computer simulations. This approach is beyond the current state of knowledge. Asphalt

content would be selected based on predicted pavement performance, which would be very close to actual performance.

In this paper, authors report a study conducted by the Arizona Department of Transportation to evaluate mixes designed using the Marshall, Superpave Level I, and a performance based procedure developed under SHRP-A003A. The mixture was placed in two 1-mile test sections on Interstate 17 near Phoenix, in November 1993. The major objective of this study was to evaluate the HMA component requirements for the Superpave system. This study used a PG 70-10 asphalt binder and a partially crushed river gravel (90 percent of coarse aggregate had two or more fractured faces; all fine aggregate was crushed gravel). One percent Portland cement was added to all mixtures to reduce moisture susceptibility. The gradation used in the study had 19 mm NMAS and passed through the Superpave restricted zone.

Marshall stability results of 75-blow Marshall designed field mix and cores were 5044 and 3760 lbs, respectively. Both results are well above the Arizona DOT's minimum requirement of 3000 lbs. Field mixtures were also compacted with the Superpave gyratory compactor at a compaction level of N_{initial} (9), N_{design} (135), and N_{maximum} (220) using the asphalt content determined by the Marshall procedure. Results indicated that the field mix would not meet the volumetric requirements for a Superpave Level I mix design. In particular, the air void content was too high (7.6 percent and 6.3 percent, with and without parafilm, respectively), and the VFA was too low (53.3 percent). [*This indicates that for this mixture, 75-blow Marshall gives more compaction effort than 135 gyrations by SGC, which is not usually observed by other researchers*] An optimum asphalt content of 5.2 percent using SGC was estimated and used to produce

some new samples for volumetric determinations. The results showed that the mixture marginally failed the VMA and the % G_{mm} at $N_{initial}$ requirements.

Field cores were evaluated in the Hamburg wheel tracking device at 55°C. The results indicated that the pavement would perform well and that it would last about 10 to 15 years. The inspections of the pavements in July 1994 showed an average rut depth of 1.5 mm, which is an indication of the good performance of the mixtures, since most of the pavement failures due to rutting in Arizona usually happen during the first summer in service.

An evaluation was also conducted to determine which laboratory compaction device yielded the best correlation with field compaction. Laboratory compaction devices evaluated consisted of UC-Berkeley rolling wheel compactor, the California kneading compactor, the Texas gyratory compactor, the Marshall hammer, the SHRP Rainhart gyratory compactor (Asphalt Institute), and the SHRP gyratory compactor (FHWA field trailer). Based on their permanent deformation resistance in the repeated simple shear at constant height test (RSST-CH), it was concluded that the rolling wheel compactor produced specimens that best correlated against field cores.

Hafez, I.H. and M.W. Witczak. “Comparison of Marshall and Superpave Level I Mix Design for Asphalt Mixes”. In Transportation Research Record 1492, TRB, National Research Council, Washington, D.C., 1995.

Hafez et al (13) described the differences on choosing compaction level when designed by two procedures: Superpave Level I and Marshall. In the Superpave Level I mix design procedure, there is a table for gyration levels, which is dependent on the anticipated traffic volume and project site climatic conditions. These design gyrations, coupled with

the specific mixture gyratory densification curves developed for each mix under different asphalt contents, can be used to determine the design asphalt content. The final design asphalt content depends on traffic level and environmental conditions.

In contrast to the Superpave gyratory mix design approach, the Marshall mix design uses an impact hammer to achieve the design level of compaction (air voids) as a basis for establishing the design asphalt content. The majority of agencies using the Marshall specify 35, 50, or 75 blow compaction consistent with the anticipated traffic level ($\leq 10^4$, 10^4 - 10^6 , $>10^6$ ESALs, respectively). Thus, the final design asphalt content will only depend on traffic level.

This study performed mix designs for 20 different mixes using both the Marshall procedure and the Superpave gyratory compactor Level I procedure. The mixes evaluated included dense graded mixtures and SMA-like [*in this paper, it was referred to as open grading Plus Ride mixtures*] mixtures. Optimum asphalt contents for all mixes in the study were determined by the Marshall 75 blow and Superpave Level I procedures. The Marshall procedure consisted of preparing three replicates at 1.0 percent asphalt content increments in order to cover an air voids range of 3.0 to 5.0 percent. The Superpave design consisted of compacting 100 mm diameter specimens at three different N_{design} values corresponding to a traffic level less than 10 million ESALs and design air temperatures of $\leq 34^\circ\text{C}$, 37 - 39°C , and 43 - 44°C . The N_{design} values corresponding to these parameters are 67, 96, and 119 gyrations, respectively.

It was concluded when the design compaction level for the SGC decreased from 119 to 67 gyrations, asphalt content increased about 1 percent for all the mixes evaluated. There were no consistent trends found between the density obtained using the Superpave

procedure and the Marshall procedure. [*Explanation of this result and aggregate properties related to breakdown were not reported in the study.*]

D'Angelo, J. A., Paugh, C., Harman, T. P., and Bukowski, J., "Comparison of the Superpave Gyrotory Compactor to Marshall for Field Quality Control." *Journal of the Association of Asphalt Paving Technologists*, Volume 64, 1995, pp. 611-635.

In the study conducted by D'Angelo et al (14), the Superpave Level I and the Marshall procedures were compared by using five different asphalt mixes produced at five different asphalt plants. Two mixes were designed using the SGC at N_{design} levels of 86 and 100 gyrations. These two mixes were evaluated with the Marshall hammer using 112 blows (6 inch sample) and 50 blows, respectively. The other three mixes were designed using the Marshall hammer with 112 (6 inch sample), 50, and 75 blows. The SGC was used to evaluate these mixes at N_{design} levels of 100, 126, and 109 gyrations, respectively. Samples of the five mixes were obtained and compacted with both the SGC and the Marshall hammer to compare the results of the SGC and Marshall hammer when used for quality control.

The results of the analysis indicated that samples compacted with the SGC had slightly less variability in air voids than did the Marshall samples. Based on air voids alone, the SGC and the Marshall hammer could both be expected to perform well in quality control applications and they would be interchangeable.

As an indication of the aggregate structure, the voids in mineral aggregate (VMA) appears to distinguish between the two compaction devices. The results showed that for all mixtures tested, the SGC samples had lower VMA than Marshall samples. The general trend of lower VMA with the SGC indicates that the compaction effort obtained

with the SGC is greater than with the Marshall hammer. Although the high variability existed in VMA comparison, it can still be observed that the VMA determined from the SGC specimens did not respond the same as from the Marshall samples to the changes in asphalt content. For three mixtures, the slopes of the VMA to asphalt content for two compaction devices had the same trend. For the other two mixtures, the slopes had the opposite trend, with the increase of asphalt content, VMA of SGC specimens decreased, and VMA of Marshall specimens increased. This indicates that the asphalt contents are on the low and high side of VMA curve for the SGC and the Marshall compacted samples. The different trends and the high degree of variability of the data indicate that the SGC and the Marshall are not interchangeable for quality control.

The overall conclusion of the study was that the SGC was better able to track plant production variability than the Marshall hammer. The mixtures designed with the SGC can not be tested and controlled in the field using the Marshall.

McGennis, R.B., R.M. Anderson, D. Perdomo and P. Turner. “Issues Pertaining to Use of Superpave Gyrotory Compactor”. In Transportation Research Record 1543, TRB, National Research Council, Washington, D.C., 1996.

McGennis et al (15) reported the results of the Superpave gyrotory compactor study to determine the effect of various compaction parameters on the mixture volumetric properties. Parameters included mold diameter, short-term aging time, and compaction temperature. Differences between different brands of SGC were also compared.

Mold Diameter

The compaction characteristics resulting from two mold sizes of 150 mm and 100 mm were compared. For the comparison, five 19 mm and two 12.5 mm nominal maximum

size aggregate blends were used, with seven gradations ranging from gap-graded to finer gradations. The optimum asphalt content for these mixes was selected to achieve 4 percent air voids at a design gyration level of 172. Three asphalt contents: optimum, optimum plus 0.5 percent, optimum minus 0.5 percent were used for compaction with two mold sizes for all seven mixtures. The volumetric properties at gyration levels of 10, 100, 150 and 250 were observed for the analysis. Two sample t-tests were performed at a level of significance of 5 percent and indicated that for 47 out of 84 comparisons (56 percent), there was a significant difference between the 150 mm and 100 mm diameter specimen. The overall trend is that the 150 mm mold produces the same or, more likely, a higher density than the 100 mm mold.

Compaction Temperature

Based on only one design aggregate which was predominately crushed limestone and two binders PG 64-28 and PG 76-28, it was found that variation in compaction temperature (120, 135, 150, 165 and 180°C were used) did not seem to substantially affect volumetric properties of a mixture containing an unmodified binder. However, variation in compaction temperature did significantly affect the volumetric properties of the same mixture containing a modified binder. To explain this result, authors used a hypothesis, which is: with the unmodified binder, the aggregate structure dominated the compaction characteristics of the mixture, whereas with the modified binder the binder properties dominated.

Short Term Aging

The study also compared the variable short-term aging period effect on the volumetric properties of mix. The results indicate the expected trend: as aging time increased, the

theoretical maximum specific gravity G_{mm} increased and bulk specific gravity of mixture G_{mb} decreased. This is because increasing the asphalt absorption will lower the effective volume of the aggregate therefore increasing the aggregate effective specific gravity G_{se} , and G_{mm} , and increasing the asphalt absorption will lower the effective asphalt content, thereby decreasing the compactibility of the mix and G_{mb} . The combination of increasing the G_{mm} and decreasing the G_{mb} will result in higher air voids.

Gyratory Compactor Comparison

This study also compared the compaction characteristics of several different units, including Pine SGC, Troxler SGC, Rainhart SGC and the modified Texas SGC. The compactor comparison testing program consisted of the preparation and compaction of three mixture specimens at design asphalt content for each of six mixtures. Specimens were prepared to determine differences in the percent G_{mm} at $N_{initial}$ (10 gyrations), at N_{design} (100 gyrations), and at $N_{maximum}$ (152 gyrations). The results showed that there were significant differences in volumetric properties produced among the four SGCs evaluated. At N_{design} , the modified Texas and Pine SGCs tended to produce similar results. The Troxler and Rainhart devices also produced similar results at N_{design} . However, the modified Texas and Pine units tended to produce lower air voids and thus lower optimum asphalt content at N_{design} than the Troxler and Rainhart devices. In addition, the modified Texas and Pine SGC produced flatter compaction slopes than the Troxler and Rainhart SGC.

Brown, E.R., D.I. Hanson, and R.B. Mallick. "Evaluation of Superpave Gyratory Compaction of Hot-Mix Asphalt". In Transportation Research Record 1543, TRB, National Research Council, Washington, D.C., 1996.

The main objective of this study (16) was to compare the density of specimens compacted with the SGC at different gyration numbers, with the density of in-place cores obtained from test sections with different levels of cumulative traffic.

Field cores were obtained from six test sections having different combinations of age and traffic levels: two in Alabama (US-280 and AL-86), and one each in Idaho (I-90), New Mexico (I-40), South Carolina (I-385), and Wisconsin (STH-67). For all the sections, the cores were drilled immediately after construction and after one year of traffic. For four of six sections, cores were also obtained after two years of traffic.

In the laboratory, two sets of specimens were produced using the Superpave gyratory compactor for the six sections. One set used original plant-produced loose mixture, and another set used the same aggregate and asphalt to produce mixture in the laboratory similar to the plant-produced mixture. The field core densities were compared to the density data obtained from these two sets of laboratory specimens.

It was concluded that 100 gyrations of laboratory compaction produced higher density than either the 1 or 2 year in place density for all the mixes. At similar gyration levels, it was found that reheated specimens had an average about 1 percent higher density than laboratory prepared specimens that were not reheated. It was also concluded that the density of the test sections varied linearly with logarithm of cumulative traffic, an average increase of 4.8 percent of theoretical maximum density corresponding with a cumulative traffic application of 1 million ESALs.

Forstie, D. A. and Corum, D. K., “Determination of Key Gyratory Compaction Points for Superpave Mix Design in Arizona.” ASTM Special Technical Publication, Volume 1322, September 1997. ASTM, Philadelphia, PA., pp. 201-209.

Forstie et al (17) conducted a study to evaluate the level of Superpave laboratory compaction necessary to equal the in-place field density after various levels of traffic. The further evaluation of SHRP recommendations for the number of design gyrations was necessary because of the following reasons:

1. The angle of gyration used by SHRP researchers to develop the current levels of N_{design} was 1.0 degree, while the angle currently specified in AASHTO TP-4 is 1.25 degrees.
2. The N_{design} experiment was conducted using 100 mm diameter specimens, not the currently used 150 mm specimens.
3. The mixes used in the N_{design} experiment were predominately fine-graded mixes, not the coarse-graded mixes, which are most commonly used today.
4. Only two cores at each project location were obtained for testing and evaluation in the original N_{design} experiment. More specimens may have provided a greater confidence in the field density.

Field cores from seven projects on Interstate 10 were obtained within and between the wheel paths. Cores obtained from the field were tested to determine bulk specific gravity and theoretical maximum specific gravity, and then processed through the ignition oven to determine asphalt content and gradation. The salvaged aggregate from each project was re-mixed with the same amount of asphalt cement and compacted in the Troxler SGC to determine its volumetric properties at N_{design} . The N_{design} level of gyrations was determined based on the project traffic and temperature. All of the projects evaluated were from a hot or warm climate location and ranged in age from 5 to 8 years and had N_{design} values ranging from 113 to 135 gyrations. Statistical analysis (t-tests at a

level of significance of 5 percent) indicated that average bulk specific gravities from the Superpave gyratory compactor were significantly higher (2.355 to 2.318) than the field cores.

Based on test results, it was concluded that the current N_{design} compaction levels table should be revised to account for the 1.0 to 1.25 gyration angle change that occurred after the original SHRP research. Mixes designed at the original N_{design} levels using a gyration angle of 1.25 degrees will likely have higher laboratory densities (lower optimum asphalt content) than mixes designed using a gyration angle of 1.0 degrees, which was the angle used to establish the original N_{design} levels. This over-compaction could lead to unnecessary difficulties in the field compaction.

Mallick, R.B., S. Buchanan, E.R. Brown and M. Huner. “An Evaluation of Superpave Gyratory Compaction of Hot Mix Asphalt”, NCAT Report No. 98-5, Auburn, AL, 1998.

Mallick et al (18) conducted a study to evaluate some issues with the Superpave gyratory compactor. One of the objectives of this study was to evaluate the correction factor used to back calculate the bulk specific gravity of a compacted specimen at any gyration. This correction factor was determined at N_{maximum} and usually assumed to be constant at all gyration levels.

One aggregate type (traprock) and a PG 64-22 asphalt were used. Two aggregate gradations including a typical SMA and a typical dense graded mixture were used.

The samples were compacted with the SGC at different gyration levels and the bulk specific gravities were determined. Back calculations were also conducted for these different gyration levels by using the correction factor determined at N_{maximum} . These two

sets of bulk specific gravities were compared. It was found that the correction factor first decreased and then became constant at higher gyration levels. Densities were found to be greater than that obtained by back calculation for lower gyration samples. Also, there was a greater difference between back calculated and actual air voids for coarse textured mixtures. SMA had a greater error in back calculation of air voids compared to a dense graded mix.

It was concluded that the correction factor was not constant at different gyration levels, and it was recommended that mixtures be compacted to N_{design} to determine the optimum asphalt content.

Anderson, R. M., R.B. McGennis, W. Tam, and T. W. Kennedy, “Sensitivity of Mixture Performance Properties to Changes in Laboratory Compaction Using the Superpave Gyrotory Compactor ”, Journal of Association of Asphalt Paving Technologists, Vol: 69, 2000.

Anderson et al (19) presented a study to evaluate and adjust the N_{design} table based on the sensitivity of mechanical properties (other than the volumetric properties in NCHRP 9-9). The purpose of this study was to estimate the consequences, in terms of change in performance properties, of using different numbers of design gyrations.

The experimental design included six Superpave mix designs (two aggregates, three design gyrations). The two aggregate types were crushed limestone and crushed gravel. All mixtures had a NMAS of 12.5 mm. Three design gyrations were used: 70, 100, and 130 to represent low, medium, and high traffic level, respectively.

The performance properties used in this study included complex shear modulus (G^*) from the shear frequency sweep test and permanent shear strain (γ_p) from the repeated shear test at constant height.

The results indicated that a general trend can be observed of decreasing shear stiffness ($G^*_{10\text{Hz}}$) with decreasing design gyrations. It was concluded that with other factors (asphalt content, asphalt binder stiffness and volume of air voids) held relatively constant, this trend reflected the change in aggregate structure produced as design gyrations were reduced. This trend was more notable as N_{design} changed from 100 to 70 gyrations. It was observed that a decrease of 30 gyrations could lower the design shear stiffness of an asphalt mixture by as much as 35 percent, and approximately 15 percent for average.

It was also observed that limestones have a significantly lower permanent shear strain (γ_p) value (average 1.29 percent) at 60°C than the gravel mixtures (average 2.02 percent). [*No explanation was given in the literature and aggregate properties were missing*] However, for each aggregate, there were no significant differences in permanent shear strain apparent between mixtures designed at 130 gyrations and 70 gyrations.

Buchanan, MS and E.R. Brown, “Effect of Superpave Gyratory Compactor Type on Compacted Hot-Mix Asphalt Density” In Transportation Research Record 1761, TRB, National Research Council, Washington, D.C., 2001

Buchanan et al (20) presented an effort to evaluate the effect of SGC type on compacted HMA density. One major concern was the degree of reproducibility between laboratories having different brands of approved SGC. The objective of this study was to present

observed precision values and practical differences between the currently used SGC and to discuss the possible project implications of the differing results.

The data used in this study include the Southeast Superpave Center gyratory compactor proficiency sample testing, results from the initial six projects from NCHRP 9-9: verification of the gyratory levels in the N_{design} table, and mix design and quality control (QC) and quality assurance (QA) results from a state DOT.

Based on the analysis of the observed data, the following conclusions are drawn:

1. The SGC has higher precision for both the single- and multi-laboratory compared to the past data with the mechanical Marshall hammer. Average values for the gyratory compactor of 0.0094 and 0.0133 were determined for single- and multi-laboratory precision, respectively. For comparison, the mechanical Marshall hammer had an average single-operator precision of 0.012 and a multi-laboratory precision of 0.022 (21).
2. Significant difference in compaction efforts was observed for different SGCs, even after proper calibration. This difference resulted in significant differences in air void content (in some cases up to 2 percent) of compacted samples, significant differences in optimum asphalt content (up to 1.3 percent) between designed mixtures and verified mixtures, and significant differences between QC and QA air void results (0.79 percent).

It is indicated that the magnitude of changes in the gyration angle during compaction contributes to the difference of compaction efforts for different SGC. Therefore, it is suggested by the authors that a protocol for an independent gyration angle-measuring device should be developed as soon as possible to ensure the gyration

angle of all gyratory compactors remains within the specification range of 1.23 to 1.27 degrees during compaction, and consequently to ensure all gyratory compactors are providing similar compactive efforts.

Tashman, L., E. Masad, R. Peterson, and H. Saleg. “Internal Structure Analysis of Asphalt Mixes to Improve the Simulation of Superpave Gyratory Compaction to Field Conditions”. *Journal of the Association of Asphalt Paving Technologists*, Vol. 70, 2001.

Tashman et al (22) compared laboratory compaction with SGC to field cores that were compacted using three field compaction patterns. The internal structure, i.e. the distribution of aggregates and air voids inside the mix was used to evaluate the similarity of laboratory compacted samples and field cores. Computer automated image analysis techniques and X-ray computed tomography were used to capture and quantify the internal structure distribution. The properties related to internal structure included in this study were air voids distribution, aggregate orientation, aggregate segregation and aggregate contacts.

Three test sections were constructed for this study. Each section was about 90 meters in length. A transition section of about 30 meters was placed between each test section for changing directions or stopping. The three sections used the same materials (limestone and a PG 70-22 asphalt with Superpave 12.5mm NMAS gradation) and a similar construction temperature. The variables among these sections were the compaction equipment and the number of passes used in order to achieve target air voids of 7 percent.

Field cores were obtained from the test sections directly after construction and before trafficking. Loose mix samples that represent the three sections were obtained from loaded trucks and tested for asphalt content and aggregate gradation, to ensure the laboratory samples had similar material properties as in the field. All mixes were reheated to the field compaction temperature (149°C) before compacting in the gyratory compactor. The gyratory compactor used in this study had various levels of several key parameters, including the angle of gyration (1.25, 1.5 and 2.0 degree), height of specimen (50, 75 and 135 mm), and compaction pressure (400, 600 and 800 kPa). Another temperature (175°C) of base plate and mold was also used at an angle of 1.25 degree, 50 mm height, and 600 kPa pressure for studying air voids distribution.

The results indicated that different field compaction patterns didn't affect the internal structure much. However, the compaction parameters (angle, pressure, height, and temperature) of SGC influenced the internal structure of lab compacted samples and changes of these parameters could make the internal structure of lab samples similar to field cores. The findings suggest the use of an angle of 1.5 degree and a specimen height of 50 mm to 75 mm in the SGC to better simulate the internal structure of field cores. Authors also indicated that this specimen height may be affected by the NMAAS of mixture, which is 12.5 mm in this study. Pressure was not a significant influencing factor for the internal structure. However, using 600 kPa gave the closest results to field cores.

The stiffness test using the shear frequency sweep test at constant height (FSCH) was also conducted to verify the usefulness of simulation in internal structure. The results showed that improving the simulation of field cores in SGC samples reduced the difference in stiffness between SGC samples and field cores.

Harman, T., J.R. Bukowski, F. Moutier, G. Huber, and R. McGennis. “The History and Future Challenges of Gyrotory Compaction 1939 to 2001”. In Transportation Research Record 1789, TRB, National Research Council, Washington, D.C., 2002.

Harman et al (23) reviewed the history of gyrotory compaction and presented the evolution of gyrotory compaction as shown in the Table 2.3.

TABLE 2.3 Evolution of Gyrotory Compaction (23)

Timeline	Device/Agency	Specimen Size	Compaction Effort
1939	Concept TX Highway Department	D – 4” H – 2”	P – Unknown A – Manual S – Manual
1946	TX Highway Department	D – 4 & 6” H – 2 & 3”	P – Variable A – Fixed 6° S – 60 rpm
1957	US Corps Engineers GTM	D – 6” H – Variable	P – Variable A – Floating 0 to 3° S – Variable 12 to 18 rpm H – Heated mold
1960’s	First Prototype Texas at LCPC, France	D – ? H – ?	P – Variable A – Variable S – Variable
1968	Second Prototype Texas at LCPC, France	D – 80 or 120 mm H – Variable	P – Variable A – Floating 0.5 to 5° S – Variable H – Heated mold
1974 to 1985	PCG1, PCG2 at LCPC, France	D – 160 mm H – Fixed 80 to 300 mm	P – 600 kPa A – Fixed 1 to 4° S – Fixed 6 to 30 rpm H – Heated mold
1991	Modified Gyrotory Shear Test Machine, FHWA	D – 4” H – 2.5”	P – 600 kPa A – Fixed 0.5 to 3° S – 30 rpm
1991	Modified TX Highway Department, SHRP	D – 6” H – 3.75”	P – 600 kPa A – See History S – Variable H – Heated mold
1993	SHRP/Superpave Gyrotory Compactor in USA	D – 150 mm H – 115 mm	P – 600 kPa A – Fixed 1.25° S – 30 rpm
1996	PCG3 at LCPC, France	D – 150 mm H – Fixed 100 to 160 mm	P – Fixed 500 to 800 kPa A – Fixed 0.5 to 2° S – Fixed 6 to 30 rpm

Key: D – diameter, H – height, P – consolidation pressure, A – external mold wall angle,
S – speed of gyration, and H – heated mold.

It is reported that over 2000 SGCs manufactured by five companies are currently in use in the United States for design and field control of asphalt mixtures. A total of eight different models from the five companies are using totally different methods of setting, inducing, and maintaining the angle of gyration. A calibration system is required in each device to measure the angle of gyration. All measurements are made externally relative to the mold wall. However, the difference in internal angle of gyration is believed to result in the different compaction effort for different types of SGC even when the external angle is controlled. In response to this issue, FHWA has developed an angle validation kit (AVK) to measure the internal angle of gyration in any SGC. However, before the AVK can be considered in standard practice, the target and tolerances for a standard internal angle must be established.

Peterson, R.L., K.C. Mahboub, R.M. Anderson, E. Masad and L. Tashman.

“Superpave Laboratory Compaction versus Field Compaction”. In Transportation Research Record 1832, TRB, National Research Council, Washington, D.C., 2003.

Peterson et al (24) presented a follow-up study on evaluation of Superpave compaction versus field compaction for the previous one (19). The mechanical properties were used to evaluate the similarity of laboratory compacted samples and field cores. The field compaction consisted of three test sections with different compaction patterns. The laboratory compaction used the Superpave gyratory compactor with adjustments to several parameters, including sample height, compaction pressure and gyration angle.

Performance tests conducted with the Superpave shear tester in accordance with AASHTO TP 7 [updated version is AASHTO T320 (25)] were used to evaluate field and laboratory compaction. Frequency sweep at constant height (FSCH) testing was

conducted at 30°C and 40°C. Repeated shear at constant height (RSCH) testing was conducted at 50°C.

It was concluded that current gyratory protocol produces specimens with significantly different mechanical properties than those of field cores produced with the same material and compacted to the same air voids. It was indicated that adjustments to certain parameters of the gyratory can produce specimens that better simulate the mechanical properties of pavement cores. It was suggested that the use of 1.5 degree angles and a specimen height of 50 or 75 mm would better simulate mechanical properties of roadway cores tested in the Superpave shear tester.

2.1.2 Summary of Literature

Historically, three compaction methods: impact compaction (Marshall), kneading compaction (Hveem) and gyratory compaction (SGC) have been used in routine HMA mix design. Several studies (5-7, 9, 12-14) were conducted to determine the best available laboratory compaction device that could simulate field compaction. The results indicate that the gyratory compaction is a promising compaction procedure in simulating field degradation, density and engineering properties.

During the Strategic Highway Research Program (SHRP), intense debate focused on the effectiveness and appropriateness of the gyratory compaction. Some research studies (9, 12) indicated that the rolling wheel compactor produced specimens that best correlated against field cores. However, other studies (7, 11) indicated the impracticality of the rolling wheel compactor as a means of mix design compaction. The equipment proposed was large and required very large batches of mixture. Although the performance test results of the gyratory specimens did not correlate with field cores as

well as rolling wheel compacted specimens, the air voids produced during compaction were very repeatable and the compactor was easy to use. This ease of use and repeatability are desirable because mix designs are based on the volumetric properties of the specimens.

Two major factors favor using a gyratory compactor for laboratory compaction for mixture design: 1) the close simulation of field compaction (5-7, 14), including volumetric properties, engineering properties, and aggregate breakdown; and 2) the ease of use and good repeatability (5, 7).

Gyratory compaction was first developed in the 1930s in Texas (5). The compaction process involved applying a vertical load while gyrating the mold in a back-and-forth motion. This gyratory compactor produced a kneading action on the specimen by gyrating the specimen through a horizontal angle.

The gyratory compaction has evolved since its first development, resulting in several unique devices and a variety of methods (23). Compaction using gyratory action was further developed and applied by the Army Corps of Engineers as well as the Central Laboratory for Bridges and Roads (LCPC) in France.

The Superpave gyratory compactor (SGC) was developed during the SHRP program. It is similar to the French gyratory but with some modifications. It operates with a vertical load of 600 kPa, a gyration speed of 30 rpm, and a constant angle of gyration of 1.25 degrees.

The gyration angle and applied pressure were found to be critical for consistent compaction results. Some studies (22, 24) have shown that adjusting these compaction parameters would make gyratory samples better simulate field compaction. Some studies

(11, 15, 20, and 23) have also indicated that different brands of SGCs result in different compaction results, and the difference in internal angle was believed to be one of the primary reasons. Therefore, it is necessary to calibrate the internal angle during compaction in order to get consistent compaction results between different brands of compactors (20, 23). An angle validation kit (AVK) has been developed as a response to this issue (23).

2.2 THE DEVELOPMENT OF SMA MIX DESIGN

2.2.1 Individual Literature

The literature reviews in this section are conducted to specifically answer the following questions:

- What are the design criteria for designing SMA mixture?
- What is the compaction effort used for designing SMA mixture?
- What are the conclusions and recommendations of researchers who have evaluated the compaction effort used in SMA mix design?
- What are the performance tests used to evaluate SMA mixtures?

AASHTO, “Report on the 1990 European Asphalt Study Tour”, Washington D.C., June 1991.

This report (1) is an outcome of the European Asphalt Study Tour (EAST) in 1990. One of the objectives of this study tour was to review and evaluate European pavements and asphalt technology. A section of this report addresses SMA. The report describes the origin of SMA and its development. Some general design criteria that had been in common practice in Europe are also summarized.

SMA was first developed in the 1960's in Germany as an HMA mixture that was especially resistant to studded tire damage. The term splittmastixasphalt is used in the German "*Supplemental Technical Specifications and Guidelines on Asphalt Surface Course.*" SMA continues to evolve in Europe, and was introduced into several European countries including Sweden and Denmark. The report indicates that SMA mix design in Europe generally follows a recipe-type approach from standard designs.

In Europe, the Marshall mix design method is usually used for voids analysis and the selection of target bitumen content. For a selected aggregate gradation, the Marshall specimens are compacted at 50 blows per side for several asphalt contents mixed at $135\pm 5^{\circ}\text{C}$. The asphalt content that yields an air void content of 3 percent is selected as the target value for the job mix formula. European specifications require a maximum 6 percent of air void content for SMA field construction.

**Stuart, K.D. "Stone Mastic Asphalt (SMA) Mixture Design", FHWA-RD-92-006
Federal Highway Administration, March 1992.**

Stuart (26) documented SMA mixture design information from Europe and a SMA project conducted by the Georgia Department of Transportation. There are two chapters in this report. Chapter 1 presents information on European SMA mixture design technology, which was obtained primarily from sources in Sweden and Germany.

The Marshall method of mixture design is used in Sweden and Germany for designing SMA mixtures. However, stability and flow values are often not used, many designs are based on air void requirements and minimum asphalt content. The compaction temperature in the lab in Sweden is generally between 293 and 302°F (145 and 150°C) and rarely exceeds 311°F (155°C). But when a fiber is used as the stabilizing

additive, temperatures up to 338°F (170°C) are allowed. Germany generally uses a temperature of 275°F (135°C). Neither loose mixtures nor compacted specimens are aged in an oven in either country.

Based on their experiences, the Swedes and the Germans to date are satisfied with the 50-blow Marshall compaction effort for mix design. Increasing the number of blows is not recommended by them because this may increase the number of fractured aggregates with little to no increase in density. Therefore, all optimal binder contents reported by the Swedes and Germans and minimum binder contents contained in their specifications were obtained through a 50-blow Marshall compactive effort.

It is also indicated that SMA design air void levels are often slightly lower than those used for dense-graded mixtures. The high stone-on-stone contact allows the use of lower air void levels. There are no requirements for voids in the mineral aggregate (VMA) or voids filled with asphalt (VFA). However, there is a minimum asphalt content requirement which has the similar overall effect. For a nominal maximum aggregate size (NMAS) of 12.5 mm, these properties are generally above 16.5 percent and 78 percent, respectively.

The air voids level requirement in an SMA pavement layer after compaction is lower than for a dense-graded mixture using the same type of aggregate and maximum aggregate size. The Swedes and Germans report that field air void levels are typically 3 to 5 percent and are specified to be less than 6 percent. When the design air voids level is 3 percent, mixtures with fibers often compact to a 3 to 4 percent level. It is also indicated that SMA mixtures at their ultimate or refusal density after traffic will not have air voids

levels significantly lower than the design level. This may be because SMA normally uses the 50-blow Marshall hammer which provides adequate compaction.

The author reports that very little evaluation testing has been done on SMA in Europe. At the time of writing the report, the author indicated that research was underway in Germany and the Netherlands on the resistance of SMA mixtures to permanent deformation using creep, repeated load, and wheel-tracking tests.

Chapter 2 documents the work performed for Georgia Department of Transportation (GDOT). GDOT performed mixture designs and requested assistance from other organizations with designs.

The lab mixing temperature was 325°F (163°C) and the compaction temperature was 310 to 315°F (154 to 157°C). These temperatures were based on past experiences of GDOT using Novophalt-modified binders. It was indicated that there was no firm basis for choosing mixing and compaction temperatures in this project.

A 50-blow Marshall design was used. The optimum binder content was taken at a 3.5 percent (requires a 3 to 4 percent design air voids level) air voids level.

Kenepohl, G.J., and J.K. Davidson. "Introduction of Stone Mastic Asphalt (SMA) in Ontario", *Journal of Association of Asphalt Paving Technologists*, Vol 61, 1992.

Kenepohl et al (27) presented the results of SMA mix designs for three projects in Ontario, which were constructed between December 1990 and October 1991. Three projects were Miller Avenue project, Highway #7N project and Highway #404 project.

The Marshall mix design method was used in all three projects. The mixes were designed to have an asphalt content that would give a value of 3 percent air voids. The compactive effort to achieve the proper air voids was the equivalent mechanical blow

count to provide a density equal to that provided with the 75-blow hand hammer or 50-blow hand hammer. In the Miller Avenue project, 75-blow was chosen because it was felt that the expected heavy traffic conditions would cause over-densification of the mix. SMA mixtures were used in both surface and base courses. The mixing and compacting temperature for these designs were 150°C and 145°C, respectively. For the other two projects, the samples were compacted with 37 blows mechanical (compactor has a rotating base and a beveled foot, equivalent with 50 blows manual) on each side at a temperature of 135°C.

Several slabs were removed from the Miller Avenue and Highway #7N projects for rutting tests, using the Ministry of Transportation (MTO) wheel tracking machine. The MTO rutting test is done at controlled temperature of 60°C using a rubber tired wheel rim along the test slab for 4000 cycles. The results indicated that the SMA surfacing and base courses demonstrated significantly better rutting resistance compared with the control section of asphalt concrete.

In the discussion on comparing the results between 50 and 75-blow Marshall designs for SMA, the authors stated: *“The 50 blow seems to do what we want it to do. Based on the results we are getting in the field, it is more than adequate”*.

Brown, E.R. “Evaluation of SMA used in Michigan (1991)”, NCAT Report No. 93-3, National Center for Asphalt Technology, Auburn, AL, 1993.

Brown (28) evaluated the sensitivity of SMA mixture properties to changes in proportions of various mixture components. This study was performed using the same materials and job mix formula as that used in the Michigan project, which is one of the first SMA projects conducted in the U.S. The mixture components that were varied to

evaluate sensitivity included amount of cellulose fiber, asphalt content, percent passing No.4 (4.75 mm) sieve, and percent passing No. 200 (0.075 mm) sieve.

The properties evaluated in this study included tensile strength, Marshall stability and flow, Gyrotory properties (gyrotory stability index, gyrotory elastic plastic index, and shear stress to produce 1 degree angle), resilient modulus, confined creep, and volumetric properties including voids, voids in mineral aggregate, and voids filled.

It was indicated that all the test samples in this study were compacted in the Corps of Engineers Gyrotory Testing Machine (COE GTM), which was set to produce a density equivalent to 50 blows with the Marshall hammer. Based on a calibration curve, the gyrotory machine was set at 120 psi, 1 degree angle and 120 revolutions. [*The calibration information was not given in the report*]

It was concluded that in most laboratory tests, the HMA performed better than the SMA. However, these tests had not been shown to be closely related with performance. SMA performed reasonably well in the confined creep test and generally performed better than the dense-graded HMA in the procedure for the gyrotory shear stress to produce one degree angle. The author notes that these two tests are indicators of rutting resistance and appear to be the best tests conducted for predicating performance of the SMA mixture.

Brown, E.R. “Experience with Stone matrix Asphalt in United States”, NCAT Report No. 93-4, National Center for Asphalt Technology, Auburn, AL, 1993.

Brown (29) summarized the construction information of the first five major SMA sections placed in the U.S. in 1991. These were in Georgia, Indiana, Michigan, Missouri, and Wisconsin. Some mix design and construction control data are presented.

All mix designs of these five SMA sections were performed with the 50 blows Marshall compaction. It was indicated that SMA mixtures compact quickly, so additional blows would not likely significantly increase the density but only cause excessive breakdown in the aggregate.

It was summarized that SMA mixtures have been designed to have as low as 3 percent voids in some cases and as high as 4 percent voids in others. The author commented that hotter climates should probably design closer to 4 percent voids, and cold climates should design closer to 3 percent. The author also indicated that SMA appeared to be able to tolerate lower voids better than dense-graded HMA, but a minimum 3 percent air voids was desirable to prevent the potential of rutting problems.

Brown, E.R., and H. Manglorkar. "Evaluation of Laboratory Properties of SMA Mixtures", NCAT Report 93-5, National Center for Asphalt Technology, Auburn, AL, 1993.

Brown et al (30) evaluated laboratory properties of SMA by using some tests developed for dense graded mixtures. These tests include Marshall stability and flow, gyratory properties (include gyratory shear index, gyratory elasto plastic index and shear stress to produce 1° angle), resilient modulus at various temperatures (40, 77, and 104°F or 5, 25, and 40°C), static and dynamic confined creep at 140°F (60°C), and indirect tensile strength at 77°F (25°C). One major objective of this study was to evaluate the potential of those tests to predict the performance of SMA mixtures.

Two typical aggregate types, a granite with a L.A. abrasion value of 35% and a siliceous gravel with a L.A. abrasion value of 46.5%, were used in this study. The asphalt cement was AC-20 grade. Three fibers were used, including U.S. and European cellulose

fibers, and European mineral fiber. The filler was obtained by screening a local agricultural lime.

The optimum asphalt content was selected at the design air void content of 3.5 percent by 50 blows Marshall compaction. The samples were compacted at optimum asphalt content using the Corps of Engineering Gyrotory Testing Machine set at 75 revolutions (the machine had a vertical pressure of 120 psi (0.83 MPa) and 1 degree gyration angle). This compaction level was selected because it provided similar density as 50 blows Marshall hammer compaction [*In literature 27, the equivalent compaction level using GTM was 120 revolutions*]. It is also reported that dense graded mix samples used to compare with SMA samples were compacted using 300 revolutions by the same gyrotory machine. [*This indicates the dense graded mix samples were compacted at a much higher compaction effort than SMA mixtures, which is also mentioned in literature 30, 33.*]

It was concluded that only some of the tests may have the potential to predict the performance of SMA mixtures. These tests included gyrotory shear, confined creep, and permanent deformation by means of dynamic creep. [*Similar conclusion is drawn in literature 27, by using the Michigan Project material*]

Carpenter, R.H. “Mix Design Considerations for SMA Mixes”, Presented in Transportation Research Board Annual Meeting, 1994.

Carpenter (31) believed that a performance test was necessary for SMA mixtures to determine at what extent the stone-on-stone skeleton has been developed. One can not assume that two different mixes prepared with the same gradation would develop the same degree of a stone skeleton. There were significant differences in these mixtures

even though the gradations were precisely controlled by blending individual sieve sizes. Therefore, gradation alone cannot be relied on when different aggregate types are used.

The author commented that SMA should not be significantly densified during compaction if properly designed. However, if the gradation does not allow a stable stone skeleton developed in the mixtures, the sand/asphalt matrix will experience densification during compaction and the volumetric properties will show a distinct relation with asphalt content. A real SMA mixture should not show a great effect of compaction on volumetric properties because there is essentially no densification on the matrix. Thus, the change of asphalt content will not significantly change compaction characteristics.

For example, the VMA curve should not change much with the change of asphalt content in an SMA mixture. Because there is little densification, the VMA should be relatively constant, and the void space between the aggregates in the sand sized fraction should remain unchanged as the extra asphalt cement being added would only serve to reduce air voids, and not alter compactability of the aggregate portion of the mixture. The author cites two cases in Illinois, one of them had developed a problem. In the problem mix, the VMA increased with increasing asphalt content, whereas, in the other mix the VMA was virtually stable at between 15.5 and 16% for asphalt contents between 6 and 7.5%.

To illustrate the presence of a skeleton, samples at optimum asphalt content (designed at 3 percent air voids) were compacted at various compactive efforts of 35, 50, 75, and 110 blows per side with the Marshall hammer. The change in air void content (VTM) is plotted in Figure 2.1.

Based on the test results, it was concluded that compaction at 50 blows should be selected as the minimum level for developing the SMA skeleton structure in the lab. The density increase from 50 to 75 blows may not be significant enough to recommend a higher compaction effort. One should never use compaction effort higher than 75 blows.

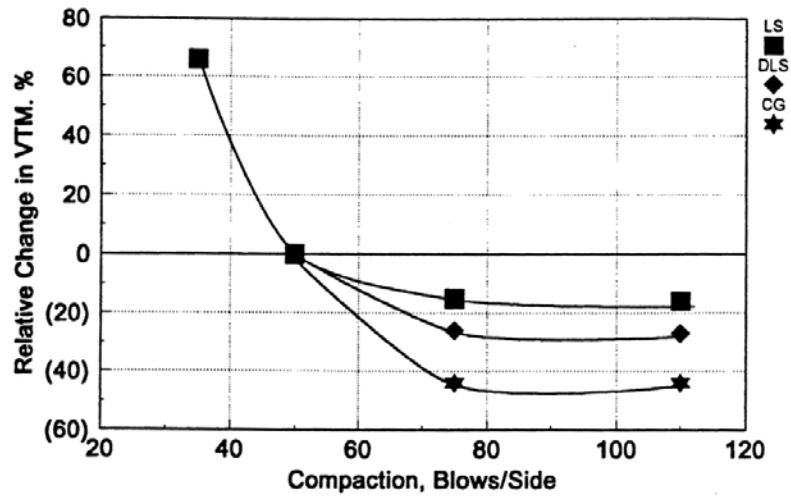


FIGURE 2.1 Effect of increase in compaction effort on limestone SMA mixture (31).

**“Guidelines for Materials, Production, and Placement of Stone Matrix Asphalt”,
National Asphalt Pavement Association, Information Series 118, 8/94, 1994.**

This publication (2) is a product of the SMA Technical Working Group (TWG) and provides general guidelines for the use of SMA paving mixtures, including composition of an SMA mixture, aggregates and additives, production, hauling and paving, and compaction.

A set of volumetric requirements of SMA mixtures was set in this guideline. Design air void content (VTM) was set at 3 to 4 percent by using 50-blow Marshall compaction. A minimum asphalt content of 6 percent and a minimum VMA content of 17 percent were also specified.

Mixing temperature was also specified in this guideline. Asphalt cement shall be mixed at a temperature as required to achieve a viscosity of 170 ± 20 centistokes. Typical plant mixing temperature for SMA is 155 to 163°C (310 to 325°F). However, at no time shall the mixing temperature exceed 177°C (350°F).

Brown, E.R., and R.B. Mallick. “Stone Matrix Asphalt- Properties Related to Mixture Design”, NCAT Report No. 94-2, National Center for Asphalt Technology, Auburn, AL, 1994.

Brown et al (32) conducted a study on SMA volumetric properties. One of objectives of this report was to develop a relationship of laboratory densities of SMA mixes prepared by a gyratory machine to those prepared by the mechanical Marshall hammer.

Two aggregates, granite and limestone, were used to do the comparison. Gyratory compaction was performed by the Corps of Engineers Gyratory Testing Machine (GTM). Mix designs were conducted by using 50 blows with the mechanical Marshall hammer, and optimum asphalt content was selected at 3.0 percent air voids. Samples were compacted with the GTM at various numbers of revolutions by using the optimum asphalt content obtained by the Marshall method of design. The number of revolutions required to produce 3.0 percent air voids was determined from plots of air voids versus number of revolutions.

The test results showed that for gravel mixes, 73 revolutions in the GTM correlated with 50 blows with a mechanical Marshall hammer in terms of air voids; for limestone approximately 103 revolutions in the GTM, set at one degree and 120 psi, produced similar air voids as produced by 50 blows with a mechanical Marshall hammer. *[The authors did not give the possible reason why these two aggregates gave two*

different numbers, some basic aggregate properties such as L.A abrasion, F&E content were not listed in the report.]

It was concluded that 90 revolutions in the GTM is a reasonable estimate of 50 blows mechanical Marshall for SMA mixes. It was also addressed that the 90 revolutions required for SMA is much less than the 300 revolutions that have been used to compact dense graded mixtures to a density equivalent to 75 blows Marshall compaction.

Dynamic creep tests were performed on a number of mixes with different percentages passing the #4 sieve. A dense-graded mix with 5.1% asphalt content was used for comparison. [*Test temperature and confining condition are not stated.*] The results showed that both gravel and limestone SMA mixtures had higher strain values and lower creep modulus values compared with the corresponding dense-graded mixes. The authors noted that these findings are contrary to observed field performance. It may be explained by the significant difference in optimum asphalt content between SMA and dense-graded mixes. The optimum gradation for the two aggregates appears to be approximately 25 percent passing the No.4 sieve; at this gradation evaluated mixtures provided the highest creep modulus and lowest strain.

Mogawer, W.S., and K.D. Stuart. “Evaluation of Stone Matrix Asphalt versus Dense-graded Mixtures”, In Transportation Research Record 1454, TRB, National Research Council, Washington, D.C., 1994.

Mogawer et al (33) conducted a study on evaluation of SMA versus dense-graded mixtures. The objectives of this study were to 1) compare SMA with dense-graded mixtures in terms of their resistance to rutting, moisture damage, low-temperature cracking, and aging; 2) determine which mechanical tests can be used to predict the rutting susceptibility of SMA.

Dense-graded mixtures and SMA mixtures with NMAS of 12.5 mm and 9.5 mm were used. The aggregate was a crushed diabase and asphalt binder was AC-20. Marshall mix design procedure was used to determine the optimum asphalt contents. The SMA mixtures were compacted using 50 blows and targeting 3 percent air voids. The dense-graded mixtures were compacted using 75 blows and targeting 4 percent air voids. The Corps of Engineers gyratory testing machine (GTM) was used to evaluate rutting resistance. The mixtures were tested at 60°C, and tested with a vertical pressure 120 psi (0.83MPa) and a 1° (0.0175-rad) gyratory angle. Samples were compacted to 300 revolutions.

Extractions were performed on the SMA mixtures before and after the GTM testing. The effect of the Marshall compaction on the SMA gradations were also examined. Both compactions fractured the aggregate and resulted in a significant increase in the percentage of aggregate passing the No.4 (4.75 mm) and No.8 (2.36 mm) sieves. At these two sieves, Marshall compaction broke slightly more aggregate than did the GTM. The results are shown in the Table 2.4.

TABLE 2.4 Aggregate Gradations of Mixtures Tested (33)

Sieve Size mm	SMA 9.5mm NMAS			SMA 12.5mm NMAS		
	Design	GTM	Marshall	Design	GTM	Marshall
19				100	100	100
12.5	100	100	100	95	95.5	94.6
9.5	95	95.1	94.5	71	74.5	76.1
4.75	46	50.8	52.9	25	33.4	34.4
2.36	25	29.6	31.0	20	24.1	24.2
1.18	20	23.4	23.4	18	20.7	20.5
0.6	16	19.0	18.8	16	18.1	17.9
0.3	13	15.6	15.4	13	15.2	14.9
0.15	12	13.7	13.6	12	13.3	13.3
0.075	10	11.4	11.2	10	10.9	11.1

Several testing devices were used to evaluate rutting potential, including LCPC pavement rutting tester, Georgia loaded wheel tester (GLWT), GTM, and unconfined repeated load tests at 40°C on samples compacted to design air voids by kneading compaction. The vertical stress was 0.45 MPa. Two confined repeated load tests were also conducted on the 12.5 mm NMAS SMA. The confining pressure used was 0.14 MPa, with 0.45 and 0.31 MPa deviator stress.

The results indicated that there was no significant difference among SMA and dense-graded mixtures when using the LCPC rut tester, the GLWT, and the GTM. SMA mixtures can pass LCPC rut tester and the GLWT, however, SMA had more permanent deformation than dense-graded mixtures by unconfined, compressive, repeated load test, and applying a confined pressure did not improve the results. [*No information on whether membrane was used for the confined test.*] The authors concluded that a test using 101.6 mm by 203.2 mm specimens might not be applicable to SMA.

Other properties evaluated in this study were moisture damage, low temperature cracking and aging cracking. The visual observation of stripping and tensile strength test results indicated that the SMA mixtures were more resistant to moisture damage than dense-graded mixes. 12.5 mm NMAS SMA showed significantly lower diametral modulus than the 12.5 mm NMAS dense-graded mixture, which indicated that SMA will be less susceptible to low temperature cracking. After aging, both 12.5 and 9.5 mm NMAS dense-graded mixtures had significant increases in dynamic modulus and tensile strength results compared with both SMA mixtures, indicating that the dense-graded mixtures might be more susceptible to cracking after aging than the SMA mixtures.

Partl, M.N., T.S. Vinison, R.G. Hicks, and K. Younger. “Performance-Related Testing of Stone Mastic Asphalt” Journal of Association of Asphalt Paving Technologists, Vol 64, 1995.

Partl et al (34) evaluated the influence of several material parameters of SMA mixtures by using several selected Strategic Highway Research Program (SHRP) tests and aging conditioning methods. The influence of long-term oven aging (LTOA), low temperature cracking, resilient modulus, rutting, and moisture sensitivity of SMA mixtures were evaluated.

The test methods used to evaluate those properties included thermal stress restrained specimen test (TSRST), the indirect tensile test (IDT), the constant height repetitive simple shear test (CHRSST), the Environmental Conditioning System (ECS), and the Laboratoire Centrale des Ponts et Chaussées (LCPC) wheel tracking device.

Two types of SMA mixtures were investigated: slabs from a road in Switzerland, and laboratory samples produced with two extreme air void contents using the same aggregate gradation as the Swiss SMA. The laboratory prepared SMA mixtures were compacted with a kneading and a steel wheeled roller compactor.

The TSRST results showed that six of the fourteen SMA specimens tested displayed a drop in stress without a clear fracture. This is possible due to the continuous change of interlock within the aggregate skeleton combined with local multiple micro-fracture resulting in a successive redistribution and reorientation of stresses. It was noted by the authors that this behavior did not occur regularly and was observed on specimens with and without LTOA.

The CHRST frequency sweep test results indicated that the shear phase angle decreases as frequency decreases. The shear phase angle also decreases at low frequencies as temperature increases. The authors concluded that SMA behaves like a viscoelastic solid and thus may show different behavior when compared with dense-graded HMA due to its different structure. The CHRST cumulative permanent deformation test results indicated that two SMA specimens with low air voids (2.6%) required more cycles (3600 and more than 5000 compared to 600 and 800 cycles) than those with high air voids (7.7%) to reach a strain limit of 5.5 percent.

The LCPC tested specimens were found to deform laterally, and had visible shear flow zones under the wheel track. It indicates that an aggregate skeleton without sufficient lateral confinement and interlocking becomes unstable and tends to shove.

The ECS test results showed that SMA specimens with lower air voids were found to be practically impermeable. However, water was found in the center of all the specimens after testing and splitting. The specimens with 4.8 percent air voids showed no stripping, whereas those with high air void contents showed some stripping.

It is concluded that because of the coarse aggregate skeleton of SMA mixtures, conventional laboratory test procedures will need modifications in order to properly evaluate SMA mixtures. Appropriate confinement and the use of realistic specimen dimensions are needed.

West, R.C. and B.E. Ruth. "Compaction and Shear Strength Testing of Stone Matrix Asphalt Mixtures in the Gyrotory Testing Machine", Journal of Association of Asphalt Paving Technologists, Vol: 64, 1995.

West et al (35) presented an effort to identify a more appropriate design procedure compared to the Marshall procedure for SMA mixture. The authors first stated that there are some existing problems in SMA mix design by 50 blows Marshall hammer, which include 1) the lack of correlation between the Marshall compaction and field compaction, resulting in adjustments of the binder content during the field production of SMA, and 2) the lack of basis for evaluating SMA performance in the Marshall procedure.

This paper investigated the results from a laboratory compaction and characterization study of SMA mixtures. Eleven SMA mixtures were compacted in the laboratory with a Corps of Engineering gyratory testing machine (GTM) with an air roller to simulate initial construction and traffic densification. It is believed that with the air roller the strain applied to a mix is an indication of stability of the mix. When applied to a stable mix the strain would decrease with an increase in shear strength of the mix, whereas the strain would increase with loss in shear strength in the case of a low strength mix.

One objective of this study was to determine a standard compactive effort which could be used to prepare future SMA mixtures for design and evaluation. An analysis of variance was performed on the available data to determine the number of gyrations which produced sample air void contents closest to the initial field air voids for each mixture. Based upon this study, to produce samples having similar initial in-place air void contents, the following compactive effort using the Model 6B/4C GTM appears to provide the best results for SMA mixtures: 9 psi initial air roller pressure, 100 psi ram pressure, 3 degree initial angle of gyration and 12 gyrations. It is noted that the compaction effort for SMA mixtures is less (i.e. fewer gyrations) than typically used for dense-grade mixtures, and

this finding reflects the practice of using 50-blow Marshall rather than 75 blows to design SMA mixtures.

Using the above settings, three compacted samples from each SMA mixture were further tested at 60°C to 300 gyrations with height and air roller pressure recorded at periodic intervals of gyrations. Two parameters, percent densification and gyratory shear strength, were determined from recorded information as a measure of mixture quality. To evaluate the rutting susceptibility of mixes, the percent densification and the gyratory shear strength at 200 gyrations were determined. Percent densification is defined as the change in air voids of the sample at any point during densification from initial in-place density. The general criteria used for dense-graded mixtures have been: ≤ 2.5 percent is good, ≤ 3.5 percent is acceptable, ≥ 4.0 percent is undesirable [*The reference for this criteria was not given*]. The critical value of gyratory shear strength at 200 gyrations has been established at 372 kPa (54 psi), which was correlated with a Hveem Stability value of 37.2 and has been subsequently shown to distinguish poor rutting performance from good performance for a variety of dense-graded mixtures.

Three of the eleven mixtures showed declining gyratory shear strength and were below the critical value of 372 kPa at 200 gyrations. At 200 gyrations, most mixtures had densified to between 2 and 3 percent air voids. Four of the mixtures had air void contents more than 4.0 percent, however, the shear strength of these mixtures remained very stable and did not indicate potential for a loss of shear resistance. It was noted as indicated that the SMA mixtures are less sensitive to low air void contents.

It was concluded that compaction of SMA for volumetric design and or further strength testing can be accomplished with the Corps of Engineers GTM with an air roller,

and the GTM is sensitive to the shear strength characteristics of SMA mixtures. The authors expected that if the shear strength proves to be a good indicator of rutting resistance, it may be used in the future to optimize mix design for SMA mixtures. It is also recommended that an N-design experiment specifically for SMA mixtures is necessary to determine appropriate compactive effort.

Brown, E.R, and J.E. Haddock, T.A. Lynn and R.B. Mallick. “Designing SMA Mixtures Volume II- Research Results”, NCHRP 9-8/2 Draft Final Report, September 1996.

Brown et al (36) conducted the NCHRP 9-8 project on mix design of SMA mixtures, which was completed in two distinct parts. Part 1 began in April 1994 and had its main goal as the development of a tentative SMA mixture design method. Part 2 began in early 1995, and its main goals were to evaluate and finalize the proposed design procedure, analyze the SMA mixtures produced using the method, and produce a final report detailing the research project. The final report was published in 1999 as a NCHRP report (42). The Volume II presents the detailed laboratory research results of Part 2. Some interesting topics are included and summarized below.

Compaction Effort

One objective of this study was to adapt the Superpave volumetric mixture design procedure for use with SMA. A total of 8 aggregates were used in this study to provide a wide variety of particle shapes, surface textures, absorption and L.A abrasion values. There were two limestone aggregates, two granite aggregates, one traprock, one dolomite, one blast furnace slag, and one gravel aggregate.

Two sets of SMA mixtures were designed for each of the 8 aggregate sources. One set was designed using 50 blows Marshall compaction, and the other set was designed using 100 gyrations of SGC. The Marshall hammer in this study was a flat-faced, static base, mechanical Marshall hammer. The SGC used in this study was Troxler SGC, model 4140.

A comparison of the optimum asphalt contents for SMA mixtures compacted with 50-blow Marshall and 100 gyrations of the SGC is shown in the Figure 2.2. *[It should be noted that there is a slight difference in aggregate gradation for the SMA mixtures designed with the two compaction efforts.]*

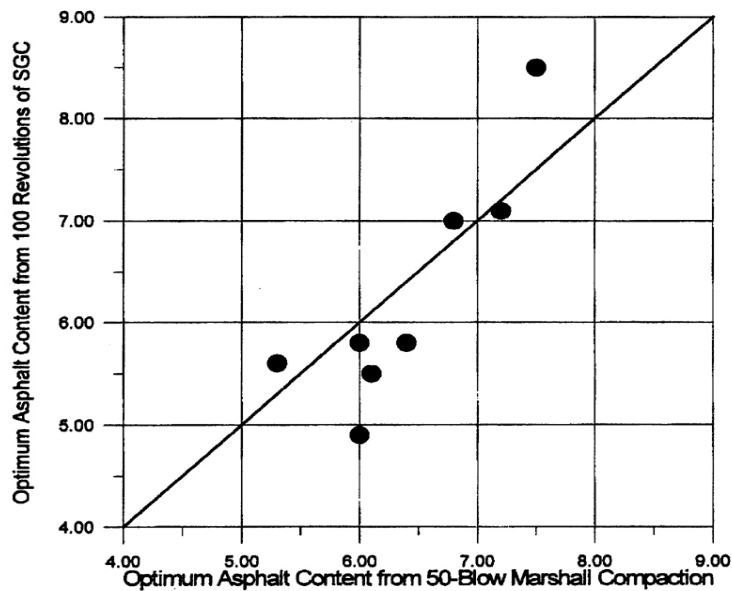


FIGURE 2.2 Optimum asphalt content from two compaction efforts (36).

The results show that the SGC on the average gave a lower optimum asphalt content than the Marshall hammer. It also appears that the SGC at 100 gyrations gave higher optimum asphalt contents than 50 blows Marshall when the asphalt content was high but lower optimum asphalt content when the asphalt content was low. Only one

mixture had less than 6 percent optimum asphalt content when compacted with 50 blows of the Marshall hammer while five mixtures had less than 6 percent optimum asphalt content when compacted with 100 gyrations of the SGC. This indicates that the SGC is forcing the aggregate closer together than the Marshall hammer, or it may be causing more aggregate breakdown. *[The comparison of aggregate breakdown results by two compaction efforts didn't support the higher aggregate breakdown concept.]*

The effect of compaction level was determined by compacting SMA mixtures for 4 of the aggregates with three levels of blows of the Marshall, and three gyration levels of the SGC. The comparison on SMA mixture design volumetric information of 35, 50 and 75 blows with the Marshall hammer is summarized in Table 2.5. *[This Table is combined from Tables 4.28, 4.29, 4.30]* The comparison of 75, 100, and 125 gyrations of the SGC is summarized in Table 2.6. *[This table is combined from Tables 4.33, 4.34, and 4.35].*

TABLE 2.5 Volumetric Properties of SMA Mixtures Compacted by the Marshall Hammer (36)

Agg.	Limestone (1)			Granite (1)			Traprock			Granite (2)		
Blows	35	50	75	35	50	75	35	50	75	35	50	75
Opt. AC, %	7.1	6.4	5.8	6.8	6.1	5.6	5.5	5.3	4.7	6.5	6.0	5.2
VTM, %	3.8	3.8	3.8	3.7	3.8	3.8	3.6	3.6	3.8	3.7	3.6	3.7
VMA, %	19.4	17.9	16.5	18.7	17.3	16.2	17.6	17.3	17.8	16.2	15.2	13.5
VFA, %	80	78.8	77.0	80.1	78.0	76.5	79.5	79.2	78.6	77.5	76.3	72.5
VCA, %	31.9	32.2	31.3	35.2	34.2	33.3	38.6	35.4	37.8	32.0	31.1	30.5

TABLE 2.6 Volumetric Properties of SMA Mixtures Compacted by the SGC (36)

Agg.	Limestone (1)			Granite (1)			Traprock			Granite (2)		
Gyrations	75	100	125	75	100	125	75	100	125	75	100	125
Opt. AC, %	6.2	5.8	5.5	6.2	5.5	5.3	5.7	5.6	5.1	5.3	4.9	4.8
VTM, %	3.7	3.7	3.7	3.6	3.6	3.8	3.8	3.8	3.8	3.7	3.8	3.7
VMA, %	17.6	16.8	16.2	17.3	15.7	15.5	17.8	17.3	16.4	13.3	12.6	12.2
VFA, %	79.0	78.3	76.9	79.5	77.4	75.5	78.2	78.2	76.9	72.0	70.9	69.2
VCA, %	37.0	36.2	35.3	33.3	32.1	32.2	38.2	36.5	34.3	26.9	29.7	26.1

The differences in the optimum asphalt contents between 35 and 50 blows averages about 0.5 percent, and between 50 and 75 blows averages about 0.6 percent. The differences between the various SGC compactive efforts are less than that for the Marshall hammer. The average difference between 75 and 100 gyrations is 0.4 percent and the average difference between 100 and 125 gyrations is 0.3 percent. The difference was thought to be due to aggregate breakdown, but the breakdown results indicated that the higher compactive effort did result in the aggregate being forced closer together and not so much the result of aggregate breakdown.

It was concluded that 50 blows Marshall compactive effort appears reasonable. The compactive effort with the SGC should be 100 gyrations [*in report page 82*].

Breakdown

This subtask was developed in an attempt to determine how aggregate breakdown affects SMA characteristics and to correlate the amount of aggregate breakdown experienced during laboratory and field compaction. The amount of aggregate breakdown experienced during the mixture design phase was determined for both 50 blows Marshall compaction and 100 gyrations of SGC for each of the 8 aggregates. For 4 of these aggregates, the compaction level was varied to determine how compaction effort affects the aggregate breakdown for both compaction devices. Two additional compaction levels for the Marshall compaction were 35 and 75 blows, the additional SGC compaction levels were 75 and 125 gyrations. The amount of aggregate breakdown produced in dense-graded mixtures using 3 of the aggregates was also determined, and the compaction efforts used were 75 blows Marshall hammer and 128 gyrations of the SGC. A total of 4 field projects were investigated to determine the aggregate breakdown.

Breakdown in the laboratory tends to be 5 to 10 percent on the 4.75 mm sieve for harder aggregates and more for softer aggregates. The Marshall hammer (50 blows) tends to breakdown the aggregate more than the gyratory compactor (at 100 gyrations). Both laboratory compactors provided breakdown approximately equal to in-place compaction.

Mixture designs compacted with 75, 100, and 125 gyrations of the SGC, and 35, 50, and 75 blows of the Marshall hammer were completed for the limestone, traprock, and two granite aggregates. The results indicate little difference in the amount of breakdown produced by the three compaction levels, but the type of compactor has an effect for some aggregates.

Since the aggregate type was found to be significant to the amount of aggregate breakdown, an attempt was made to correlate one or more aggregate properties to the amount of aggregate breakdown. The L.A. abrasion value was shown to have a good correlation with the aggregate breakdown. And it appears that an L.A. abrasion requirement of 30 which is often used is reasonable to separate these aggregate with extreme breakdown and reasonable breakdown.

For the construction projects evaluated in this study, there was no significant difference in aggregate breakdown for static and vibratory rollers. The L.A. Abrasion appeared to have little effect on the in-place breakdown of aggregate. [*Final report Volume III, page 62*]

Permeability

The objective of this subtask was to determine if SMA mixtures are more or less permeable to water than are conventional dense-graded HMA mixtures. A falling head permeometer was used to determine how permeability varies as a function of air voids.

The permeability of the SMA mixture was found to be very sensitive to the air void content and may change by a factor of 10 with very little change in air void content. The results also showed that the percent of absorbed water and the permeability start to increase rapidly at approximately 6 to 6.5 percent air voids.

Based on the test results, it was concluded that SMA mixes are more permeable than Superpave mixes with similar void contents and similar nominal maximum size aggregates. Therefore, SMA must be compacted to a lower in-place void content of approximately 6 percent or less.

Performance Tests

The performance tests were used to modify design criteria if necessary, and to further refine the design method. Two tests were conducted in this study, including Wheel Tracking (WT), and Indirect Tensile Creep (ITC).

The wheel tracking test was used to estimate the rutting potential of SMA mixtures. The test equipment used in this study was manufactured by Couch Construction, and was very similar to the Hamburg equipment. The loads were applied under water. Four aggregates (limestone, slag, traprock, and granite) and 4 mortars were evaluated in the wheel tracking device. Each mixture was tracked at 55°C with up to 20,000 passes unless failure occurred earlier. The ITC test was conducted at -10°C to evaluate the low temperature properties of the mixture. The tensile strength and strain at failure for the 4 aggregates and 4 mortars were determined.

The comparison between four aggregate types indicated that limestone aggregate had a significantly higher average rutting rate of 5.02 mm/hr compared to the other three aggregates. The rutting rates for slag, traprock, and granite were 0.31, 0.22, and 0.21

mm/hr, respectively. The reason for this is not clear. The poor performance of the limestone compared with other three aggregates was also identified by the low Marshall stability (5010 N versus 6100-9700 N) and low tensile strength (526 kPa versus 668-1050 kPa).

The comparison between wheel tracking results at 55°C and mortar dynamic shear rheometer (DSR) results at 58°C indicated a reasonable correlation between DSR and rutting rate based on the limited data. No indication of a good correlation between ITC test results of mixtures and the bending beam rheometer (BBR) test results of mortar was shown in this study.

Based on this study, it was suggested that the wheel tracking test should probably be a part of mix design of SMA mixture to predict rutting performance. The indirect tensile test should also be included in SMA mixture design to evaluate the potential for low temperature cracking if its correlation with performance is further verified.

Brown, E.R., R.B. Mallick, J.E. Haddock, and J. Bukowski. Performance of Stone Matrix Asphalt (SMA) Mixtures in the United States. In Journal of the Association of Asphalt Paving Technologists, Volume 66, 1997.

Brown et al (37) evaluated a total of 86 SMA projects built from 1991 to 1996 in USA. Data on SMA material and mixture properties, and performance were collected and summarized.

At the time this paper was presented, some SMA mixtures were beginning to be designed using the Superpave gyratory compactor. However, all the SMA pavement sections evaluated in this study were designed with 50-blow Marshall compaction.

It was summarized that early SMA mixtures (1991-1993) were typically designed to have 3.5 percent air voids or less, and later on from year 1994, the design air voids became close to 4 percent to reduce the possibility of fat spots and permanent deformation. Authors also indicated that the design air voids were generally lower for the northern states compared to the southern states.

More than 90 percent of the SMA projects had VMA ranging from 15 to 20 percent based on the collected information, and 53 percent of the projects met the requirement of minimum 17 percent VMA. In the mean time, about 50 percent of the projects satisfied the 6.0 percent minimum recommended asphalt content. It was indicated that a minimum asphalt content requirement is not necessary if the minimum VMA is required.

Over 90 percent of the projects had rutting measurements of less than 4 mm, and about 25 percent of the projects had no measurable rutting. SMA presented excellent rutting resistance considering most of the projects were located in high traffic areas.

Thermal and reflective cracking have not been a significant problem for SMA. SMA mixtures appear to be more resistant to cracking than dense mixtures, which is likely due to the relatively high asphalt content resulting in high film thickness.

Asphalt flushing (fat spots) appeared to be the biggest performance problem. The possible reasons for this include segregation, draindown, high asphalt content, or improper type or amount of stabilizer.

Based on the findings in this study, it was concluded that SMA mixtures should continue to provide good performance in high volume traffic roads. The extra cost for SMA construction should be more than offset by the increased performance.

Louw, L., C.J. Semmelink, and B. Verhaeghe. “Development of a Stone Mastic Asphalt Design Method for South African Conditions”, Eighth International Conference on Asphalt Pavements, Vol. I., Seattle, Washington, August 1997.

Louw et al (38) presented a research study performed to develop a volumetric approach for designing SMA mixture. Two compaction methods, the gyratory compaction and the Marshall compaction, were compared in this study. The Marshall compaction used 50 blows on each face with standard Marshall hammer and 100 mm molds. The gyratory compactor used was a Troxler Gyratory Compactor (with gyration angle of 1.25°, compaction pressure of 0.6 MPa, and speed of gyration of 30 rpm), with cylindrical molds having diameters of 100 mm, and 200 gyrations were used.

Seven mixtures were designed according to the recipe approach with the same asphalt content of 6.5 percent. These mixtures were compacted by the two compaction devices. The really low Marshall stabilités at 60°C indicated these mixtures were unstable even though the volumetric properties (VMA values of seven mixtures were between 17.7 and 20.1 percent, air voids were between 2.9 to 5.7 percent) indicated that these mixtures were suitable. [*European experience(1) indicates the Marshall stability should not be used to evaluate the performance of SMA mixtures, the research in the U.S. (28, 30) also indicates that Marshall stability of SMA mixture is normally lower than dense-graded mixture*]

It is stated in this report that the gyratory compaction information gives the indication of compactibility, workability and rutting resistance of SMA mixtures. A compactibility index number (C) is determined by carrying out a regression analysis on the gyratory results. A linear regression analysis is performed on the compaction (%Gmm)

versus the natural log of the number of gyrations between 20 and 200. An equation is given as following:

$$C = C_i + k \times \ln (N) \quad (2.1)$$

Where:

- C = compactibility index
- C_i = intercept on the y-axis
- K = slope of the regression analysis
- N = number of gyrations

The authors believe that a high value of C_i indicates a good workability of evaluated mixture, and a high value of k indicates a high tendency of permanent deformation during the design life of the mixture. However, a high C_i value combined with a low k-value could also indicate that the mix is susceptible to deformation, especially if the asphalt content is very high and overfilling the air voids.

Based on test results, it was recommended that the gyratory compaction rather than Marshall compaction be used to design SMA. The gyratory compactor can give an indication of the rut resistance of the mixtures and volumetric properties during the design life of the SMA mixtures.

Brown, E.R., J.E. Haddock, R.B. Mallick, and T.A. Lynn. “Development of a Mixture Design Procedure for Stone Matrix Asphalt (SMA)”, Journal of Association of Asphalt Paving Technologists, Vol 66, 1997.

Brown et al (39) presented a mixture design procedure for SMA mixtures developed by the National Center for Asphalt Technology. Most of the content of this paper has also been reported in the Final report of NCHRP project 9-8 (36).

Some selected conclusions from this study are:

1. There is a good correlation between the Los Angeles abrasion loss and aggregate breakdown (Marshall compaction $R^2=0.62$, SGC $R^2=0.84$),
2. The 3:1 or 2:1 flat and elongated particles appear to provide much better classification for the various aggregates than a 5:1 ratio,
3. There is an excellent correlation between the flat and elongated particle ratio and aggregate breakdown (Marshall compaction $R^2=0.89$),
4. It was observed that a VMA significantly lower than specified VMA can be obtained due to aggregate breakdown. Therefore, the mix designer must consider aggregate type, compactor type and compaction effort along with the gradation in meeting the required VMA criteria.
5. It was found that 50 blows of Marshall hammer produced about the same density as 100 revolutions of the SGC. The SGC was found to produce less aggregate breakdown than the Marshall hammer.

Brown, E.R., and J.E. Haddock. "Method to Ensure Stone-on-Stone Contact in Stone Matrix Asphalt Paving Mixtures", In Transportation Research Record 1583, TRB, National Research Council, Washington, D.C., 1997.

Brown et al (40) presented a method for determining when stone-on-stone contact exists. The proposed method first determines the voids in the coarse aggregate (VCA) for the coarse aggregate-only fraction of the SMA mixture. Second, the VCA is determined for the entire SMA mixture. When the two VCA values are compared, the VCA of the SMA mixture should be less than or equal to the VCA of the coarse aggregate-only fraction to ensure that stone-on-stone contact exists in the mixture.

Five different methods for determining the VCA of the coarse aggregate-only fraction were used to see which performed best and was the most practical. The five methods were Marshall hammer, SGC, dry-rodded test, vibrating table, and vibrating hammer. When using Marshall hammer, SGC, and vibrating hammer, 2 percent AC-20 asphalt by total specimen mass was added to aid in the compaction process. While in the dry-rodded method, and the vibrating hammer test, no asphalt cement was added.

In general, the Marshall hammer and SGC produced the lowest VCA values, while the vibrating hammer gave the highest. The dry-rodded and vibrating table methods produced VCA values that were approximately equal and between the high and low extremes. It was also indicated that for a given compaction method and aggregate gradation combination, the coarse aggregate-only fraction produced approximately the same VCA regardless of aggregate type. [*Data shown in the paper still have as high as 8.7 and 8.9 percent difference between FL limestone and Traprock when compacted by Marshall hammer and SGC, respectively.*]

It was concluded that the reason for the lower VCA with the Marshall hammer than with the SGC was aggregate breakdown. It was also indicated that the method ultimately selected to measure coarse aggregate stone-on-stone contact should result in breakdown similar to that occurring during construction.

Samples of SMA mixtures compacted in the laboratory with the Marshall hammer were extracted to evaluate the amount of breakdown in the total SMA mixtures. [*The extraction data from SGC compacted SMA mixtures can not be found in the paper, no indication that the tests had been conducted*]. Test results showed that the breakdown of SMA mixtures compacted by Marshall were similar to the coarse aggregate-only SMA

compacted by SGC, lower than the coarse aggregate-only SMA compacted by Marshall, and much higher than the coarse aggregate-only SMA compacted by the other three compactors.

It was concluded that the SGC and dry-rodded methods produced the best results, and further study is needed to compare the aggregate breakdown they produce with aggregate breakdown during the SMA mixture design. Also, aggregate breakdown that occurs during construction should be quantified to determine whether it is similar to that produced by laboratory compaction.

**Kuennen, T. “Gap-Graded Maryland Mixes Meld SMA, Superpave Designs”,
HMAT, Vol. 4, No.2, 1999.**

Kuennen (41) stated that Maryland was defining the area where the Superpave mix design system and high performance Stone Matrix Asphalt designs complement each other. Maryland used the term “Gap-graded” Superpave to describe SMA mixes designed with Superpave Performance-graded (PG) asphalts, fiber filler, and Superpave testing equipment, including the gyratory compactor.

**Brown, E.R. and L.A. Cooley, Jr. NCHRP Report 425. “Designing SMA Mixtures
for Rut-Resistant Pavements”. Transportation Research Board, Washington, D.C.,
1999.**

Brown et al (42) reported the findings for NCHRP Project 9-8, “Designing Stone Matrix Asphalt Mixtures”. This report includes Volumes III and IV of the original five-volume final report. So this report has two parts, the first part contains a summary of research results in the areas of SMA mixture design and performance evaluation, the second part

presents a mix design method and construction guidelines for SMA in AASHTO standard format.

Two distinct phases of research were conducted to achieve the overall objective of developing a mixture design procedure for SMA. Phase I included evaluating critical material and mixture properties of SMA and choosing laboratory tests to evaluate the selected material and mixture properties. Phase II included the field validation of the proposed mixture design procedure and give the construction guidelines for SMA.

In phase I, the volumetric properties for SMA were compared between 50 blows of Marshall hammer and 100 gyrations of the SGC. It was concluded that a good correlation existed between the two compactive efforts, and 100 gyrations of the SGC would provide about the same density as 50 blows with the Marshall hammer. [*The results are shown in Figure 2.2 in literature 35*] The data indicated that the Marshall hammer tended to give higher optimum asphalt contents at lower asphalt contents, while at higher asphalt contents, the SGC gave higher optimum asphalt contents. [*The report didn't give any explanations for this trend*]

In phase II, field projects were used to verify that 100 gyrations with SGC was equal to 50 blows of the Marshall hammer. Since the 50 blows Marshall hammer compaction was widely used and proved to have good performance, the compaction effort with SGC was set to provide a density approximately equal to that of 50 blows with the Marshall hammer. The results showed a lot of scatter on the gyrations with SGC to produce the same density as 50-blow Marshall compaction. The range was from less than 60 gyrations to more than 100 gyrations, and averaged about 80 gyrations.

The further analysis on the variation of gyrations indicated that aggregate L.A. abrasion loss may be a possible source. The analysis showed that with L.A. abrasion loss 20 to 40 percent, ranges from 68 to 82 gyrations with SGC were needed to produce a similar density as 50 blows of the Marshall hammer (results are shown in Figure 2.3).

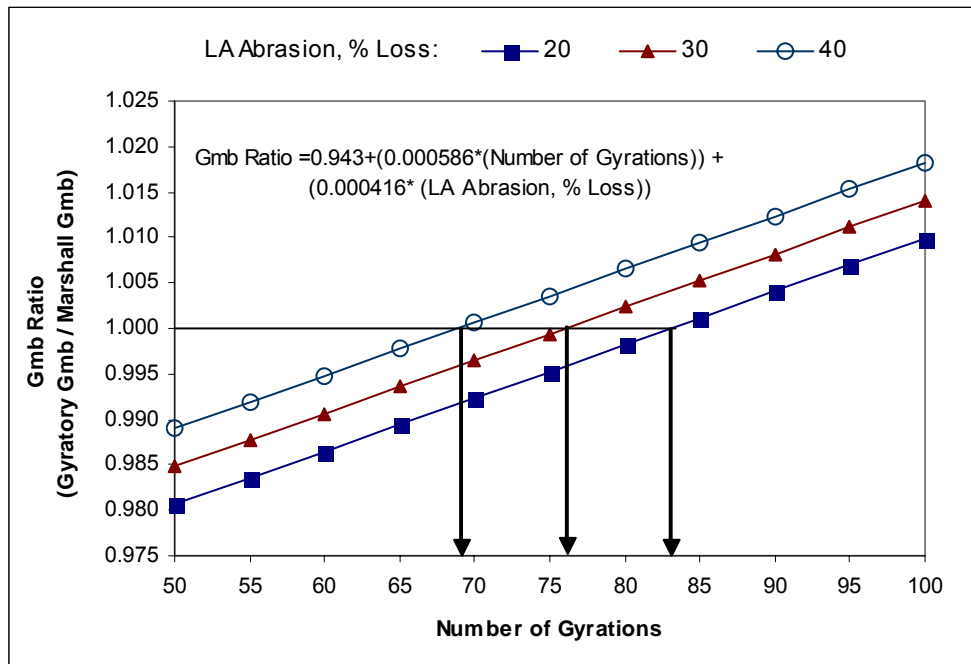


FIGURE 2.3 Gmb ratio as a function of gyratory level and L.A. abrasion loss (42).

Therefore, it was recommended that 70 gyrations should be used with L.A. abrasion loss of 30 or more, while 100 gyrations should be used when harder aggregate with L.A. abrasion less than 30 was used. It was also indicated that these two gyration levels will result in a difference in optimum asphalt content of about 0.4 percent.

NAPA, “Designing and Constructing Stone Matrix Asphalt (SMA) Mixtures - State-of-the-Practice”, 1999 (Updated edition is published in 2002).

This NAPA publication (43) is usually referred to as the SMA guidelines, which is an update version from 1994 SMA guidelines (2). The updated research results from

NCHRP project 9-8 are reflected in these guidelines. Some concerns about the SMA mixture design, especially compaction method and design air void content are listed below.

The compaction temperature is determined in accordance with AASHTO T245 (25), section 3.3.2, or that recommended by the producer when polymer-modified binders are used. Laboratory samples of SMA should be compacted using either 100 gyrations of the Superpave Gyrotory Compactor (SGC) with 150 mm diameter specimens or 50-blows of the flat-faced, static base, mechanical Marshall hammer with 100 mm diameter specimens. Higher compactive efforts than these can cause excessive aggregate breakdown and should not be used.

The optimum asphalt content is chosen to produce 4 percent air voids in the mixture. The NCAT performance evaluation of SMA pavement suggests that choosing the asphalt content to produce an air void content near 4 percent will provide protection against fat spots after laydown and provide better rut resistance, particular in warm climates. Cold climates may use an air void content near 3.5 percent.

It is indicated in these guidelines that with the increased emphasis on the use of Superpave mixtures and the SGC, more SMA mixtures are being designed with the SGC. When using the SGC, 100 gyrations is typically used for aggregates with L.A. Abrasion value less than 30, and 75 gyrations may be used for L.A. Abrasion value between 30 and 45. A compactive effort of 78 gyrations of the SGC was comparable to the 50-blow Marshall compaction based on NCHRP project 9-8, and this number can be rounded off to 75 gyrations to correspond to N_{design} gyrations used in AASHTO PP28 (44).

[No performance evaluation test is included in this publication. However, it is indicated that triaxial test and wheel tracking test have potential to evaluate the rut resistance of SMA mixtures, and further research is need to develop the necessary test criteria.]

Kuennen, T. “Stone Matrix Asphalt is Catching on in the U.S.”, in Better Roads, Sep. 2003.

Kuennen (45) gave a general idea in this newsletter how SMA compared to Superpave designed dense mixtures, and how these two asphalt mixtures integrated together.

Maryland is one of the first few states that integrated Superpave design technology into SMA mixes, also called gap-graded Superpave, which is in fact SMA designed using Superpave, including gyratory compaction, PG-binders, etc.

In 1998 the Superpave lead states recommended the following modifications:

- SMA should use asphalt binders at least one grade higher at high temperature grade than selected in accordance with AASHTO MP-2 (44).
- A fiber modifier should be used to facilitate placement regardless of the binder grade selected.
- Design air voids should be 4 percent. There are no recommended N_{initial} or N_{maximum} values.
- Use 150-mm diameter Superpave specimens in SMA mixture design.

It was concluded that SMA and the Superpave mix design procedures actually complement each other. In some respects, Superpave mix design methods are making SMA even more durable.

Aschenbrener, T. “Results of Survey on Stone Matrix Asphalt”, Colorado Department of Transportation, April 2004.

A comprehensive survey on mix design and construction practices of SMA mixtures was conducted by the Colorado Department of Transportation (46). The survey mainly included 4 questions, which concerned paving requirements, use of fiber, use of mineral filler, and compaction effort for SMA mixture design.

A total of 43 responses from different states were received and summarized. Sixteen states had no or little experience with SMA and provided no answers to questions. Eleven states had limited experience and answered the questions. Sixteen states had significant experience and answered the questions.

For the question on compaction efforts used for SMA mixture design, 2 states use 50 gyrations, 4 states use 75 gyrations , 16 states use 100 gyrations, 2 states use various gyrations based on traffic level, and 4 states continue using 50 blow Marshall compaction.

2.2.2 Summary of Literature

SMA was first developed in Germany in 1960’s (1) to decrease the excessive wear and damage caused by studded tire use. SMA continues to evolve in Europe, and has been introduced into several European countries as well as other countries outside of Europe. Due to its exceptional rut resistance and good durability, the use of SMA has become widespread throughout the world.

The early SMA mixture design in Europe was essentially a recipe-type method, which dictated mixture ingredients and proportions that seemed to work well. As the use of SMA became more widespread in Europe, various specifications evolved to suit the regional materials. These specifications and empirical methods were not directly

applicable to all situations; therefore, similar satisfactory results could not be expected when different materials were used. Despite these facts, few SMA failures are reported in the literature.

SMA was first introduced into the United States in 1990 as a result of the European Asphalt Study Tour (1). The first SMA trial in the United States was built in Wisconsin in June 1991, and many subsequent projects were built in North America thereafter (26-27, 29). However, there was no standard mix design procedure available in the early 1990's. Consequently, most specifications and design procedures used for early U.S. trials were a reflection of those of the Europeans.

In 1994, guidelines (2) for materials, production and placement of SMA were developed by the SMA Technical Working Group (TWG) and then published by the National Asphalt Pavement Association (NAPA). These guidelines summarized the experience from Europe and the United States, and set volumetric requirements for SMA mixture, including a design air void content at 3 to 4 percent by using 50-blow Marshall compaction, a minimum asphalt content of 6 percent and a minimum VMA content of 17 percent.

In the middle 1990's, several studies (31-32, 40) addressed mixture volumetric properties and establishment of the stone-on-stone contact that provides SMA with excellent rutting resistance. The importance of stone-on-stone contact was validated by using laboratory shear strength measurements made with the GTM (35). The measurement of stone-on-stone contact in the SMA mixture design procedure has made a definite improvement in the mix design procedure.

The current mix design method for SMA mixtures was developed in the NCHRP project 9-8 (36), and was summarized in the final report (42). One objective of this study was to adapt the Superpave volumetric mixture design procedure for use with SMA. The results of this project suggested that the equivalent compaction effort as the 50-blow Marshall hammer depended on the L.A. abrasion value of aggregates used, and averaged about 80 gyrations. Therefore, it was recommended that 70 gyrations should be used when the L.A. abrasion loss was 30 or more, while 100 gyrations should be used when the L.A. abrasion was less than 30. The establishment of stone-on-stone contact is required in this mix design method by comparing VCA_{mix} and VCA_{drc} (40, 42).

Although SMA mixtures have excellent performance in the field, there is no generally accepted performance test to evaluate it in the laboratory. Several studies (28, 29, 31-33, 35) evaluated various performance tests that could best evaluate SMA mixtures. Several evaluation tests for dense-graded mixture were proven not appropriate for evaluating performance of SMA mixtures, including Marshall stability and flow, resilient modulus, and indirect tensile strength etc. It is generally believed (30, 32-33, 36) that loaded wheel tracking tests and/or the confined repeated load permanent deformation test have the best potential to evaluate rutting resistance of SMA mixtures.

2.3 FINDINGS ON COMPACTION EFFORT FOR DESIGNING SMA MIXTURES

SMA mixtures have been commonly designed with the 50-blow Marshall compaction, and this compaction effort has proven to be adequate for several projects in Europe and North America (1, 27, 29, 36). Several studies (30, 32, 35) have also indicated that the compaction effort for SMA mixture was less than typically used for dense-graded

mixture, and this finding reflects the practice of using 50-blow Marshall rather than 75 blows to design SMA mixtures.

However, with increased emphasis on the use of Superpave mixtures and the SGC, SMA has been incorporated into the Superpave mix design system, and more SMA mixtures are being designed with the SGC. Studies (38, 45) have shown more interest in using SGC instead of the Marshall compaction procedure. At the time this report was prepared, only four States in the United States continued to use the Marshall procedure to do SMA mix design (46). One of the most important reasons for using the SGC instead of the Marshall hammer is because the SGC better simulates the degradation and aggregate orientation found in field compaction (5-7).

A comparative study on SGC compaction and Marshall compaction was performed during NCHRP 9-8 (36) and indicated that about 78 gyrations with SGC produced a similar density as 50 blows of Marshall compaction. However, 100 gyrations was adopted in the final report (42). Current SMA design guidelines (43) list two compaction options to design SMA: 50 blow Marshall or 100 Gyrations by SGC. The design guidelines also note that 75 gyrations should be used if the aggregate has a L.A abrasion value higher than 30 percent loss. Therefore, one of three compaction efforts is typically used in the SMA mix design procedure.

Some states such as Georgia have found that 100 gyrations with the SGC is excessive for their materials and results in mixtures with lower than desired optimum asphalt contents. Georgia has many aggregate sources with L.A abrasion value above 30. The high level of density obtained in the laboratory is also difficult to obtain in the field in some cases without excessive fracturing of aggregate particles. Experience from

Georgia indicates that for their materials the optimum SGC compactive effort should be between 50 and 75 gyrations. The recent survey on SMA (46) showed that some states had already used either 50 or 75 gyrations to design SMA mixtures. Georgia, for example, requires 50 gyrations in their SMA mixture design specification.

Based on the literature review, the preference of using a compaction level lower than the standard 100 gyrations has little research support. The major reason for choosing a lower compaction level is to produce a more durable mixture by designing a mixture with higher optimum asphalt content. Using a decreased compaction level may result in the SMA mixture becoming unstable and having rutting problems if the compaction level is too low. No study is available that evaluates performance of SMA mixture designed with lower compaction levels. Therefore, a study is needed to characterize the performance of SMA mixtures designed with lower compaction levels using a wide range of aggregates and different NMAAS.

In this study, several compaction levels will be evaluated by volumetric properties, aggregate degradation, and rutting resistance. Recommendations will be made about adopting a lower compaction level based on the overall performance of the mixtures designed in this study.

2.4 OTHER RELEVANT TESTS RELATED TO TOPICS

This section includes several other relevant tests that will be performed in this study. The background information of these individual tests is provided for each test.

2.4.1 Vacuum Seal Method (CoreLok)

The air voids is determined by comparing the bulk specific gravity and the theoretical maximum specific gravity of hot mix asphalt (HMA). The standard method currently

used to measure the SMA bulk specific gravity is AASHTO T166 (25), commonly known as the saturated surface dry (SSD) method. Another alternative method recently used is the CoreLok method following ASTM D6752 (47). Both methods have advantages to some other alternative methods such as the parafilm method, and cut and measure method (48).

The study conducted by Cooley et al (49) showed there was not a significant difference between the variability of the CoreLok method and SSD method in six of nine cases, while in another three cases the SSD method was less variable. However, Hall et al (50) indicated that the CoreLok method had smaller multi-operator variability compared to the SSD method in 82 percent of 144 samples with a wide range of air voids.

Research by Buchanan (51) has indicated that the CoreLok vacuum-sealing device provides a better measure of internal air void contents of coarse graded mixtures than other conventional methods because of the increased repeatability. Cooley et al (49) also reported a significant difference in air voids measured by the CoreLok and SSD methods for the mixes having coarse gradations. The study also suggested that the CoreLok procedure was a better measure of density for samples with high air void contents. The primary reason for this is the high potential for overestimating sample density due to the water draining out of the mixture when determining the SSD weight in the SSD method.

This study will determine if the CoreLok method should be used for SMA mixtures. As part of this evaluation the study will look at how much difference there is between the CoreLok and SSD methods for different air void levels, how this difference will affect the volumetric properties and whether this difference depends on NMAS.

2.4.2 Permeability

It is generally believed (52-59) that permeability is a function of both the air voids content and the degree of interconnectivity of those voids. Therefore, besides the total air void contents, permeability also depends on gradation, NMAS, and other factors that may affect the air voids shape and air voids distribution.

Many researchers (52-58) have suggested that permeability depends on gradation. It is generally believed that mixtures with coarse gradations have larger individual voids which increase the potential for interconnected air voids. Fine-graded mixtures tend to have smaller individual air voids and have less potential for interconnectivity. An early study (52) indicated that permeability of aggregate materials depends more on the size of the voids than the volume of voids. They found that fine aggregates with VMA of 30 to 35 percent were less permeable than well-graded coarse aggregates with VMA of 12 to 15 percent. SMA has been found (53) to be more permeable compared to dense-graded mixtures at a given air voids content. It was especially significant that the 9.5 mm NMAS SMA mixtures were found to be permeable at a 5 to 7 percent void range, while a 9.5 mm Superpave designed mixtures above the maximum density line was not permeable at an air voids content of 9 percent (59). However, experience in Virginia (56) has indicated all NMAS (25 mm, 19 mm, and 9.5 mm) SMA mixtures were impermeable with in-place air void contents below 6 percent. In current SMA design guides (36), the suggested air voids level after field compaction is 6.0 percent or less.

Several studies (53-58) also suggested that NMAS had an effect on permeability. As the NMAS increases, the size of the individual air voids also tend to increase which could result in higher potential for interconnected air voids. Therefore, the larger NMAS

mixtures would be expected to be more permeable than the smaller ones at a given air voids level. A thin overlay study (54) indicated that at 7 percent air voids, only two 4.75 mm NMAS SMA mixtures complied with permeability requirement, while 19 mm and 12.5 mm NMAS mixtures had permeability values as much as 50 times of that generally specified. The Virginia experience (56) also showed that 9.5 mm NMAS SMA was less permeable at the same air voids level compared to the more commonly used 19 and 25 mm NMAS SMA mixtures.

This study will determine at what air voids the SMA mixtures will become permeable for different NMAS mixtures, and how compaction level affects the permeability.

2.4.3 Aggregate Breakdown

Several studies (7, 60-65) have focused on aggregate degradation. Generally speaking, the most influential factors affecting the degradation of aggregates in HMA include aggregate gradation, aggregate toughness, particle shape, and compactive effort.

Among all the factors, aggregate gradation was found to be the most important factor controlling degradation (60). As the gradation becomes denser (closer to the maximum density line), degradation decreases. The LA Abrasion value also became more critical when coarse graded mixture were used. For a given aggregate, degradation in SMA mixtures would be expected to be more severe than in dense graded HMA because of the stone-on-stone contact.

Aggregate toughness, mostly indicated by LA abrasion, was another important factor (60, 62-64). Collins et al (62) found that aggregates with high abrasion loss degrade more. It was suggested that when high abrasion loss aggregate was used, the

gradation should be designed to compensate for the effect of degradation during compaction. Brown et al (64) also found LA abrasion loss at 30 percent resulted in about 10 percent degradation on the 4.75 mm sieve size, and it should be set as the limit for aggregate used in SMA mixtures.

Particle shape, usually indicated by F&E content, was found to affect the degradation of aggregates. The researchers (63-65) showed that for a given gradation and aggregate type, increasing the percentage of F&E particles would increase the amount of aggregate breakdown.

The compaction method was believed to be another influential factor. Button et al. (7) compared field cores with specimens compacted by an Exxon rolling wheel compactor, a gyratory compactor, a linear kneading compactor, and a rotating base Marshall compactor. The study showed that the Marshall compactor fractured more aggregate than the other three compactors. An early study (5) on gyratory compactor concluded that gyratory compaction can closely simulated the degradation found in the field compaction because it allowed proper orientation of aggregate with low initial pressure. A recent study (22) using x-ray tomography indicated that the gyratory compaction could provide similar aggregate orientation as in the field cores.

Obviously, these factors would also interactively affect the aggregate degradation in HMA mixtures. Aggregates with high L.A abrasion values were more sensitive to the effect of F&E particles than aggregates with lower L.A abrasion values (63).

One of the purposes of laboratory compaction is to simulate the aggregate breakdown in the field. The aggregate breakdown due to the field construction was reported by Brown et al (64) and is shown in Figure 2.4. From Figure 2.4, one can

observe that the aggregate breakdown is not dependent on the L.A abrasion value of aggregate. The aggregate breakdown values in the field were between 3.7 and 6.3 percent on the 4.75 mm sieve for all the projects investigated, except for one project that had unexpected high aggregate breakdown (11.1 percent). If this project is deemed as an outlier, the average aggregate breakdown in the field construction for all projects is 4.9 percent.

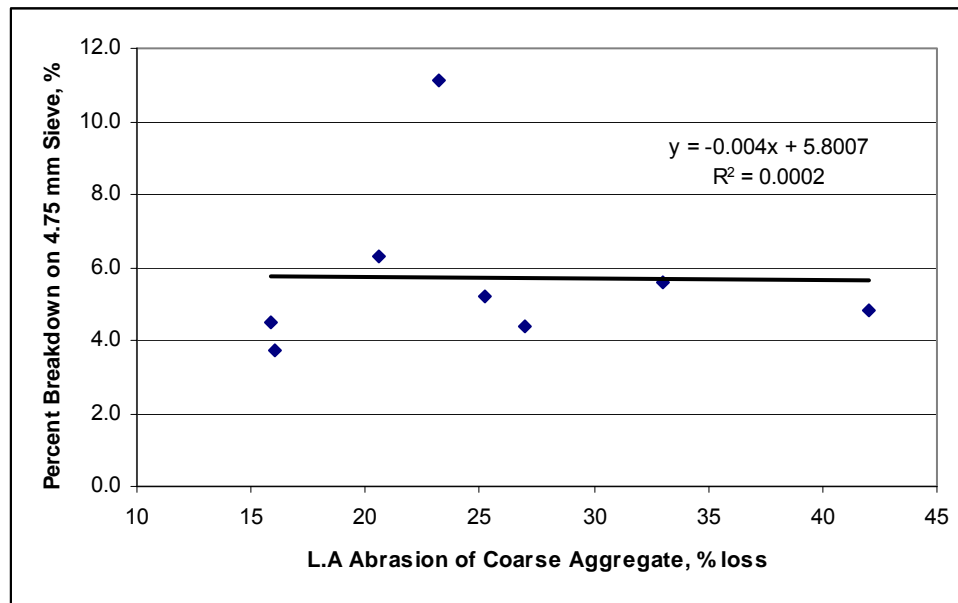


FIGURE 2.4 Correlation of L.A Abrasion values and aggregate breakdown for field compacted samples (64).

This study will determine the aggregate breakdown values in the laboratory for different compaction efforts. The influence of these factors that affect the aggregate breakdown will be determined and discussed.

2.4.4 Locking Point

The “locking point”, or the point during compaction at which the mixture exhibits a marked increase in resistance to further densification, was first developed by Illinois (4,

66) to prevent the over-compaction of their designed mixtures and better back-calculate the specimen densities at prior levels of compaction. The locking point is defined by the authors as the first of three consecutive gyrations producing the same sample height [*the difference in height is less than 0.1 mm*]. Generally, the densification rate of the mixture is nonlinear at any further gyration levels.

The “Locking Point” has also been found to be related to compaction tendencies in the field (67). Compaction of a mix past the “locking point” generally results in aggregate degradation that is not representative of field compaction, and thus the benefit of compacting the mix to very high gyration levels, such as 125 or even 100 gyrations is questionable.

As a result, several states have already included the locking point concept into their mix design specifications. In the Georgia DOT provisional specification (68), two locking points are defined and used as maximum allowed gyration levels for two traffic conditions. The “first” and “second” locking points are defined as the number of gyrations at which, in the first occurrence, the same height has been recorded for the third time and the fourth time, respectively. It was also reported (68) that for Georgia materials, typical first and second locking points are around low 60’s and high 80’s, respectively. In the Alabama DOT provisional specification (69), the locking point is defined as the first occurrence at which the sample height remains the same for two consecutive gyrations.

This study will use 100 gyrations, a compaction level that is above the locking point for most mixtures as the second gyration level, and a third level that is lower than the locking point. The influencing factors that affect the locking point will also be discussed.

2.4.5 Asphalt Pavement Analyzer Rutting Test

The loaded wheel rut tests are simulative test methods used for evaluating rut resistance of HMA mixtures. In simulative tests, the load and environmental conditions in the field are simulated in the laboratory, and the response of the mixture in the laboratory is recorded and used for field performance prediction.

Several loaded wheel testers (LWT) have been used in the past and are currently being used to evaluate rutting performance. Some of these methods include the Asphalt Pavement Analyzer (APA, second generation of Georgia Loaded Wheel Tester, GLWT), Hamburg Wheel-Tracking Device, French Rutting Tester (LCPC wheel tracker), Purdue University Laboratory Wheel Tracking Device, Model Mobile Load Simulator, Dry Wheel Tracker (Wessex Engineering), and Rotary Loaded Wheel Tester (Rutmeter) (70). Out of all LWTs, the APA is one of the most commonly used and most readily available.

Brown et al (71) recommended using the APA as a temporary simple performance tests for evaluating rutting. Their recommendation was based on a comparative assessment for almost all available test methods. The ability to predict permanent deformation was one of the most important characteristics for the comparison. The GLWT, then the APA has been used by numerous researchers in an attempt to evaluate rutting resistance of HMA mixtures. The capability of this device to estimate field rutting performance has been validated by many studies (72-77).

Lai (72) evaluated rut-prediction capability of the GLWT using four mixes from Georgia with known field rut performance. Three of the four mixes had shown a tendency to rut in the field. Results of this work showed that the GLWT was capable of ranking mixtures similar to actual field performance. West et al (73) conducted a study to

verify that the GLWT can be used to predict actual field performance. Three field projects with known rutting performance were included in the study. They found that there was a good correlation between the GLWT results and the actual rutting performance of the mixtures. Miller et al (74) evaluated the feasibility of the GLWT to predict rutting at the University of Wyoming. Core specimens from 13 pavement sections with known field performance were selected for evaluation. The sections had a wide range of rutting performance. The APA test results had a good correlation with actual field measurement when project elevation and pavement surface type were considered. Choubane et al (75) from Florida DOT used three mixes of known field performance to evaluate the suitability of APA for predicting pavement rutting. The rutting performances of these three mix types were good, very poor, and moderate. The results indicated that APA ranked the mixes according to their field performance. This ranking is the same using either beam or gyratory specimens. Mohammad et al (76) evaluated three Superpave implementation projects using the APA test. The APA test results were found to correlate well with the field rutting data. The WesTrack Forensic Team (77) conducted a study on the performance of coarse-graded mixes at WesTrack sections. Their results on the actual field performance and the predicted performance using the APA showed a good correlation with an R^2 value of 0.797.

West (78) conducted a ruggedness study to evaluate APA testing factors that have the greatest influence on the outcome of test results. Factors included in the study were air void content of test specimens (6% vs 8%), specimen preheating time (6-hour vs 24-hour), test temperature (55°C vs 60°C), wheel load (95 lb vs 105 lb), hose pressure (95 psi vs 105 psi), and specimen type (cylinder vs beam). The specimen type factor was actually

a confounded factor in that the cylinders were compacted with an SGC and beams were compacted with an Asphalt Vibratory Compactor (AVC). They found that three of the six main factors were significant: air void content, test temperature and specimen type.

Many test conditions have been used for APA rutting tests. A New Jersey study (79) summarized a range of APA test specifications used by various state agencies.

TABLE 2.7 APA Testing Specifications Used by Various State Agencies

State	Test Temp, °C	Air Voids, %	Compactor Type	Seating Cycles	Cycles
AL	67	4±1	SGC	25	8000
AR	64	4±1	SGC	25	8000
CN	PG	7±1	SGC/AVC	25	8000
DE	67	7±0.5	AVC	25	8000
FL	64	7±0.5	AVC	25	8000
GA	49	6±1	SGC	50	8000
IL	64	7±1	SGC	25	8000
KS	(<PG)	7±1	SGC	25	8000
KY	64	7±1	SGC	25	8000
LA	64	7±1	AVC	25	8000
MI	PG	4to7	SGC/LKC	25	8000
MS	64	7±1	SGC	50	8000
MO	64	7±1	SGC	25	8000
NJ	60	4&7±1	SGC	25	8000
NC	64	7±1	SGC/AVC	25	8000
OK	64	7±1	SGC	25	8000
SC	64	7±1	AVC	25	8000
TN	64	7±1	SGC	----	8000
TX	64	7±1	SGC	50(25)	8000
UT	64	7±1	LKC	50	8000
WV	60	7±1	SGC	----	8000
WY	52	6±1	AVC	25	8000

SGC = Superpave Gyratory Compactor; AVC = Asphalt Vibratory Compactor
LKN = Linear Kneading Compactor; PG = Performance Grade for asphalt binder

The air void contents of tested samples for APA typically included two air void levels: the initial air voids after placement in the field, i.e. 7%; or design air voids after several years in service, i.e. 4%. From Table 2.7, most states used the initial air voids to address the premature rutting problem. For SMA mixtures, normally 6% was used as initial air voids.

Kandhal et al (80) evaluated several test configuration combinations for APA testing. Ten mixes with known field performance were selected from three full-scale pavement research projects, WesTrack, the Minnesota Road Research Project (MnRoad) and the FHWA Accelerated Loading Facility (ALF). Test conditions that give the best correlation with the measured rut depths for WesTrack, MnRoad test sections were recommended for use in the APA test. Based on the finding that 10 of 14 individual projects that were most related to field results used the low level of the air void content, they suggested using 4% air voids in cylinder samples to better simulate the field rutting performance. However, for ALF projects, 4 out of 6 individual projects that had the highest R^2 used 7% air voids.

Test temperatures used for the APA have ranged from 40.6°C to 67°C (70, 79). Most states have specified the test temperature at or near expected maximum pavement temperatures (79). Kandhal et al (80) found the samples tested in the APA at a temperature corresponding to the high temperature of the standard performance grade for a project location better predicted field rutting performance.

Kandhal et al (80) also indicated that both gyratory (cylinder) and beam specimens are acceptable, and a 25 mm standard, small hose gave acceptable results.

Wheel load and hose pressure for the APA basically stayed the same as for the GLWT, 445 N and 690 kPa (100 lb and 100 psi), respectively. One recent research study (81) did use a wheel load of 533 N (120 lb) and hose pressure of 830 kPa (120 psi) with good success. However, the predominant load conditions currently used are still 100 lb and 100 psi (79-80).

Many state agencies and researchers have used or proposed the acceptance criteria for APA rut depth. As shown in Table 2.8, the 5 mm APA rut depth is the most commonly used criteria for high traffic conditions and becomes a general criteria for SMA mixtures.

TABLE 2.8 APA Rut Depth Criteria (70-71, 79, 82)

Agency or Researcher	Criteria, mm
Alabama	4.5 high traffic
Akansas	3 very high traffic (design gyration 205)
	5 high traffic (design gyration 160)
	8 medium traffic (design gyration 115)
Georgia	5 high traffic
	6 medium traffic
	7 low traffic
Kentucky	5
Mississippi (82)	6 high traffic (>3M ESALs)
	7 medium or low traffic (1-3 M or < 1 M ESAL)
New Jersey	3 very high traffic
	5 high traffic
	8 medium traffic
South Carolina	5
Utah	5
Virginia	3.5 high traffic(PG-76)
	5.5 medium traffic (PG-70)
	7 low traffic (PG-64)
West Virginia	6
Zhang et al (70)	8.2
Brown et al (71)	6.0

In summary, the APA rutting test has been successfully used to differentiate the good or bad rutting resistance, and ranked the mixtures according to their field performance. Good relationships between APA rut depth and field rut depth have also been developed for several individual studies. In this study, the APA rutting test will be employed to evaluate the rutting resistance for different compaction levels. The test conditions will follow the most commonly used ones, i.e. 6% air voids samples

compacted by SGC, at PG temperature required for location, and 100 lb load and 100 psi hose pressure.

2.4.6 Triaxial Tests

In contrast to simulative test, the fundamental tests examine the relationship between stress and strain in the laboratory, and develop prediction models for predicting field performance. The fundamental performance tests for evaluating rutting potential include triaxial (or uniaxial) tests, shear loading tests, and diametrical tests.

The triaxial (or uniaxial) tests have been widely used to estimate the rutting potential and to provide necessary input for structural analysis (71). The shear loading tests are usually conducted by Superpave Shear Tester (SST), which is expensive and complex to run, and has very limited availability (71). The diametrical test has been deemed inappropriate (83) because the state of stress is nonuniform and strongly dependent on the shape of the specimen, also the only relatively uniform state of stress is tension. The use of mechanical properties determined by diametrical testing almost always resulted in overestimates of pavement rutting (83).

Multiple members of the NCHRP 9-19 project research team (84) ranked the tests and parameters that are used for predicting permanent deformation based on comprehensive evaluation including test feasibility, relationship between field performance, repeatability of the test and the sensitivity of the test parameter to different mixture variables, and the application of test results. The top three parameters for permanent deformation were 1) the dynamic modulus term ($E^*/\sin\phi$), determined from the triaxial dynamic modulus; 2) the flow time (F_t) from the triaxial static creep; and 3)

the flow number (F_n) from the triaxial repeated load test. All these three parameters are from triaxial tests.

Uniaxial test without a confining pressure is relatively inexpensive and easy to conduct, however, without confining pressure the creep test or repeated load test usually has to be conducted at a relatively low stress (30 psi, or 207 kPa) and low temperature (can't usually exceed 104°F, or 40°C), otherwise the sample fails prematurely (71). For predicting rutting, laboratory testing was suggested (85) to be conducted at a high temperature as expected in the pavement in service, because the rate at which permanent deformation accumulates increases rapidly with higher temperatures. For the NCHRP 9-19 project (84), the triaxial tests for evaluating rutting were conducted at 100 to 130°F (37.8 to 54.4°C). The NCHRP 9-29 project (86) conducted both unconfined and confined repeated load test at 45°C. Additional analysis (87) on mixture verification in the NCHRP 9-19 project indicated that confinement is needed to capture the performance of SMA mixtures compared with dense-graded mixtures, although unconfined testing gave good results for many tests. Therefore, confinement is recommended for testing of SMA and open-graded mixtures.

To better simulate actual traffic and environmental conditions, Brown et al (88) conducted unconfined creep tests at an axial stress of 120 psi, and for confined tests, a confining pressure of 20 psi was used with an axial stress of 120 psi, both at 140°F (60°C). Brown found that for the “ideal test” conditions presented above, the unconfined test, in most cases, could not be performed due to rapid sample failure. However, the confined test could be conducted and, therefore, was recommended for future testing. Gabrielson (89) also used 140°F (60°C) in his rutting study to best simulate the average maximum

pavement temperature throughout the country, and maintained 120 psi axial stress (100 psi deviator stress with 20 psi confining stress) to best represent in situ HMA pavement and traffic interaction.

A certain minimum height to diameter ratio is necessary for the accuracy of the tests due to the end effects concern. Foo (90) found that there was no significant end effect when using samples with 2.5 inches in height and 4 inches in diameter, if a confining pressure was applied. However, during NCHRP 9-19 project (84), it was found that a minimum height-to-diameter ratio of 1.5 was required in order to ensure that the response of a sample evaluated in either the dynamic modulus or permanent deformation tests represents a fundamental engineering property.

There were some debates on the use of dynamic modulus test for predicting rutting resistance recently. The dynamic modulus term ($E^*/\sin\phi$) was selected as the top parameter for predicting rut resistance by NCHRP 9-19 project (84, 91). However, the dynamic modulus is usually conducted at relatively low stress and/or strain level, and reflects the visco-elastic behavior of the material. Neither plastic nor visco-plastic behavior exhibited in rutting is measured by the dynamic modulus test. A recent study (92) indicated that this term may not always relate to HMA rutting resistance, particularly when polymer-modified asphalts are used. The study also suggested that tests in addition to dynamic modulus should be considered to accurately assess rutting resistance of HMA mixtures. A research project in Florida (93) also indicated that there was no discernable relationship between complex modulus and rutting for mixtures of varying gradations and aggregate structure. The study concluded that the complex modulus should generally not be used to determine rutting or fracture resistance of mixtures. While the ability of using

dynamic modulus results to predict rutting resistance is questionable, the dynamic modulus test will still be conducted in this study as a part of the work plan, and provide the information for stiffness of mixtures.

The static creep test has been used for evaluating HMA rutting potential for many years and it was often conducted under unconfined test conditions. Typically, the total strain after 1 hour of loading, the creep modulus (the applied stress divided by the permanent strain after 1 hour loading and 1 hour recovery) and the slope of strain with time were used as criteria for accepting or rejecting mixtures. Sousa et al (94) reported that, under the unconfined test conditions, reasonable consistency was found in the strain level at which a variety of mixtures failed under creep loading. Failure strain levels of 0.8 percent was reported for the compressive creep. Based on a comprehensive literature review, a study in Texas (95) concluded that under typical test conditions, a creep modulus greater than 69 MPa (10ksi) indicates a mix has low sensitivity to rutting, a creep modulus between 41.4 to 69 MPa (6 to 10 ksi) represents a moderate to high sensitivity to rutting. This study (95) also summarized a criteria table suggested for use in the evaluation of compressive creep test data, as shown in Table 2.9.

TABLE 2.9 Criteria for Static Creep Test Results (95)

Total strain at 1 hour of loading, %	Slope of Steady State Creep Curve					
	< 0.17	< 0.20	< 0.25	< 0.30	< 0.35	< 0.40
< 0.25	IV	IV	IV	IV	IV	III
< 0.40	IV	IV	IV	III	III	III
< 0.50	IV	IV	III	III	III	II
< 0.80	III	III	II	II	II	II
< 1.0	I	I	I	I	I	
< 1.2	I	I	I			

Notes: I – Low traffic intensity, < 10⁵ ESALs
 II – Moderate traffic intensity, between 10⁵ and 5×10⁵ ESALs
 III – Heavy traffic intensity, between 5×10⁵ and 10⁶ ESALs
 IV – Very heavy traffic intensity, > 10⁶ ESALs

The unconfined condition generally limited the test temperature to under 40°C (104°F) and axial pressure to under 30 psi (207 kPa). As discussed before, these conditions do not represent the field conditions under which the majority of rutting happens.

A rutting study (90) used the confined static creep test to evaluate the cores from 42 pavement sites. The confining and deviator stresses were 20 psi and 120 psi, respectively. The test temperature was 60°C. The field rut depth and rut rate were used to validate the confined creep test. The permanent strain from the creep test correlated the best with the field rut depth and rut rate. And it was concluded that a laboratory permanent strain of 1.2% would be expected to result for a field rut depth of 0.5 inches. However, the low correlation as indicated by the low coefficient of determination, R^2 (0.35 and 0.21 for creep test vs rut depth and rut rate, respectively) may limit the use of this conclusion. This criterion was developed by using shorter samples (2.5 inches); a taller sample (6 inches) will likely have a higher strain criterion because of the end effects of the short samples (90). The NCHRP 9-19 report (84) suggested the constant load should be held in confined static creep test until the tertiary flow occurs or the total axial strain reaches 4 to 5 percent. Although the flow time and strain slope in static creep test showed a fair to good correlation with field rutting of three field sites (84), additional work is needed to establish the criteria for these test parameters using taller samples (6 inches).

Several studies (71, 89, 96-99) reported that the confined repeated load test was found to give a better correlation with field rut depths and more responsive to the

presence of modified binders in HMA mixtures than the static constant load (creep) tests. The greater suitability of the dynamic test for rating the effect of the binder modification is due to the recovery effects of the tests (98). Gabrielson (89) also reported that variability of the static creep tests is substantially higher than that for repeated load tests.

Brown et al (100) discussed the failure conditions in the repeated load. The failure point was defined as the point at which the deformation rate starts to increase rapidly. Strains at failure measured in the study were about 2 percent for unconfined tests. In another study, Pell et al (101) reported the failure strains for the repeated load tests were also about 1 to 2 percent for unconfined tests, and 4 to 5 percent for confined tests. Hofstra et al (102) reported in-situ strains up to 15 percent. Based on a national study on rutting, Gabrielson (89), Brown and Cross (96) provided information to show that 13% strain was a good pass/fail criteria for triaxial repeated load tests. Pavement cores were tested to validate the confined repeated load test. The cores were from pavements identified as “good” pavements or “rutted” pavements based on the rate of rutting with respect to traffic (89). The original test results are plotted in Figure 2.5.

Based on the same set of data, a relationship between the field rut depth and permanent strain by repeated load was developed. As shown in Figure 2.6, a laboratory strain less than 10% would help ensure that the rut depth does not exceed 0.5 inches. Achieving high strain levels in the laboratory more clearly shows the difference between rut susceptible mixes and rut-resistant mixes. These differences may be subtle at low strain levels (96).

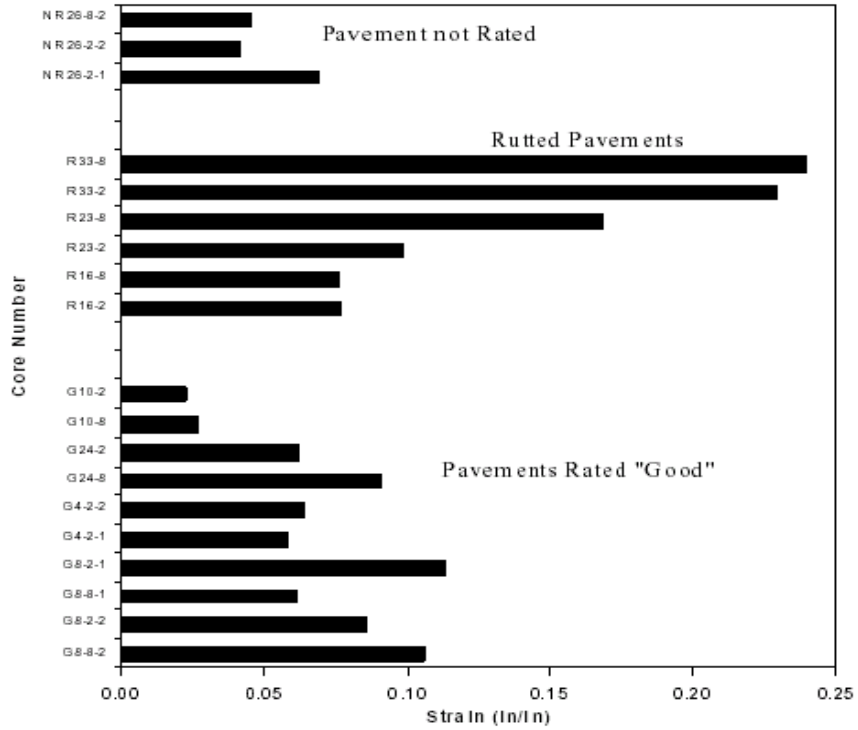


FIGURE 2.5 Permanent strains of core samples by triaxial repeated load test (89).

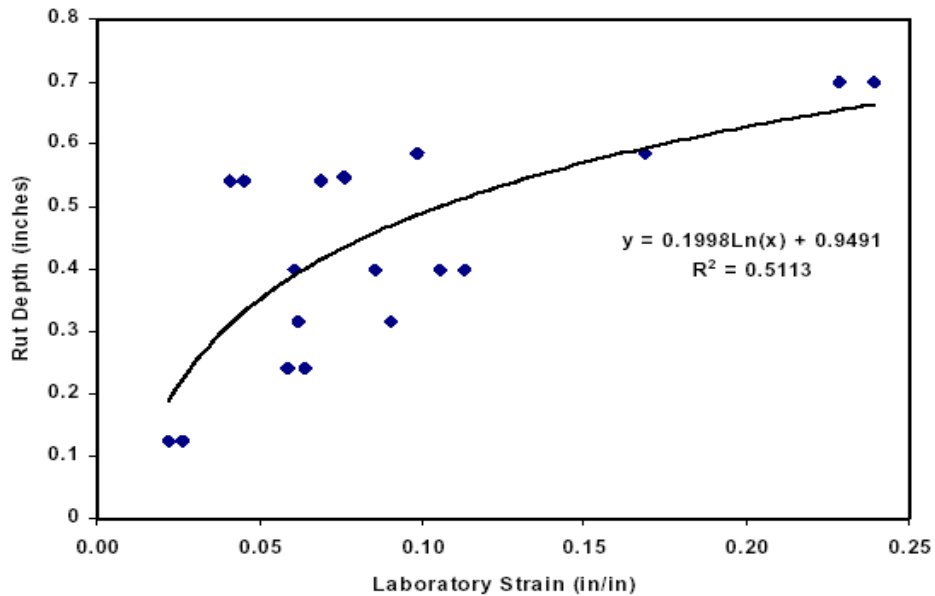


FIGURE 2.6 Field rut depth versus the lab strain from repeated load test (96).

In summary, triaxial tests are the most commonly used fundamental tests for predicting rutting performance, and have been recently recommended by the NCHRP 9-

19 project as the simple performance tests to complement the Superpave Level 1 volumetric mixture design procedure. In this study, all three triaxial tests, including the dynamic modulus test, static creep test, and repeated load test will be used to compare the effects of different compaction levels on rutting performance. The triaxial test will be performed at a high temperature and with confinement to better simulate the field conditions.

CHAPTER 3 EXPERIMENTAL PROCEDURES

3.1 RESEARCH PLAN

A three-phase test plan was developed to accomplish the project objectives. The first phase consisted of selecting aggregates, asphalt and fiber, and determining their properties. This phase was used to choose a wide range of aggregates and determine proper filler content and gradation. The second phase involved the SMA mixture designs, and evaluation of volumetric properties, permeability and aggregate degradation of several compaction efforts. The third phase involved the performance evaluation of designed SMA mixtures, including wheel track APA testing, repeated load confined creep, dynamic modulus and static creep testing.

The general description of each work plan phase is discussed below. Detailed descriptions of tests conducted in each phase are given in later sections. All the test results are shown in chapters 4 and 5.

3.1.1 Materials Selection

This phase included the selection of materials and determination of their properties. The test plan for this phase is shown in Figure 3.1. Five aggregates with a range of L.A. abrasion loss values were selected for the study. L.A abrasion value, flat and elongated (F&E) content, fine aggregate angularity (FAA), and specific gravity of all five aggregates were determined and are shown in chapter 4.

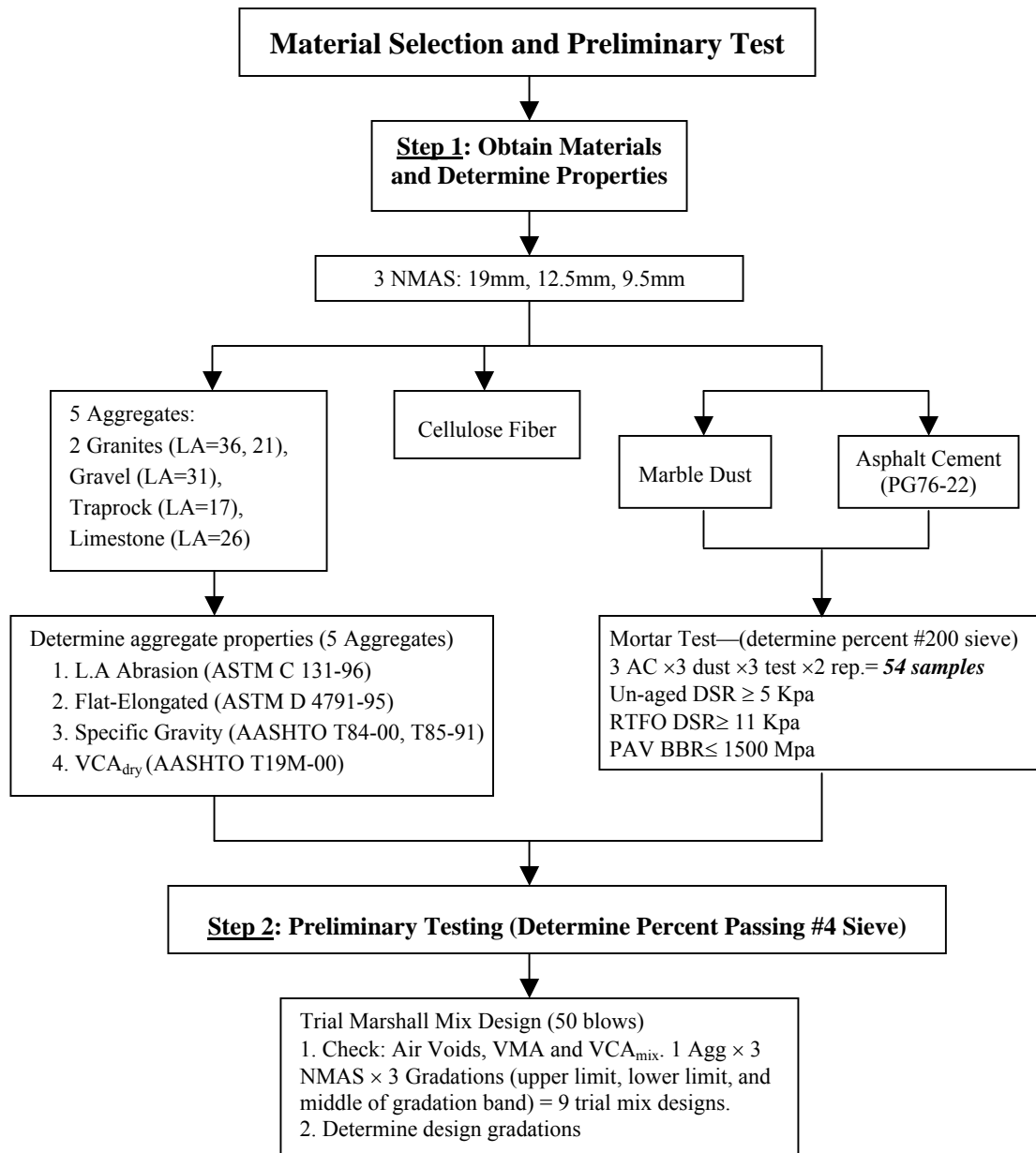


FIGURE 3.1 Work plan for phase I: material selection and preliminary test.

The asphalt grade used in this study was a PG 76-22. This PG grade is typically used for SMA mixtures in the southeastern U.S., as well as other areas in the U.S. Also 0.3 percent stabilizing fiber by weight of total mixture as a common practice was used to help eliminate any potential for draindown. Superpave binder tests were employed to help determine acceptable filler contents based on fine mortar properties.

Trial mix designs were conducted to determine the proper gradation based on volumetric properties resulting from 50 blow Marshall compaction. A total of 9 trial mix designs were conducted for the following combinations: 1 aggregate (crushed gravel), 3 NMAS, and 3 trial gradations (upper limit, lower limit and middle value of specified SMA mix gradation band). The trial gradations are shown in Table 3.1.

TABLE 3.1 Trial Gradations Used in Preliminary Mix Designs

NMAS	Gradation Codes	Percent Passing, %										
		1"	3/4"	1/2"	3/8"	#4	#8	#16	#30	#50	#100	#200
19	U		100	88	60	28	24	19.8	16.2	14	12.5	11
	M	100	95	69	42.5	24	20	16.7	13.9	12	11	10
	L	100	90	50	25	20	16	13.6	11.6	10	9	8
12.5	U		100	99	85	40	28	22.2	18	15	13	11
	M	100	100	94.5	67.5	30	22	17.9	14.7	12.5	11	10
	L	100	100	90	50	20	16	13.6	11.4	10	9	8
9.5	U			100	95	50	30	21	18	15	13	12
	M			100	82.5	40	25	18.5	15.5	13	11	10
	L			100	70	30	20	16	13	11	10	8

The preliminary mix design results are shown in Table 3.2. As shown in Table 3.2, the VCA ratio (VCA_{mix}/VCA_{drc}) for U gradation for all NMAS are either higher than 1 or close to 1. The M gradation for 12.5 mm NMAS is close to 1. With a lower compaction level, the VCA ratio will be expected to be higher indicating that stone on stone contact does not exist. Therefore the gradation should be coarser than the middle of the gradation band as shown in Table 3.1 to ensure stone on stone contact. A set of normal (named N) gradations that are located between the middle of the gradation band

and lower limit were suggested to be used for designing the SMA mixtures for this study (N gradations are shown in Table 3.3. Later results indicated that finer gradations, named F gradations, were necessary for ruby granite and traprock to keep reasonable optimum asphalt content. The F gradations are also shown in Table 3.3).

TABLE 3.2 Preliminary Mix Design Results

NMAS	Gradation	VCA _{drc} , %	Opt. AC, %	VMA, %	VCA _{mix} , %	VCA ratio
19	U	42.2	6.3	17.0	40.2	0.953
	M	40.3	6.4	17.1	36.8	0.913
	L	40.7	6.7	17.5	33.2	0.816
12.5	U	42.4	6.7	17.5	48.0	1.132
	M	42.6	6.5	17.1	41.9	0.984
	L	42.4	6.7	18.0	34.2	0.807
9.5	U	43.0	6.2	17.0	41.8	0.972
	M	41.4	6.4	17.1	37.7	0.911
	L	42.0	7.0	17.7	34.1	0.812

VCA_{drc} - Void in coarse aggregates by dry rodded method
VCA_{mix} - Void in coarse aggregates in compacted mixture
Opt. AC - Optimum asphalt content, at 4 percent air voids
VMA - Void in mineral aggregates

3.1.2 Mixture Design and Volumetric Properties

The test plan for the second phase is shown in Figure 3.2. This phase included conducting mix designs and tests to evaluate mix design samples. Three NMAS mixtures were selected: 19 mm, 12.5 mm and 9.5 mm. SMA mixtures were designed with three different compaction efforts, including 50 blows with Marshall hammer, 100 gyrations with the SGC and a lower gyration level near the locking point with SGC for comparison. A third gyration level which is below the locking point was also used to design 12.5 mm NMAS SMA mixtures for two aggregates. This lower gyration level is lower than that presently being used but was included to provide some idea of the performance at this lower level. Thus, a total of 47 mix designs were conducted.

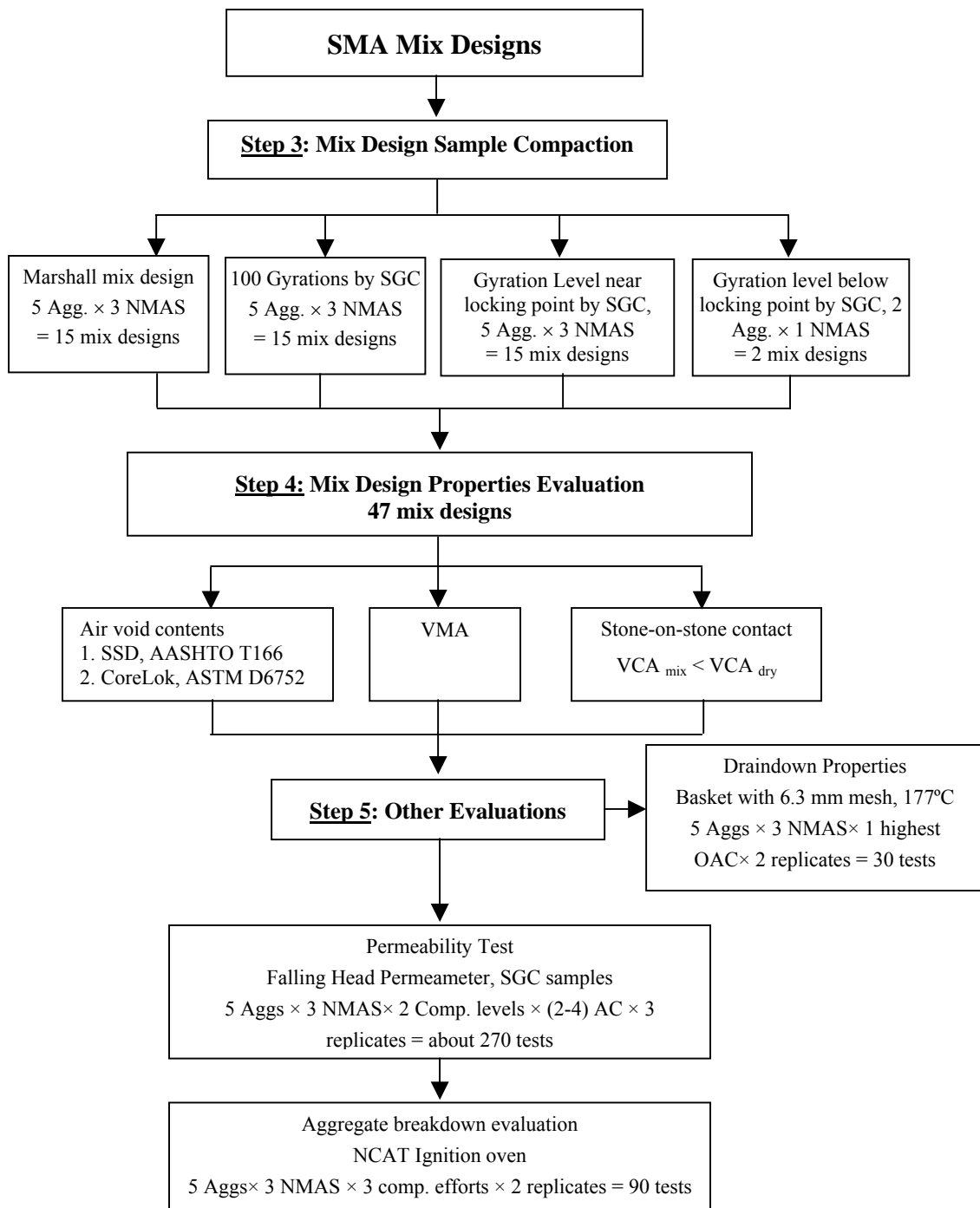


FIGURE 3.2 Work plan for phase II: SMA mix designs.

For easy comparison of the effects of aggregate properties, the same gradation (the N gradations) was initially used for all five aggregates. However, for ruby granite and traprock, the optimum asphalt contents for a lower gradation level were higher than would realistically be used (as high as 8.5 percent) when the N gradations were used. This is likely due to two aggregate characteristics: L.A abrasion and F&E content. These two aggregates have the lowest L.A abrasion loss and lowest F&E content (as shown in Table 4.1). Less aggregate breakdown during compaction and more cube-shaped aggregate will result in higher VMA values and higher optimum asphalt content. Therefore, finer gradations (named F gradations) were used for these two aggregates. The gradations used in this study are summarized in Table 3.3 and shown in Figure 3.3.

TABLE 3.3 Gradations Used in This Study

Gradation Code	Sieve Size (mm)	Percent Passing, %										
		1"	3/4"	1/2"	3/8"	#4	#8	#16	#30	#50	#100	#200
N	19	100	93	59	33	20	16	14	12	10	9	8
	12.5		100	93	59	24	18	15	12	10	9	8
	9.5			100	82	35	22	17	14	11	9	8
F	19	100	95	69	42	24	19	15	12	10	9	8
	12.5		100	95	65	26	22	18	15	13	12	11
	9.5			100	82	35	22	18	16	14	12	11

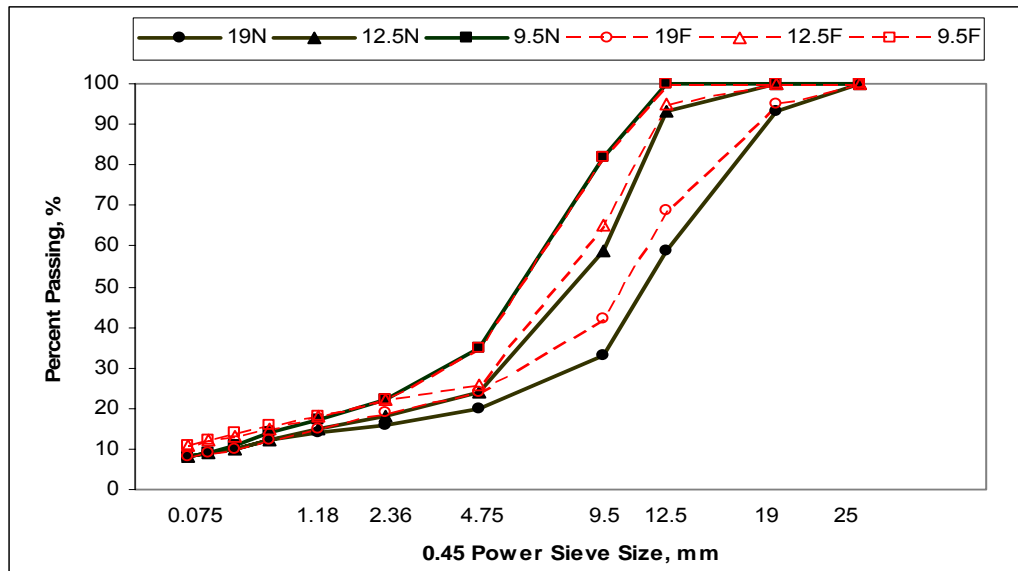


FIGURE 3.3 Gradations used in this study.

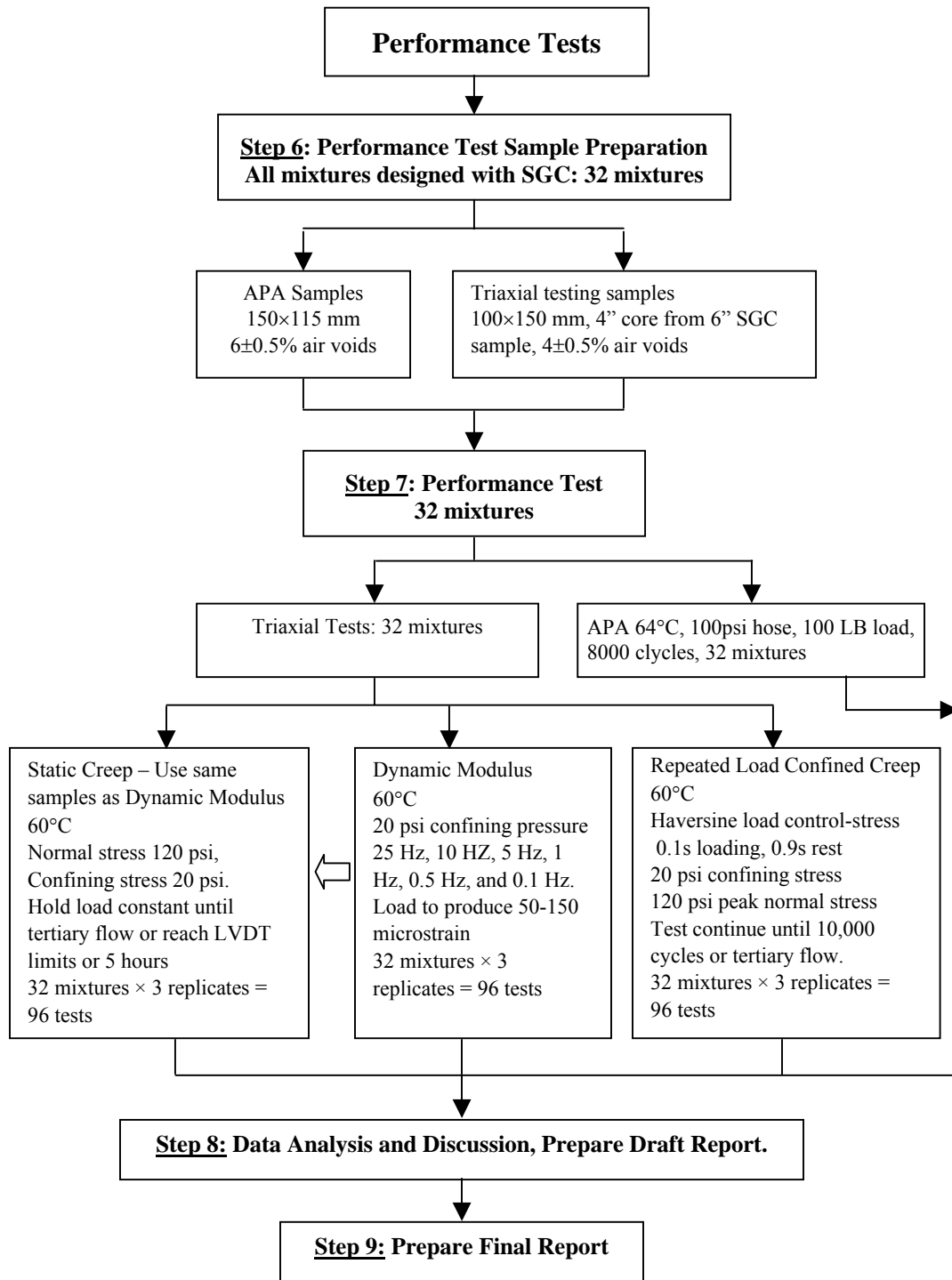


FIGURE 3.4 Work plan for phase III: performance tests.

The SMA mixtures with higher asphalt content are more susceptible to draindown problems if all other influencing factors are identical. Draindown tests were conducted on all 15 combinations of aggregate sources and NMAAS with the highest optimum asphalt content from the three compaction efforts, to ensure all the designed SMA mixtures can meet the draindown test requirement. Two replicated tests were conducted for each mixture.

The volumetric properties of SMA mixtures are very important to ensure the durability and stone-on-stone contact of SMA mixtures. Volumetric properties were determined for the mix design samples, including air void content, voids in mineral aggregate (VMA), and voids in coarse aggregate in mixture (VCA_{mix}).

Based on the literature review, SMA mixtures tend to become permeable at lower air voids content than that for dense-graded mixtures. Permeability tests were conducted on all mix design samples, to determine the threshold air voids value for SMA mixtures becoming permeable.

Ignition oven tests were conducted for all the mix design samples that had air voids close to 4 percent, or that were near optimum asphalt content. This test was used for removal of asphalt binder, and to determine the aggregate breakdown due to compaction after correcting the aggregate breakdown due to the ignition process.

3.1.3 Performance Testing

The test plan for the third phase is shown in Figure 3.4. One of the most remarkable characteristics of SMA mixtures compared to the conventional dense-graded mixtures is its excellent rutting resistance. Also, the most critical property that must be evaluated when increasing the asphalt content is rutting potential. Therefore, the performance tests

conducted in this study mainly focused on the evaluation of rutting resistance, which included APA test, repeated load confined creep, dynamic modulus and static creep tests.

3.2 MATERIALS SELECTION

3.2.1 Aggregate Tests

3.2.1.1 Specific gravity test

In this study, the bulk specific gravity of coarse aggregate and fine aggregate were conducted following the AASHTO T85 and T84 test methods (25), respectively. The coarse aggregate portion is generally defined as the portion that remains on the 4.75 mm sieve. For the coarse aggregate portion, the samples were tested in individual size fractions. The fine aggregate portion was tested together for the specific gradation. The bulk specific gravity of the mineral filler is hard to test and therefore the apparent specific gravity was used as a substitution to calculate the combined bulk specific gravity of aggregate. The equation used to calculate the combined specific gravity of the aggregate sample is shown as follows:

$$G = \frac{P_1 + P_2 + \dots + P_n}{\frac{P_1}{G_1} + \frac{P_2}{G_2} + \dots + \frac{P_n}{G_n}} \quad (3.1)$$

where,

G = combined specific gravity;

G₁, G₂,... G_n = specific gravity values for fraction 1, 2, ..., n; and

P₁, P₂,... P_n = weight percentages of fraction 1, 2, ..., n.

3.2.1.2 L.A abrasion test

The Los Angeles (L.A.) abrasion test is most often used to evaluate the toughness and abrasion of the aggregates. When the L.A abrasion is too high, excessive aggregate breakdown may occur during handling, compaction, and traffic, resulting in potential

bleeding, rutting, or raveling. The L.A. abrasion test was conducted in this study following ASTM C131 (3). The gradation used in this study was the B grading (2500 gram 12.5 mm aggregates and 2500 gram 9.5 mm aggregates).

3.2.1.3 Flat and elongated content test

Flat and elongated particles tend to break during compaction and under traffic, thus they may adversely affect the stability and durability of the compacted HMA. The flat and elongated particles in coarse aggregates were determined following ASTM D4791 (47), using a proportional caliper device.

The individual fractions of each sieve size equal to or greater than 4.75 mm were tested separately. For each sieve size aggregate, approximately 100 particles were obtained following AASHTO T248 (25). The percent by weight of particles that had a ratio of the longest dimension to the shortest dimension greater than 3:1 or 5:1 were recorded. The flat and elongated content of certain blended aggregate depends on the gradation and can be calculated based on the weight fraction of individual sizes and the flat and elongated content of each size.

3.2.1.4 Fine aggregate angularity

The Superpave mix design system specifies a minimum angularity for the fine aggregate portion of asphalt mixtures to increase internal friction (shear strength) and reduce the rutting potential of the mix. However, there have been many controversies on whether fine aggregate angularity (FAA) related to rut resistance (103). In this study, The FAA values for each aggregate type were determined, and used as an input in the data analysis. The particle shape and surface texture of the fine aggregate can be quantified by the use of AASHTO T304 (25), “*Uncompacted Void Content of Fine aggregate*”. In this method,

a 100 cm³ cylinder is filled with fine aggregate of a certain gradation by allowing the sample to flow through the orifice of a funnel into the calibrated cylinder. Excess material is struck off and the cylinder with aggregate is weighed. Uncompacted void content of the sample is then calculated using the weight and the bulk specific gravity of the aggregate. A high uncompacted void content is an indication of good aggregate angularity and coarse surface texture.

$$U = \frac{V - (F / G)}{V} \times 100 \quad (3.2)$$

where:

- U = uncompacted voids in the material, percent;
- V = volume of cylinder, mL;
- F = net mass of fine aggregate, g; and
- G = bulk dry specific gravity of fine aggregate.

3.2.1.5 Uncompacted air voids of coarse aggregate

Coarse aggregate angularity is believed to have a significant effect on mixture rutting performance. The uncompacted air voids of coarse aggregate was recommended by the NCHRP 4-19 project (113) to specify the combination effects of aggregate shape, angularity, and texture.

The uncompacted air voids of coarse aggregate test followed AASHTO TP56 (106), and use the standard gradation for Method A. For 12.5 mm NMAS, the aggregate combination is 1970 grams of 9.5 mm aggregates and 2020 grams of 4.75 mm aggregates. The test procedure and calculation is similar to that of the FAA test, but in a large scale to accommodate the larger aggregate sizes.

3.2.1.6 Voids in coarse aggregates

The stone on stone contact is one of the key criteria for designing SMA mixtures. The existence of stone on stone contact can be determined by comparing VCA_{mix} and VCA_{drc} . The VCA_{mix} can be calculated (104) from the bulk specific gravity G_{mb} of a compacted SMA sample, aggregate gradation, and bulk specific gravity of total aggregate G_{sb} . The dry rodding test for VCA_{drc} followed AASHTO T 19 (25), “Unit weight and Voids in Aggregate”. In this method, the coarse aggregate fraction (retained on 4.75 mm sieve for 19 mm and 12.5 mm NMAS gradation, and retained on 2.36 mm sieve for 9.5 mm NMAS gradation) are filled and dry rodded in three layers into a metal cylinder container. Excess material is struck off and the cylinder with aggregate is weighed. When the dry-rodded density of the coarse aggregate fraction has been determined, the VCA_{drc} for the fraction can be calculated using the following equation:

$$VCA_{drc} = \left(1 - \frac{\gamma_s}{G_{ca}\gamma_w}\right) \times 100 \quad (3.3)$$

where:

VCA_{drc} = voids in coarse aggregate in the dry-rodded condition, percent;

γ_s = unit weight of the coarse aggregate fraction in the dry-rodded condition;

γ_w = unit weight of water (998kg/m³), and

G_{ca} = bulk dry specific gravity of the coarse aggregate.

3.2.2 Fine Mortar Tests

3.2.2.1 Dynamic shear rheometer test

The dynamic shear rheometer (DSR) test was conducted following the AASHTO T315 procedure (25). Although the DSR test is not designed for testing mortar, it is a good method to characterize fine mortars (42). The fine mortar is a mix of asphalt binder and

mineral filler that passes 0.075 mm sieve. In this study, the DSR test was conducted on 9 fine mortars, i.e. 9 combinations of 3 binder contents and 3 filler contents. The binders used for the DSR test were both original PG 76-22 asphalt and the rolling thin-film oven (RTFO) aged asphalt binder. The test temperature was set at 76°C in order to evaluate fine mortar properties at high pavement service temperature.

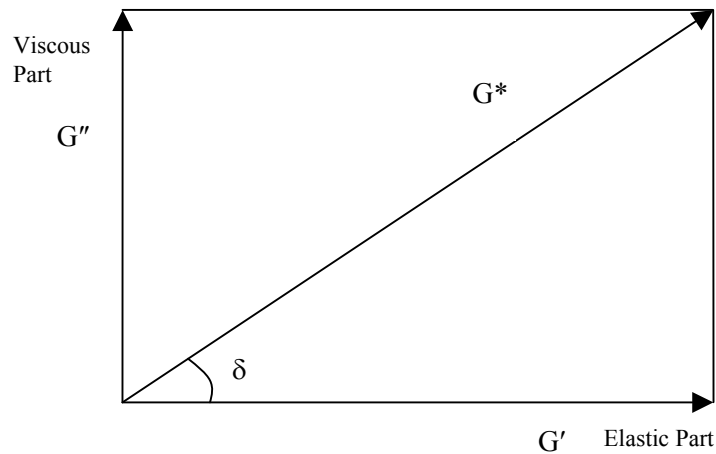


FIGURE 3.5 Components of complex modulus G^* .

The DSR measures the complex shear modulus G^* and phase angle δ of fine mortar at the desired temperature and frequency of loading. Complex modulus G^* can be considered as the total resistance of the fine mortar to deformation when repeatedly sheared. As shown in Figure 3.5, complex modulus G^* consists of two components: storage modulus G' or the elastic part and loss modulus G'' or the viscous part.

For rutting resistance, a high complex modulus G^* value and low phase angle δ are both desirable. A higher G^* value indicates the fine mortar is stiffer and thus more resistant to rutting. A lower δ value indicates a more elastic fine mortar thus more resistance to permanent deformation. In the Superpave asphalt binder specification, the $G^*/\sin\delta$ parameter was chosen as the rutting parameter. And for fine mortar, a

recommended specification of the rutting parameter is listed in Table 3.4. The minimum requirements for $G^*/\sin\delta$ are 5 and 11 kPa for original and RTFO aged mortar, respectively.

TABLE 3.4 SMA Mortar Quality Requirements (43)

Test	Material	AASHTO Method	Property	Specification
Dynamic Shear	Original Mortar	TP 5	$G^*/\sin\delta$	$\geq 5.0\text{kPa}$
Dynamic Shear	RTFO Aged Mortar	TP 5	$G^*/\sin\delta$	$\geq 11.0\text{ kPa}$
Bending Beam	PAV Aged Mortar	TP 1	S	$\leq 1500\text{ MPa}$

3.2.2.2 Bending beam rheometer test

The bending beam rheometer (BBR) test was conducted following the AASHTO T313 (25) procedure. The BBR test was conducted at -12°C in this study to evaluate the fine mortar properties at low pavement service temperature. The asphalt binder in the fine mortar for this test was pressure aging vessel (PAV) aged to simulate the long term aging after several years in service.

Two parameters were recorded during the BBR tests. One is creep stiffness, $S(t)$, which is a measure of how the asphalt binder resists the constant loading. The other is m -value, which is a measure of the rate at which the creep stiffness changes with loading time.

As $S(t)$ increases, the thermal stresses developed in a pavement due to thermal shrinking increases proportionally to temperature change. The thermal cracking becomes more likely with higher $S(t)$ values. Therefore, a recommended maximum limit for PAV aged fine mortar is 1500 MPa as shown in Table 3.4.

3.3 MIXTURE DESIGN PROCEDURES

3.3.1 Mixture Design by Marshall Hammer

The majority of the early SMA projects in the United States were designed with the Marshall procedure. However, the Marshall stability and flow were generally not included in the acceptance criteria.

The compaction effort used in the Marshall procedure to design SMA mixtures was typically 50 blows with a manual hammer. Since the mechanical hammer is normally used and available in the laboratory, a calibration was conducted to give an equivalent blow number by mechanical hammer that results in a similar density as the manual hammer. The Marshall compactor used in this study was a mechanical hammer with a static base. The calibration used lab granite and 12.5 mm NMAS with 6.5 percent asphalt content to represent a typical SMA mixture. The equivalent blow number was calibrated to be 59 blows. The calibration data is shown in Table 3.5 and Figure 3.6.

TABLE 3.5 Automatic Marshall Hammer Calibration Data

Method	Blows	Sample No.	T166	Average
Manual	50	1	2.328	2.332
		2	2.334	
		3	2.335	
Auto	50	1	2.318	2.318
		2	2.321	
		3	2.316	
	60	1	2.329	2.333
		2	2.338	
		3	2.332	
	70	1	2.342	2.345
		2	2.344	
		3	2.350	

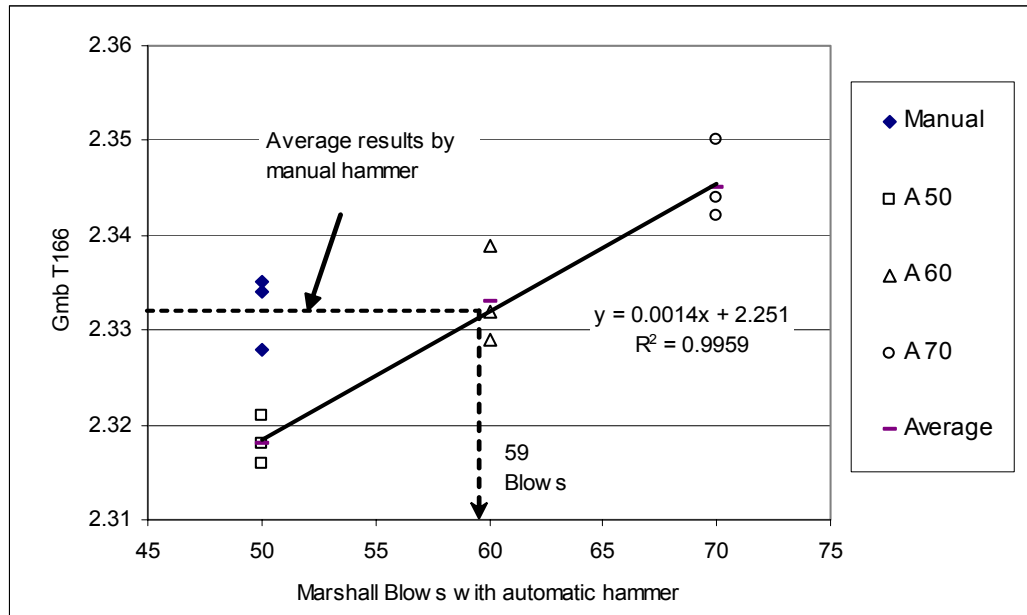


FIGURE 3.6 Automatic Marshall hammer calibration.

A few trial asphalt contents were used to determine the optimum asphalt content that produced the SMA mixture with 4 percent air void content under the designated compaction effort. The number of trial asphalt contents used was as few as possible, as long as the 4 percent air void content was achieved.

The compaction temperature was controlled within 149 and 154°C (300 and 310°F). This temperature range was selected based on supplier information. The loose mixture was packed into the Marshall mold and placed in an oven at this compaction temperature until the temperature was satisfactory for compaction. No short term aging was conducted before the compaction.

3.3.2 Mixture Design by Superpave Gyrotory Compactor

The Superpave gyrotory compactor used in this study was manufactured by the Pine Instrument Company. It had an average internal gyration angle of 1.23° (average external gyration angle was 1.27°) and contact pressure of 600 kPa.

The compaction of SMA samples with the SGC followed the AASHTO PP41 (44) procedure. Short term aging of the loose mix was performed in the oven set at 149°C (300°F) for two hours in accordance with the AASHTO PP2 (44). The compaction temperature was set at 149°C (300°F).

Several trial asphalt contents were used to determine the optimum asphalt content that could produce the SMA specimens with 4 percent air void content under the designated compaction levels. The number of trial asphalt contents used was as few as possible, as long as the 4 percent air void content was achieved.

3.3.3 Draindown Test

The draindown test conducted in this study followed the AASHTO T-305 (25) test procedure. A sample of the SMA mixture with a mass of approximately 1200 grams was prepared in the laboratory. The sample was placed in a wire basket, which was positioned on a plate of known mass. The sample, basket, and plate were placed in a forced draft oven for one hour at a pre-selected temperature. At the end of one hour, the basket containing the sample was removed from the oven along with the plate and the mass of the plate was determined. The amount of draindown was then calculated. The draindown test result was recorded as a percent of the total mixture, by subtracting the initial plate mass from the final plate mass and dividing this by the initial total sample mass.

For each mixture, two replicates were tested. The test temperature used in this study was 177°C (350°F), which is approximately 15°C above the anticipated plant production temperature for the SMA mixtures. The sieve cloth size of the wire basket was 6.3 mm.

3.4 TESTS CONDUCTED ON MIX DESIGN SAMPLES

3.4.1 Air Void Content Determination

The air void content is defined as the total volume of the small pockets of air between the coated aggregate particles throughout a compacted paving mixture, expressed as a percent of the bulk volume of the compacted paving mixture. The formula used for calculating the percent air voids is shown below:

$$VTM = \left(1 - \frac{G_{mb}}{G_{mm}}\right) \times 100 \quad (3.4)$$

Where,

VTM = voids in total mix;

G_{mb} = bulk specific gravity of compacted specimen; and

G_{mm} = the theoretical maximum specific gravity of mixture.

Since G_{mm} can be obtained by following AASHTO T 209 (25), *Theoretical Maximum Specific Gravity and Density of Bituminous Paving Mixtures*, the value of VTM depends primarily on how G_{mb} is measured. There are several different methods to measure the bulk specific gravity. The difference in the various methods is primarily due to the difference in the volume measured for each sample since the sample mass is identical.

Two methods were used in this study to determine the air void content of compacted SMA mixtures. One was the standard method used to measure the SMA bulk

specific gravity by following AASHTO T166 (25), *Bulk Specific Gravity of Compacted Bituminous Mixtures Using Saturated Surface-Dry Specimens*, commonly known as the saturated surface dry (SSD) method. The other method used was the vacuum seal method, by following ASTM D6752 (47), *Standard Test Method for Bulk Specific Gravity and Density of Compacted Bituminous Mixtures Using Automatic Vacuum Sealing Method*.

The SSD method consists of first weighing a dry sample in air, then obtaining a submerged mass after the sample has been placed in a water bath for a specified time interval. Upon removal from the water bath, the SSD mass is determined after patting the sample dry using a damp towel. The bulk specific gravity of the sample can then be calculated by using the following formula:

$$G_{mb} = \frac{W_{dry}}{W_{SSD} - W_{sub}} \quad (3.5)$$

Where,

G_{mb} = Bulk specific gravity of compacted specimen by SSD method

W_{dry} = Dry weight of compacted sample

W_{SSD} = SSD weight of compacted sample

W_{sub} = Submerged weight of compacted sample

The major error of this method typically comes from the SSD weight. During G_{mb} testing for SMA with the SSD method, water can quickly infiltrate into the sample. However, after removing the sample from the water bath to obtain the SSD condition, the water can also drain from the sample quickly. This draining of the water from the sample results in an incorrect SSD weight, and usually results in the measured G_{mb} being higher than the actual G_{mb} .

The vacuum seal method uses a vacuum-sealing device (manufactured by CoreLok) to keep water from entering the sample and thus avoid the water-draining

problem. This vacuum-sealing device utilizes an automatic vacuum chamber with a specially designed, puncture resistant, plastic bag. Under vacuum, the bag tightly conforms to the sides of the sample and prevents water from infiltrating into the sample. The volume of the specimen encapsulated by the bag is considered as the bulk volume of the sample.

3.4.2 Flexible Wall Falling Head Permeability

The permeability test was conducted by following ASTM PS 129 (105) test procedure. Specimens used for permeability testing were produced in the SGC in the mix design phase. For each mixture, several trial asphalt contents resulted in a range of air void contents. This variability in air void content was used to examine the effect of aggregate type, air void content, and NMAAS on permeability.



FIGURE 3.7 Flexible wall falling head permeameter.

A falling head permeability test was used in this study. The test device is shown in Figure 3.7. Water from an upright standpipe was allowed to flow through a saturated sample. The sides of the sample were sealed by a confining rubber sleeve to prevent the

possible leaking from sample sides. The time interval to reach a known change in head was recorded. The coefficient of permeability was then calculated from Darcy's law as follows:

$$K = \left(\frac{aL}{At}\right) \ln\left(\frac{h_1}{h_2}\right) \quad (3.6)$$

Where,

- K = coefficient of permeability, cm/s;
- a = area of standpipe;
- L = specimen height, cm;
- A = cross section area of specimen, cm²;
- t = the measured time of flow;
- h₁ = initial water head, cm; and
- h₂ = final water head, cm.

3.4.3 Ignition Oven Test

The asphalt removal procedure used in this study was performed by the ignition oven test, which was developed at the National Center for Asphalt Technology (NCAT). The ignition oven test followed ASTM D6307 test procedure (47).

This method determines the asphalt content and provides a clean aggregate sample. The gradation analysis on the samples after ignition was compared with the original gradations used in the SMA mixtures. The changes in each sieve were recorded to indicate the total degradation due to compaction and possibly due to additional breakdown in the ignition oven. The loose mixtures were also put into the ignition oven and followed the same procedure to get the possible gradation changes due to the high temperature in the ignition oven. Hence, the degradation due to compaction could be

obtained and used in the data analysis after the correction of possible breakdown in the ignition oven.

3.5 PERFORMANCE TESTING EQUIPMENT AND METHODS

3.5.1 Asphalt Pavement Analyzer (APA) Wheel Tracking

The APA is an automated, new generation of Georgia Loaded Wheel Tester (GLWT). The APA is shown in Figure 3.8. The device uses a wheel to apply a load to a rubber hose, which is in contact with the test specimens. The hose is air pressurized to the desired pressure. The device is configured with three loading stations so that three tests can be conducted simultaneously. Both rectangular slabs and cylindrical specimens can be tested in the device. This test has been used by many States to measure the rutting potential of HMA mixture during the mix design and construction process.

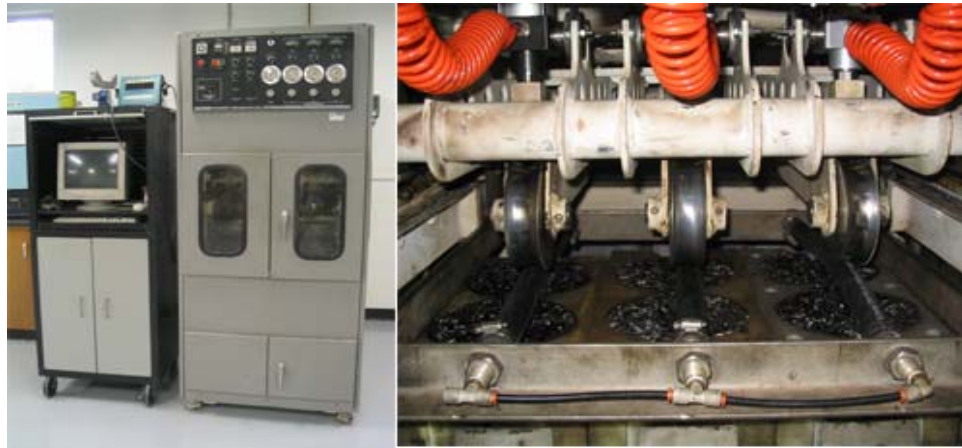


FIGURE 3.8 Asphalt Pavement Analyzer.

In this study, APA testing was used to evaluate the rutting potential for SMA mixtures designed with different compaction levels. Testing with the APA was conducted at 64°C. This temperature corresponds to the standard high temperature performance grade of asphalt cement for most project locations within the southeast. The air void

content of test specimens was 6.0 ± 0.5 percent. Hose pressure and wheel load were 690 kPa and 445 N (100 psi and 100 lb), respectively. Testing was carried out to 8,000 cycles and rut depths were measured continuously. Rut depths were also measured manually after 8,000 cycles as recommended in AASHTO TP 63-03 (106).

3.5.2 Dynamic Modulus

3.5.2.1 Testing setup

The dynamic modulus test is one of the oldest and best documented of the triaxial compression tests. It was standardized in 1979 as ASTM D3497 (47), “*Standard Test Method for Dynamic Modulus of Asphalt Concrete Mixtures*.” The test consists of applying a uniaxial sinusoidal (i.e. haversine) compressive stress to an unconfined or confined HMA cylindrical test specimen, as shown in Figure 3.9.

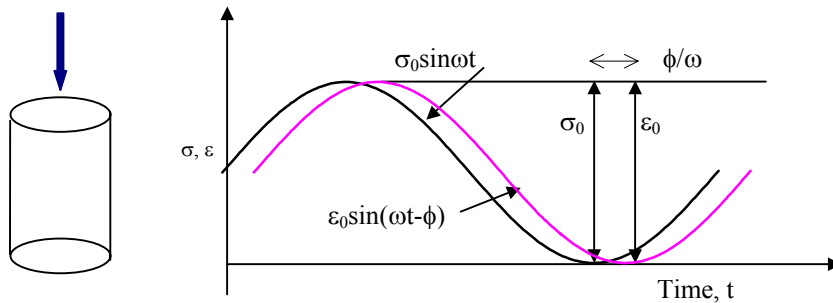


FIGURE 3.9 Haversine loading pattern or stress pulse for the dynamic modulus test.

Within a small stress and strain range, the asphalt mixture tested is deemed as viscoelastic material. If a cyclic stress with a constant amplitude σ_0 is applied to a specimen made of viscoelastic material, the strain response will be an oscillation at the same frequency as the stress but lagging behind a phase angle ϕ as shown in Figure 3.9, where ϵ_0 is the amplitude of strain, and ω is the angular frequency.

In this study, the test was conducted in an environmental chamber at a temperature of 60°C (140°F) with a 20 psi confining pressure. The vertical load was applied by a servo-hydraulic system: the Material Testing System (MTS). The magnitude of the applied load was decided by controlling the responding strain within a range of 50 to 150 microstrain. The MTS and environmental chamber used for this study are shown in Figure 3.10. The specimens were tested in an order of decreasing load frequency including 25Hz, 10Hz, 5Hz, 1Hz, 0.5Hz, and 0.1Hz. This frequency sequence was carried out to cause minimum damage to each specimen before the next sequential test.

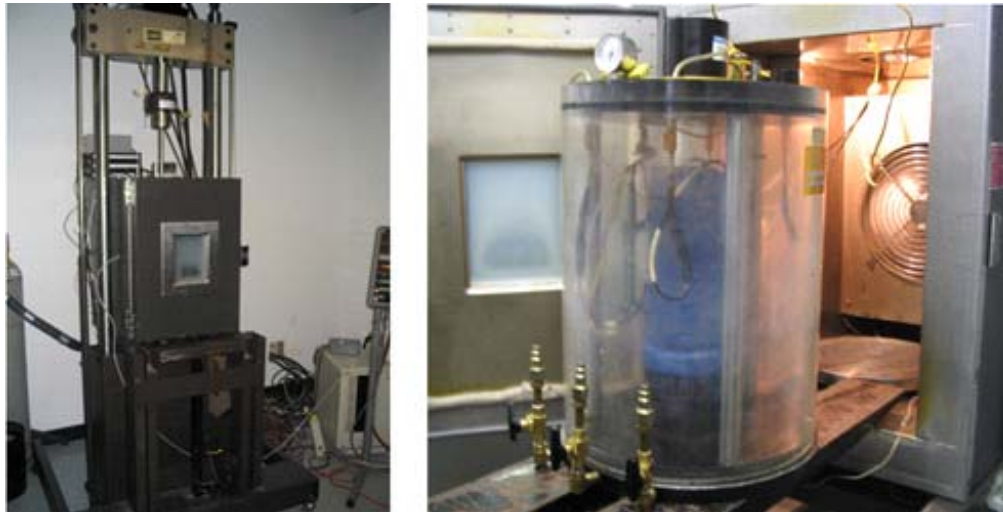


FIGURE 3.10 The MTS and environmental chamber used for triaxial testing.

The deformations were measured through three spring-loaded linear variable differential transformers (LVDTs). The LVDTs were evenly and vertically placed on the side of the specimens, which resulted in the LVDTs being approximately 120° apart. Parallel brass studs that were glued 100 mm apart and located approximately 25 mm from the top and bottom of the specimens were used to secure the LVDTs in place. A sample ready for the triaxial testing is shown in Figure 3.11.

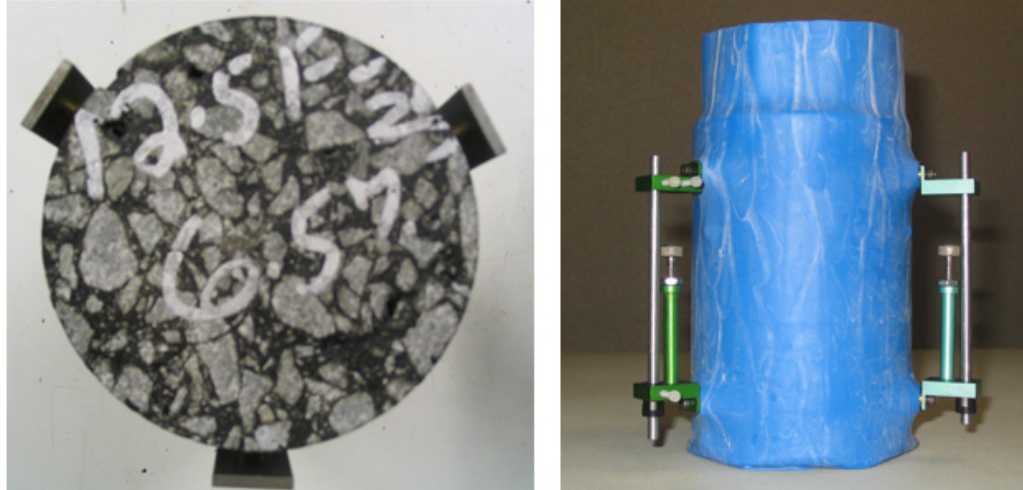


FIGURE 3.11 A sample prepared for triaxial testing.

Since it was a confined test, a flexible membrane with the 4 inches diameter and 0.025 inch thickness was used to cover the tested sample. The flexible membrane was extended over the top and bottom platens and confined with two O-rings to seal the sample from the confining air.

3.5.2.2 Method of analysis

In the raw data analysis phase, two equations: equations 3.7 and 3.8 were used to simulate the stress and strain measured data, respectively. The columns were set up in a data file to predict stress and strain using these equations, and then columns for the square of the error were set up. The Microsoft Excel solver program then was employed to minimize the sum of squares error cell by changing the cells with the equation coefficients. The fitted data was plotted against the measured data to ensure the simulation was correct, since the solver may give a solution that is wrong, depending on the initial values assumed.

$$\sigma = a_1 + b_1t + \sigma_o \times \sin(\omega t + c_1) \quad (3.7)$$

$$\varepsilon = a_2 + b_2t + \varepsilon_o \times \sin(\omega t + c_2) \quad (3.8)$$

where,

σ = predicted stress at time t ;

ε = predicted strain at time t ;

σ_0 = predicted peak stress;

ε_0 = predicted peak axial strain;

ω = angular frequency of dynamic stress and strain; and

$a_1, a_2, b_1, b_2, c_1, c_2$ = other coefficients of simulative equations.

Once the fitted equations were determined, the coefficients of the equations could be used to conduct further analysis. The stress-to-strain relationship under a continuous sinusoidal loading for linear viscoelastic materials is defined by a complex number called the “complex modulus” (E^*). The absolute value of the complex modulus, $|E^*|$, is defined as the dynamic modulus. The dynamic modulus is mathematically defined as the maximum (i.e., peak) dynamic stress (σ_0) divided by the peak recoverable axial strain (ε_0).

$$|E^*| = \frac{\sigma_0}{\varepsilon_0} \quad (3.9)$$

The real and imaginary portions of the complex modulus (E^*) can be written as

$$E^* = E' + iE'' \quad (3.10)$$

E' is generally referred to as the storage or elastic modulus component of the complex modulus; E'' is referred to as the loss or viscous modulus. The phase angle, ϕ , is the angle by which ε_0 lags behind σ_0 . It is an indicator of the viscous properties of the material being evaluated. Mathematically, this is expressed as

$$E^* = |E^*| \cos \phi + i|E^*| \sin \phi \quad (3.11)$$

$$\phi = \frac{t_i}{t_p} \times 360 \quad (3.12)$$

$$\text{or } \phi = (c_1 - c_2) \times \frac{180}{\pi} \quad (3.13)$$

where

t_i = time lag between a cycle of stress and strain (s);

t_p = time for a stress cycle (s); and

i = imaginary number.

For a pure elastic material, ϕ is equal to 0, and the complex modulus (E^*) is equal to the absolute value, or dynamic modulus. For pure viscous materials, ϕ is equal to 90°.

At high temperature, a higher complex modulus E^* indicates a stiffer asphalt mixture, therefore more resistance to deformation. A lower phase angle ϕ indicates a more elastic asphalt mixture resulting in quicker recovery and less permanent deformation. The dynamic complex modulus term $E^*/\sin\phi$ under high temperature has been suggested (84) to be used as an indication of rutting resistance. The dynamic modulus is also very important for mechanic pavement design.

3.5.3 Static Creep

3.5.3.1 Background of Creep Behavior

In a static compressive creep test, a total strain-time relationship for a mixture is measured in the laboratory under unconfined or confined conditions. The static creep test, using either one load-unload cycle or incremental load-unload cycles, provides sufficient information to determine the instantaneous elastic (i.e., recoverable) and plastic (i.e., irrecoverable) components (which are time independent), as well as the viscoelastic and viscoplastic components (which are time dependent) of the material's response.

These four components of creep strain can be expressed as:

$$\varepsilon_t = \varepsilon_e + \varepsilon_p + \varepsilon_{ve} + \varepsilon_{vp} \quad (3.14)$$

where

ϵ_t = total strain;

ϵ_e = elastic strain, recoverable and time independent;

ϵ_p = plastic strain, irrecoverable and time independent;

ϵ_{ve} = viscoelastic strain, recoverable and time dependent and

ϵ_{vp} = viscoplastic strain, irrecoverable and time dependent.

Figure 3.12 illustrates the creep behavior of HMA mixtures. The load duration is t_1 and the rebound time is $t_2 - t_1$. When the load is applied at $t = t_0$, a strain ϵ_0 containing the elastic and plastic components appears instantaneously. During the load duration, viscoelastic and viscoplastic strain occur. Once the load is removed ($t = t_1$), the elastic strain is recovered instantaneously. In the rebound period, the viscoelastic strain is recovered. At the end of the rebound period ($t = t_2$), the permanent creep strain consists of the plastic and viscoplastic strains.

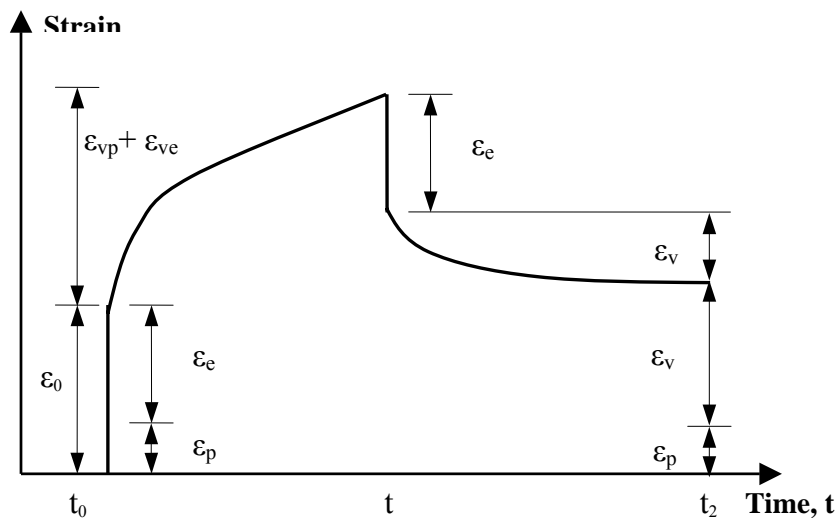


FIGURE 3.12 HMA creep behavior in static creep test.

This creep behavior can be modeled by Krass's model (107). As shown in Figure 3.13, Krass's model consists of a skidding block, a Maxwell model and a Kelvin model in series. The constitutive equation for Krass's model is given as

$$\varepsilon_t = \varepsilon_{psk} + \frac{\sigma_0}{E_1} + \frac{\sigma_0 t_1}{\eta_1} + \frac{\sigma_0}{E_2} (1 - e^{-E_2 t_1 / \eta_2}) \quad (3.15)$$

where

ε_{psk} = plastic strain due to skidding block;

σ_0 = applied constant stress;

E_1 = elastic constant of spring in series;

E_2 = elastic constant of spring in parallel;

η_1 = viscous constant of dashpot in series;

η_2 = viscous constant of dashpot in parallel; and

t_1 = time when constant stress was removed.

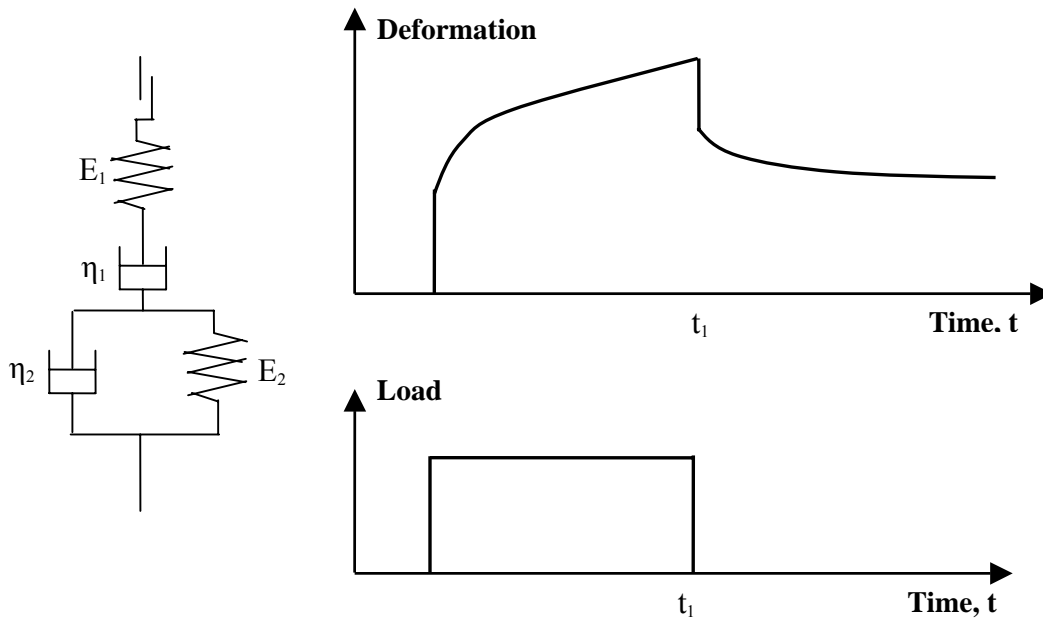


FIGURE 3.13 Krass's model for creep behavior (107).

Comparing the equations 3.14 and 3.15, elastic strain $\varepsilon_e = \sigma_0 / E_1$, plastic strain $\varepsilon_p = \varepsilon_{psk}$, viscoelastic strain $\varepsilon_{ve} = (\sigma_0 / E_2)(1 - e^{-E_2 t_1 / \eta_2})$, and viscoplastic strain $\varepsilon_{vp} = \sigma_0 t_1 / \eta_1$.

3.5.3.2 Testing Setup

Since the dynamic modulus test is generally recognized as a non-destructive test because of the low stress/strain applied, the same specimens and setup were used to conduct static creep tests after testing for dynamic modulus. The equipment setup and condition were the same as those used in dynamic modulus test. The test temperature for the static creep test was 60°C. The confining pressure was 20 psi. The static compressive load, or the continuous applied load used in this study was 1257 lb, which resulted in the contact pressure of 100 psi. Therefore, the major and minor principle stresses for this test were 120 and 20 psi, respectively.

The program was set to automatically stop the test when any LVDT reached the maximum limit. The valid range for the LVDTs used in this study was 5 mm. While measuring the deformation between two points at 100 mm apart, the LVDT displayed the individual strain up to 5 percent. The test was also stopped when a test time was longer than 5 hours and no indication was shown that the test would be completed within a short period of time (usually less than 1 hour).

3.5.3.3 Method of analysis

A typical relationship between the calculated total compliance and loading time is shown in Figure 3.14.

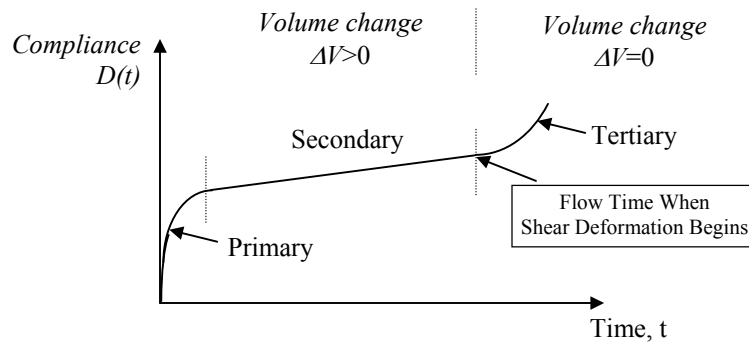


FIGURE 3.14 Typical test results between compliance and loading time.

As shown, the total compliance can be divided into three major zones:

1. The primary zone: the portion in which the strain rate decreases with loading time;
2. The secondary zone: the portion in which the strain rate is constant with loading time; and
3. The tertiary flow zone: the portion in which the strain rate increases with loading time.

Ideally, the large increase in compliance occurs at a constant volume within the tertiary zone (84). The starting point of tertiary deformation is defined as the flow time, which has been found to be a significant parameter in evaluating an HMA mixture's rutting resistance (84). The flow time also is viewed as the minimum point in the relationship of the rate of change of compliance to loading time. The flow time, FT , is therefore defined as the time at which the shear deformation under constant volume begins (84).

Details on compliance models and regression parameters are available in the NCHRP reports on simple performance test (84, 86). In general, power models are used

to model the secondary (i.e., linear) phase of the creep compliance curve, as illustrated in Figure 3.15.

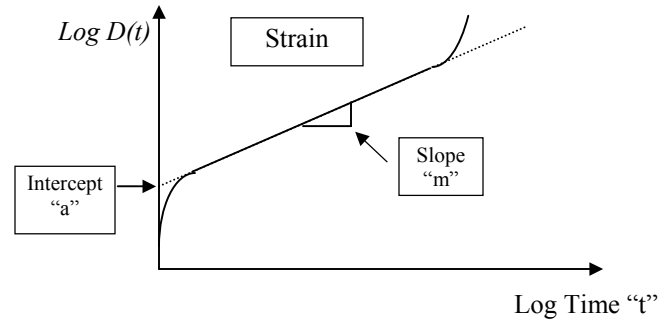


FIGURE 3.15 Regression constants a and m obtained from the secondary zone of the log compliance–log time plot.

$$D' = D(t) - D_0 = at^m \quad (3.16)$$

where

D' = viscoelastic compliance component at any time;

$D(t)$ = total compliance at any time;

D_0 = instantaneous compliance;

T = loading time; and

a, m = materials regression coefficients.

The regression coefficients, a and m , are generally referred to as the compliance parameters. These parameters are general indicators of the permanent deformation behavior of the material. In general, the larger the value of a , the larger the compliance value, $D(t)$, the lower the modulus, and the larger the permanent deformation. For a constant a -value, an increase in the slope parameter m means higher rate of permanent deformation.

3.5.4 Repeated Load Confined Creep

3.5.4.1 Testing setup

Another promising approach to measuring the permanent deformation characteristics of an HMA mixture is to conduct several thousand repetitions of a repeated load test and to record the cumulative permanent deformation as a function of the number of load cycles (i.e., repetitions). A schematic graph of stress and strain relationship in repeated load test is shown in Figure 3.16.

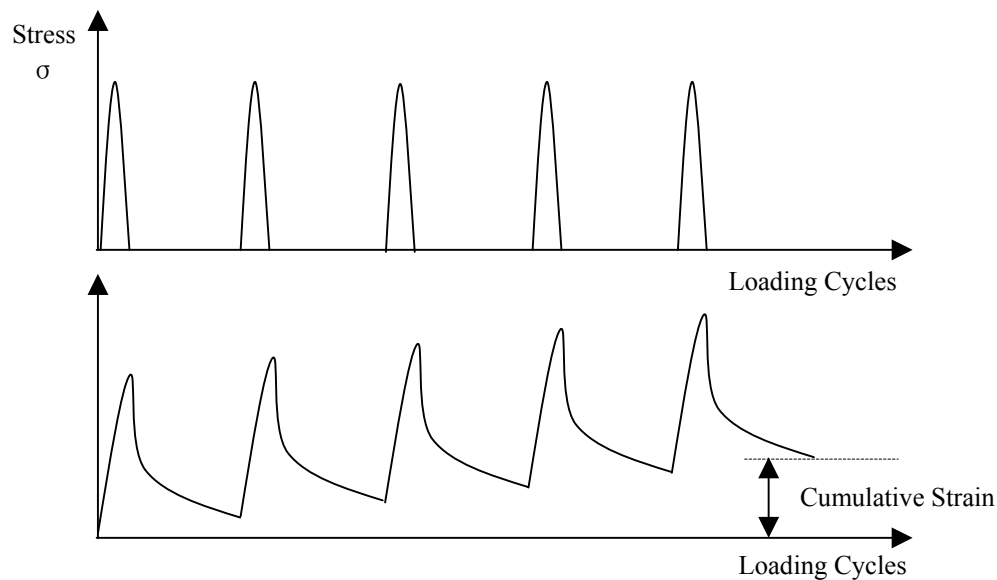


FIGURE 3.16 Repeated load test schematic graph.

A load cycle consisting of a 0.1 second haversine pulse load and a 0.9 second dwell (i.e., rest) time is applied for the test duration—10,000 loading cycles or about 3 hours in this study. The sample setup and test environmental conditions were the same as those used in the dynamic modulus and the static creep test. The test temperature for the static creep test was 60°C and the confining pressure was 20 psi. The load magnitude (peak value) used in this study was 1257 lb, which resulted in a peak contact pressure of

100 psi. Therefore, the major and minor principle stresses at the peak for this test were 120 and 20 psi, respectively.

3.5.4.2 Method of analysis

Results from repeated load tests are typically presented in terms of the cumulative permanent strain versus the number of loading cycles. Figure 3.17 illustrates such a relationship. Similar to the creep test, the cumulative permanent strain (ϵ_p) curve can be divided into three zones: primary, secondary, and tertiary. The cycle number at which tertiary flow starts is referred to as the “flow number”.

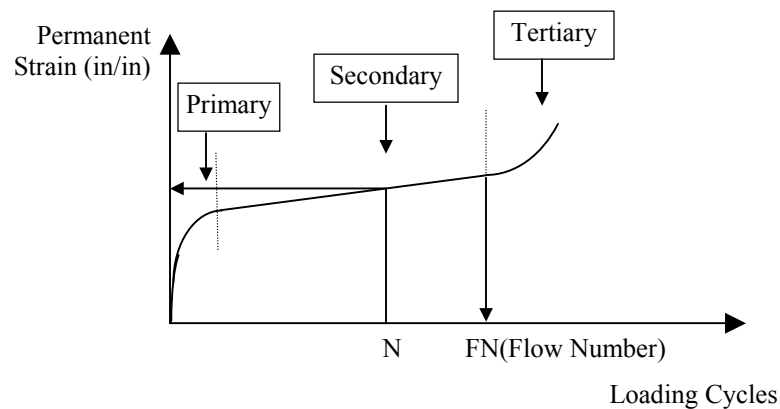


FIGURE 3.17 Typical relationship between total cumulative plastic strain and loading cycles.

Figure 3.18 illustrates the same relationship plotted on a log–log scale. The intercept a represents the permanent strain at $N = 1$ whereas the slope b represents the rate of change of the permanent strain as a function of the change in loading cycles ($\log [N]$). These two permanent deformation parameters are derived from the linear (i.e., secondary) portion of the cumulative plastic strain–repetitions relationship.

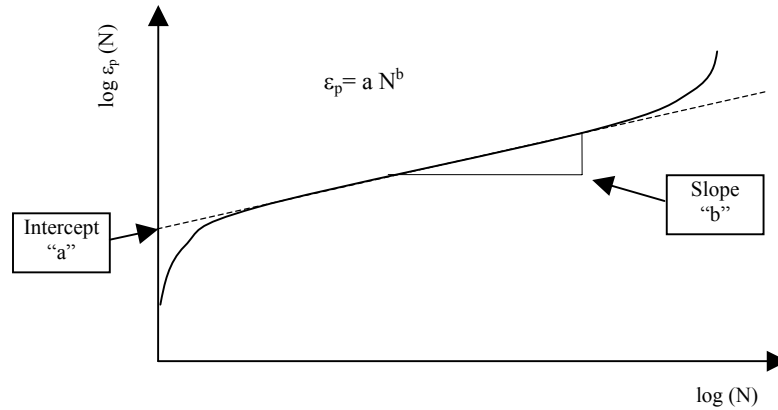


FIGURE 3.18 Regression constants a and b when plotted on a log–log scale.

The classic power-law model, mathematically expressed by Equation 3.17, is typically used to analyze the test results:

$$\varepsilon_p = aN^b \quad (3.17)$$

The regression constants a and b ignore the tertiary zone of material deformability (Figure 3.17) and are dependent on the material–test combination conditions. The estimation of parameters a and b are obtained from a regression analysis of the linear portion of the permanent strain versus number of cycles. The flow number is recorded where the minimum slope occurs (84), or just before the slope begins to increase.

3.6 PERFORMANCE TEST SPECIMEN PRODUCTION

3.6.1 APA Specimen Production

The test specimens prepared for APA rut testing had a diameter of 150 mm, a height of 115 ± 5 mm, and air void content of 6.0 ± 0.5 percent. For each mixture, a set of six specimens was prepared.

The specimens were compacted at optimum asphalt content with a reduced gyration level based on the compaction curve obtained from the mix design phase to

obtain the appropriate air voids. Accordingly, the amount of loose mixture was also reduced in order to get the 6 percent air void content and the designated height range. The intent of these procedures was to produce specimens having densities representative of those present in-place after construction and to produce specimens having similar air voids in order to make comparisons between the different design compaction levels.

3.6.2 Triaxial Test Specimen Production

The specimens prepared for triaxial tests had average dimensions of 100 mm in diameter and 150 mm in height. The test specimens were cored and sawn from gyratory compacted mixtures. The target air void content for the test specimens was 4 ± 0.5 percent. The detailed requirements on the geometric properties of triaxial samples follow NCHRP report 465 and 513 (84, 86), and are listed in Table 3.6.

TABLE 3.6 Geometric Requirements for Triaxial Samples (84, 86)

Item	Test Procedure	Requirements
Diameter	Measure at the mid height and third points along axes that are 90 degrees apart, a total of six measurement for each sample	Within 102 ± 2 mm Standard deviation \leq 2.5 mm
Height	At least three measurements at approximately 120° intervals for each sample	Within 150 ± 2.5 mm
Air Void Content	AASHTO T269	Within target ± 0.5 percent
End Smoothness	Check a minimum of three positions at approximately 120° intervals using a straight edge and feeler gauges approximately 8-12.5 mm wide or an optical comparator	Within ± 0.05 mm across any diameter
Perpendicularity	Measure angle between the specimen end and the axis of the specimen by using a machinists square and feeler gauges	Not depart from perpendicular by more than 0.5 degrees

This preparation can provide more homogeneous test specimens (108), also provide a height-to-diameter ratio of 1.5, which is recommended as the minimum ratio to

ensure the response of a sample evaluated represents a fundamental engineering property (84). The smooth, parallel specimen ends were needed to eliminate the end friction and violation of the theoretical boundary effects of the specimen during the test. The smooth surface also allows better mounting for the LVDTs.

In order to get the test specimens described above, SMA mixtures were compacted in the SGC with the final height of 170 mm. About 10 mm from both ends of the compacted specimen was removed, and a 100 mm (4 inches) core was drilled from each 150 mm (6 inches) specimen. The gyratory specimen, sawing and drilling devices should be adequately supported to ensure the resulting test specimen is cylindrical with parallel ends, and with sides that are smooth, parallel, and free from steps, ridges, and grooves. Figure 3.19 shows a comparison of a 150 mm (6 inches) sample and a 100 mm (4 inches) cored sample side by side.



FIGURE 3.19 Whole and cored sample prepared for triaxial testing.

The air void content of the whole specimen is generally higher than that of the test specimen after coring and sawing because of the distribution of the air voids (108). The

surface of the lab compacted sample is likely to have higher air voids because the surface friction and other edge effects between the mixture and mold provide resistance to densification during compaction. Therefore, a higher target air void content for the whole gyratory specimens were used in order to get a 4 percent air void content for test specimens. The specific target air voids varied for different mixtures with different aggregates and NMA. The gyratory compaction was controlled by sample height and adjusting the sample mass of the mixtures, therefore, the gyration number varied for individual specimen. A maximum gyration number was also set to eliminate the chance of over compaction due to errors in estimation for various mixtures.

CHAPTER 4 TEST RESULTS, ANALYSIS AND DISCUSSION ON MIX DESIGN PROPERTIES

This chapter presents the material properties, mix design results using different compaction efforts, effects of test methods on air void content, permeability test results, and aggregate breakdown results due to different laboratory compaction efforts.

Discussion is emphasized on the volumetric properties comparison for different compaction efforts, air voids measurement effects on volumetric properties, influencing factors on permeability of SMA mixtures, and degradation comparison for different compaction efforts.

4.1 MATERIAL PROPERTIES

Five aggregates with a range of LA abrasion loss values were selected for this study. They were crushed gravel, lab stock granite, ruby granite, limestone, and traprock. All aggregates were used to design three NMA mixtures: 19 mm, 12.5 mm, and 9.5 mm. In addition, each SMA mixture incorporated the same mineral filler “marble dust”, cellulose fiber stabilizer and a polymer modified PG 76-22 asphalt binder. This section documents the properties of each of these materials used in the preparation of each mixture.

4.1.1 Coarse Aggregate Properties

The specific gravity, L.A. abrasion, flat and elongated (F&E) content, and the uncompacted air voids of coarse aggregates are shown in Table 4.1.

TABLE 4.1 Aggregate Properties

<i>Aggregate Type</i>	<i>Bulk Specific Gravity¹</i>	<i>LA Abrasion Loss², %</i>	<i>F&E Content¹ 3:1 ratio, %</i>	<i>F&E Content¹ 5:1 ratio, %</i>	<i>Uncompacted Air Voids of Coarse aggregate³, %</i>	<i>Fine Aggregate Angularity, %</i>
C. Gravel	2.600	30.7	35.2	9.4	48.4	50.0
L. Granite	2.666	36.4	28.1	2.4	47.8	49.2
Limestone	2.730	26.4	25.5	3.6	46.6	47.1
R. Granite	2.702	20.6	23.4	4.4	47.1	48.9
Traprock	2.927	16.6	17.7	3.9	48.5	48.7

1. The bulk specific gravity and F&E content depends on the combined gradation and NMAS; the value shown is for 12.5mm NMAS gradation.

2. LA abrasion values are based on B grading in ASTM C131.

3. Uncompacted air voids of coarse aggregate results are based on AASHTO TP56, method A with 12.5 mm NMAS.

The L.A. abrasion value of the five aggregates ranged from 16.6 to 36.4 percent, and two of five aggregates exceeded the suggested high limit of 30 percent for SMA mixture (43). The reasons for choosing the range of L.A. abrasion were to represent the various aggregates that have been used in SMA mixtures and to determine the effect of aggregate L.A. abrasion on the design compaction level.

The F&E content (3:1 ratio) of aggregates ranged from 17.7 to 35.2 percent. Only one of five aggregates has the F&E content below the suggested maximum limit of 20 percent for SMA mixture (43). However, two of the other aggregate sources (lab granite and ruby granite) have been used on Georgia SMA projects, and it was believed the range in F&E content values would provide an opportunity to evaluate the effect of F&E on SMA performance properties.

The uncompacted air voids of coarse aggregate were within a narrow range from 46.6 to 48.5 percent. There is no specific requirement for this aggregate property in the SMA mix design guides (43). However, this aggregate property was tested because some studies (103, 113) have shown it to have a good correlation with rutting performance.

4.1.2 Fine Aggregate Angularity

The fine aggregate angularity (FAA) which is determined from the uncompacted air void content of fine aggregate is also shown in Table 4.1. All of the fine aggregates had uncompacted air void contents higher than the suggested minimum limit of 45 percent (43), and ranged from 47.1 to 50.0 percent.

4.1.3 Mineral Filler Properties

Marble dust was used as mineral filler for all SMA mixtures in this study. The properties of the mineral filler are shown in Table 4.2.

TABLE 4.2 Mineral Filler Properties

Particle Size Analysis	
Sieve Size, mm	Cumulative Percent Passing ¹ , %
1.18	100
0.6	100
0.3	100
0.15	100
0.075	99.6
0.045	90.7
0.02	61.1
0.01	40.1
Property	Value
Apparent Specific Gravity ²	2.566
Dry-Compacted Voids ³ , %	37.3

1. Determined using a Coulter LS-200 laser particle size analyzer.
2. Determined by AASHTO T-100.
3. Determined by modified Rigden voids method (109).

4.1.4 Asphalt Binder Properties

The asphalt binder used in this study was tested using the Superpave binder tests and graded according to the Superpave binder grading specification. The PG 76-22 asphalt binder was selected since it is the most common grade appropriate for SMA mixture in

the southeastern United States. The asphalt was modified with a styrene-butadiene-styrene (SBS) polymer.

The binder characterization and performance grading summary for the PG 76-22 is shown in Table 4.3.

TABLE 4.3 PG 76-22 Asphalt Binder Properties

Test	Temperature (°C)	Test Results	Requirement
Specific Gravity		1.0277	
Original DSR, $G^*/\sin\delta$ (kPa)	76	1.650	1.00 min
RTFO Aged DSR, $G^*/\sin\delta$ (kPa)	76	3.304	2.20 min
PAV Aged DSR, $G^*/\sin\delta$ (kPa)	25	2831	5000 max
PAV Aged BBR, Stiffness (MPa)	-12	137	300 max
PAV Aged BBR, m-value	-12	0.370	0.300 min

4.1.5 Fiber Properties

Cellulose fiber was selected for inclusion in the SMA mixtures since it had been used extensively in SMA in the United States and Europe. The properties of the cellulose fibers are shown in Table 4.4. The ash content, Ph value, average fiber length and mesh sieve analysis shown were provided by the manufacturer.

TABLE 4.4 Cellulose Fiber Properties

Property	Value	Requirements
Fiber length (Method A), mm	6	6 max
Passing through 0.15 mm (No. 100) sieve, %	66.71	70 ± 10
Ash Content, %	18.76	18 ± 5
Ph value	7.5	7.5 ± 1
Oil Absorption, times of fiber weight	5.15	5 ± 1
Moisture Content, %	2.97	5 max

4.1.6 Fine Mortar Properties

The Superpave binder tests including the DSR test and BBR test were conducted on fine mortars that consist of various asphalt binder contents, various mineral filler contents and 0.3 percent cellulose fiber by total mix weight. The test results are shown in Table 4.5.

TABLE 4.5 Mortar Test Results

Asphalt content, %	Dust content, %	Dust / Asphalt ratio	DSR (Orig.), G*/sin ϕ , 76°C, kPa	DSR (RTFO) G*/sin ϕ , 76°C, kPa	BBR (PAV) Stiffness, S -12 °C, MPa
5.5	8	1.37	9.29	18.64	710
	10	1.71	11.08	22.71	999
	12	2.06	13.86	30.26	1045
6.0	8	1.25	7.86	17.13	637
	10	1.56	9.53	19.87	837
	12	1.87	11.20	27.46	958
6.5	8	1.15	7.36	16.17	607
	10	1.43	8.70	19.33	766
	12	1.72	10.59	23.55	891
Criteria	--	--	≥ 5	≥ 11	≤ 1500

The mortar was evaluated at three levels of asphalt content: 5.5, 6.0, and 6.5 percent, which covered the most commonly used range of asphalt content for SMA mixtures. The mineral filler content also had three levels: 8, 10, and 12 percent by total weight of aggregates (the aggregate type was not specified), which covered the gradation band limit on the No. 200 (0.075 mm) sieve for SMA mixtures. For all the combinations of asphalt content and mineral filler content, the DSR test results on the fine mortar with original and RTFO aged asphalt binder ranged from 7.36 to 13.86 kPa and 16.17 to 30.26 kPa, respectively. These results were higher than the minimum recommended criteria of 5 kPa and 11 kPa (43) recommended for SMA fine mortar with original and RTFO aged asphalt binder, respectively.

For the same combinations of asphalt binder and mineral filler content, the BBR test results on fine mortar with PAV aged asphalt binder ranged from 607 to 1045 MPa. All the results were less than the recommended maximum limit of 1500 MPa (43) set for SMA fine mortar.

The results of mortar tests indicated that the fine mortars with all the combinations of asphalt content and mineral filler content could meet the recommended

requirements for SMA fine mortar. Therefore, with the PG 76-22 asphalt binder and marble dust mineral filler used in this study, no restriction on asphalt content and mineral filler content were incurred from fine mortar property requirements. All of the asphalt contents and mineral filler contents evaluated in this study can be used if the volumetric and performance properties of SMA mixture are satisfactory.

4.2 MIXTURE DESIGN PROPERTIES

In this study, SMA mixtures were designed using both a Marshall compactor and a gyratory compactor. The Marshall compaction was conducted with a static base, automatic Marshall hammer. The number of blows with the automatic hammer was calibrated to 50 blows with a manual hammer. It was determined that 59 blows with the automatic hammer were needed to correlate with the 50 blow density of the manual hammer. The gyratory compactor used in this study had an average internal gyration angle of 1.23° and contact pressure of 600 kPa. A standard compaction level of 100 gyrations, a compaction level near the locking point and a compaction level below the locking point were used. This section includes the mix design volumetric properties from different compaction efforts, the draindown test results, and the discussion on these results.

4.2.1 Marshall Mix Design

The volumetric properties of SMA mixtures designed with the Marshall method are shown in Table 4.6. Crushed gravel (C.GVL), limestone (LMS), and lab granite (L.GRN) used a normal (N) gradation in the middle to coarse side of the gradation band (Table 3.1), while traprock (TRAP) and ruby granite (R.GRN) used a finer (F) gradation to keep the optimum asphalt content in a reasonable range.

TABLE 4.6 Marshall Mix Design Volumetric Properties¹ Summary

Agg.	NMAS	VCA _{drc} , %	Opt. AC, %	VMA, %	VCA _{mix} , %
C. GVL	19	40.7	6.5	17.7	34.1
	12.5	41.2	6.6	18.4	38.0
	9.5	41.5	6.6	18.0	35.9
L. GRN	19	39.4	6.3	18.0	34.5
	12.5	41.0	6.3	18.1	37.8
	9.5	41.4	6.3	17.7	35.8
LMS	19	41.7	6.1	17.8	34.6
	12.5	41.6	5.9	17.4	37.5
	9.5	41.1	5.8	17.1	35.6
R. GRN	19	41.1	6.7	18.4	36.4
	12.5	42.1	6.4	18.0	39.0
	9.5	42.0	6.8	18.7	37.8
TRAP	19	42.4	6.5	19.0	37.6
	12.5	42.1	6.3	18.4	40.0
	9.5	42.1	6.6	19.1	39.2

1. Volumetric properties are based on 4.0 percent air voids by AASHTO T166 method.

For all fifteen designed SMA mixtures, the optimum asphalt contents were in a practical range of 5.8 to 6.8 percent based on 50 blow Marshall designs. Thirteen of fifteen mixtures had the optimum asphalt content greater than the general requirement of 6.0 percent minimum asphalt content. All VMA values were greater than the minimum value of 17.0 percent and ranged from 17.1 to 19.1 percent. Stone on stone contact was achieved for all designed SMA mixtures, as indicated by VCA_{mix} values being less than their corresponding VCA_{drc} values. The volumetric property results confirmed the gradations chosen for all aggregate types were reasonable.

4.2.2 Gyratory Mix Design

4.2.2.1 Locking points

The standard gyration level used was 100 gyrations since this is the level typically specified. The lower gyration level was selected based on the locking point concept (4, 66). Based on the compaction information obtained from the 100 gyrations mix design,

the first occurrence of a gyration number that gave a change in height less than 0.1 mm for two successive gyrations was recorded as the locking point. For each mixture, three samples were compacted as replicates at each trial asphalt content, and up to four trial asphalt contents were used in the SMA mix design. For each mixture, the average locking point is provided in Table 4.7. The average locking point for each mix ranged from 51 gyrations to 63 gyrations.

To equal or exceed the locking points for all mixtures, 65 gyrations was selected as the comparative lower compaction level. For comparison, a third level of 40 gyrations that represents a level below the locking point was used to design two 12.5 mm NMAS SMA mixtures, with lab granite and ruby granite aggregate sources.

TABLE 4.7 Locking Point Results Summary

<i>Aggregate</i>	<i>NMAS</i>	<i>Gradation</i>	<i>Number of Samples</i>	<i>Locking Point, gyrations</i>	
				<i>Average</i>	<i>St. Dev</i>
C.GVL	19	N	12	57	4.8
	12.5	N	9	57	4.0
	9.5	N	9	51	5.1
L.GRN	19	N	12	61	6.4
	12.5	N	12	61	2.9
	9.5	N	6	59	2.4
LMS	19	N	9	62	4.7
	12.5	N	12	63	3.7
	9.5	N	9	59	5.3
R.GRN	19	N	9	59	2.5
	12.5	N	12	56	3.5
	9.5	N	12	53	4.8
TRAP	19	N	12	54	4.1
	12.5	N	12	53	5.0
	9.5	N	12	52	3.5
R.GRN	19	F	9	55	3.8
	12.5	F	9	56	4.8
	9.5	F	12	57	2.7
TRAP	19	F	9	55	3.5
	12.5	F	6	54	5.1
	9.5	F	6	55	3.2

A histogram of locking point results for all 210 mix design samples (including 69 samples for ruby granite and traprock with the N gradation) with 100 gyrations is shown in Figure 4.1.

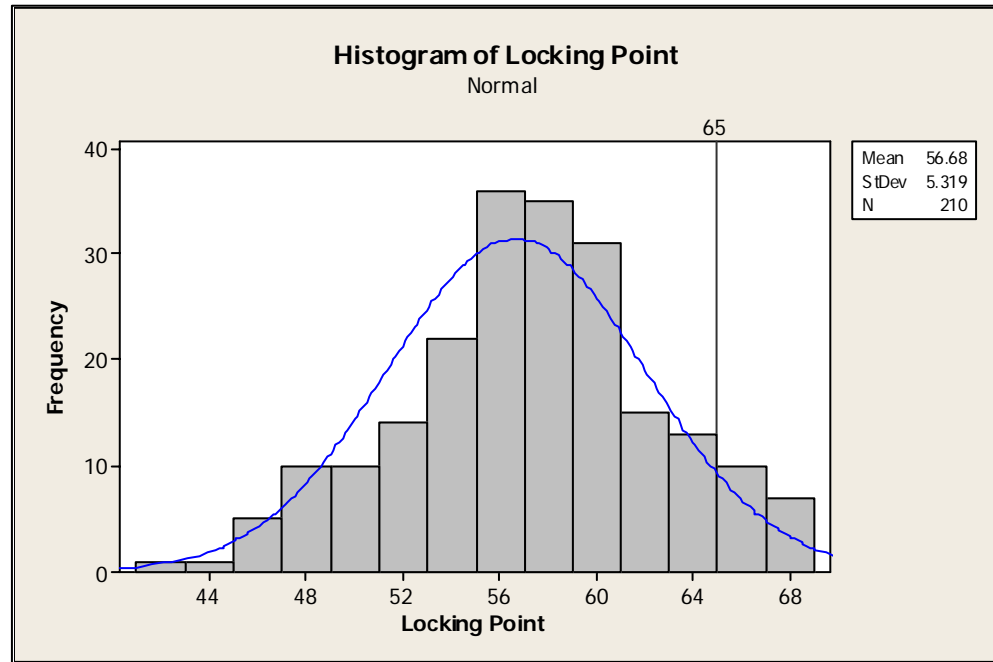


FIGURE 4.1 Histogram of locking point results.

As shown in Figure 4.1, the locking point results had an average of 57 gyrations and a standard deviation of 5.3 gyrations. If a normal distribution is assumed, the 65 gyrations provided about 95 percent confidence level to cover the locking point of designed SMA mixtures.

A forward stepwise regression was employed to evaluate the influencing factors on locking point results. The factors evaluated include aggregate properties (L.A. abrasion, uncompacted air voids for coarse aggregates -- represents coarse aggregate angularity or CAA, FAA, F&E content), NMAS, and asphalt content. The regression results are shown in Table 4.8.

TABLE 4.8 Forward Stepwise Regression Results for Locking Point

Step	1	2	3	4	5	6
Constant	79.96	160.95	155.27	172.2	181.37	180.62
AC	-3.74	-3.15	-2.33	-1.84	-1.68	-1.67
T-Value	-7.95	-6.57	-4.43	-3.4	-3.03	-3.02
P-Value	0.000	0.000	0.000	0.001	0.003	0.003
CAA		-1.78	-1.85	-2.23	-1.66	-1.5
T-Value		-3.92	-4.18	-4.92	-2.72	-2.36
P-Value		0.000	0.000	0.000	0.007	0.019
L.A			0.17	0.284	0.303	0.278
T-Value			3.42	4.56	4.76	4.03
P-Value			0.001	0.000	0.000	0.000
F&E				-0.197	-0.16	-0.1
T-Value				-2.95	-2.22	-1.05
P-Value				0.004	0.028	0.296
FAA					-0.79	-0.98
T-Value					-1.37	-1.6
P-Value					0.173	0.111
NMAS						0.1
T-Value						0.95
P-Value						0.341
S	4.67	4.52	4.4	4.32	4.31	4.32
R-Sq	23.31	28.62	32.46	35.2	35.79	36.08
R-Sq(adj)	22.95	27.93	31.47	33.94	34.22	34.19
Mallows C-p	37.5	22.7	12.5	5.8	5.9	7

As shown in Table 4.8, four factors are significant with the significant level of 95 percent ($\alpha=0.05$) and the regression equations are shown in Equation 4.1:

$$LP = 172 - 1.84AC + 0.284L.A. - 2.23CAA - 0.197F \& E \quad (R^2 = 0.352) \quad (4.1)$$

From regression equation 4.1, the locking point value is associated with four factors, while it still has a relatively low coefficient of determination ($R^2=0.352$). Any prediction based on an equation with such a low coefficient of determination is likely to have significant error. However, this equation did show some interesting trends about how these factors affect the locking point.

With the increase of asphalt content, the locking point tends to decrease. This is likely due to the increased amount of asphalt providing a better lubrication of aggregates during compaction, resulting in quicker compaction. With the increase of L.A abrasion loss value, the locking point tends to increase. This is likely due to the breaking of aggregate associated with high L.A abrasion causing additional densification thus a higher locking point. The aggregate breakdown during compaction is found to have good correlation with L.A abrasion value, and will be shown in a later section. With the increase of uncompact air voids for coarse aggregates (CAA) and F&E content, the locking point tends to decrease. This is not as expected. It is believed that more angular aggregates are more difficult to be compacted and therefore should have higher locking points. This misleading result in equation 4.1 is likely due to the limited range of CAA values (from 46.6 to 48.5%), and high variability or low coefficient of determination value in the regression model.

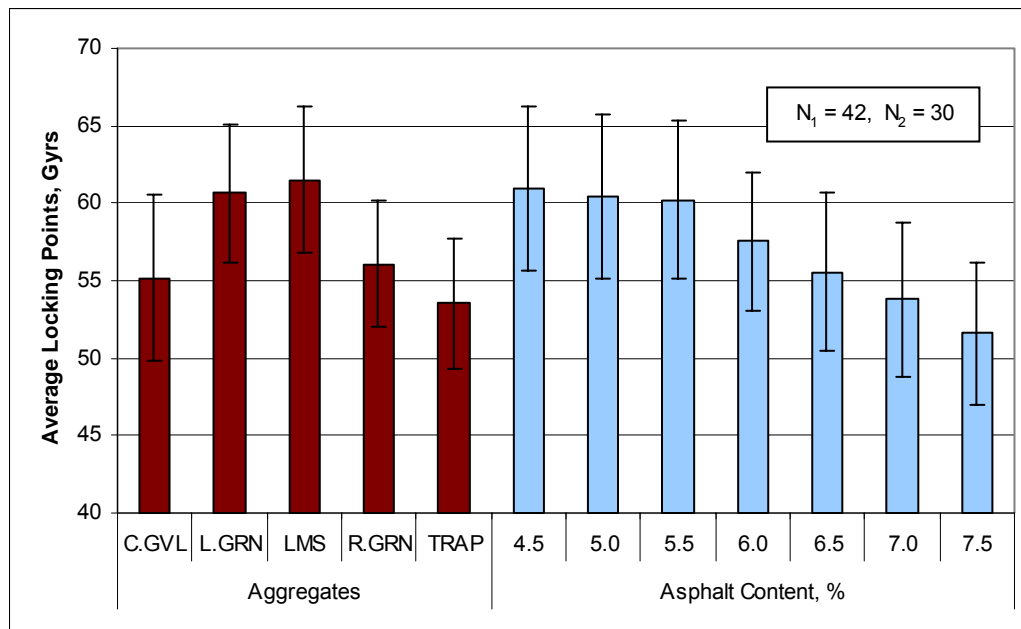


FIGURE 4.2 Average locking point results.

The average locking points for different aggregate types and different asphalt contents are shown in Figure 4.2. N_1 and N_2 represent the number of samples used for average for each group. Error bars that stand for one standard deviation of results are also shown in the graph.

For different aggregates, the average locking point varied from about 54 to 62 gyrations. Limestone and lab granite had high average locking points which were more than 60 gyrations, while crushed gravel and traprock had low average locking points which were equal or less than 55 gyrations. The difference in average locking point for different aggregates is likely due to the difference in aggregate L.A. abrasion value and asphalt content range. For example, the limestone and lab granite had high locking points, which is likely due to combination effects of low asphalt contents (average of 5.3 percent versus 6.3 percent for the other three aggregates, as shown in Table 4.9) and high L.A abrasion value (average of 32.3 percent versus 22.6 percent for the other three aggregates, as shown in Table 4.1).

As shown in the right side of Figure 4.2, with the increase of asphalt content from 4.5 to 7.5 percent, the average locking point dropped from about 61 to 52 gyrations. A close look at the effects of asphalt content on locking point is shown in Figure 4.3. There is a strong tendency that the locking point decreases with an increase of asphalt content. The regression in Figure 4.3 showed a significant higher coefficient of determination, R^2 , than the Equation 4.1, because the data used in Figure 4.3 are average values thus showing reduced variability.

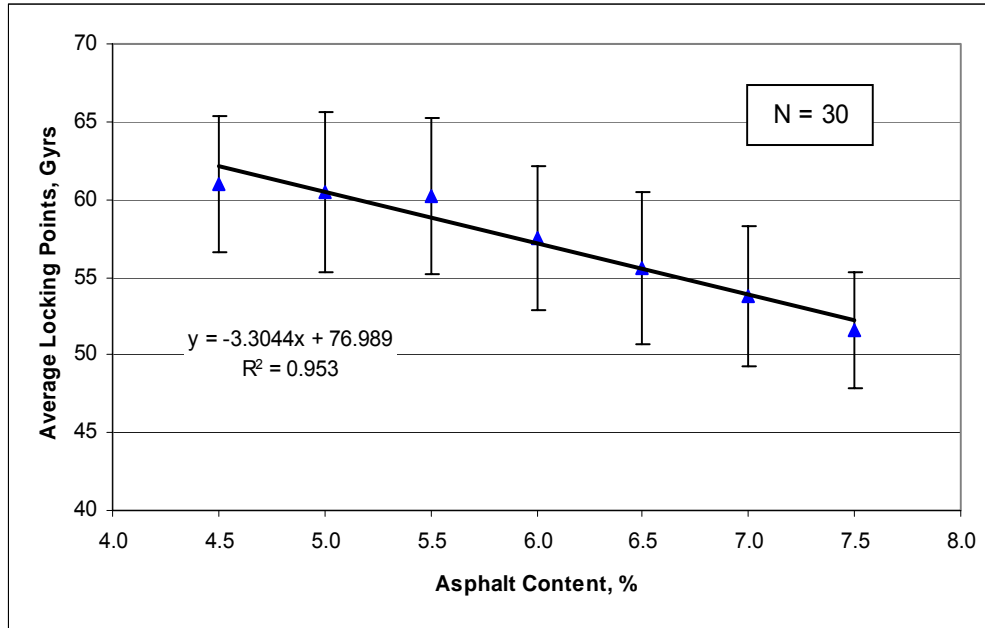


FIGURE 4.3 Average locking point values versus asphalt content.

4.2.2.2 Gyratory mix design results

The volumetric properties of designed SMA mixtures using the SGC at 100, 65, and 40 gyrations levels are shown in Tables 4.9, 4.10 and 4.11, respectively. As expected, a lower design compaction level resulted in higher optimum asphalt contents and higher VMA values. SMA mixtures designed with 100 gyrations had optimum asphalt contents ranging from 4.8 to 6.7 percent, and VMA ranging from 15.0 to 19.3 percent. SMA mixtures designed with 65 gyrations had optimum asphalt contents ranging from 6.0 to 7.2 percent, and VMA ranging from 17.4 to 20.0 percent. SMA mixtures designed with 40 gyrations had optimum asphalt contents of 7.2 and 7.5 percent, and VMA of 20.0 and 20.2 percent for lab granite and ruby granite, respectively.

TABLE 4.9 100 Gyration Mix Design Volumetric Properties¹

Aggregate Type	NMAS, mm	VCA _{drc} , %	Opt. AC, %	VMA, %	VCA _{mix} , %
C.GVL	19	40.7	5.8	16.4	33.0
	12.5	41.2	6.4	17.7	37.4
	9.5	41.5	6.2	17.3	35.5
L.GRN	19	39.4	4.8	15.0	32.1
	12.5	41.0	5.4	16.2	36.4
	9.5	41.4	5.7	16.6	34.9
LMS	19	41.7	5.1	15.4	32.6
	12.5	41.6	5.5	16.6	36.9
	9.5	41.1	5.3	16.1	34.9
R.GRN	19	41.1	6.2	17.5	37.6
	12.5	42.1	6.0	17.1	38.9
	9.5	42.0	6.7	18.9	37.0
TRAP	19	42.4	6.7	19.3	39.5
	12.5	42.1	6.1	17.9	40.5
	9.5	42.1	6.5	18.7	37.7

1. Volumetric properties are based on 4.0 percent air voids by AASHTO T166 method.

TABLE 4.10 65 Gyration Mix Design Volumetric Properties¹

Aggregate Type	NMAS, mm	VCA _{drc} , %	Opt. AC, %	VMA, %	VCA _{mix} , %
C.GVL	19	40.7	6.6	18.0	34.3
	12.5	41.2	7.1	19.1	38.5
	9.5	41.5	6.5	18.0	35.9
L.GRN	19	39.4	6.0	17.4	34.0
	12.5	41.0	6.5	18.6	38.2
	9.5	41.4	6.6	18.5	36.4
LMS	19	41.7	6.0	17.6	34.4
	12.5	41.6	6.5	18.7	38.5
	9.5	41.1	6.1	17.9	36.2
R.GRN	19	41.1	6.6	18.3	38.0
	12.5	42.1	6.7	18.6	40.1
	9.5	42.0	7.2	19.8	37.7
TRAP	19	42.4	7.0	20.0	40.0
	12.5	42.1	6.5	18.9	40.9
	9.5	42.1	7.0	20.0	38.7

1. Volumetric properties are based on 4.0 percent air voids by AASHTO T166 method.

TABLE 4.11 40 Gyration Mix Design Volumetric Properties¹

Aggregate Type	NMAS, mm	VCA _{drc} , %	Opt. AC, %	VMA, %	VCA _{mix} , %
L. GRN	12.5	41.0	7.2	20.0	39.2
R. GRN	12.5	42.1	7.5	20.2	41.3

1. Volumetric properties are based on 4.0 percent air voids by AASHTO T166 method.

As shown in Table 4.9, all mixtures using lab granite and limestone can not meet the volumetric property requirements for SMA when designed with 100 gyrations. The discussion for this result is shown in the next section.

4.2.3 Effects of Compaction on Volumetric Properties

The volumetric properties of SMA mixture are critical to ensure its structural properties and durability. The requirement of minimum asphalt content and minimum VMA is to ensure the durability of SMA mixtures. The requirement of VCA ratio is to ensure the stone-on-stone contact and eliminate possible unstable mixtures.

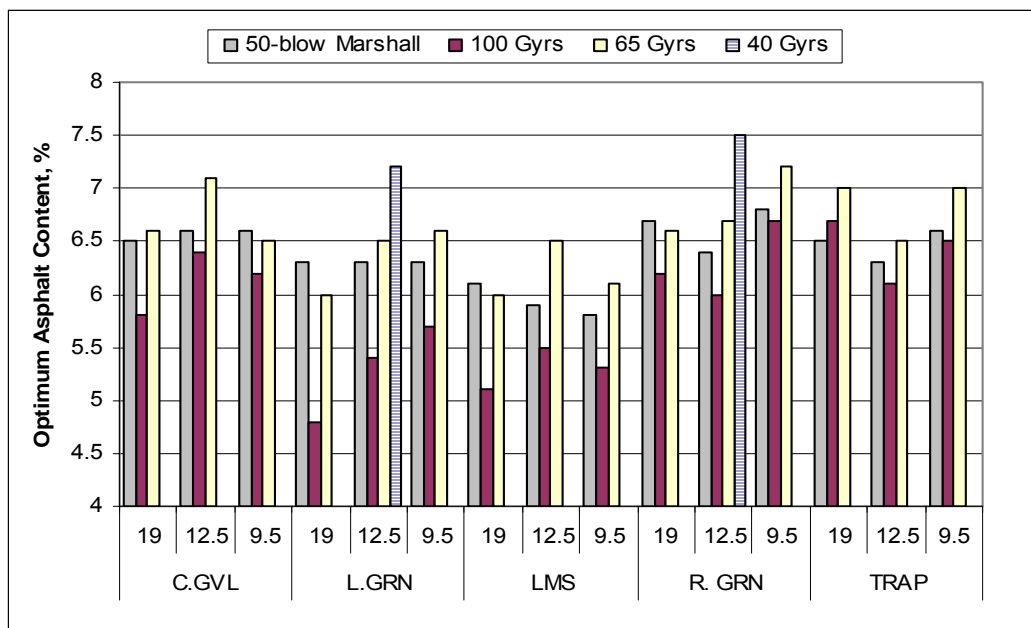


FIGURE 4.4 Comparison of optimum asphalt content.

The side by side comparison of different compaction efforts on optimum asphalt content is shown in Figure 4.4. As shown in the Figure, going from 100 to 65 gyrations resulted in an average 0.7 percent increase in optimum asphalt content. For individual comparison the increase ranged from 0.3 percent to 1.2 percent. Going from 65 to 40 gyrations for lab and ruby granite 12.5 mm NMA mixtures resulted in 0.7 and 0.8 percent increase in optimum asphalt content, respectively. SMA mixtures designed with 65 gyrations had an average of 0.2 percent higher optimum asphalt content than those designed with Marshall compaction. Higher asphalt content is believed to provide more durability for SMA mixtures as long as the mixtures maintain stability and rutting resistance.

Also shown in Figure 4.4, all SMA mixtures designed with 65 gyrations met the general requirement for minimum asphalt content of 6.0 percent. However, only 8 of 15 (53 percent) mixtures designed with 100 gyrations met this requirement. Even with L.A abrasion values less than 30, the three mixtures using limestone designed with 100 gyrations all failed this minimum asphalt content requirement. For example, limestone with 19 mm NMA by 100 gyrations had an optimum asphalt content of 5.1 percent. The gradation used for this mixture was N gradation, which is near the lower limit of the gradation band in SMA design guides (N gradation with 19 mm NMA has 20 percent passing the 4.75 mm sieve, and 8 percent passing the 0.075 mm sieve). So there was no space to adjust the gradation in order to increase the optimum asphalt content, which means if 100 gyrations is used, SMA mixtures designed with limestone aggregate will not meet the design requirements. For the same aggregate and same gradation, when the

compaction level dropped to 65 gyrations, the optimum asphalt content increased to 6.0 percent and was able to meet the minimum asphalt content requirement.

From Figure 4.4, one can also observe that ruby granite and traprock were less sensitive to compaction level than the other three aggregates. For ruby granite and traprock, going from 100 to 65 gyrations resulted in an average 0.5 percent increase of optimum asphalt content, while the other three aggregates had an average 0.9 percent increase. This may be explained by the fact that these two aggregates had lower L.A. abrasion values, and used finer gradations than the other three aggregates. For these two aggregates, the additional 35 gyrations would be expected to break less aggregate, therefore, resulting in less change in optimum asphalt content.

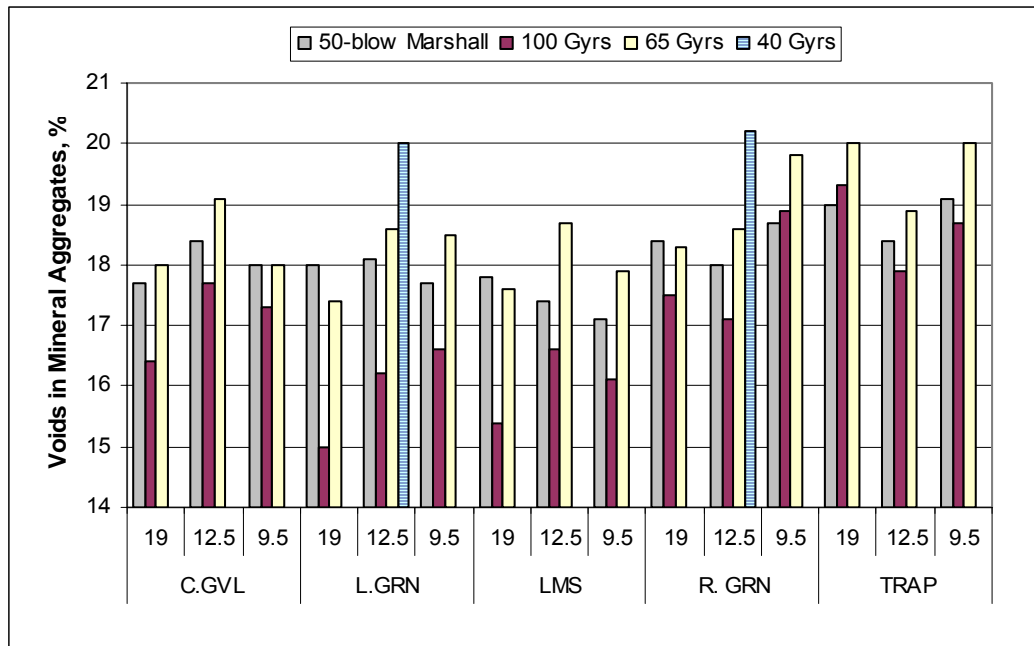


FIGURE 4.5 Comparison of VMA for various compaction levels.

The side by side comparison of different compaction efforts on VMA value is shown in Figure 4.5. VMA comparison results showed very similar observations as optimum asphalt content results. Going from 100 to 65 gyrations resulted in an average

1.5 percent increase in VMA. All SMA mixtures designed with 65 gyrations met the minimum VMA requirement of 17 percent for SMA mixture, while only 8 of 15 (53 percent) of mixtures designed with 100 gyrations met this requirement. All mixtures designed with the Marshall method also met this minimum VMA requirement, and had an average 0.5 percent less than those designed with 65 gyrations.

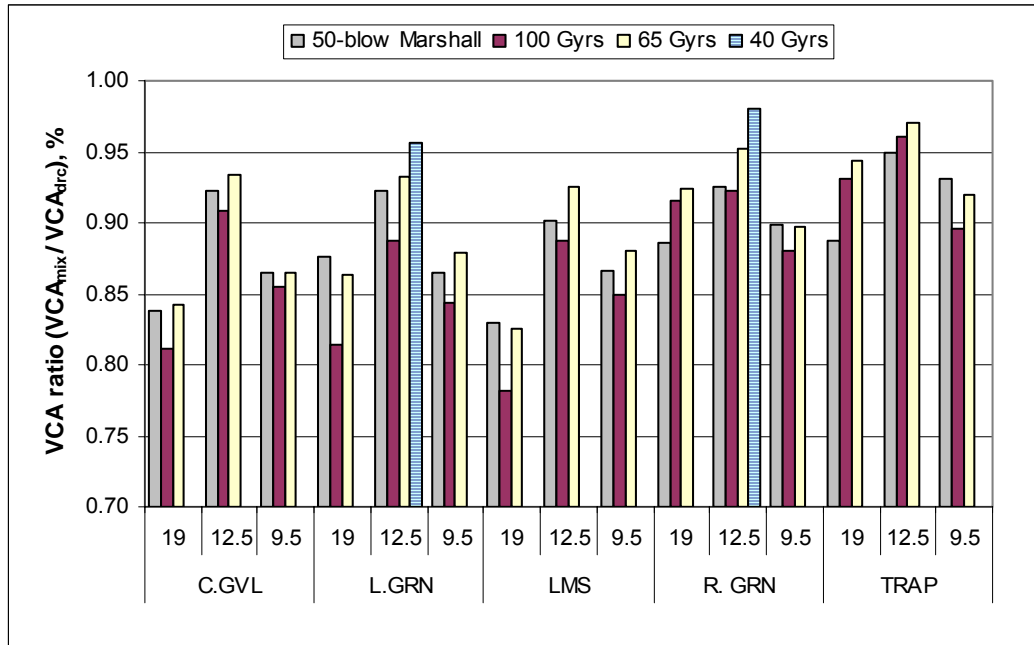


FIGURE 4.6 Comparison of VCA ratio for various compaction levels.

The side by side comparison of different compaction efforts on VCA ratio is shown in Figure 4.6. As shown in Figure 4.6, all designed SMA mixtures have the VCA ratio less than one, which indicates that stone-on-stone contact existed for all designed mixtures. The VCA ratios for Marshall compaction are similar to those compacted with 65 gyrations. The VCA ratio decreases with the increase of gyration level, which indicates the coarse aggregate skeleton gets tighter with the additional compaction. However, additional aggregate breakdown with the high compaction level will also result

in the actual aggregate gradation getting finer and therefore the calculated VCA ratio based on the original gradation will be smaller than the actual VCA ratio.

In summary, in consideration of durability, the order from the best to the worst is 40 gyrations, 65 gyrations, 50 blow Marshall, and 100 gyrations. In consideration of rutting resistance, the order from the best to the worst may be the reverse ranking of durability. The present recommended gyration level is 100. If the performance test results support a lower level, this will be lowered to improve durability without affecting rutting potential.

4.2.4 Draindown Test Results

A lower compaction level tends to result in higher asphalt content; therefore draindown may be a concern for a low compaction level. The asphalt contents selected for draindown test were the highest optimum asphalt contents resulting from all compaction efforts. Two replicate tests were conducted for each mixture.

During testing of the different mixes, it was noted that aggregate particles were able to fall through the wire mesh onto the plate when using the standard ¼ inch (6.3 mm) mesh basket. Some fine aggregate particles that fell through the openings of the basket were counted as draindown following the test procedure AASHTO T305 (25). This phenomenon became more common when smaller NMAS mixtures were tested, and resulted in relatively high draindown results for 9.5 mm NMAS mixtures. The draindown test results are summarized in Table 4.12.

TABLE 4.12 Draindown Test Results Summary

Aggregate Type	NMAS, mm	Asphalt Content, %	Percent Draindown, %	St. Dev of Draindown, %
C.GVL	19	6.6	0.028	0.017
	12.5	7.1	0.126*	0.023
	9.5	6.5	0.170*	0.106
L.GRN	19	6.0	0.029	0.041
	12.5	7.2	0.047	0.001
	9.5	6.6	0.283*	0.014
LMS	19	6.0	0.073	0.057
	12.5	6.5	0.084	0.039
	9.5	6.1	0.212*	0.061
R.GRN	19	6.6	0.167*	0.135
	12.5	7.5	0.118*	0.022
	9.5	7.2	0.059	0.005
TRAP	19	7.0	0.020	0.006
	12.5	6.5	0.020	0.005
	9.5	7.0	0.060	0.028

* Aggregate particles were observed in the plate, and counted as draindown.

As shown in Table 4.12, the draindown results ranged from 0.02 to 0.28 percent.

The results showed high variability because some aggregate particles were included as draindown. Even without the correction, all draindown results met the maximum limit of 0.3 percent as required in the SMA design specifications (44). Therefore, in terms of the draindown test requirement, all compaction levels including 40 and 65 gyrations are satisfactory for all the mixtures evaluated in this study. The use of modified asphalt binder and 0.3 percent cellulose fiber effectively prevents the draindown problem. If fiber was not used, the draindown amount would almost certainly be a problem.

4.3 AIR VOID CONTENT MEASUREMENT

The amount of air voids is one of the most important mixture properties evaluated in this study. Accurate determination of air void content is critical to ensure proper mix design, and to provide a pavement with good performance and durability. For this research, air voids were measured in two commonly used methods: the SSD method following

AASHTO T166 (25) and the vacuum seal method following ASTM D 6752 (47). The comparison of the test results by using these two test methods and the effects on mix design volumetric properties were analyzed and evaluated. In addition, the air void results of whole samples and cored-and-sawn triaxial samples are also included in this section. An error with the software for the CoreLok method was identified and a further study on direct calculation based on the original concept of vacuum sealing method for CoreLok results was also conducted to provide a better method of making correction factors. Some guidance was provided to let the user know when each method should be used.

Four different air voids were used in this study relating to the vacuum sealing method:

- 1) CoreLok air voids, which is calculated by the CoreGravity™ program created by IntroTEK, Inc (110). This air voids reflects the embedded correction by the program, and it is generally known as the air voids by the CoreLok method.

- 2) Corrected CoreLok air voids, which is CoreLok air voids with additional correction factor. This correction factor is determined by the difference between the SSD and CoreLok air voids using a sample with low air voids.

- 3) Uncorrected vacuum sealing air voids, which is a calculation based on the concept of vacuum sealing test method without any corrections.

- 4) Corrected vacuum sealing air voids, which is a vacuum sealing air voids with a correction factor. The correction factor is determined by the difference between the SSD and uncorrected vacuum sealing air voids using a sample with low air voids and similar surface condition.

These air voids will be discussed in detail later and used throughout this section.

4.3.1 Concepts of Air Voids

As discussed in the literature review and the test procedure, air voids is defined as the total volume of the small pockets of air between the coated aggregate particles throughout a compacted paving mixture, expressed as a percent of the bulk volume of the compacted paving mixture. The value of air voids depends on the bulk specific gravity G_{mb} and the measured theoretical maximum specific gravity G_{mm} . Hence accurate measurement of G_{mb} and G_{mm} is very important in the calculation of air voids in a mixture. This report will provide a detailed discussion concerning measurement of G_{mb} .

There are several different methods to measure the bulk specific gravity G_{mb} . The difference between various methods is primarily due to the different methods of measuring sample volume since the sample mass can be measured very accurately.

Figure 4.7 (49) illustrates volumes and air voids that are associated with compacted HMA. Each of the diagrams within Figure 4.7 are divided into halves with each half representing the volumes and air voids of mixes with coarse and fine gradations.

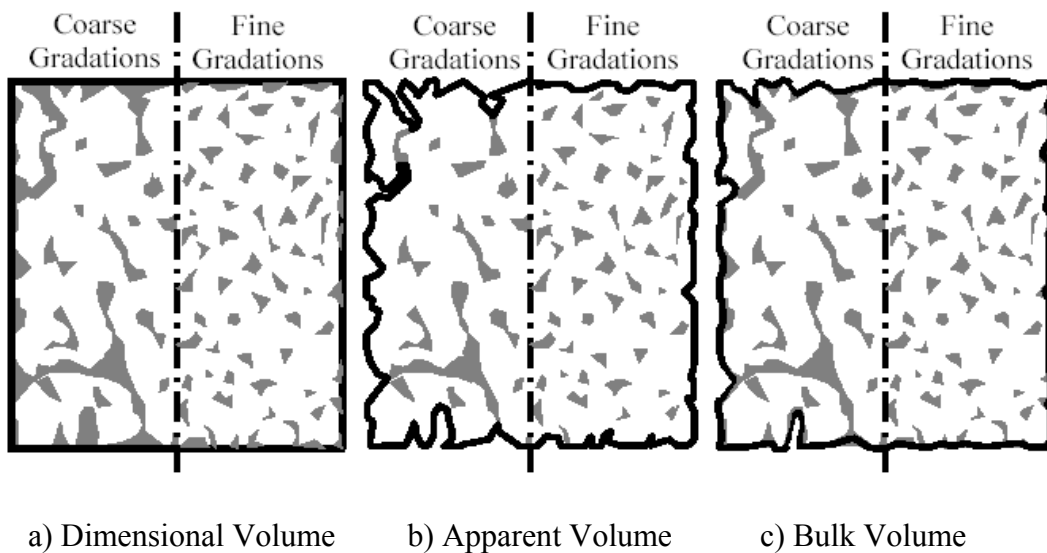


FIGURE 4.7 Volumes associated with compacted HMA (49).

The dark black line in Figure 4.7a shows the volume that is associated with the dimensional procedure. This volume includes any surface irregularities on the outside of the sample and thus overestimates the internal air void content. Figure 4.7b illustrates the apparent volume of compacted HMA samples. This volume can be calculated by the difference of dry weight and submerged weight of sample based on Archimedes' Principle. This calculated volume does not include any of the surface irregularities on the sample or the air voids that are interconnected to the surface. Water that infiltrates the sample through the interconnected surface voids is not considered a portion of the sample volume. Therefore, the apparent volume underestimates the sample's true internal voids. This problem is more prevalent with mixes having coarser gradations, as there are more voids interconnected to the surface of the sample. Figure 4.7c illustrates the bulk volume determined from the SSD method. The difference between the bulk and apparent volume is that the bulk volume includes the voids that are interconnected to the surface. This is accomplished by using the SSD weight instead of dry weight when using the Archimedes' Principle to calculate the sample volumes. Therefore, the volume of water retained in the sample at the SSD condition is included as internal voids. The bulk volume lies between the dimensional and apparent volumes and is desired for HMA volumetric calculations.

The CoreLok and SSD methods both attempt to determine the bulk volume of the HMA sample. A high amount of surface texture makes it more difficult to differentiate between mixture air voids and surface texture for the vacuum sealing method, because much of the surface texture in some HMA samples, especially in SMA samples, lies within the pore space rather than the outer geometrical area. The texture does not increase

the internal air voids, however, it may result in a higher measured air voids. The rate and extent of water penetration into SMA mixtures during the SSD test depend not only on the total air voids content but also on the actual void size inside the mixture. It is easier for water to enter into and drain out from SMA mixture during the SSD test due to large voids with a higher percentage of coarse aggregate particles. Water draining from the large interconnected voids within SMA mixtures leads to a lower SSD weight, or lower calculated sample volume. Consequently it becomes difficult to define the volumetric properties of compacted SMA mixtures if the voids are high. If the voids are low one can get an accurate measure of air voids by weighing the sample in air and water. Since it is not possible to know the true sample volume, one can never accurately know the true air void content. However, the most accurate, repeatable, and feasible method to measure the true volume should be determined and adopted. The volumetric requirements should be specified based on this most accurately measured volume.

For the SSD test procedure, the water draining out of compacted samples with high air voids could result in a lower SSD weight of the sample, therefore resulting in a lower calculated sample volume and higher calculated bulk specific gravity. Therefore, the SSD method may only be accurate for a certain air void range, which is also affected by mixture type. For the CoreLok test method, the bridging effect of high surface texture (the plastic bag can't tightly conform to rough sample surface due to bag stiffness and not unlimited vacuum pressure) may result in higher enclosed volume than the true sample volume, therefore a proper correction factor is needed to reduce this measured volume and increase the calculated bulk specific gravity.

4.3.2 Comparison of Two Test Methods

The air void content of compacted SMA mixture samples including the Marshall samples, SGC mix design samples, APA samples, triaxial testing (before and after coring) samples, were determined by using two methods, the SSD method and the vacuum seal (CoreLok) method. However, the SMA samples included in this analysis consist of SGC mix design samples only. The reason for using this part of the data is because of the wide distribution of air void content results, identical sample size, and all of these samples had permeability information, which is presented in section 4.4. The permeability information can be used as an indication of error potential for the SSD method.

The air void results for SMA mixtures are shown in Appendix Table A1 and in Figure 4.8. As shown in Figure 4.8, the air void content measured had a range from 1.1 to 8.0 percent by the SSD method, and a range from 1.6 to 10.9 percent by the CoreLok method. The Corelok air void results were calculated using the computer program CoreGravity™ created by IntroTEK, Inc. It is noteworthy that correction factors are applied in the program based on bag size and the ratio of sample weight and bag weight (110). For all the test results, the difference of these two methods ranged from 0.4 to 4.6 percent. The CoreLok method provided an average of 1.2 percent higher air voids than the SSD method. This is as expected, because the SSD method is likely to underestimate the air voids due to the water draining out problem while the CoreLok method is likely to overestimate the air voids due to high surface textures for the SMA samples. A true air void content is likely between the results from these two methods. For samples with low air voids, the error potential for the SSD method is limited and should provide a measurement of air voids close to the true value.

A paired t-test was employed to compare air void content results by using the CoreLok and SSD methods. Statistical results are shown in Table 4.13. There is a significant difference at the 95 percent confidence level between these two methods as indicated by a P-value equal to 0.000. Keep in mind that these 372 samples are lab compacted SMA samples with variable air voids.

TABLE 4.13 Paired T-Test for CoreLok and SSD air voids

	<i>N</i>	<i>Mean</i>	<i>StDev</i>	<i>SE Mean</i>
CoreLok	372	5.391	1.555	0.0806
SSD	372	4.200	1.199	0.0622
Difference	372	1.190	0.559	0.0290

95% CI for mean difference: (1.133, 1.247)

T-Test of mean difference = 0 (vs not = 0): T-Value = 41.08, P-Value = 0.000

A linear regression between the results of the two methods along with the R² value is shown in Figure 4.8. It is noticed that all the data points are above the equality line, which indicates the CoreLok air void content is higher than the air void content by the SSD method for all the tested samples.

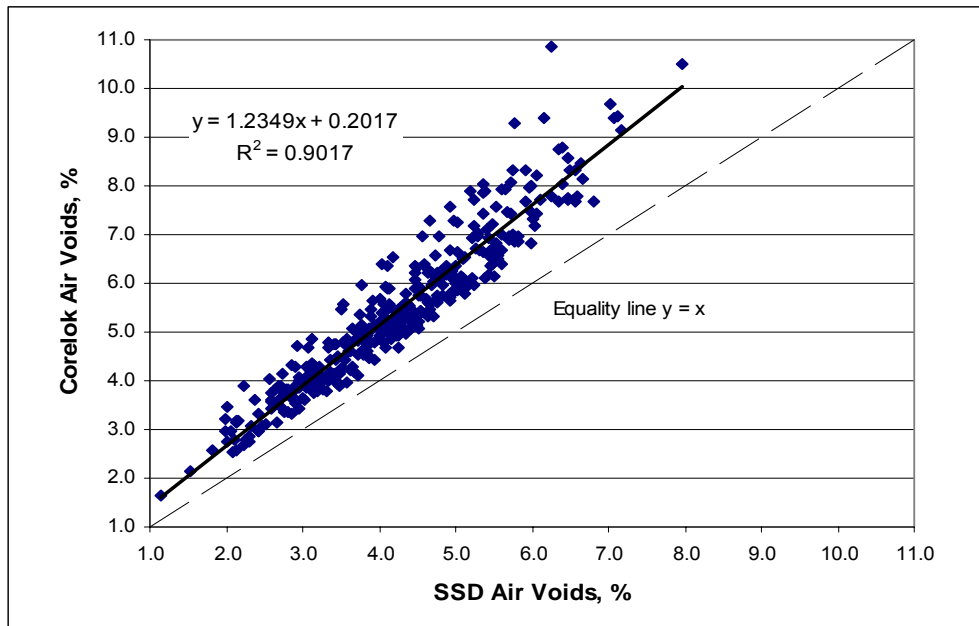


FIGURE 4.8 Comparison of the CoreLok and SSD air voids.

Also, the slope of the trendline is higher than one, which indicates that the difference between these two methods increases with an increase in air void content. This is likely due to the increasing error potential for the SSD method with an increase of air voids. For SMA samples with high air void contents, the water was observed to drain out of the samples quickly and a significant amount of water was retained on the scale after the SSD weight was measured. The SSD weight depends on how quick a sample can be patted to surface dry and be weighed, and it usually results in decreased calculated air void contents when compared to the actual air voids. This water draining problem is difficult to correct and resulted in higher test variability with the increase of air voids as shown in Figure 4.8.

A ratio of the air void contents by the CoreLok and SSD method is used for representing the difference between the two methods. A general linear model (GLM) analysis on this ratio was conducted to evaluate the effect of the main factors, such as aggregate type, asphalt content, NMA and air void content by SSD method. GLM is used because it can be used to analyze unbalanced test results. Statistical results are shown in Table 4.14.

TABLE 4.14 GLM for Influencing Factors on VTM Ratio

<i>Source</i>	<i>DF</i>	<i>Seq SS</i>	<i>Adj SS</i>	<i>Adj MS</i>	<i>F</i>	<i>P Value</i>
AGG. Type	4	0.112	0.025	0.006	1.05	0.384
NMA	2	1.775	0.482	0.241	39.82	0.000
Asphalt Content	6	0.140	0.039	0.006	1.07	0.387
VTM by SSD	253	2.390	2.390	0.009	1.56	0.005
Error	106	0.641	0.641	0.006		
Total	371	5.059				

From Table 4.14, the significant factors were NMA S and air void content by the SSD method based on a level of significance of 95 percent. The fact that NMA S was a significant factor is likely due to the different amount of air trapped in the surface texture of compacted samples, and the larger NMA S likely results in more connected internal air voids therefore resulting in higher permeability and higher error potential for the SSD method. The surface texture for three samples with different NMA S and similar air voids are shown in Figure 4.9. The average surface texture depths for these 19, 12.5, and 9.5 mm NMA S samples are 1.80, 1.55, and 1.36 mm following the sand patch method ASTM E965 (3), respectively. The fact that air void content was a significant factor indicated that water draining out of samples during the SSD test became a problem for the SMA samples with high air voids.



FIGURE 4.9 Surface textures for different NMA S mixtures.

Since the NMA S is a significant factor affecting the ratio of air void contents by the CoreLok and SSD methods, the air void content data was separated for three subsets based on the three NMA S. Linear regressions were conducted for these subsets of data respectively. The regressions along with the respective R-squares are shown in Figure 4.10.

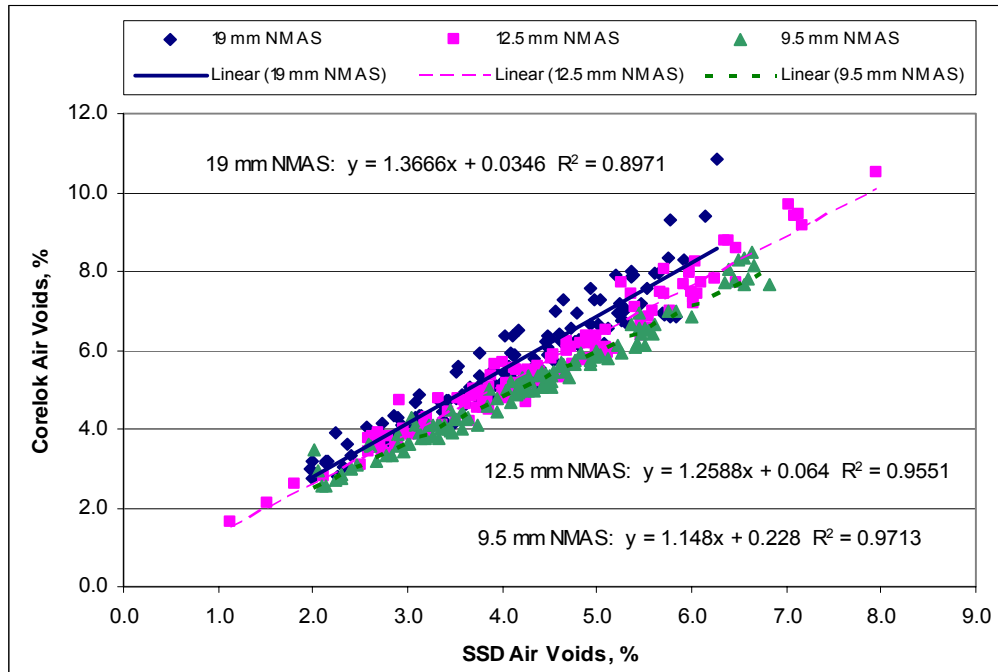


FIGURE 4.10 Relationships between the CoreLok and SSD air voids for three NMA.

One can observe from Figure 4.10 that slopes of these three trendlines are all larger than one, and the magnitude of these three slopes are in order of NMA. As expected, with the increase of NMA, the ratio of the slope of the two air void methods increases. This is likely explained in that with the increase of NMA, the surface macro-texture depth tends to get larger. In the meanwhile, the larger NMA results in a greater chance of internal air voids becoming connected to the surface at high air voids, and more bridging of surface texture by CoreLok bag. Therefore, the SSD method tends to underestimate the air voids because water drains out of samples quicker for larger NMA mixtures at a high air void level when determining the SSD weight, and the CoreLok method tends to overestimate the air voids because of more bridging for larger NMA mixtures with high coarse aggregate content. As a combined result, there is a bigger

difference between the CoreLok and SSD air voids for larger NMAS mixtures. For samples with high air voids, the error in the SSD method due to the water draining out problem is hard to correct, however, an appropriate correction factor can be determined for the CoreLok method if one assumes the surface texture for the mixture with various air voids is similar.

The difference between the CoreLok and SSD method versus air void content by SSD method for three NMAS is shown in Figure 4.11. It is noticeable that at the lowest air voids level (1.1 percent by the SSD method) of all the data, the difference between the two methods was still as high as 0.5 percent. It is believed that at low air void content, when mixtures are impermeable, these two methods should give similar results. If not, the SSD method is believed to be more reliable.

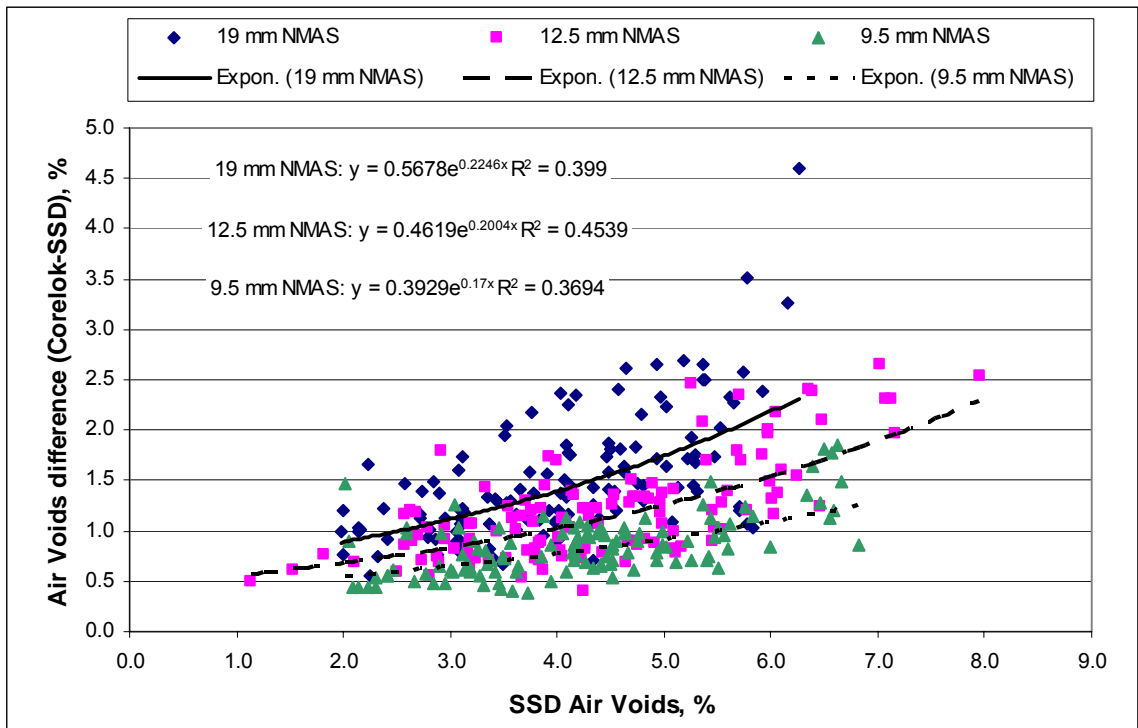


FIGURE 4.11 Air voids difference between the CoreLok and SSD method versus the SSD air voids.

To estimate the difference between the SSD and CoreLok method, a comparison was made between the two methods by using a steel cylinder 100 mm (4 in) in diameter × 63 mm (2.5 in) in height. The steel cylinder had a smooth surface and no internal voids connected to the surface. The G_{mb} result by the SSD method was considered to be very accurate since there was no voids in the cylinder. This resulted in G_{mb} and G_{mm} being equal for the cylinder. The calculated air void content by the CoreLok method was 0.6 percent based on the average of two replicates. This result indicates that there is not only an error for the CoreLok method for samples with rough surface textures (lab compacted SMA mixtures), but also for samples with very smooth surface and no internal voids (steel sample). The CoreLok air voids calculated by CoreGravity™ are not accurate for all types of tested samples. Since bag stiffness, vacuum pressure and bag sizes are standardized by the manufacturer and considered into the embedded correlation factors (110), the user should use caution when a new type of material is tested.

Another error may be introduced into the procedure if samples are not tested immediately or within a reasonable time frame. After vacuum sealing, the bags may relax and allow air to leak into the bags. Samples for this study were tested immediately after sealing so that this potential for error was minimized. Also, the sample weight before vacuum sealing and after submerging was compared. A weight gain more than 5 grams due to water penetration was considered excessive by the CoreGravity™ program and a new test was run after drying the sample.

Based on the trendlines and regression equations shown in Figure 4.11, the average difference between the two methods for three NMA SMA mixtures is approximately 0.5 percent when the air void content by the SSD method approaches zero.

Therefore, an additional correction factor of 0.5 percent was suggested for the CoreLok device used in this study since it was assumed the system error for all the NMAS and air voids levels was similar. The air voids with this additional correction factor are defined as corrected CoreLok air voids in this study.

From Figure 4.11, if the additional correction factor is applied to the CoreLok air voids, a difference between the two methods of more than one percent occurs for 19 mm NMAS samples with air voids greater than 4.3 percent, for 12.5 mm NMAS samples with air voids greater than 5.9 percent, and for 9.5 mm NMAS samples with air voids greater than 7.9 percent by the SSD method. The threshold air voids increase with the decrease of NMAS is likely due to the decreased permeability and error potential for the SSD method with lower NMAS mixture at the same air void level.

The difference between the SSD and CoreLok methods for SMA samples with low air voids indicate that the correlation factors embedded into the computer program CoreGravity™ seem insufficient for laboratory compacted SMA samples. A study on comparing uncorrected air voids by vacuum seal method and program corrected (CoreLok) air voids is necessary to provide a set of better correlation factors. The results and discussion are shown in section 4.3.5.

The CoreLok device was designed to aid in density determination of asphalt cores or laboratory specimens that are porous (water absorption during the SSD test is greater than 2 percent). However, even though all the samples used in this study had water absorption less than 2 percent, these two methods still showed a significant difference. This indicated that the allowable water absorption for using the SSD method should be a level less than 2 percent. A GLM analysis was conducted to determine the most

significant influencing factors on water absorption during the SSD test. As shown in Table 4.15, the NMAS and air void content are the two most significant influencing factors. This is as expected because the water absorption during the SSD test depends not only on the total air voids, but also on the actual void size inside the mixture. As shown in Figure 4.11, the mixture with higher NMAS has greater water absorption because of the larger void size.

TABLE 4.15 GLM for Influencing Factors on Water Absorption

Source	DF	Seq SS	Adj SS	Adj MS	F	P Value
AGG. Type	4	1.181	0.075	0.019	2.57	0.042
NMAS	2	0.353	0.116	0.058	7.99	0.001
Asphalt Content	6	2.974	0.057	0.009	1.30	0.264
VTM by SSD	253	8.805	8.805	0.035	4.79	0.000
Error	106	0.770	0.770	0.007		
Total	371	14.083				

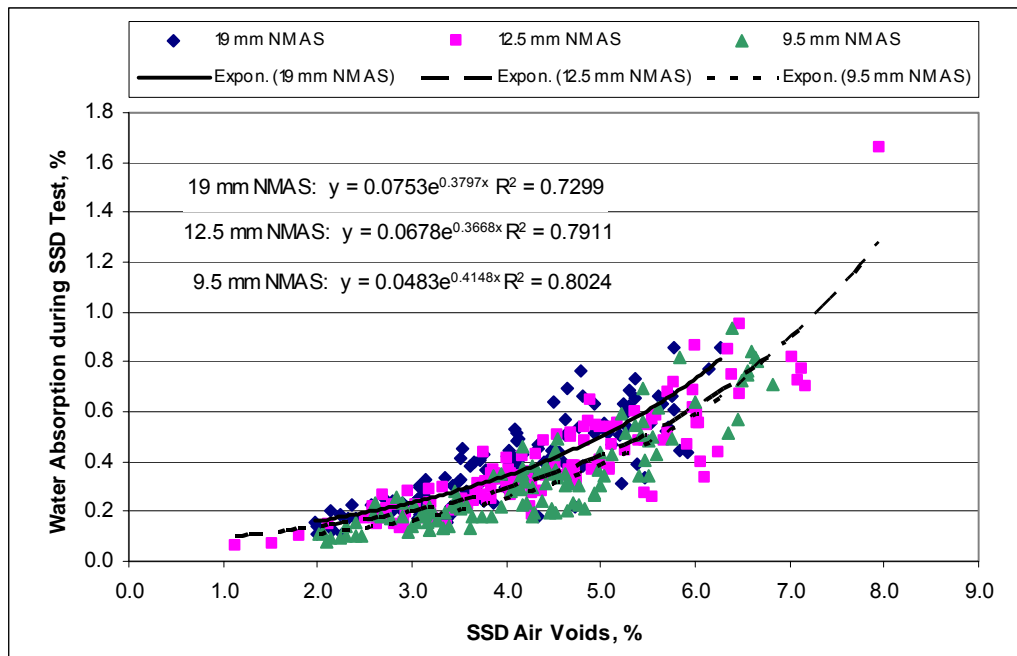


FIGURE 4.12 Relationships between absorbed water and air void content.

Figure 4.12 demonstrates the absorbed water during the SSD test procedure versus the air void content by the SSD method. As expected, the water absorption increased with an increase of air voids.

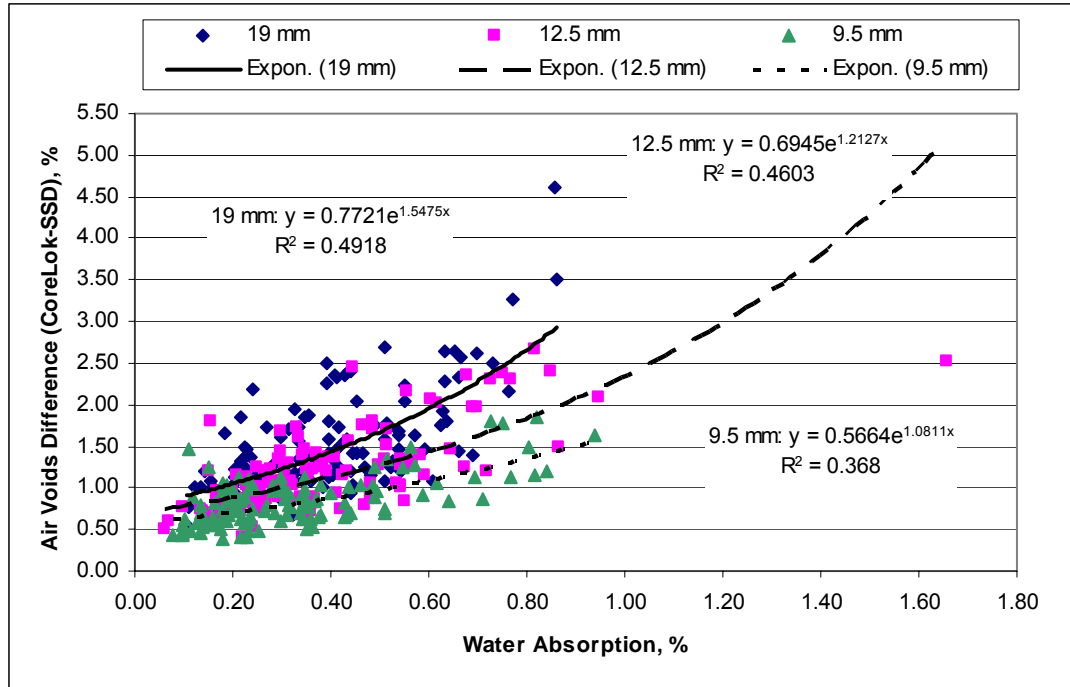


FIGURE 4.13 The difference between the CoreLok and SSD air voids versus absorbed water content.

Figure 4.13 combines some information from Figure 4.11 and 4.12. As shown in Figure 4.13, if the tolerance between Corrected CoreLok air voids and the SSD air voids is set as 1 percent (difference between the CoreLok and SSD air voids is 1.5 percent), the threshold water absorption values are 0.4, 0.6 and 0.9 for 19 mm, 12.5 mm and 9.5 mm NMAS mixtures, respectively. This concept is important because the absorbed water can quickly be determined by the SSD test, and used to indicate if a substantial error for the SSD method is occurring.

4.3.3 Effect on Mix Design Volumetric Properties

The measured air void content is the primary property used in the mix design process to select the optimum asphalt content. The difference in mix design volumetric properties by these two methods is summarized in Table 4.16.

Table 4.16 shows that there was as much as 0.8 percent difference in optimum asphalt content between the SSD and CoreLok method when the design air voids was set at the same level of 4 percent. The average difference in optimum asphalt content for the two methods was 0.45 percent. Figure 4.14 shows graphically the difference in optimum asphalt content by aggregate type and NMA for each of the two methods of determining G_{mb} . This amount of difference is significant because many State agents limit asphalt content to a range of 1 percent, for example California DOT requires the asphalt content within ± 0.5 percent of the target value. This study indicates that most of the asphalt content tolerance may be used just by the difference in G_{mb} measurement.

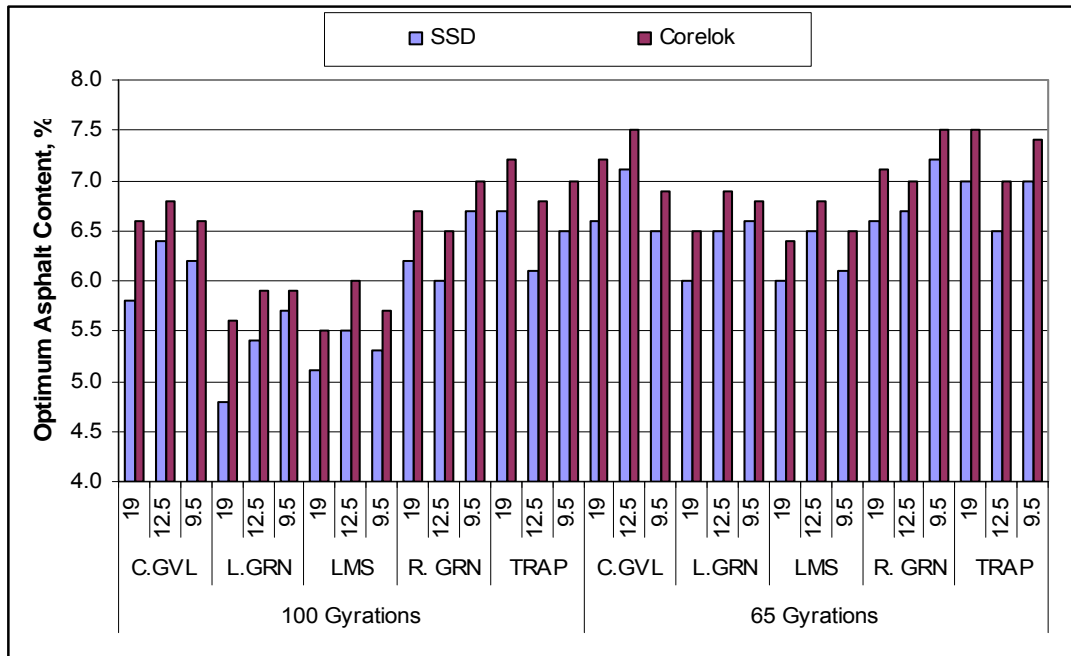


FIGURE 4.14 Effect of CoreLok and SSD methods on optimum asphalt content.

TABLE 4.16 Mix Design Volumetric Properties¹ Summary

Comp. Level	AGG.	NMAS	Grad.	AASHTO T166		CoreLok		Difference		
				Opt. AC	VMA	Opt. AC	VMA	Opt. AC	VMA	
100 Gyrs	C.GVL	19	N	5.8	16.4	6.6	18.0	0.8	1.6	
		12.5	N	6.4	17.7	6.8	18.5	0.4	0.8	
		9.5	N	6.2	17.3	6.6	18.0	0.4	0.7	
	L.GRN	19	N	4.8	15.0	5.6	16.6	0.8	1.6	
		12.5	N	5.4	16.2	5.9	17.3	0.5	1.1	
		9.5	N	5.7	16.6	5.9	17.2	0.2	0.6	
	LMS	19	N	5.1	15.4	5.5	16.6	0.4	1.2	
		12.5	N	5.5	16.6	6.0	17.7	0.5	1.1	
		9.5	N	5.3	16.1	5.7	16.8	0.4	0.7	
	R. GRN	19	F	6.2	17.5	6.7	18.6	0.5	1.1	
		12.5	F	6.0	17.1	6.5	18.3	0.5	1.2	
		9.5	F	6.7	18.9	7.0	19.5	0.3	0.6	
	TRAP	19	F	6.7	19.3	7.2	20.6	0.5	1.3	
		12.5	F	6.1	17.9	6.8	19.5	0.7	1.6	
		9.5	F	6.5	18.7	7.0	19.9	0.5	1.2	
	65 Gyrs	C.GVL	19	N	6.6	18.0	7.2	19.2	0.6	1.2
			12.5	N	7.1	19.1	7.5	19.9	0.4	0.8
			9.5	N	6.5	18.0	6.9	18.7	0.4	0.7
L.GRN		19	N	6.0	17.4	6.5	18.6	0.5	1.2	
		12.5	N	6.5	18.6	6.9	19.2	0.4	0.6	
		9.5	N	6.6	18.5	6.8	18.9	0.2	0.4	
LMS		19	N	6.0	17.6	6.4	18.5	0.4	0.9	
		12.5	N	6.5	18.7	6.8	19.3	0.3	0.6	
		9.5	N	6.1	17.9	6.5	18.6	0.4	0.7	
R. GRN		19	F	6.6	18.3	7.1	19.4	0.5	1.1	
		12.5	F	6.7	18.6	7.0	19.4	0.3	0.8	
		9.5	F	7.2	19.8	7.5	20.4	0.3	0.6	
TRAP		19	F	7.0	20.0	7.5	21.1	0.5	1.1	
		12.5	F	6.5	18.9	7.0	19.8	0.5	0.9	
		9.5	F	7.0	20.0	7.4	20.7	0.4	0.7	

1. Optimum asphalt content and VMA are based on 4.0 percent air voids.

Voids in mineral aggregate (VMA) is an important volumetric property specified in most mix design procedures. This property is defined as “the volume of intergranular void space between the aggregate particles of a compacted paving mixture that includes the air voids and volume of the asphalt not absorbed into the aggregates” (104). When the target air voids is chosen, VMA is an indication of the void space to be partially filled with asphalt binder. Therefore, a minimum VMA is needed to ensure the long-term durability and an upper limit is also desirable to prevent an unstable asphalt mixture.

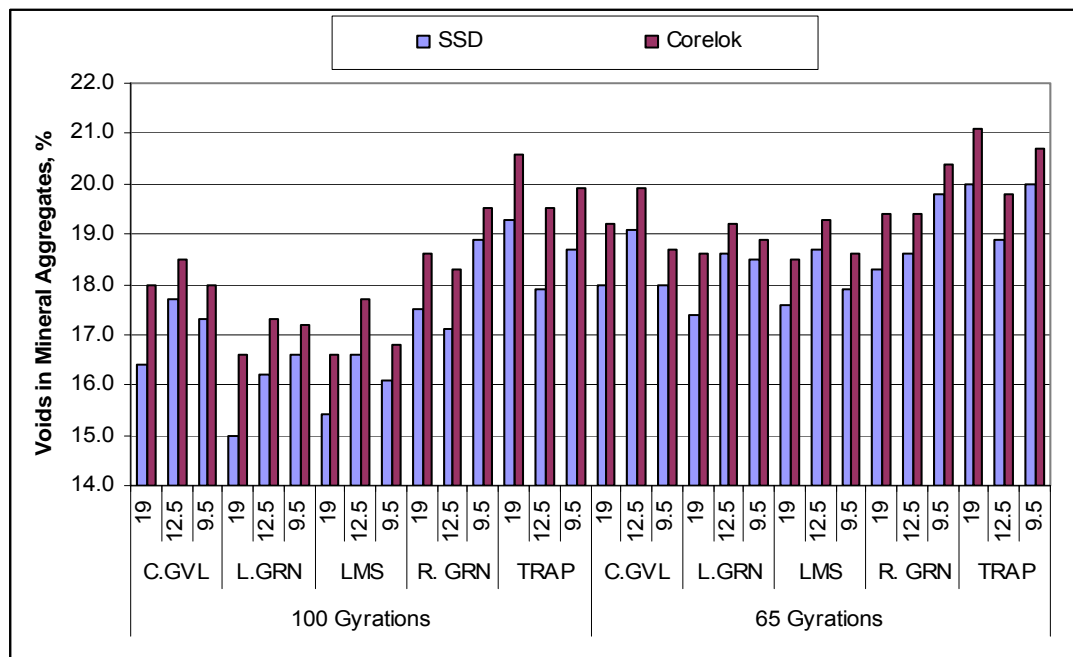


FIGURE 4.15 Effect of CoreLok and SSD methods on voids in mineral aggregate.

As shown in Figure 4.15, there is as much as 1.6 percent difference in calculated VMA depending on whether SSD or CoreLok method is used to determine G_{mb} of the specimens. This difference is critical because some agencies limit VMA to a range of 2 percent. In this study most of the VMA tolerance may be nullified just by the difference between G_{mb} measurements. Therefore, in determining VMA values, specifying agencies

must clearly define the method that is to be used for determining G_{mb} . The same test method should be followed throughout the mix design and quality control in construction. However, one test method may be more appropriate than the other for different types of mix or with different air void levels. The correction for CoreLok method will help to solve some of these problems. This study will recommend when a specific test method should be used based on the air voids, water absorption, and permeability data analysis.

As shown in Figures 4.14 and 4.15, the effects of the two test methods on these volumetric properties are greater for larger NMA mixtures. This is consistent with the greater difference in air void measurements for larger NMA mixtures.

4.3.4 Triaxial Test Sample Preparation

As expected, the cored samples for the triaxial test had different air void contents from the whole samples compacted by the SGC because of the significant difference in air voids in the middle of the compacted sample and that around the top, bottom and sides. The target air void content for the cored samples was 4.0 ± 0.5 percent by the SSD method. However, the target air void content for the whole samples had to be higher to provide 4.0 percent air voids in the cored sample, therefore a trial-and-error method was used. Based on some literature (86, 108), an initial air void level for the whole sample was targeted at around 5.5 percent. With the feedback of air voids of sawn-and-cored samples, the target air voids for the whole sample were adjusted. In order to get enough cored samples with air voids in range of 4.0 ± 0.5 percent, generally about 50 percent more samples were compacted. The samples with the closest air void contents to 4.0 percent and in good physical shape were selected to conduct the triaxial tests. A total of 277 samples were compacted and prepared for triaxial tests.

The air void content for all whole samples and cored samples were measured by both SSD and CoreLok method. The comparison of these two test methods for the whole samples is demonstrated in Figure 4.16.

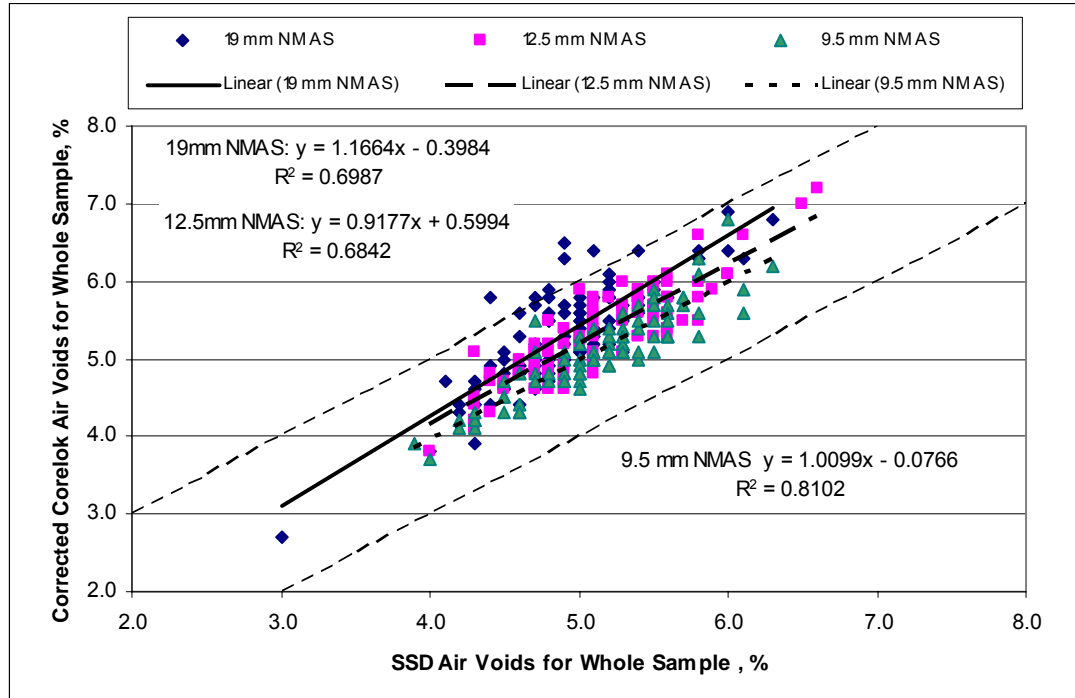


FIGURE 4.16 Corrected CoreLok and SSD Air Voids for Whole Samples.

As shown in Figure 4.16, after applying the 0.5 percent correction factor from the pervious discussion for CoreLok air voids, the difference between these two methods for 12.5 mm and 9.5 mm NMA SMA samples and most of 19 mm NMA SMA samples were less than 1 percent. This verifies that the 0.5% correction factor, which is developed using standard SGC samples of 115 mm in height, is applicable to the taller samples with about 170 mm in height. This also indicates that the correction factor mainly depends on the surface texture, and not the amount of air voids in the mixture. For 19 mm SMA samples, a higher correction factor is needed to bring all the data points within the 1 percent difference.

The comparison of the CoreLok and SSD method for the core samples is demonstrated in Figure 4.17. The air void results for the core samples showed a different trend from the whole samples prior to coring. This again verifies the significant effect of surface condition on the test results of the CoreLok method. The CoreLok results for the core samples were very similar to the results measured by the SSD methods. The difference between these two methods was within 1 percent for all the core samples.

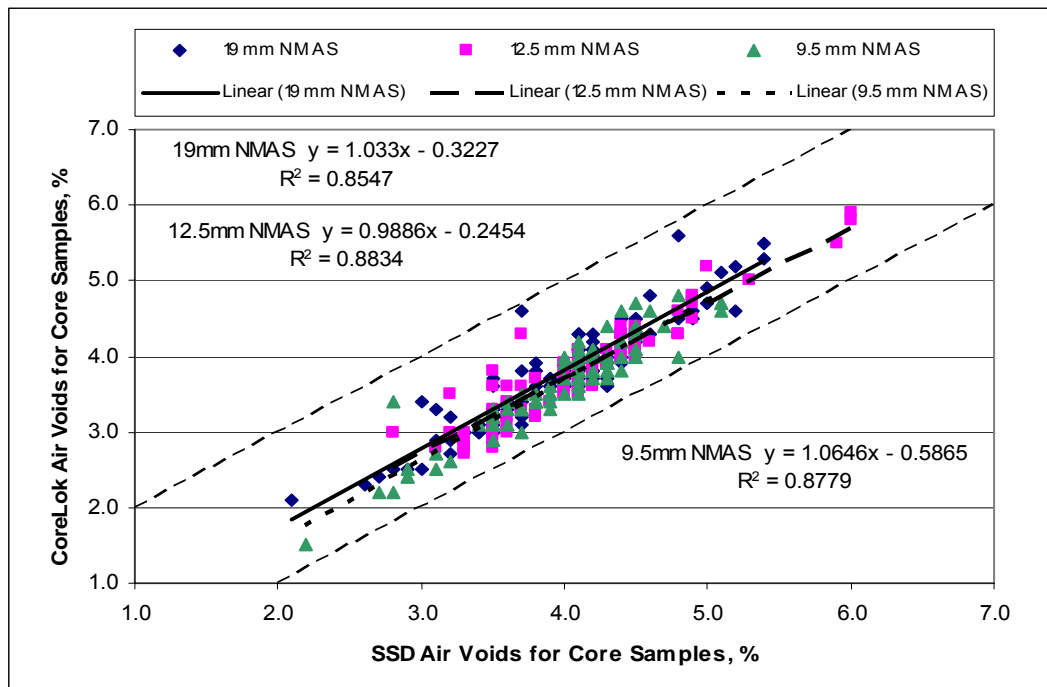


FIGURE 4.17 CoreLok and SSD air voids for core samples.

For samples with 4 percent air voids by the SSD method, the Coregravity™ program provided the air voids of 3.8, 3.7, and 3.7 percent for 19 mm, 12.5 mm, and 9.5 mm cored SMA mixtures. It is important to say that all lines plotted on top of each other and the SSD and corelok voids were very similar. The cored sample is smooth therefore the effect of surface texture is removed. This indicates that the accuracy of CoreLok method mainly depends on the surface condition regardless of NMA. The significance

of NMAS for lab compacted samples is likely due to difference in surface texture provided by different NMAS. The correlation factor embedded in the CoreGravity™ program (Appendix B) seems to work well on core samples; therefore no additional correction factor was needed for the air voids results calculated by the CoreGravity™ program.

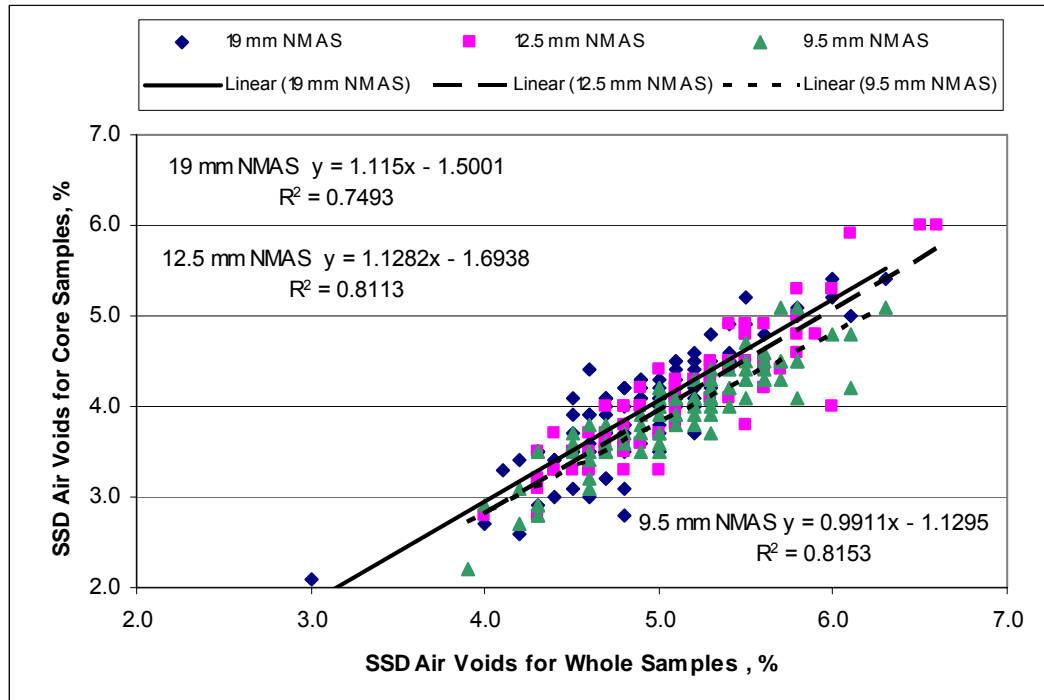


FIGURE 4.18 Air voids relationships between the whole and core samples by the SSD method.

Based on air void content results of 277 samples, the air void content relationships between whole and cored samples were developed. The relationships between the whole and cored samples are demonstrated in Figure 4.18. There is approximately a 1 percent difference between the whole and cored samples because of the inhomogeneous distribution of the air voids. These relationships were developed separately based on the different NMAS. However, the results showed the difference between these three NMAS

was not large (Table 4.17). In order to get the cored samples with 4.0 percent air void content (using the SSD method), the whole samples should be compacted to 4.9, 5.0, and 5.2 percent air void content (using the SSD method) for the 19 mm, 12.5 mm and 9.5 mm NMAS mixtures, respectively. The larger NMAS SMA mixtures require slightly lower air voids for the whole sample in order to get the core samples with 4 percent air voids. This may be due to the greater error potential when measuring air voids by the SSD method for the whole samples with larger NMAS. The threshold air voids value for the 19 mm NMAS whole samples may be higher than 4.9 percent if the water draining problem is prevented.

TABLE 4.17 Targeting Whole Samples VTM¹ for Triaxial Samples

NMAS, mm	Core VTM V_c , %	Regression Equations	Whole VTM V_w , %
19	4.0	$V_c = 1.1150V_w - 1.5001$ $R^2=0.7493$	4.9
12.5	4.0	$V_c = 1.1282V_w - 1.6938$ $R^2=0.8113$	5.0
9.5	4.0	$V_c = 0.9911V_w - 1.1295$ $R^2=0.8153$	5.2

1. VTM measured by the SSD method.

The difference in air void content between the whole and core samples is likely due to the edge effects and surface friction around the side of the mold during compaction (108). The surface of lab compacted samples is likely to have higher air voids because the loss in freedom for re-orientation for the surface portion of samples and the surface friction during compaction provide resistance to densification. The amount of difference depends on the degree of non-uniformity in the air voids and aggregate structure between the surface and the interior of the samples. In comparison with core samples, the whole samples are less homogeneous in their distribution of air voids. Many

studies have shown the air voids around the outside of a core are higher than the inside of the core (84, 86, 108).

4.3.5 Uncorrected Vacuum Seal Method Calculation

From the test results shown in previous sections, the CoreGravity™ program provided similar air voids for some type of samples (cored-and-sawn samples) with the SSD method, however significantly different results were provided for other type of samples (lab compacted SMA sample or steel sample). The lab compacted SMA sample will have higher air voids by CoreGravity™ because the embedded correction factor in the program is not sufficient for the high surface texture. The steel sample will have higher air voids by CoreGravity™ because there is no internal air voids therefore less path comparing to cored sample for air trapped on the surface to go out during vacuuming, which resulted in some air remaining trapped after vacuum. A CoreLok test on a solid steel sample showed about 0.6 percent air voids. Therefore, a study on how to appropriately apply the correlation factor for the vacuum sealing method is needed because the correlation factor embedded into the Coregravity™ is not applicable for all situations.

In the vacuum seal method, a plastic bag tightly conforms to the sides of the sample by the vacuum and prevents water from infiltrating into the sample. The volume of the specimen encapsulated by the bag is considered as the bulk volume of the sample.

The equation used to calculate the bulk specific gravity is shown as follows:

$$G_{mb} = \frac{A}{[C + (B - A)] - E - \frac{B - A}{F_T}} \quad (4.2)$$

where:

A = initial mass of dry specimen in air, g,

- B = mass of dry, sealed specimen, g,
C = final mass of specimen after removal from sealed bag, g,
E = mass of sealed specimen underwater, g, and
F_T = apparent specific gravity of plastic sealing materials at 25°C.

The automatic calculation of CoreLok test results was provided by the Coregravity™ program. A set of correction factors was embedded into the program by the manufacturer (110) and shown in the Appendix Table B1. The correction factors are given based on three regression equations (110) for three test situations and are functions of ratio of sample mass and bag mass. The three test situations are using different bags, i.e. small bags (10×14 inch), big bags (14.75×18 inch) and double bags. These correlation factors are used as specific gravity of plastic bags in the Coregravity™ program following Equation 4.2. In other words, the correlation on CoreLok test results was conducted by adjusting the specific gravity of plastic bags in the Coregravity™ program, or part of the air trapped in the bag was deemed as part of the bag. As shown in Appendix Table B1, the specific gravity of bags can be varied from 0.142 to 0.843 depending on the test situations. This correlation approach seems reasonable, but depends on an empirical regression relationship. The difference between the CoreLok and SSD results for cored-and-sawn samples were within one percent for all tested samples as shown in Figure 4.17, and for samples with 4 percent air voids by the SSD method, the CoreLok program provided only 0.2 to 0.3 percent difference, which indicates this correlation approach works very well for cored samples. For lab compacted SMA samples with high surface texture, however, this correlation seems insufficient and results in higher air voids than those using the SSD method, as shown in Figure 4.10. For impermeable samples with low air voids, this difference is mainly due to the bridging effect of high surface texture

for the CoreLok method. Based on the previous discussion, this difference is about 0.5 percent.

To clarify the effect of these embedded correlation factors on air voids calculation, the air voids calculated by Equation 4.2 without adjusting the specific gravity of the plastic bags needs to be investigated. The specific gravity of the plastic bags was determined as 0.916 following the ASTM D 792 (47). It is noteworthy that this specific gravity value is higher than all the specific gravity values used in the CoregravityTM program. This indicates that the specific gravity value used in the program is reduced for correcting the tendency of overestimating the air voids in the vacuum sealing method. Calculations were conducted by using Equation 4.2 with actual bag specific gravity for all tested samples with different sizes, including the mix design samples (150×115 mm), whole samples for triaxial tests (150×170 mm), and cored samples (100×150 mm) for triaxial tests. The uncorrected vacuum sealing air voids based on Equation 4.2 were compared to those from the CoregravityTM program (CoreLok air voids) and are shown in Figure 4.19.

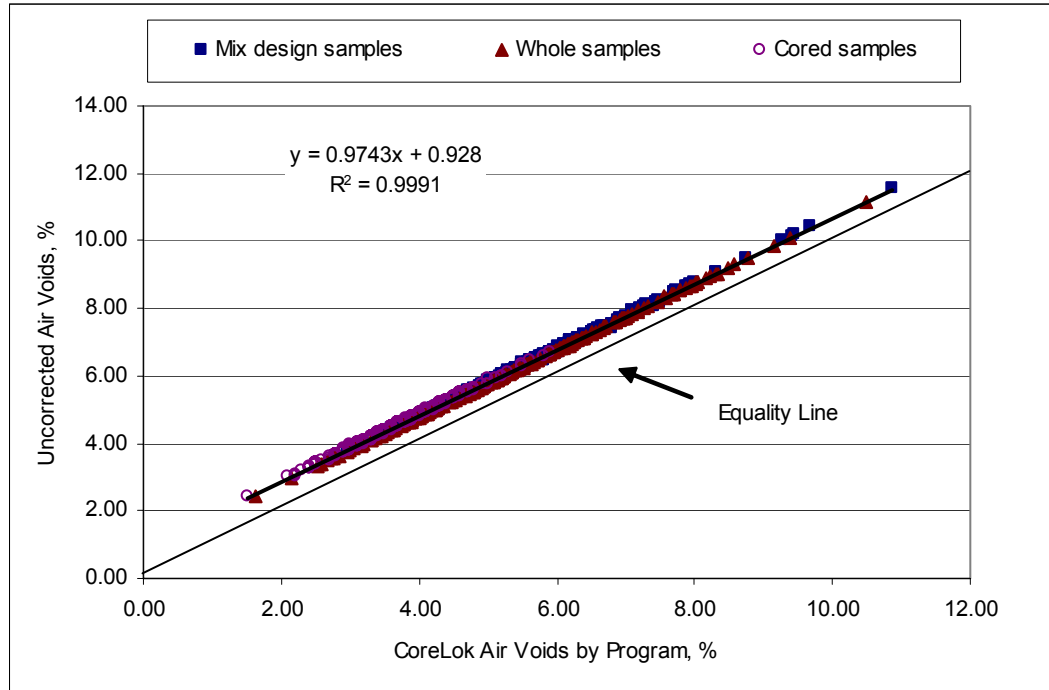


FIGURE 4.19 CoreLok air voids by program versus uncorrected air voids.

As shown in Figure 4.19, the different sample sizes do not make a significant difference and basically overlap each other. The regression equation showed very high coefficient of determination R^2 of 0.999. The program had lower air voids than the uncorrected results because the embedded correlation factors reduced the specific gravity of plastic bags. This resulted in higher volume for the bags and thus lower volume of tested samples, and consequently higher bulk specific gravity of tested samples resulting in lower air voids. The differences between the uncorrected calculation (uncorrected vacuum seal air voids) and the program calculation (CoreLok air voids) are shown in Figure 4.20.

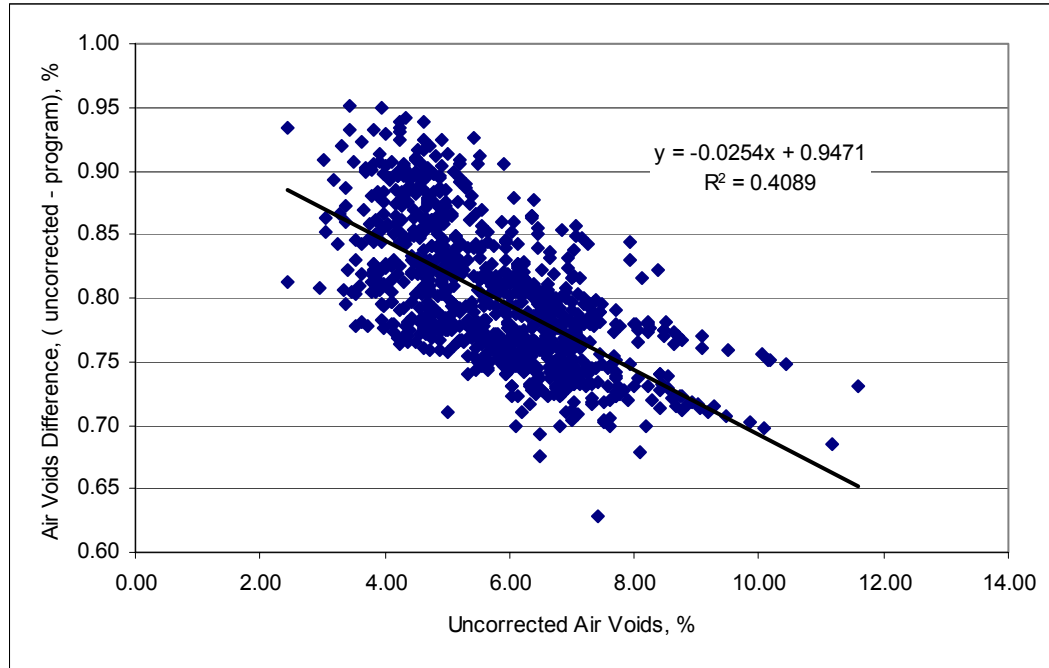


FIGURE 4.20 Air voids difference between program and uncorrected calculation.

From Figure 4.20, one can observe that the difference between the two calculation approaches ranged from 0.63 to 0.95 percent, and had an average of 0.80 percent with a standard deviation of 0.05 percent. The correction in air voids by the program decreases with the increase of air voids. This trend is not desirable since it is believed that for the same type of mixture at higher air void content, the surface texture of compacted samples should be at least similar or even higher. Therefore, the CoreLok bag tends to overestimate the sample volume more, as a result a higher or at least an equal amount of correction is needed.

In consideration of the difference between the uncorrected air voids using Equation 4.2 and the Coregravity™ program (0.9 percent), and the difference between the SSD method and the CoreLok method (0.5 percent), the combined difference between the uncorrected air voids for vacuum seal method and the SSD method is around 1.4

percent for SMA with low air voids. This difference should be the average correlation factor used for the vacuum seal method when lab compacted SMA samples are tested.

The correlation factor for vacuum seal method can be determined by the difference between the SSD air voids and uncorrected vacuum seal air voids using a test sample with similar surface condition and low air voids. The similar surface condition is critical because a different correlation between the SSD and the CoreLok test results had been found for the sawn-and-cored samples and untreated lab compacted samples. Mixtures with different NMAS, which resulted in different surface conditions, also showed different relationships between the SSD and CoreLok test results. The low air void content is necessary because the SSD method results are believed to be accurate at low air voids.

In summary, for impermeable samples with low air voids, the SSD method has little error potential therefore it should be used for air voids measurement. For permeable samples with high air voids, the water draining problem associated with the SSD method is difficult to correct, therefore the vacuum sealing method with correction factor should be used. The correlation factor can be determined by comparing the SSD air voids and uncorrected vacuum sealing air voids using test samples with similar surface conditions and low air voids. The water absorption can be easily used to determine if a significant error potential exists for the SSD method, a threshold value is approximately 0.4 to 0.9 percent for different NMAS mixtures. The threshold air voids for permeable samples will be discussed in the next section.

4.4 PERMEABILITY TEST

Permeability tests were conducted on all the mix design samples compacted by the SGC with 100 gyrations and 65 gyrations. The samples were tested as compacted without sawn or cored treatment. The permeability test results are shown in Appendix Table A1. The relationship between permeability and air voids for SMA mixtures, and effect of compaction level on permeability are evaluated in this section.

4.4.1 The Relationship between Permeability and Air Voids

Permeability test results had a range from 0.00 to 6343.9 (1×10^{-5} cm/s). Based on the literature study (53-58), the NMAS affects the permeability at similar air void contents because of different size of voids, therefore the data was separated into three subsets based on NMAS. The relationships between permeability and total air voids for three NMAS are shown in Figures 4.21, 4.22 and 4.23, respectively. The impermeable (permeability less than 0.01×10^{-5} cm/s) samples were not included in the analysis. There were 56 impermeable samples (out of 372 tested samples), with an air voids range from 1.8 to 4.5 percent by the SSD method.

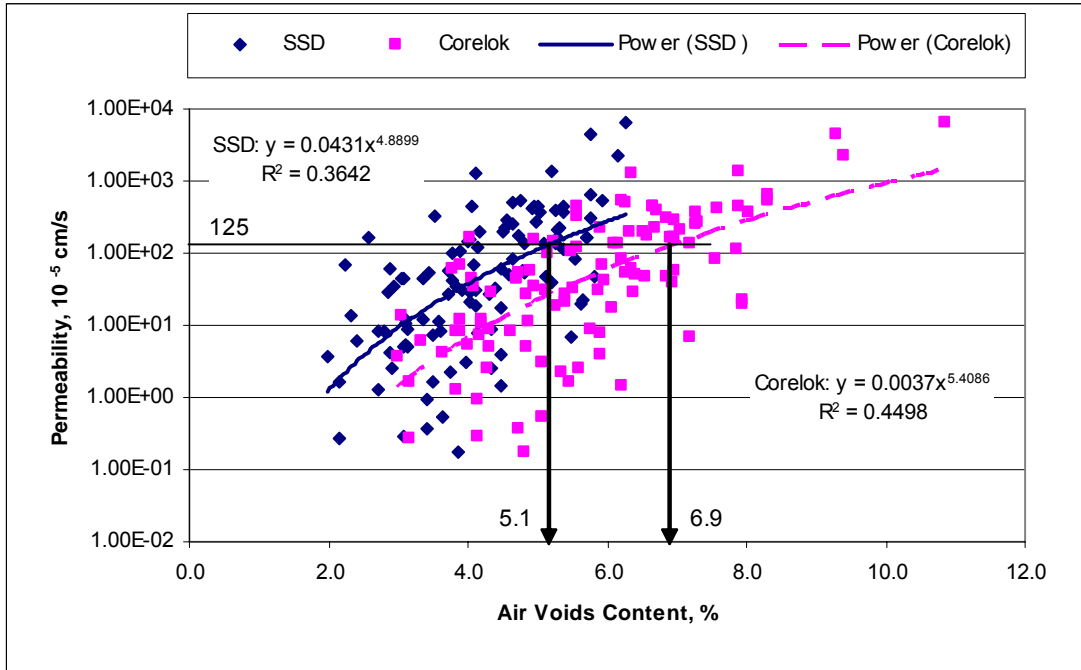


FIGURE 4.21 Relationship between permeability and VTM for 19 mm NMASS.

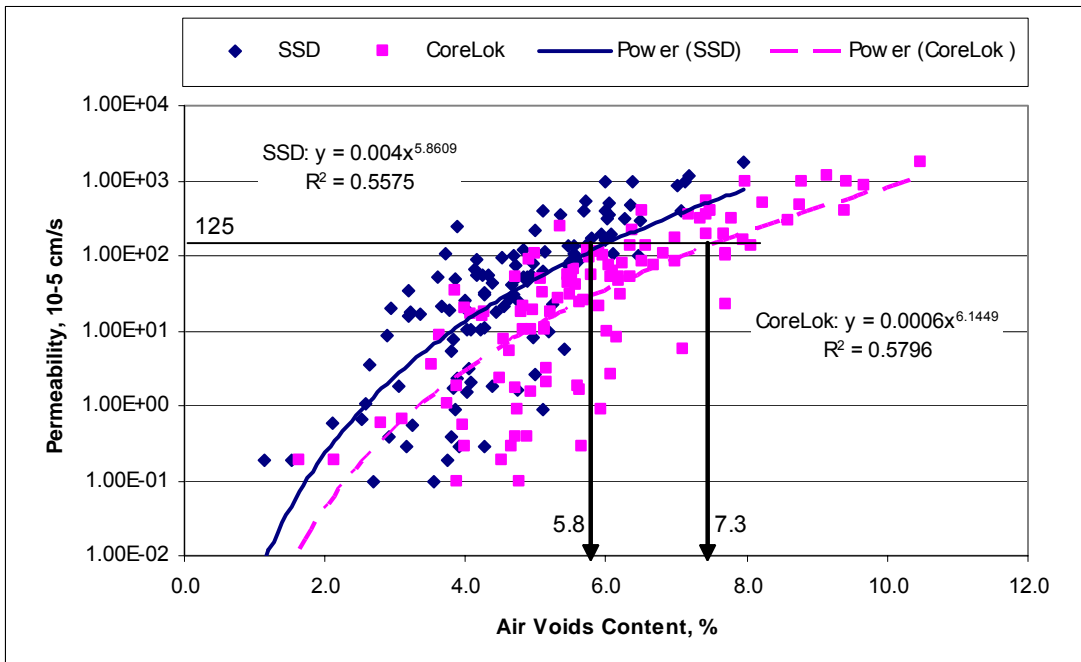


FIGURE 4.22 Relationship between permeability and VTM for 12.5 mm NMASS.

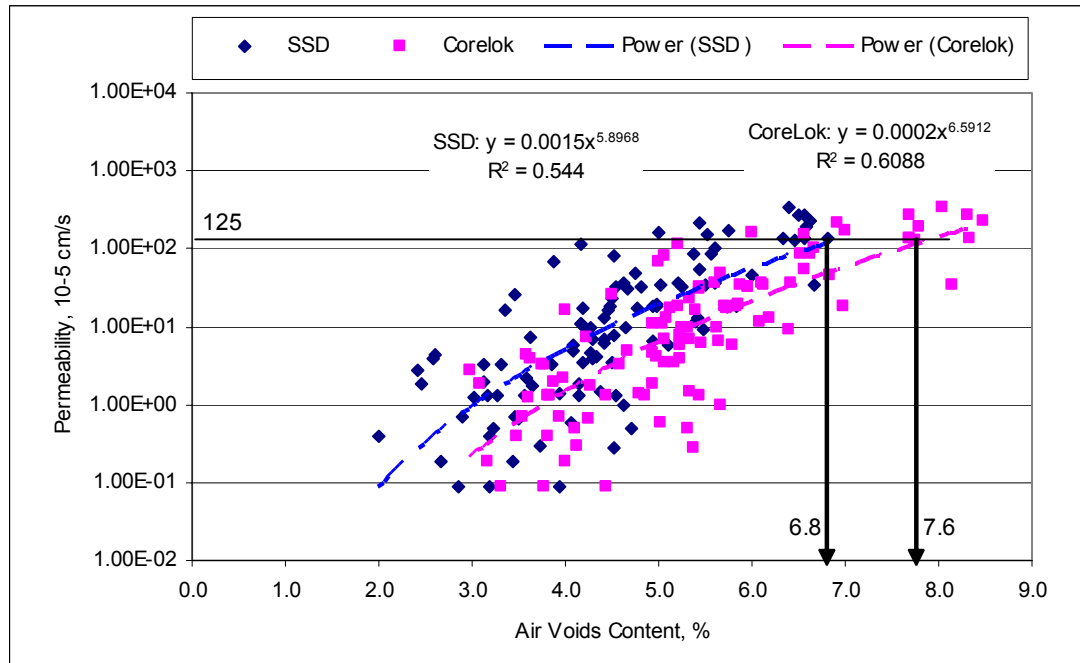


FIGURE 4.23 Relationship between permeability and VTM for 9.5 mm NMA.

It is noteworthy that the coefficients of determination R^2 for the regressions in all Figures are not high (from 0.36 to 0.61). This is because the data for each regression includes variation in aggregate type and AC content, and these factors will affect the size, shape, and connectivity of the air voids. Therefore the amount of interconnected air voids will vary even if the total air voids are the same. The amount of interconnected air voids is believed to have a better correlation with permeability but it is difficult to measure.

If the threshold value for permeable SMA mixtures is set at 125×10^{-5} cm/s (III), the critical air voids values by both SSD and CoreLok methods are shown in Table 4.18. From Table 4.18, one can observe that the critical air void content increases with the decrease of NMA. In other words, SMA mixtures become permeable at higher air void content for lower NMA. The critical air void contents by the SSD method are 5.1, 5.8, and 6.8 percent for 19 mm, 12.5 mm, and 9.5 mm NMA mixtures, respectively.

TABLE 4.18 Critical Air Void Content for Permeable SMA Mixtures

<i>NMAS</i>	<i>Test Method</i>	<i>Regression Equation</i>	<i>Critical¹ VTM, %</i>
19 mm	SSD	$k = 0.0431V_a^{4.8899}$, $R^2=0.3642$	5.1
	CoreLok	$k = 0.0037V_a^{5.4086}$, $R^2=0.4498$	6.9
12.5 mm	SSD	$k = 0.004V_a^{5.8609}$, $R^2=0.5575$	5.8
	CoreLok	$k = 0.0006V_a^{6.1449}$, $R^2=0.5796$	7.3
9.5 mm	SSD	$k = 0.0015V_a^{5.8968}$, $R^2=0.5440$	6.8
	CoreLok	$k = 0.0002V_a^{6.5912}$, $R^2=0.6088$	7.6

1. Critical VTM calculation based on threshold permeability 125×10^{-5} cm/s

The critical air void contents were consistent with the discussion in air voids comparison for the CoreLok and SSD method. As shown in Figures 4.21 to 4.23, for 19 mm NMAS, the critical air voids for a permeable SMA mixture was 5.1 percent by the SSD method, which corresponds to a corrected CoreLok air voids of 6.4 percent. For 12.5 mm NMAS, the critical air void content by the SSD method was 5.8 percent, which was the similar air voids level (5.9 percent, as shown in Figure 4.11) at which the two methods began to have more than one percent difference. For 9.5 mm NMAS, most of the tested samples were not considered permeable, and the difference between the corrected CoreLok and SSD results for most of the tested samples were within one percent (Figure 4.11). For air voids higher than the critical value, the SSD method was considered inaccurate because of the problem of water draining out of the specimen during the SSD procedure.

Based on the air voids and permeability comparison information (Figure 4.11, Figures 4.21 to 4.23), both the SSD and CoreLok methods can be used for SMA 9.5 mm NMAS mixtures with similar results to be expected. This is because the relatively low surface texture and relatively high threshold air voids to become permeable for 9.5 mm mixtures. For 12.5 mm NMAS mixtures with about 6.0 percent or more air voids and for

19 mm NMAS mixtures with more than about 5.0 percent air voids, the SMA mixtures become permeable and therefore there is a greater potential for error by the SSD method than when the vacuum sealing method is used.

4.4.2 Effect of Compaction level on Permeability

At similar air voids, different compaction levels may result in a different air voids distribution and a different degree of interconnectivity of those voids, therefore different permeability. The effect of compaction level on permeability was determined by comparing permeability test results for two compaction levels.

The comparisons of the permeability test results for three NMAS mixtures are shown in Figures 4.24, 4.25, and 4.26, respectively. The coefficients of determination R^2 for the regressions in all Figures are not high (from 0.39 to 0.66). However, these values are compatible with other permeability studies (55, 58-59). The correlation would be better if the effective or interconnected air voids could be used. As discussed in the literature review, permeability did not only depend on the total air voids, but also depended on the size, shape, and distribution of these voids.

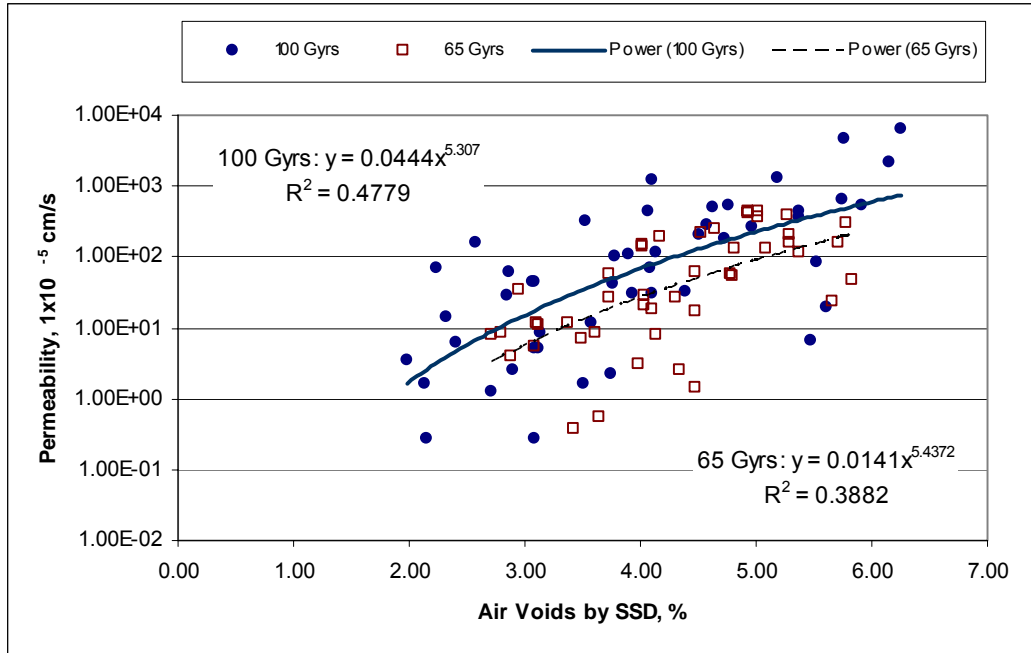


FIGURE 4.24 Permeability results for 65 and 100 gyration levels for 19 mm NMA.

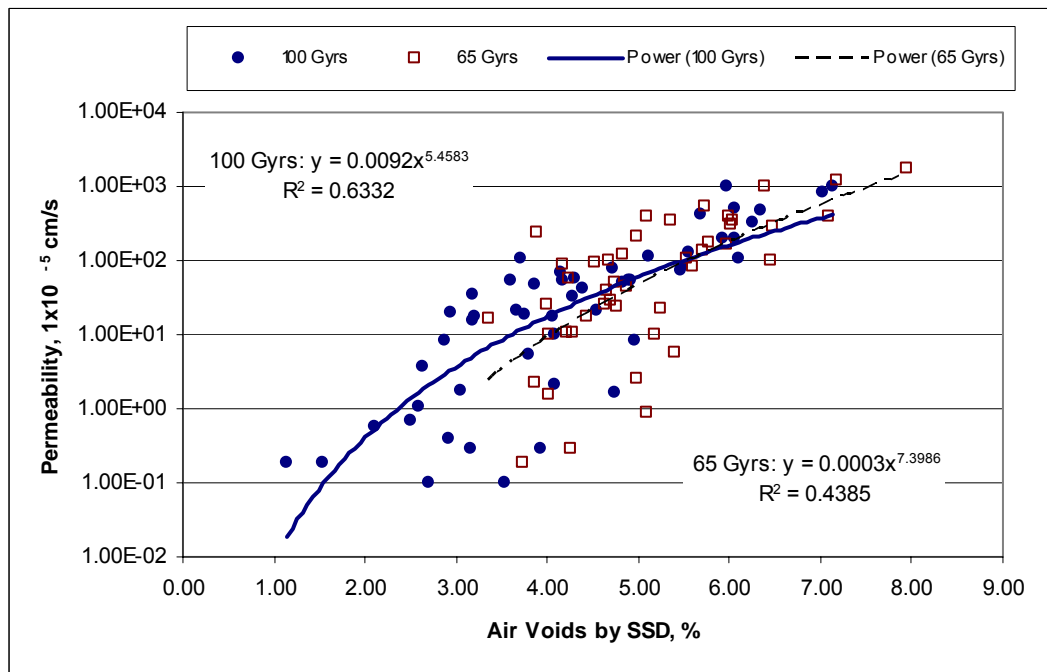


FIGURE 4.25 Permeability results for 65 and 100 gyration levels for 12.5 mm NMA.

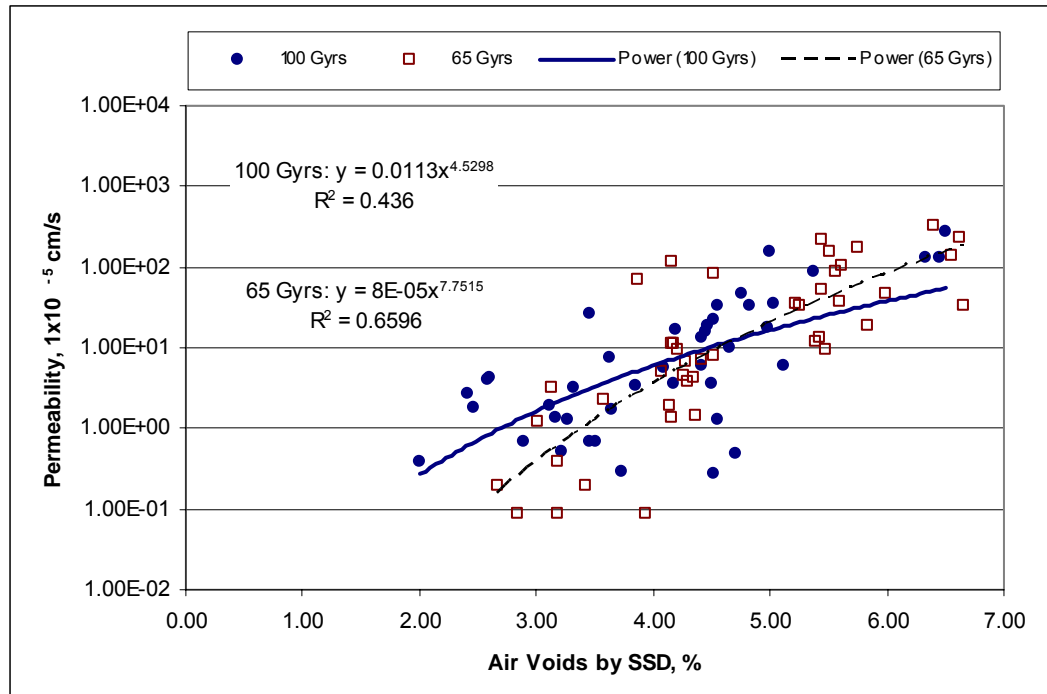


FIGURE 4.26 Permeability results for 65 and 100 gyration levels for 9.5 mm NMA.

As shown in Figure 4.24, 19 mm NMA SMA mixtures designed with 65 gyrations generally had lower permeability than those designed with 100 gyrations at similar air voids. This indicates one of the advantages of using 65 gyrations for designing SMA mixtures.

For 12.5 and 9.5 mm NMA mixtures as shown in Figure 4.25 and 4.26, the permeability test results for the two compaction levels are mixed at similar air voids. SMA mixtures designed with 65 gyrations had a slightly higher slope than those designed with 100 gyrations. The two best-fitted regression lines crossed at an intermediate air void content.

SMA mixtures designed with 65 gyrations had higher asphalt content than those designed with 100 gyrations at similar air voids (Figure 4.4). The high asphalt content will help seal the air voids and prevent the connectivity of internal air voids. At low air

void levels, this sealing effect of the asphalt binder becomes more significant and makes those designed with 65 gyrations more impermeable. At high air void levels, the asphalt binder seems not enough to seal the interconnected voids and the mixture becomes permeable.

The critical air voids calculated from the best-fitted regression lines for two compaction levels are shown in Table 4.19. As shown in Table 4.19, the critical VTM is lower for larger NMAS mixture. This is because the size of air voids tends to become larger and more interconnected with larger NMAS mixture, resulting in higher permeability at the same level of total air voids.

TABLE 4.19 Critical Air Void Content for Permeable SMA Mixtures

<i>NMAS</i>	<i>Gyrations Level</i>	<i>Regression Equation</i>	<i>Critical* VTM, %</i>
19 mm	100	$k = 0.0444V_a^{5.307}$, $R^2=0.4779$	4.5
	65	$k = 0.0141V_a^{5.4372}$, $R^2=0.3882$	5.3
12.5 mm	100	$k = 0.0092V_a^{5.4583}$, $R^2=0.6332$	5.7
	65	$k = 0.0003V_a^{7.3986}$, $R^2=0.4385$	5.7
9.5 mm	100	$k = 0.0113V_a^{4.5298}$, $R^2=0.4360$	7.8**
	65	$k = 0.00008V_a^{7.7515}$, $R^2=0.6596$	6.3**

* Critical VTM calculation based on threshold permeability 125×10^{-5} cm/s, by SSD method.

** The critical VTM is extrapolated from regression equation or at the end of data range.

For 19 mm NMAS, the SMA mixture designed with 65 gyrations become permeable at higher air voids than those designed with 100 gyrations. For 12.5 mm NMAS, the critical air voids for the two compaction levels are the same at 5.7 percent. For 9.5 mm NMAS, the critical air voids for those designed with 65 gyrations are lower than those designed with 100 gyrations. It is notable that for 9.5 mm NMAS, the critical air voids results are extrapolated at the high end of the sample air voids range. As shown in Figure 4.26, the low permeability results for those designed with 65 gyrations resulted

in a higher slope than those designed with 100 gyrations. This high slope may result in a misleading extrapolated critical air voids at the very high end of the air voids range.

Three F tests were employed to examine the difference between the regression equations of the two compaction levels for the three NMAS. For each of the F test, a sum of square error (SSE) for each individual regression of one compaction level and an SSE for a new regression of combined data were calculated. Then an F statistics was formulated by the SSD difference (SSD (D)) between combined and individual regressions and the total SSD (SSD (T)) of two individual regressions. The results for the F tests are summarized in Table 4.20.

TABLE 4.20 F-tests for permeability regressions of two compaction levels

	SSE (D)	DF (D)	SSE(T)	DF(T)	F stat	P value
19 mm	7060603	2	54394245	89	5.776	0.004
12.5 mm	1263962	2	3100691	93	18.955	0.000
9.5 mm	9294	2	241115	81	1.561	0.216

As shown in Table 4.20, the difference between the regression for 100 and 65 gyrations are significant for 19 mm and 12.5 mm SMA mixture results. For 9.5 mm SMA mixtures, the difference between the permeability results for the two compaction levels is not significant even though the two regressions showed big difference. This is logical because as shown in Figure 4.26, the two sets of data are mixed together and the two regression lines are crossed in the middle. In the overall range of tested air voids, there is no significant difference between two compaction levels.

In summary, the SMA mixtures designed with 65 gyrations generally had similar or lower permeability than those designed with 100 gyrations at a given level of air voids. For 19 mm NMAS mixtures, 65 gyrations resulted in a lower permeability than 100

gyrations at similar air voids. For 12.5 and 9.5 mm NMAS mixtures, the effects of two compaction levels on permeability were not significant.

4.5 AGGREGATE DEGRADATIONS

Samples were tested in the NCAT ignition oven for each aggregate and NMAS combination (loose samples, Marshall compacted samples, and the SGC samples) to determine the aggregate breakdown. Washed gradation analyses were conducted on the remaining aggregates to determine the aggregate breakdown. The aggregate breakdown for the combinations of five aggregates and three NMAS using different compactive efforts are shown in Appendix C, from Figure C1 to C15. A typical result of aggregate breakdown under different compactive efforts is shown in Figure 4.27.

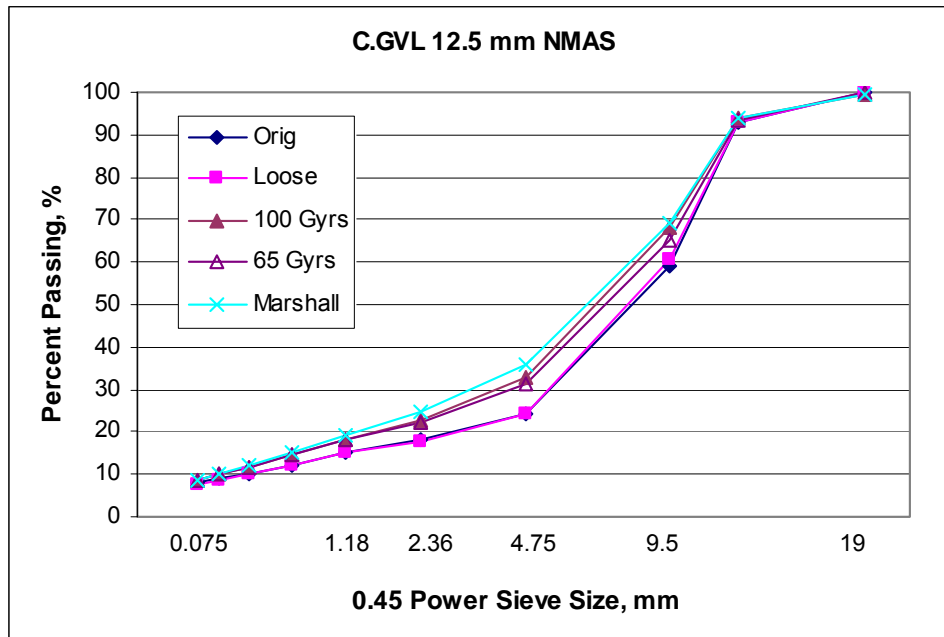


FIGURE 4.27 Typical aggregate breakdown results for different compaction efforts (C.GVL 12.5 mm NMAS).

As shown in Figure 4.27, the gradation of the loose mixture is basically the same as the original gradation, which indicates there was virtually no breakdown as a result of

mixing and testing in the ignition oven. However, there was a big difference between compacted samples to loose samples. The Marshall compactor produced more breakdown than the SGC, and therefore produced gradations that were denser and closer to the maximum density line. The 100 gyrations compaction effort generally resulted in some additional aggregate breakdown when compared to the 65 gyrations compaction. However, the difference between these two compaction levels was generally not large.

The gradation changes by using different compaction efforts, including the Marshall compaction, 100 gyrations by the SGC, and 65 gyrations by the SGC are summarized in Tables 4.21, 4.22, and 4.23, respectively. Each result shown in the tables is the average value from two replicates. The information in these tables includes the aggregate type, LA abrasion, NMA, F&E content, and selected sieve size changes due to the compaction. The deviation in results was shown as the difference in gradation between compacted samples and loose mixtures. The results therefore present the compaction effect only.

As shown in Tables 4.21 to 4.23, lab granite had the highest breakdown while traprock had the lowest breakdown. The lab granite is a major aggregate type used in Georgia and the traprock is the primary aggregate used in Maryland. These two States probably are the two biggest producers of SMA. The State of Georgia has specified the 50 gyration level for designing SMA mixture, while the State of Maryland has always insisted on 100 gyrations. The reason for the different specification is likely due to the different availability of aggregate sources. The lab granite has high breakdown therefore a lower compaction level is desired, while the traprock produces very little breakdown and therefore can use the higher compaction level.

TABLE 4.21 Marshall Compaction Aggregate Breakdown Results

Agg. Type	L.A. Abrasion, %	NMAS, mm	Grad.	F&E, %	12.5mm sieve change, %	9.5 mm sieve change, %	4.75 mm sieve change, %	2.36 mm sieve change, %	0.075 mm sieve change, %
C.GVL	30.7	19	N*	23.8	11.1	16.8	9.2	5.8	0.4
		12.5	N	35.2	--	8.4	11.9	6.9	1.1
		9.5	N	37.7	--	4.1	10.1	6.9	0.4
L.GRN	36.4	19	N	18.6	9.3	15.2	9.9	6.3	0.6
		12.5	N	28.1	--	7.8	11.7	6.1	0.1
		9.5	N	30.3	--	2.7	12.6	7.7	0.6
LMS	26.4	19	N	20.7	15.1	15.0	8.6	4.8	1.2
		12.5	N	25.5	--	8.7	11.4	5.7	1.4
		9.5	N	26.8	--	2.7	10.1	5.7	1.5
R. GRN	20.6	19	N	24.1	4.5	11.7	7.3	3.7	0.5
		12.5	N	23.4	--	6.2	9.9	4.5	0.6
		9.5	N	24.7	--	1.1	9.1	4.3	0.5
TRAP	16.6	19	N	12.8	3.7	6.8	3.0	1.0	0.0
		12.5	N	17.7	--	5.7	6.3	3.1	0.4
		9.5	N	19.5	--	0.9	7.0	3.2	0.3
R. GRN	20.6	19	F*	24.0	2.9	8.8	5.5	2.5	1.1
		12.5	F	23.8	--	4.9	9.5	3.4	0.5
		9.5	F	24.7	--	2.7	9.6	4.7	1.3
TRAP	16.6	19	F	13.9	3.1	3.9	2.5	0.3	0.5
		12.5	F	18.2	--	2.6	2.8	0.1	0.4
		9.5	F	19.5	--	2.6	2.4	1.3	0.2

Note: * N and F stand for normal and fine gradation, respectively.

-- Test result is not available for this sieve.

TABLE 4.22 100 Gyration Aggregate Breakdown Results

Agg. Type	L.A. Abrasion, %	NMAS, mm	Grad.	F&E, %	12.5mm sieve change, %	9.5 mm sieve change, %	4.75 mm sieve change, %	2.36 mm sieve change, %	0.075 mm sieve change, %
C.GVL	30.7	19	N*	23.8	5.3	10.4	6.1	4.1	0.5
		12.5	N	35.2	--	7.6	8.7	4.7	0.9
		9.5	N	37.7	--	3.0	8.1	5.2	0.7
L.GRN	36.4	19	N	18.6	4.3	9.4	8.0	5.7	1.5
		12.5	N	28.1	--	2.2	9.7	5.2	0.8
		9.5	N	30.3	--	0.4	9.7	6.0	1.1
LMS	26.4	19	N	20.7	5.9	8.1	5.4	3.8	0.7
		12.5	N	25.5	--	3.2	5.8	3.8	0.6
		9.5	N	26.8	--	1.5	5.2	4.8	1.3
R. GRN	20.6	19	N	24.1	1.4	6.7	5.5	3.2	0.7
		12.5	N	23.4	--	2.3	5.6	3.0	0.7
		9.5	N	24.7	--	0.1	6.3	3.8	0.3
TRAP	16.6	19	N	12.8	0.6	2.0	-0.1	-0.6	-0.3
		12.5	N	17.7	--	2.4	1.2	1.4	0.3
		9.5	N	19.5	--	1.1	0.9	2.0	0.5
R. GRN	20.6	19	F*	24.0	2.1	5.3	4.6	2.7	1.0
		12.5	F	23.8	--	3.0	6.2	2.5	0.7
		9.5	F	24.7	--	1.9	6.5	3.8	0.8
TRAP	16.6	19	F	13.9	1.6	0.6	1.2	-0.2	0.4
		12.5	F	18.2	--	0.9	1.7	-0.1	0.6
		9.5	F	19.5	--	2.0	0.3	0.3	0.1

Note: * N and F stand for normal and fine gradation, respectively.

-- Test result is not available for this sieve.

TABLE 4.23 65 Gyration Aggregate Breakdown Results

Agg. Type	L.A. Abrasion, %	NMAS, mm	Grad.	F&E, %	12.5mm sieve change, %	9.5 mm sieve change, %	4.75 mm sieve change, %	2.36 mm sieve change, %	0.075 mm sieve change, %
C.GVL	30.7	19	N*	23.8	4.7	8.2	5.4	3.8	0.7
		12.5	N	35.2	--	4.5	7.2	4.4	1.0
		9.5	N	37.7	--	1.6	5.3	4.2	0.7
L.GRN	36.4	19	N	18.6	5.6	8.6	7.3	5.5	1.7
		12.5	N	28.1	--	3.7	8.0	4.5	0.8
		9.5	N	30.3	--	1.8	8.1	5.4	1.1
LMS	26.4	19	N	20.7	5.1	7.5	5.1	3.2	1.2
		12.5	N	25.5	--	4.2	5.9	3.4	0.8
		9.5	N	26.8	--	1.4	5.2	3.4	1.1
R. GRN	20.6	19	F*	24.1	2.9	5.4	4.5	2.5	0.9
		12.5	F	23.4	--	3.2	5.7	2.4	0.6
		9.5	F	24.7	--	1.7	6.4	3.5	1.3
TRAP	16.6	19	F	12.8	2.4	0.3	1.1	-0.1	0.5
		12.5	F	17.7	--	1.4	1.4	0.0	0.7
		9.5	F	19.5	--	0.9	-0.2	0.0	0.1

Note: * N and F stand for normal and fine gradation, respectively.

-- Test result is not available for this sieve.

The aggregate breakdown results for N gradation of the traprock and ruby granite are also included in Tables 4.21 and 4.22. The comparison of N gradation and F gradation is shown in Figure 4.28. One standard deviation is shown as the error bar for each result. The pooled standard deviations for N and F gradations are 0.35 and 0.31 percent, respectively. The aggregate breakdown results were represented by the changes in percent passing the critical sieves. The critical sieve chosen was the 4.75 mm sieve for 19 mm and 12.5 mm NMAS mixtures, and the 2.36 mm sieve for 9.5 mm NMAS mixtures.

These sieve sizes are most critical for SMA gradations and are used to determine the existence of stone-on-stone contact. As shown in Figure 4.28, the difference between N and F gradations is generally not large and doesn't show a consistent trend. This is not as expected but not surprising. The F gradation is finer than the N gradation and closer to the maximum density line, therefore it was expected to have less degradation. However, the difference between the F and N gradations is not large, both gradations fall within the gradation band for SMA mixtures (Tables 3.1 and 3.3). Therefore the test variability overwhelmed the effect of small differences in gradation.

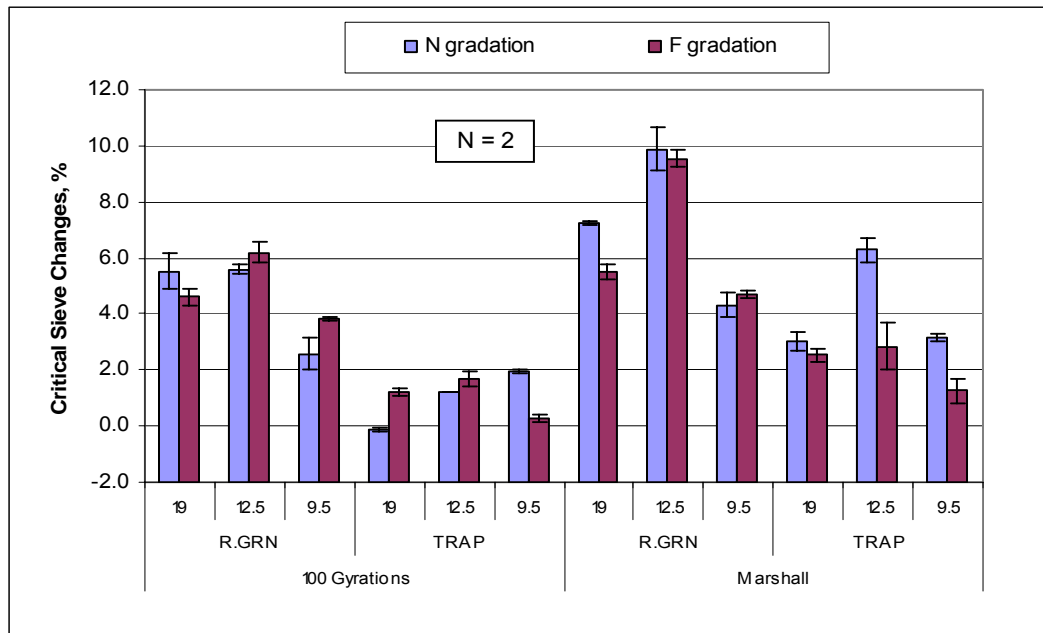


FIGURE 4.28 Comparison of N and F gradation on aggregate breakdown.

TABLE 4.24 Paired-T Test on Degradation for Two gradations

	N	Mean	StDev	SE Mean
N gradation	12	4.233	2.820	0.814
F gradation	12	3.675	2.607	0.753
Difference	12	0.558	1.458	0.421

95% CI for mean difference: (-0.367754, 1.484420)

T-Test of mean difference = 0 (vs not = 0): T-Value = 1.33, P-Value = 0.211

A paired T-test (Table 4.24) was used to compare breakdown of N and F gradations and the results indicated that these two gradations had no significant difference in terms of aggregate breakdown under compaction. Therefore, the following analysis on aggregate breakdown is limited to F gradation for the traprock and ruby granite.

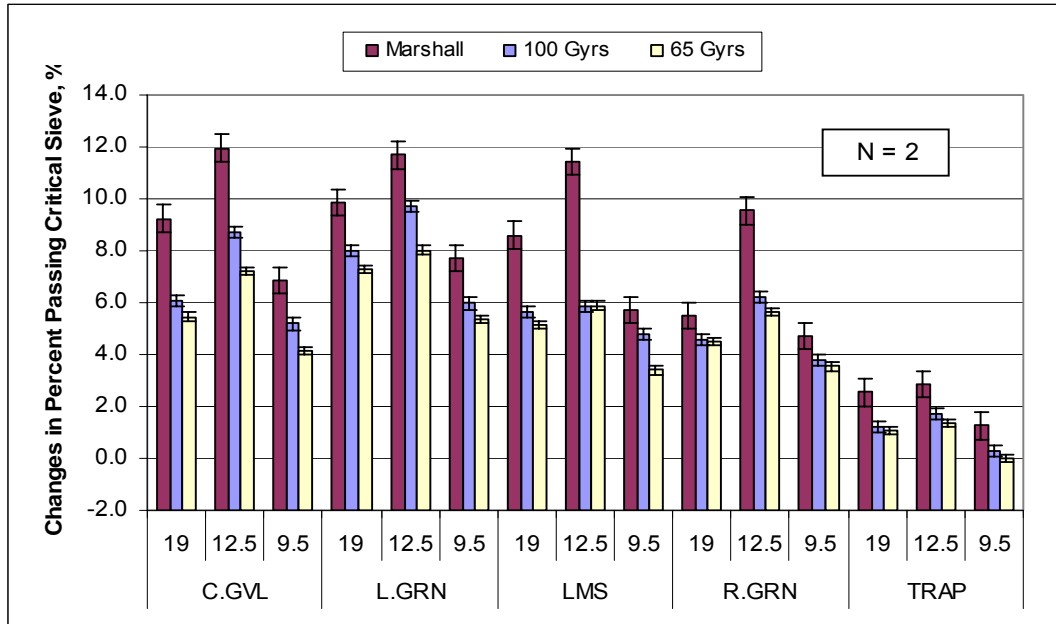


FIGURE 4.29 Critical sieve changes due to compaction.

Figure 4.29 is a schematic summary of the breakdown results due to compaction. The aggregate breakdown results were represented by the average changes in percent passing the critical sieves, from two replicates for each mixture. One standard deviation is shown as the error bar for each result. (The pooled standard deviations are 0.65, 0.29, and 0.22 percent for 50 blow Marshall, 100 gyrations and 65 gyrations, respectively).

From Figure 4.29, one can observe that Marshall compaction gave the highest aggregate breakdown of the three compaction efforts. The 100 gyrations generally broke more aggregate compared to 65 gyrations, but typically not by a significant amount. The

change in percent passing the critical sieve has a range from 0.3 to 9.7 percent for 100 gyrations SGC compaction, from 0.0 to 8.0 percent for 65 gyrations SGC compaction, and from 1.3 to 11.9 percent for Marshall compaction. The results are as expected. The Marshall hammer is considered as an impact compactor and allows little reorientation of aggregates during compaction, therefore higher aggregate breakdown was expected in order to achieve similar air voids to the gyratory compactor. On the other hand, the gyratory compactor produces a kneading action which allows the proper reorientation during compaction.

An ANOVA was conducted on the critical sieve breakdown results to evaluate the effect of main factors (aggregate type, NMAS, and compaction level) and any interaction between these main factors. The ANOVA results shown in Table 4.25 indicate that all the main factors and all the interactions are significant. This result is due to the surprising low variability in error (about 1%) in the ANOVA result. Even though the effects of interaction are much lower than those of the main factors, all the interactions are shown as significant. This small error term makes the ANOVA results very sensitive to minor effects. The effects of interactions may not be practically significant but will be shown as statistically significant.

TABLE 4.25 ANOVA on Aggregate Breakdown at Critical Sieve Size

Source	DF	Seq SS	Adj SS	Adj MS	F	P
Agg.	4	492.35	492.35	123.09	665.74	0.000
Comp	2	124.84	124.84	62.42	337.60	0.000
NMAS	2	132.92	132.92	66.46	359.46	0.000
Agg.*Comp	8	14.62	14.62	1.83	9.88	0.000
Agg.*NMAS	8	14.55	14.55	1.82	9.84	0.000
Comp*NMAS	4	12.29	12.29	3.07	16.62	0.000
Agg.*Comp*NMAS	16	9.33	9.33	0.58	3.15	0.001
Error	45	8.32	8.32	0.19		
Total	89	809.22				

The average breakdown for different aggregate types, compaction efforts and NMAS are shown in Figure 4.30. One standard deviation is shown as error bar. The numbers of results used for calculating the average values and standard deviations are also included in the Figure. The high variability as shown in the Figure 4.30 is as expected because only a single factor is considered to draw the average bar while all the other factors are significant.

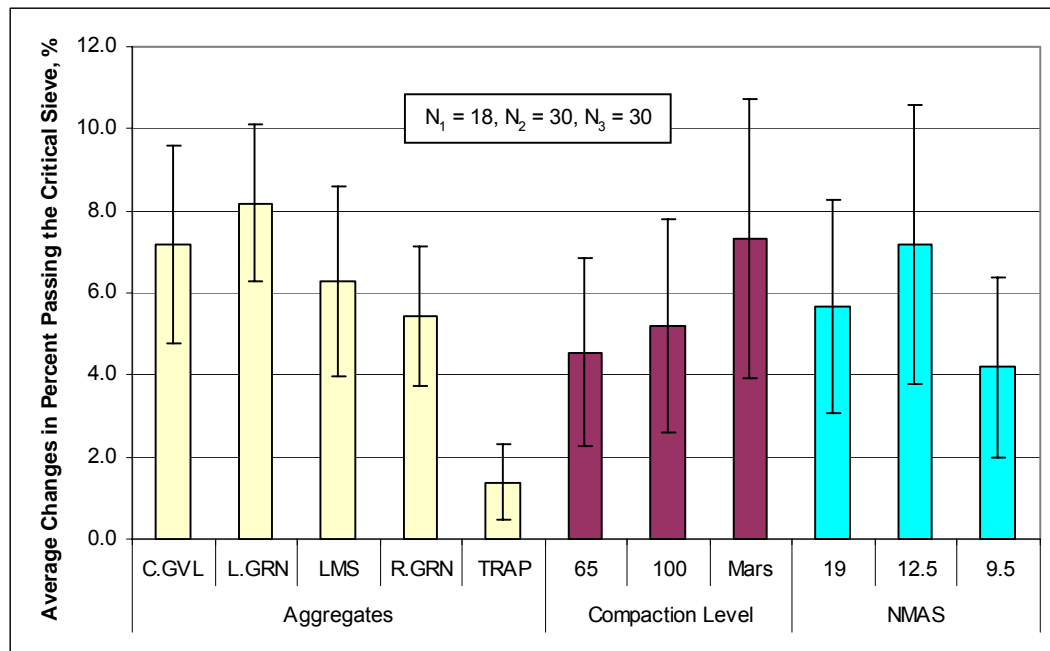


FIGURE 4.30 Average aggregate breakdown for all main factors.

The aggregate breakdown depended on the aggregate type. The traprock had the lowest aggregate breakdown of 1.4 percent on average, while the lab granite had the highest aggregate breakdown of 8.2 percent on average. Aggregate properties such as L.A. abrasion and F&E content are believed to correlate the most to the aggregate breakdown value (36). The regressions for average breakdown value versus aggregate L.A. abrasion value and F&E content (3:1 ratio) are shown in Figure 4.31 and Figure

4.32, respectively. The correlation between aggregate breakdown under laboratory compaction and the L.A. abrasion value is very strong (R^2 larger than 0.84 for all NMAS mixtures). The results indicate that with the increase of aggregate L.A. abrasion, the aggregate breakdown is greater. This result is logical because the L.A. abrasion is an indication of aggregate hardness and impact resistance, a tough and hard aggregate would be expected to have less breakdown during compaction.

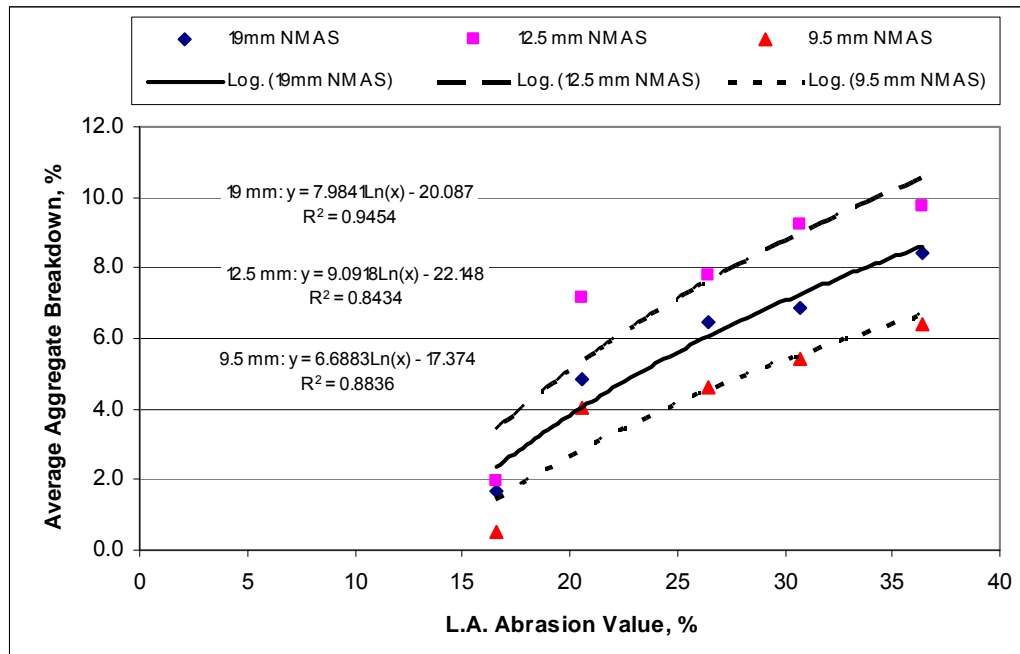


FIGURE 4.31 Relationship between aggregate breakdown and L.A abrasion value.

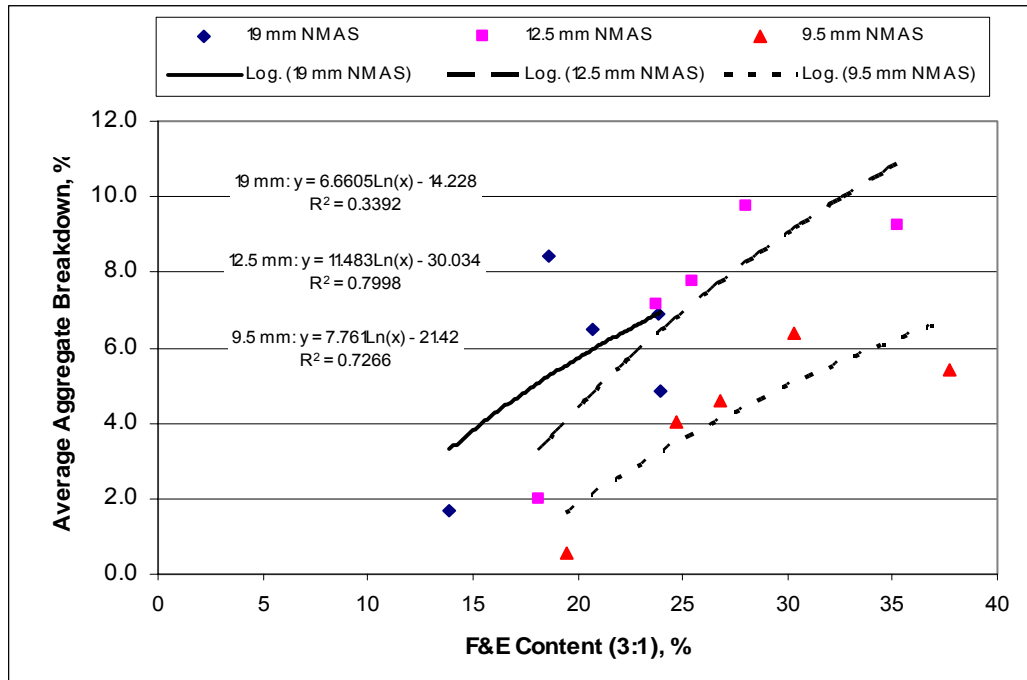


FIGURE 4.32 Relationship between aggregate breakdown and F&E content.

The aggregate breakdown under laboratory compaction didn't show a strong correlation ($R^2=0.34$) with aggregate F&E content for 19 mm NMAS mixtures. However, for 12.5 mm and 9.5 mm NMAS mixtures, the correlation between aggregate F&E content and aggregate breakdown is good ($R^2 \geq 0.73$). The general trends showed an increase in F&E content created more aggregate breakdown. This is logical because the flat or elongated particles will tend to break quicker than more cube-shaped particles.

As expected, the compaction effort was also shown to be a significant factor. The Marshall compaction, 100 gyrations with the SGC, and 65 gyrations with the SGC gave an average change of 7.3, 5.2 and 4.6 percent in percent passing the critical sieves, respectively. As discussed before, the Marshall compactor is an impact compactor which allows little aggregate re-orientation and therefore tends to break more aggregates. From the literature review, aggregate breakdown due to the field construction seems relative stable (average 4.9 percent) regardless the aggregate types (64). Both 65 gyrations and

100 gyrations resulted in similar (average difference is within 0.3 percent) aggregate breakdown as in the field construction.

Two paired t-tests were employed to compare the Marshall compaction with 100 gyrations, and the 100 gyrations with 65 gyrations for critical sieve changes. The results are shown in Tables 4.26 and 4.27, respectively. Both paired t-tests showed there were significant differences between the two compaction efforts compared. For the paired t test between 100 and 65 gyrations, even though the difference is not practically significant (0.6 percent), the statistical analysis showed a significant difference because of the consistent difference between the two compaction levels. This is logical because additional gyrations have to provide at least as much and probably more breakdown.

TABLE 4.26 Paired T Test on Degradation for 100 Gyrations and Marshall Compaction

	N	Mean	StDev	SE Mean
Marshall	15	7.287	3.448	0.890
100 Gyrs	15	5.180	2.646	0.683
Difference	15	2.107	1.316	0.340

95% CI for mean difference: (1.37784, 2.83549)
 T-Test of mean difference = 0 (vs not = 0): T-Value = 6.20, P-Value = 0.000

TABLE 4.27 Paired T Test on Degradation for 65 and 100 Gyrations

	N	Mean	StDev	SE Mean
100 Gyrations	15	5.18	2.646	0.683
65 Gyrations	15	4.54	2.337	0.603
Difference	15	0.64	0.541	0.140

95% CI for mean difference: (0.340460, 0.939540)
 T-Test of mean difference = 0 (vs not = 0): T-Value = 4.58, P-Value = 0.000

The NMAS was also shown as a significant factor in the breakdown of the aggregates. The 12.5 mm NMAS mixtures had the highest aggregate breakdown of 7.2 percent on average for the critical sieve, while the 9.5 mm NMAS mixtures had the lowest aggregate breakdown of 4.2 percent on average. The average breakdown values for the three compaction efforts at different sieve sizes are shown in Table 4.28.

TABLE 4.28 Average Percent Passing Changes at Three Sieve Sizes

NMAS	Average Breakdown Value at Sieve Size, %		
	9.5 mm	4.75 mm	2.36 mm
19 mm	8.2	5.6*	3.4
12.5 mm	4.4	7.2*	3.5
9.5 mm	2.1	6.6	4.2*

* Selected as representative value as the choosing of critical sieve size.

As shown in Table 4.28, for 12.5 mm NMAS mixtures, the critical sieve selected was the same sieve size (4.75 mm) at which the maximum breakdown happened. However, for 19 mm and 9.5 mm NMAS mixtures, the maximum breakdown due to compaction generally happened at 9.5 mm and 4.75 mm sieve size, respectively. The critical sieves selected for 19 mm and 9.5 mm NMAS mixtures were one size lower than where the maximum breakdown happened.

As shown in Table 4.25, all the interactions between these main factors were significant. This indicates that aggregate breakdown depends on specific combinations of aggregate type, NMAS, and compaction level. Any factor alone can not be used to estimate the aggregate breakdown.

The interaction between aggregate type and compaction levels is shown in Figure 4.33. One standard deviation is shown as error bar. For each aggregate, the three compaction efforts followed the same order for aggregate breakdown levels. However, the amount of breakdown was slightly different for different aggregate types. Considering the test precision of the sieve analysis test (single operator precision is 3.7%, from AASHTO T27), these differences are not significant.

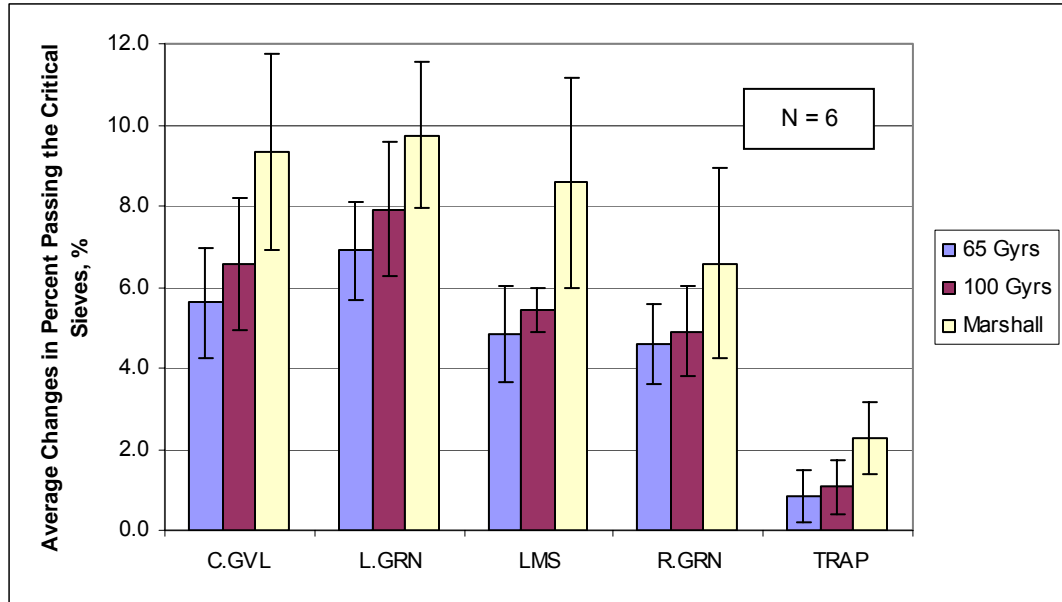


FIGURE 4.33 Interaction between aggregate type and compaction level on aggregate breakdown.

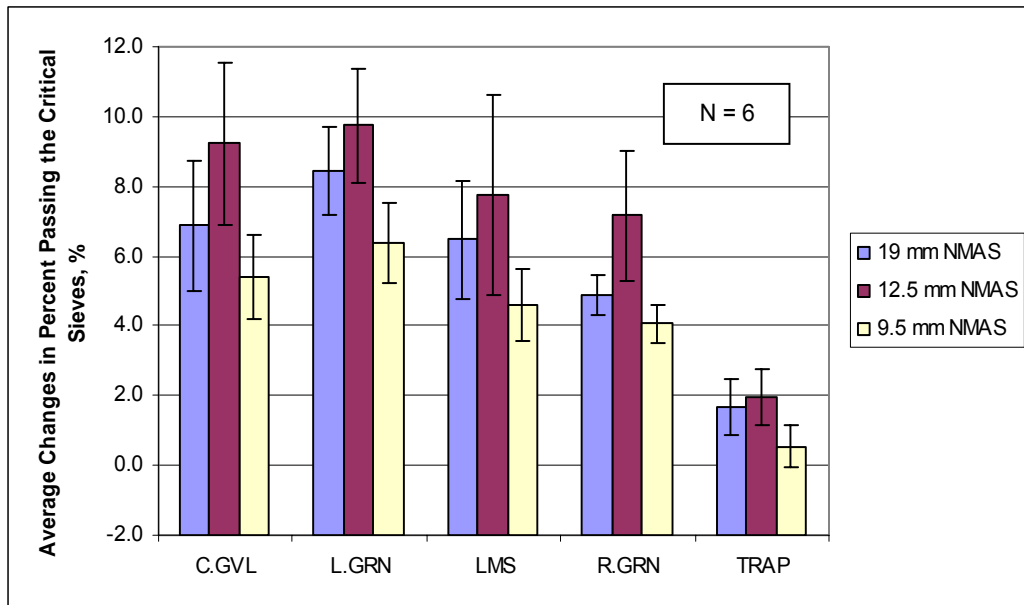


FIGURE 4.34 Interaction between aggregate type and NMAS on aggregate breakdown.

The interaction between aggregate type and NMAS is shown in Figure 4.34. One standard deviation is shown as error bar. For each aggregate type, the three NMAS

followed the same order for aggregate breakdown results. However, the differences among the three NMAS varied a little for different aggregate types. Considering the test precision of the sieve analysis test, these differences are not practically significant.

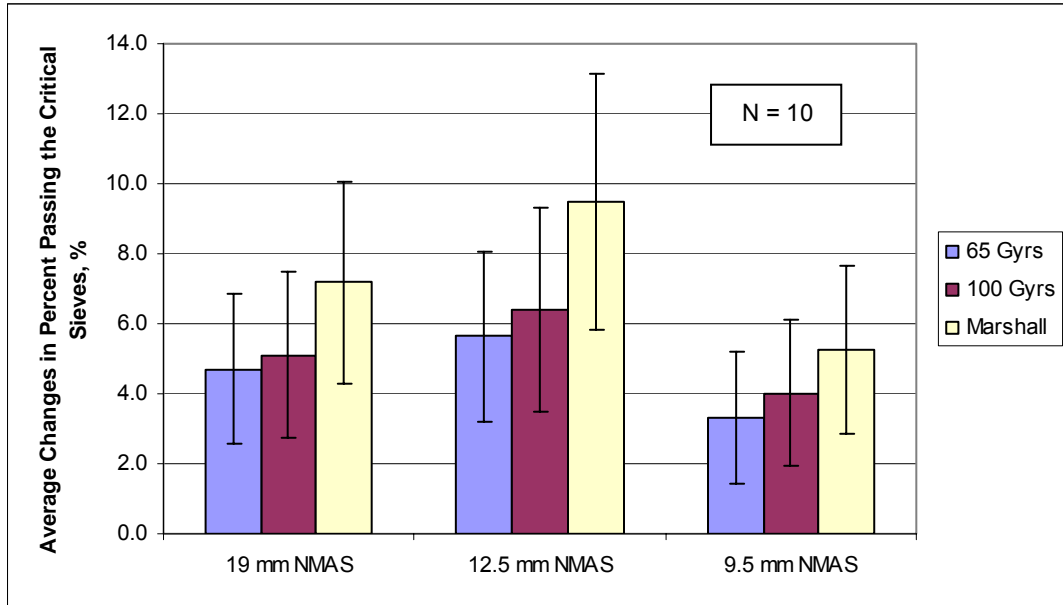


FIGURE 4.35 Interaction between compaction level and NMAS on aggregate breakdown.

The interaction between compaction level and NMAS is shown in Figure 4.35. One standard deviation is shown as error bar. For each NMAS, the compaction efforts followed the same order for aggregate breakdown results. However, for different NMAS, the amounts of change varied for different compaction levels. For example, for 19 mm NMAS mixtures, the difference between 100 gyrations and 65 gyrations was smaller when compared to that of mixtures with the other two NMAS. Considering the test precision of sieve analysis test, these differences are not significant.

In summary, three compaction efforts that were evaluated included 65 gyrations, 100 gyrations, and 50 blow Marshall. The Marshall compaction provided the most aggregate breakdown, while 65 gyrations provided the least aggregate breakdown. The

difference between 65 and 100 gyrations in terms of aggregate breakdown values at the critical sieves are shown to be statistically significant, but not large. Both 65 and 100 gyrations provided similar aggregate breakdown as in the field construction.

4.6 SUMMARY

The effects of different compaction levels on volumetric properties, permeability and aggregate breakdown were evaluated. The two test methods for determining air voids was compared and suggestions on how to properly determine air voids for SMA mixtures at different air void levels were made. The test results for different compaction levels are summarized in Table 4.29.

TABLE 4.29 Average Test Results for Different Compaction Levels

Properties\Compaction level	50 blows Marshall	100 Gyration	65 Gyration	40 Gyration ¹	Suggested Criteria
Asphalt content, %	6.4	5.9	6.6	7.4	6.0 min
VMA, %	18.1	17.1	18.6	20.1	17 min
VCA ratio	0.89	0.88	0.90	0.97	1.0 max
Draindown, %	N/A ²	N/A	0.10	0.08	0.3 max
Breakdown, %	7.3	5.2	4.6	N/A	4.9 ³
Permeability for 19 mm NMA mix at 6% air voids ⁴ , 1×10^{-5} cm/s	N/A	190	74	N/A	125 max

1. Only two mixtures were designed with 40 gyrations.
2. N/A—the tests were not conducted for this compaction effort.
3. Average value from field observation (64).
4. Air voids is the corrected vacuum sealing air voids.

The volumetric properties comparison on four compaction levels indicated that with the decrease of compaction level, the optimum asphalt content and VMA increased.

All mixtures designed with 65 and 40 gyrations met the minimum optimum asphalt content of 6.0 percent and minimum VMA of 17 percent, while only 8 out of 15 mixtures designed with 100 gyrations met these requirements. All designed SMA mixtures in this study met the VCA requirement and draindown requirement. The decrease of compaction level will result in more durable mixtures and will allow the use of more aggregate types for designing SMA mixtures if rutting is not a problem.

For determination of air voids, both the SSD and CoreLok methods can be used for SMA 9.5 mm NMAS mixtures with similar results to be expected. For 12.5 mm NMAS SMA mixtures with more than 6.0 percent air voids or more than 0.6 percent water absorption during the SSD test; and for 19 mm NMAS SMA mixtures with more than about 5.0 percent air voids or more than 0.4 percent water absorption during the SSD test, there is a greater potential for error by the SSD method than when the CoreLok method is used. Since this error is difficult to correct with the water draining problem for the SSD method, the CoreLok method is recommended for SMA mixtures with high air voids. However, the correlation factor embedded into the CoreGravity™ program is not sufficient for SMA laboratory compacted samples, an additional 0.5 percent correlation factor was recommended for use in this study. A further study of the correction factor indicated that an average 1.4 percent should be used on top of the uncorrected vacuum sealing air voids for lab compacted SMA mixtures when the vacuum sealing method was used.

From the comparison of two compaction levels on permeability, 65 gyrations resulted in a lower permeability than 100 gyrations at similar air voids for 19 mm NMAS

mixtures. For 12.5 and 9.5 mm NMAS mixtures, the effects of compaction level on difference in permeability between the two compaction levels were not significant.

Marshall compaction resulted in significantly higher aggregate breakdown than gyratory compaction. The increase of compaction level from 65 gyrations to 100 gyrations resulted in some additional aggregate degradation. But both 65 and 100 gyrations resulted in similar aggregate breakdown as that observed during field compaction.

CHAPTER 5 TEST RESULTS, ANALYSIS AND DISCUSSION OF PERFORMANCE TESTS

The rutting resistance for the SMA mixtures was evaluated by several laboratory tests, including the APA rutting test as a simulative test, and more fundamental tests such as dynamic modulus, static creep and repeated load tests. This chapter presents the results, data analysis, and discussions of these performance tests.

The discussions emphasize the effects of different compaction levels on these performance test results. The discussion of the test results will give the basis for recommending a compaction level that provides a more durable mix with satisfactory rutting resistance.

5.1 APA RUTTING TEST

5.1.1 APA Test Results and Analysis

As shown in the literature (72-77), the APA rutting test has been validated by many field projects, and can be used for differentiating rut susceptible mixtures. Many state DOTs have begun to use this test to test the rutting resistance of HMA during mix design and quality control/quality assurance. The APA rut depth results for the 32 mixes designed with the SGC at the three levels of compaction are summarized in Table 5.1.

TABLE 5.1 APA Rutting Results

Gyration Level	Agg. Type	NMAS, mm	Asphalt Content, %	APA Rutting, mm	St. Dev. Of APA rutting, mm
100	C.GVL	19	5.8	4.10	0.62
		12.5	6.4	2.80	0.50
		9.5	6.2	2.63	0.41
	L.GRN	19	4.8	2.37	0.30
		12.5	5.4	2.29	0.65
		9.5	5.7	3.61	1.01
	LMS	19	5.1	2.47	0.78
		12.5	5.5	4.42	1.22
		9.5	5.3	3.92	0.13
	R.GRN	19	6.2	2.55	0.42
		12.5	6.0	2.41	0.61
		9.5	6.7	2.59	0.21
	TRAP	19	6.7	4.46	0.87
		12.5	6.1	2.67	0.35
		9.5	6.5	3.14	0.33
65	C.GVL	19	6.6	4.17	0.58
		12.5	7.1	5.04	1.54
		9.5	6.5	4.43	1.02
	L.GRN	19	6.0	3.72	1.07
		12.5	6.5	4.68	1.37
		9.5	6.6	3.94	1.19
	LMS	19	6.0	2.97	1.22
		12.5	6.5	6.14	0.91
		9.5	6.1	4.73	1.39
	R.GRN	19	6.6	2.65	0.43
		12.5	6.7	3.01	0.64
		9.5	7.2	2.42	0.20
	TRAP	19	7.0	4.15	1.08
		12.5	6.5	3.22	0.99
		9.5	7.0	3.93	1.53
40	L.GRN	12.5	7.2	5.05	1.71
	R.GRN	12.5	7.5	4.56	0.86

A side by side comparison of the APA rut depth results for all three gyration levels (40 gyrations was used only for 12.5 mm NMAS mixture with two aggregate types:

lab granite and ruby granite) are shown in Figure 5.1. One standard deviation is shown as error bar. The pooled standard deviation values for rut depth results are 0.63, 1.08, and 1.35 mm with the compaction level of 100, 65, and 40 gyrations, respectively. These variability values are less than the maximum allowable variability (2.0 mm) specified in the AASHTO TP-63 (105). The increased test variation with lower compaction level may be due to the increased rut depth results and higher variability in aggregate orientation with lower compaction level.

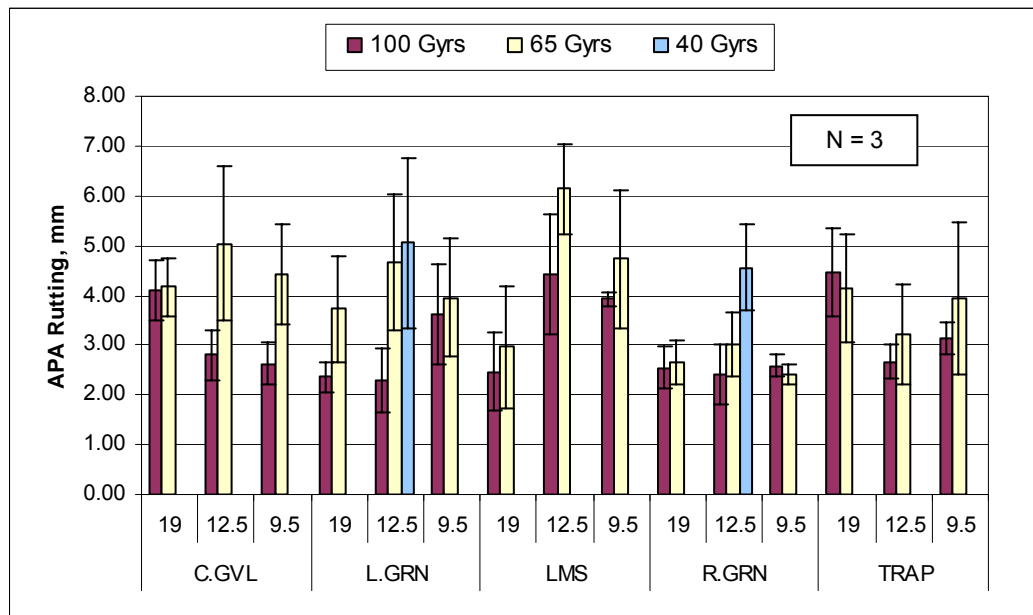


FIGURE 5.1 Comparison of APA rutting for three compaction levels.

From Figure 5.1, one can observe that the APA rut depth generally increased with a decrease of compaction level. The two SMA mixtures designed with 40 gyrations had higher APA rut depths than the same mixture designed with higher compaction levels. SMA mixtures designed with 65 gyrations generally had higher APA rut depths than those designed with 100 gyrations because of the higher asphalt content. Even with higher asphalt contents, the mixtures designed with 65 gyrations were still rut resistant except for the crushed gravel and limestone 12.5 mm mixtures. Thirteen of fifteen

mixtures (87 %) compacted with 65 gyrations still performed well when 5.0 mm was used as the maximum rut depth allowed (68). For 40 gyrations, one of two mixtures still met this requirement and had a 4.6 mm rut depth.

The rut depth of the SMA mixtures using ruby granite and traprock aggregates were less sensitive to compaction level than the mixtures using the other three aggregates. For these two aggregates, going from 100 to 65 gyrations resulted in an average 0.26 mm increase in APA rut depth while the other three aggregates had an average of 1.25 mm increase. This is likely due to the smaller change in optimum asphalt content (average 0.5 percent) and aggregate degradation (average 0.3 percent) for these two aggregates when compared to the other three aggregates (average 0.9 percent change in asphalt content, and 0.8 percent change in degradation) between the two compaction levels. The effects of compaction level on mix properties are essentially caused by the optimum asphalt content and aggregate gradation changes due to compaction. When the differences in these two properties are smaller, the difference in performance for two mixtures is likely to be smaller.

Further analysis of these APA rut depth data was performed by conducting an ANOVA to evaluate the effect of the main factors (aggregate type, NMAS, and compaction level) and any interactions between the main factors on rut depths. Since only two mixtures were designed with 40 gyrations, the comparison of mean value of APA rut depth between 40 gyrations with the other two compaction levels could not be made. Therefore, two mixtures designed with 40 gyrations were excluded from this analysis. The APA results of these two mixtures were only used for comparison to the rut depth results of mixtures using the same aggregate type and same NMAS.

Results of the ANOVA are presented in Table 5.2. From Table 5.2, aggregate type and compaction level were significant influencing factors. The interaction between aggregate type and NMAS, and the interaction between NMAS and compaction level were also significant. Side by side comparison for the effects of these significant factors and interactions were shown in the Figures 5.2, 5.3 and 5.4 to better visualize the discussion.

TABLE 5.2 ANOVA for APA Rutting Results

<i>Source</i>	<i>DF</i>	<i>Seq SS</i>	<i>Adj SS</i>	<i>Adj MS</i>	<i>F</i>	<i>P</i>
Agg.	4	23.7189	23.7189	5.9297	7.54	0.000
NMAS	2	1.4509	1.4509	0.7254	0.92	0.403
Gyrs	1	16.2053	16.2053	16.2053	20.59	0.000
Agg.*NMAS	8	27.0070	27.0070	3.3759	4.29	0.000
Agg.*Gyrs	4	5.6395	5.6395	1.4099	1.79	0.142
NMAS*Gyrs	2	5.3331	5.3331	2.6666	3.39	0.040
Agg.*NMAS*Gyrs	8	4.5286	4.5286	0.5661	0.72	0.674
Error	60	47.2138	47.2138	0.7869		
Total	89	131.097				

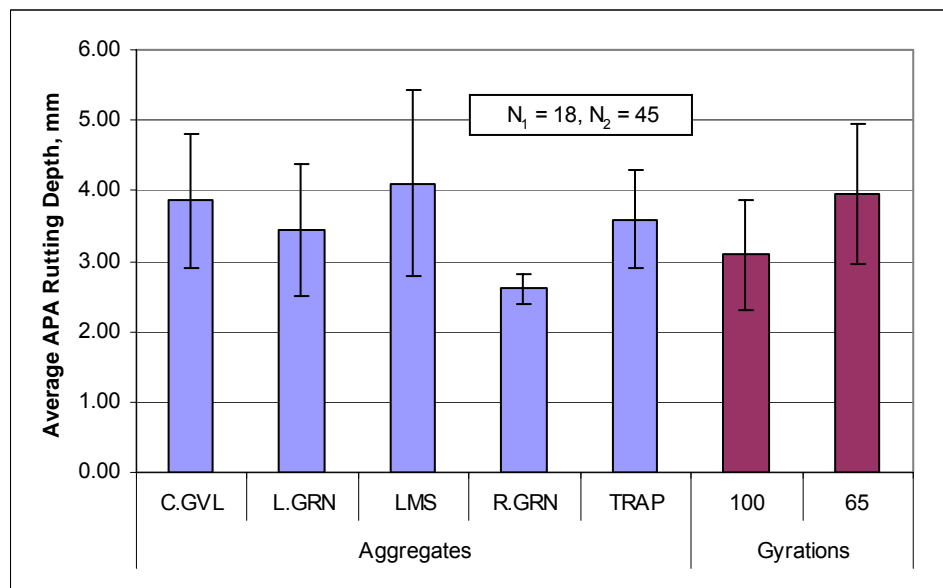


FIGURE 5.2 Comparison of average APA rut depth.

Figure 5.2 shows the comparison of the average APA rut depth for different aggregate types and two compaction levels. One standard deviation for each group is shown as error bar. N_1 and N_2 represent the number of samples used for average for each group. The ruby granite mixtures had the lowest average APA rut depth of 2.6 mm, while the limestone mixtures had the highest average APA rut depth of 4.1 mm. This is likely due to the limestone had the lowest coarse aggregate uncompacted voids of 46.6 percent as shown in Table 4.1. The uncompacted air voids was recommended by the NCHRP project 4-19 (113) as an indication of effects of aggregate shape, angularity and texture. Full-scale rutting tests (114) at Indiana DOT APT Facility indicated a good correlation between the rutting resistance and uncompacted air voids for coarse aggregate. Aggregates with high uncompacted air voids are likely to produce more rut-resistant pavement.

The differences between all different aggregate types are not large considering the test precision (allowable standard deviation in AASHTO TP63 is 2.0 mm). The low value of the APA results for all aggregate types indicates the requirements of aggregate properties such as L.A abrasion (30 percent maximum), F&E content (20 percent maximum for 3:1 ratio) for SMA mixtures seems too stringent. Two aggregates (crushed gravel and lab granite) have L.A abrasion values higher than 30 percent, and only one aggregate (traprock) has the F&E content (3:1) less than 20 percent. However, two aggregates: lab granite and ruby granite have been used on Georgia SMA projects with proven good rutting performance.

The average rut depth for mixtures designed with 100 gyrations was 3.1 mm, while the average rut depth for mixtures designed with 65 gyrations was 3.9 mm. A

higher compaction level will result in lower optimum asphalt content and a tighter aggregate structure, therefore a better rutting resistance. However, considering the test precision of the APA rutting test, there is no practical difference for rutting between the SMA mixtures with the two compaction levels. Other studies (37, 115) have shown that the rutting for SMA mixtures is not sensitive to asphalt content. This is because of the stone on stone contact and high voids in aggregates result in less build-up of pore pressure. Based on the literature review (68, 79), mixtures that have an APA rut depth less than 5.0 mm are deemed as rutting resistant. Most (29 of 32 mixtures) of the APA rut depths measured in this study are below the 5.0 mm criteria and therefore should be resistant to rutting.

The interaction between aggregate type and NMA is shown in Figure 5.3. One standard deviation value is shown as error bar. For different aggregate types, the orders of the three NMA in terms of average APA rut depth are different. However, this appears to be due to normal variations considering the precision of APA rutting test.

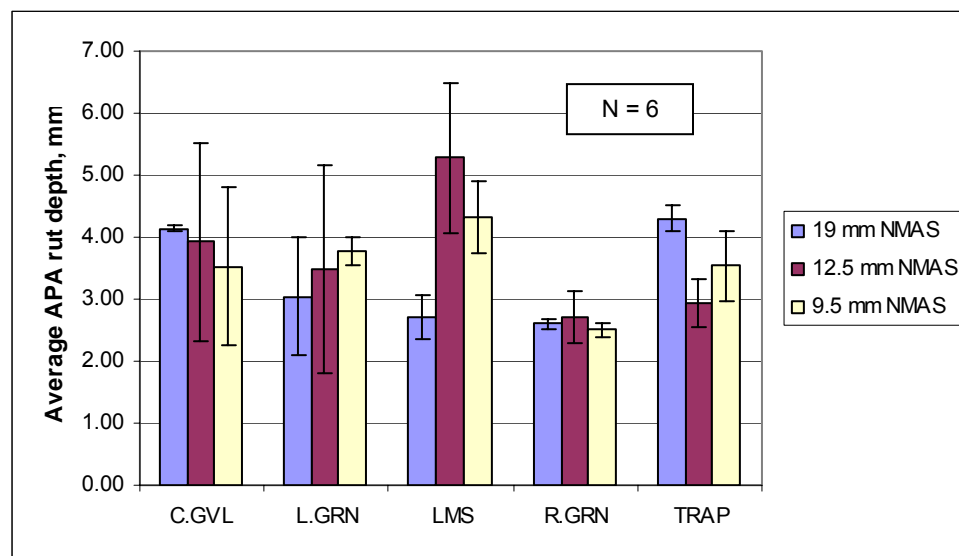


FIGURE 5.3 Interaction between aggregate type and NMA on APA rut depth.

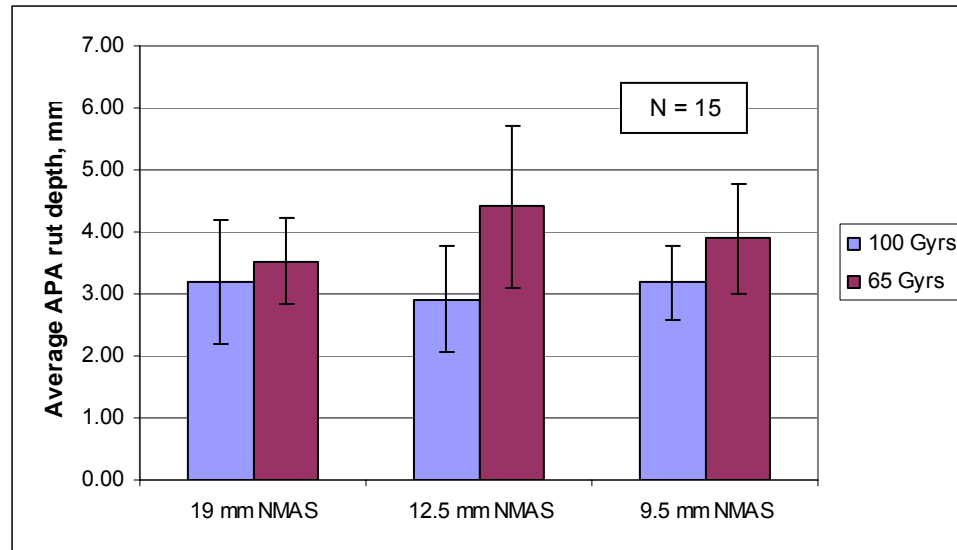


FIGURE 5.4 Interaction between NMAS and compaction level on APA rut depth.

The interaction between NMAS and compaction level are shown in Figure 5.4. One standard deviation is shown as error bar. For different NMAS, a decrease of compaction level from 100 to 65 gyrations resulted in a different amount of increase in average APA rut depth. The highest increase in APA rut depth was 1.5 mm for 12.5 mm NMAS mixtures (from 2.9 to 4.4 mm), while the lowest increase in APA rut depth was 0.3 mm for 19 mm NMAS mixtures (from 3.2 to 3.5 mm). This indicates that 12.5 mm NMAS mixtures were more sensitive to compaction level than the other two NMAS mixtures in terms of APA rut depth. However, this difference is not considered as practically significant since the highest difference is only 1.5 mm, and the same trend with compaction level are shown for all three NMAS mixtures.

5.1.2 Discussion on APA Rut Depth versus Gyration Level

The discussions in this section will focus on the effect of compaction level on the APA rut depth test results which will provide a basis to recommend a gyration level that provides as much asphalt as possible without causing potential rutting problems. All the

APA rutting results versus gyration levels are shown in Figure 5.5. Since only two mixtures (12.5 mm NMAS SMA with lab granite and ruby granite) were designed with three gyrations levels while all the rest of mixtures were designed with two gyration levels, an overall analysis on the effect of gyration level on the APA rutting result is difficult to conduct.

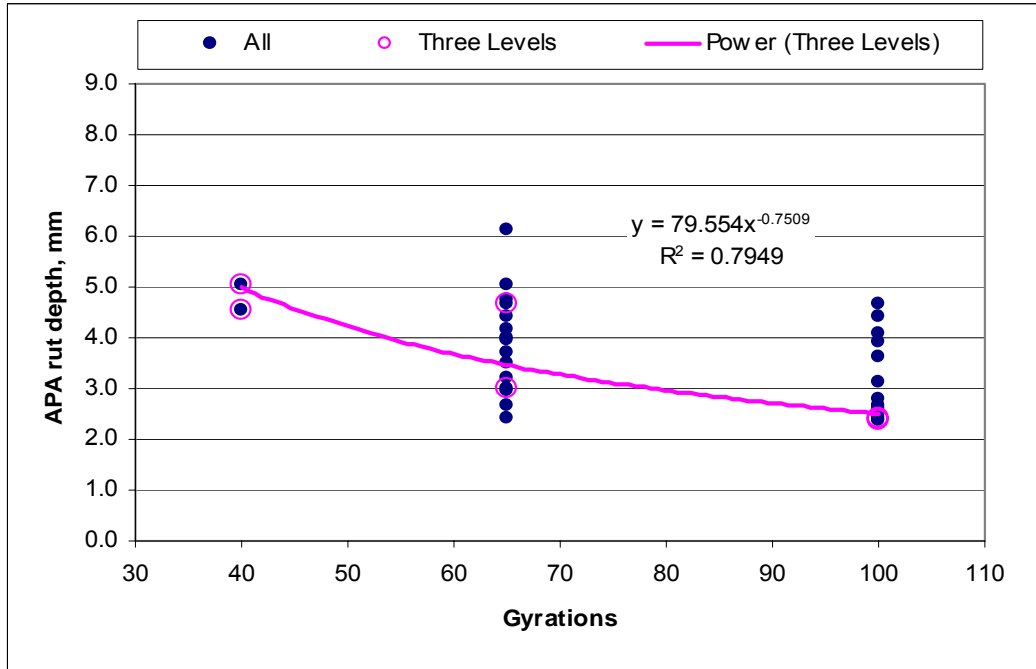


FIGURE 5.5 The relationship between APA rut depth and compaction level.

As shown in Figure 5.5, the APA rutting results for SMA mixtures designed with 65 and 100 gyrations varied within similar ranges. Even with various aggregate types and various NMAS, the ranges are not large considering the test variability. The APA results for all mixtures designed with 100 gyrations are less than the suggested criteria of 5 mm. The APA rut depths for most (13 out of 15) of the mixtures designed with 65 gyrations are less than this criteria.

The two mixtures with three gyration levels are highlighted using different data symbols. A best fitted regression line for the results of these two mixtures is also included. As shown in Figure 5.5, the APA rut depth of these two mixtures decreases with an increase of gyration level. However, the decrease in APA rut depth is not large when the compaction level increases from 65 to 100 gyrations. For these two mixtures, the APA rut depth becomes marginal when the gyration level drops to 40 gyrations.

NCHRP 9-17 project (80) provided a correlation between the laboratory rut depth and normalized field rut depth, as shown in Figure 5.6. The field rut depth data were from the MnRoad and Westrack projects. The lab rut depths were obtained by conducting APA rutting tests on cylinder samples with 4 percent air voids at PG grade temperature. A comparison between 4 and 7 percent air voids for APA rutting test is shown in Figure 5.7 from the same research. The results indicate the APA rut depth for 7 percent air voids is only slightly larger than those for 4 percent. Therefore, the correlation should be reasonably applicable for the 6 percent air voids samples used in this study.

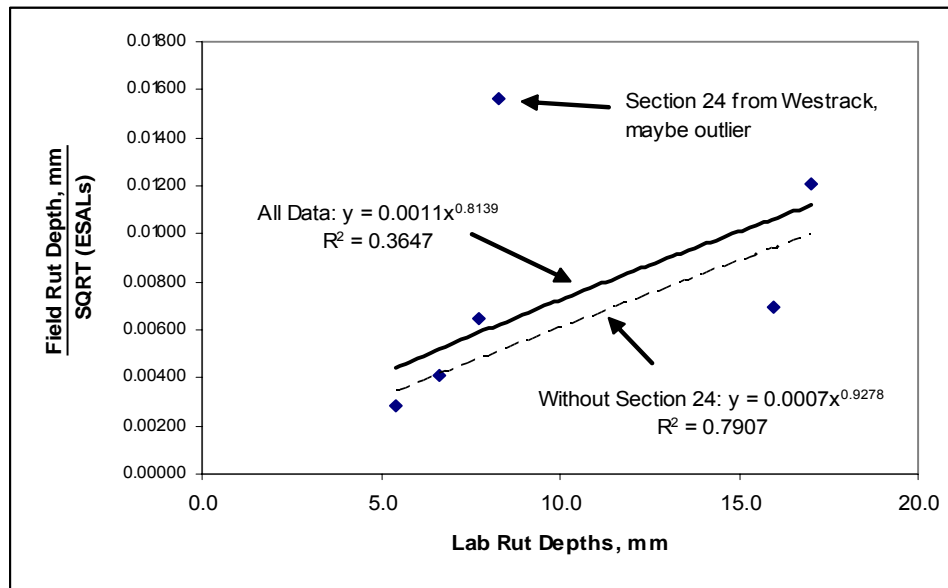


FIGURE 5.6 Correlation between field and APA rut depth from NCHRP 9-17 project (80).

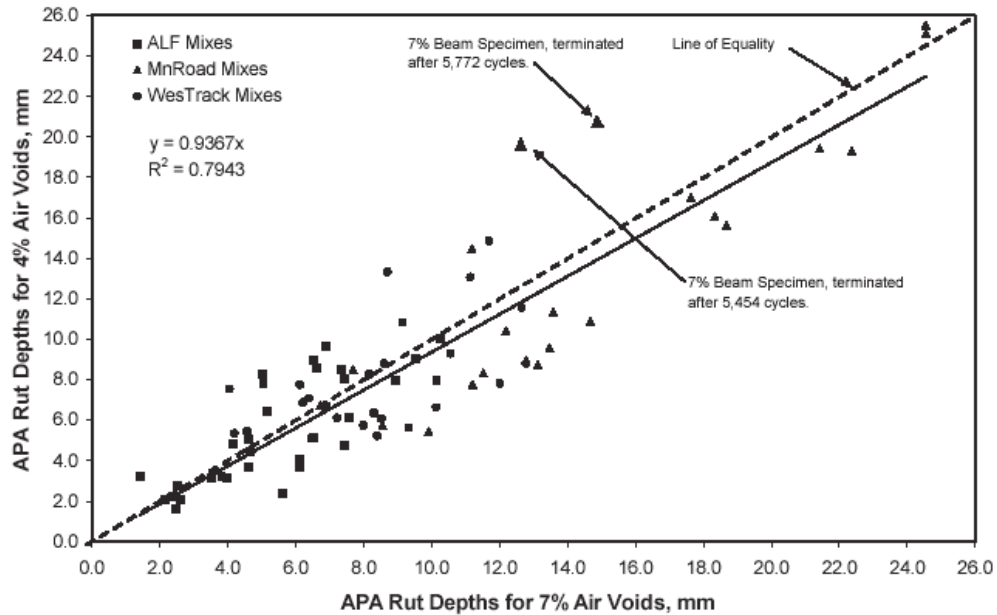


FIGURE 5.7 Effects of air voids on APA rut depths (80).

As shown in Figure 5.6, the normalized field rut depths show a positive trend with lab rut depth. If a possible outlier from Westrack project is removed from the regression, the R^2 value of the regression equation increased from 0.36 to 0.79. However, there is no strong evidence to identify this point is an outlier, therefore the researchers (80) still used the regression from all data to set up the APA rutting criteria. If we use the regression equation with all data to predict the field rut depth, the average field rut depth will be expected as 8.7 and 10.5 mm after 10 million ESALs for SMA mixture designed with 100 and 65 gyrations, respectively. This level of rutting is acceptable if we assume the maximum acceptable field rut depth is 12.5 mm, which has been used for many studies (71, 80, 89). For SMA mixtures designed with 40 gyrations, the predicted field rut depth is 12.5 mm based on the average APA rut depth of 4.8 mm. This is the maximum acceptable field rut depth and therefore SMA mixtures designed with 40 gyrations may not have enough rutting resistance.

In summary, the APA rut depth appears to be affected by the aggregate types and compaction levels. NMAS is not shown as a significant factor. However, the APA rutting results in this study are in a relatively narrow range (2.3 to 6.1 mm) therefore the precision of the test may mask the significance of these influencing factors. The good APA rutting results for all aggregate types indicate the suggested requirements for aggregate properties such as 20 percent maximum for F&E (3:1) and 30 percent maximum for L.A abrasion may be too stringent. The discussion on the effect of compaction indicates that 65 gyrations is a low compaction level that still can provide satisfactory rutting resistance.

5.2 DYNAMIC MODULUS

As discussed in the literature review, the dynamic modulus test is one of the top tests selected by the NCHRP 9-19 researchers (84) for predicting rutting resistance although many researchers (92-93) have questioned the accuracy of using this test for rutting prediction. This section will present the dynamic modulus test results and examine the influencing factors on the test results. The effect of compaction level on the dynamic modulus test results will be evaluated and the effectiveness of the dynamic modulus test for predicting rutting resistance will be discussed.

The dynamic modulus test was conducted for a total of 32 mixtures, in which 15 mixtures were designed at the 100 gyration level, 15 mixtures were designed at the 65 gyration level, and 2 mixtures were designed with 40 gyrations. Three replicates were conducted for each mixture. The individual dynamic modulus test results are shown in Appendix Table D1. Table D1 includes the dynamic modulus and phase angle results under the dynamic stress at a series of load frequencies of 25Hz, 10Hz, 5Hz, 1Hz, 0.5Hz

and 0.1Hz. At a high test temperature of 60°C, the higher complex modulus E^* indicates the stiffer asphalt mixtures, therefore higher deformation resistance; the lower phase angle ϕ indicates more elastic asphalt mixture, therefore quicker recovery and less permanent deformation. The compound index $E^*/\sin\phi$ under high temperature has been suggested (84) to be used as an indication of rutting resistance.

The ruby granite 12.5 mm NMAAS mixture designed with 40 gyrations showed unexpected high dynamic modulus values. The average dynamic modulus values for 12.5 mm ruby granite mixtures are 910, 785, and 1199 MPa at 10Hz for 100, 65 and 40 gyrations, respectively. The high value for the 40 gyrations designed mixture was noticed during the test, and extra care was taken to ensure the test conditions including test temperature and loading conditions were the same as required for the rest of the test. Although this mixture was designed and evaluated as supplemental mixtures after testing all the other mixtures was completed, the sample preparation followed the same procedure, and sample size and air void contents for this mixture were within the allowable range. To examine the possible batching problem, the asphalt content and gradation were determined by conducting the ignition oven test and sieve analysis. The investigation results showed the correct asphalt content and gradations were used. The asphalt content was within 0.1 percent from the designed value, and the values of percent passing each sieve were within a reasonable range of 1-2 percent from the gradation results for 65 gyration samples. Since only two mixtures were designed with 40 gyrations, test results for these two mixtures were not included in the following ANOVAs and discussions.

TABLE 5.3 ANOVA for Dynamic Modulus

Source	DF	Seq SS	Adj SS	Adj MS	F	P
Agg.	4	5153812	5153812	1288453	24.2	0.000
NMAS	2	893965	893965	446982	8.4	0.000
Gyrs	1	782476	782476	782476	14.7	0.000
Hz	5	16003526	16003526	3200705	60.12	0.000
Agg.*NMAS	8	1961960	1961960	245245	4.61	0.000
Agg.*Gyrs	4	948451	948451	237113	4.45	0.002
Agg.*Hz	20	454733	454733	22737	0.43	0.987
NMAS*Gyrs	2	237551	237551	118775	2.23	0.109
NMAS*Hz	10	94580	94580	9458	0.18	0.998
Gyrs*Hz	5	51347	51347	10269	0.19	0.965
Agg.*NMAS*Gyrs	8	2760676	2760676	345084	6.48	0.000
Agg.*NMAS*Hz	40	68749	68749	1719	0.03	1.000
Agg.*Gyrs*Hz	20	16681	16681	834	0.02	1.000
NMAS*Gyrs*Hz	10	52411	52411	5241	0.1	1.000
Agg.*NMAS*Gyrs*Hz	40	166726	166726	4168	0.08	1.000
Error	360	19166711	19166711	53241		
Total	539	48814354				

Initial analysis of the dynamic modulus test results was performed by conducting two ANOVAs to evaluate the effect of the main factors (aggregate type, NMAS, gyration level, and test frequency) and any interactions between the main factors on dynamic modulus and phase angle. These two ANOVAs are shown in Tables 5.3 and 5.4.

TABLE 5.4 ANOVA for Phase Angle

Source	DF	Seq SS	Adj SS	Adj MS	F	P
Agg.	4	714.12	714.12	178.53	18.16	0.000
NMAS	2	56.18	56.18	28.09	2.86	0.059
Gyrs	1	103.4	103.4	103.4	10.52	0.001
Hz	5	33586.33	33586.33	6717.27	683.25	0.000
Agg.*NMAS	8	545.77	545.77	68.22	6.94	0.000
Agg.*Gyrs	4	321.55	321.55	80.39	8.18	0.000
Agg.*Hz	20	165.73	165.73	8.29	0.84	0.661
NMAS*Gyrs	2	4.24	4.24	2.12	0.22	0.806
NMAS*Hz	10	21.31	21.31	2.13	0.22	0.995
Gyrs*Hz	5	1.25	1.25	0.25	0.03	1.000
Agg.*NMAS*Gyrs	8	325.1	325.1	40.64	4.13	0.000
Agg.*NMAS*Hz	40	101.11	101.11	2.53	0.26	1.000
Agg.*Gyrs*Hz	20	29.49	29.49	1.47	0.15	1.000
NMAS*Gyrs*Hz	10	21.51	21.51	2.15	0.22	0.995
Agg.*NMAS*Gyrs*Hz	40	68.27	68.27	1.71	0.17	1.000
Error	360	3539.26	3539.26	9.83		
Total	539	39604.63				

For dynamic modulus, all the main factors were significant and the interaction between aggregate type and NMAS, aggregate type and compaction level, and interaction among aggregate types, NMAS and compaction level were also significant. As shown in Tables 5.3 and 5.4, the load frequency is the most significant factor indicated by the highest F statistic value of 60 and 683, respectively. The effect of load frequency will be discussed first and all the other significant factors will be discussed later. The average dynamic modulus results with different test frequencies are shown in Figure 5.8. One standard deviation is shown as error bar. As shown in Figure 5.8, the standard deviation values for each load frequency depended on the average modulus values, an average COV of 19.8 percent was determined. This average COV value is not surprising because the test variability is expected to be higher for SMA mixture than dense-graded mixture. SMA is a gap-graded mix with a high percentage of coarse aggregates. With the same sample size as dense-graded mix, SMA mixture is likely to be more variable because the high potential for segregation within a sample. As expected, the dynamic modulus increased with an increase of loading frequency for all tested samples. With a decrease of load frequency, the mixtures tend to have less stiffness according to the time-temperature superposition mechanism, therefore lower dynamic modulus values occur at these lower frequencies.

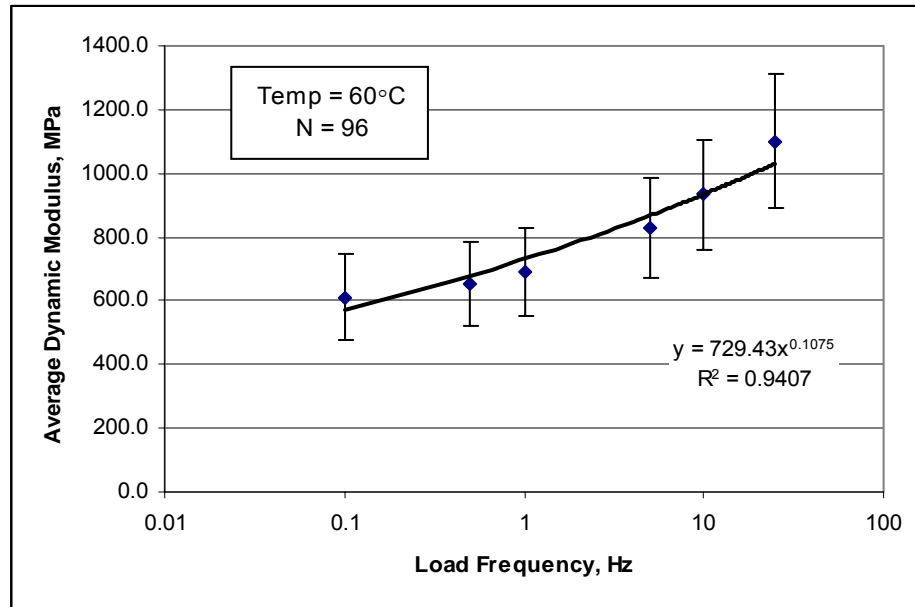


FIGURE 5.8 Average dynamic modulus versus load frequency.

The ANOVA results (Table 5.4) for phase angle were similar to those results for dynamic modulus. All the main factors except NMAS were significant and there were significant interactions between aggregate type and NMAS, aggregate type and compaction level, and between aggregate type, NMAS and compaction level. The average phase angles with different test frequencies are shown in Figure 5.9. One standard deviation is shown as error bar. The pooled standard deviation for all load frequencies is 2.2 degrees. This standard deviation is compatible to the result from other studies (84, 86), where the standard deviation for phase angle was reported from 1.8 to 2.3 degrees.

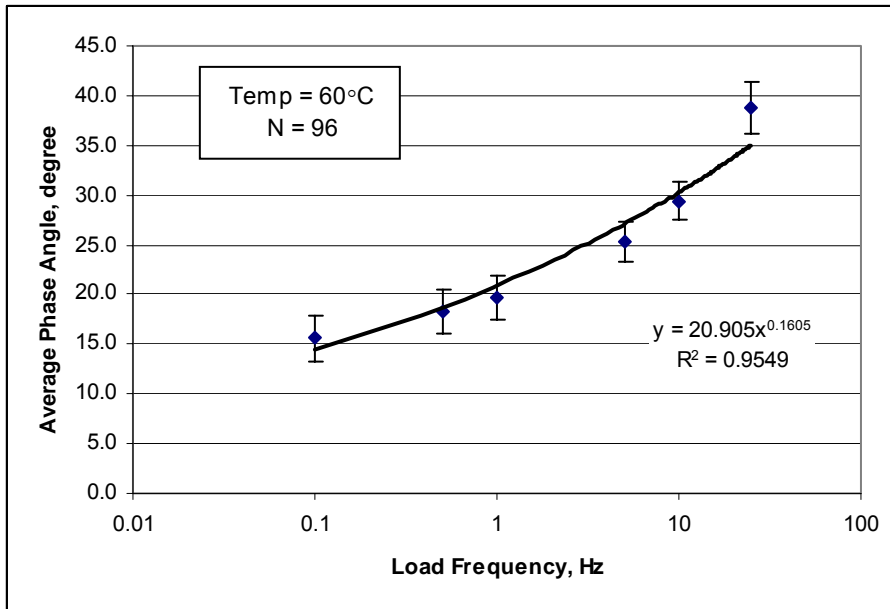


FIGURE 5.9 Average phase angle versus load frequency.

As expected, the phase angle increased with the increase of loading frequency for all tested samples. Similar phenomenon had also been reported by other researchers (87, 112). However, this trend is not usually observed at the low or normal test temperature, such as 5°C and 25°C. This phenomenon can be explained by the mechanism of composite material. The SMA mixture which had a good aggregate skeleton structure can be seen as a composite material that is composed of aggregate structure and asphalt mortar. The decrease of loading frequency, which gives the same effect as an increase in test temperature, will cause the asphalt mortar to have a small elastic component and become more viscous. At a high test temperature, when the load frequency is lowered to a certain level, the aggregate structure becomes dominant within the whole mix structure. With the confining test condition, the aggregate structure is close to becoming elastic. Therefore, with a decrease of loading frequency, the aggregate structure within the mixtures becomes more dominant, and increases the elastic component of the whole

structure, which resulted in the lower phase angle. The decrease of phase angle with the decrease of loading frequency, to some extent, indicates that a strong internal structure existed. To better explain this, the elastic and viscous parts of complex modulus were calculated based on Equation 3.11, and are shown in Figure 5.10. One standard deviation is shown as error bar. Since the standard deviation values depended on modulus values, average COV values of 20.4 and 19.3 percent were determined for storage and loss modulus, respectively.

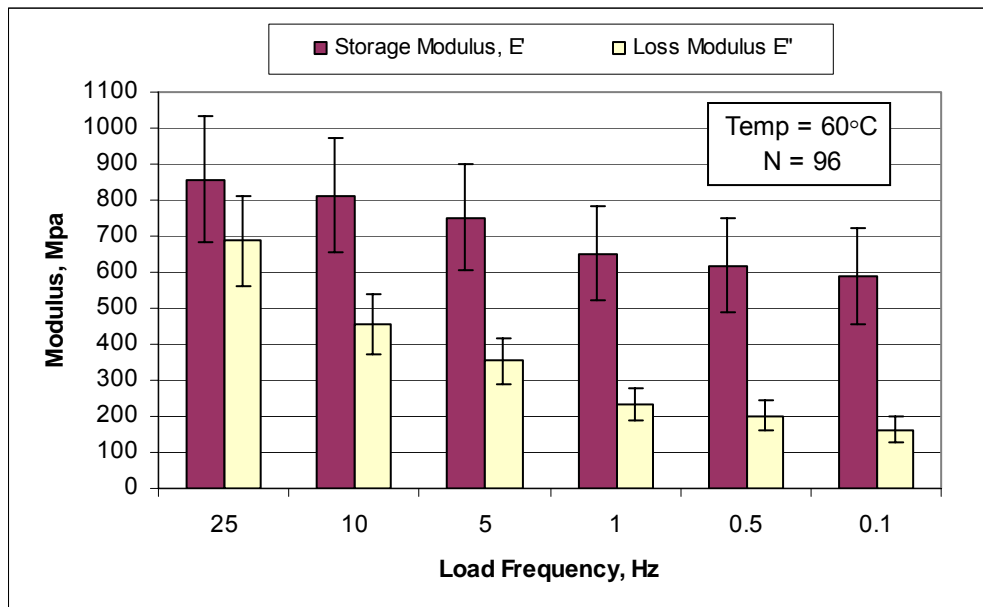


FIGURE 5.10 Average storage and loss modulus at different frequencies.

As shown in Figure 5.10, both the storage and loss modulus decreased with the decrease of load frequency. However, the decrease rate of storage modulus slowed down with the decrease of load frequency and maintained nearly a constant level, while the loss modulus had a higher decrease rate and quickly approached zero with the decrease of load frequency. The storage modulus maintained at a certain level indicates the aggregate skeleton became dominant and this structure is less dependent of load frequency. The fact

that loss modulus approached zero indicates the role of asphalt binder becomes negligible at low frequency and high temperature.

As shown in Tables 5.3 and 5.4, test frequency is the only testing condition variable in the ANOVA analysis and the most significant factor as indicated by the highest F statistics and lowest P value. Therefore, the test results are demonstrated and discussed separately regarding different frequencies. Since the 10 Hz and 0.1 Hz are typically used to simulate the high speed and low speed vehicle loading (84, 87), these two frequencies will be analyzed in more detail.

The test results for all designed mixtures are presented in Tables 5.5 and 5.6 for the load frequency of 10 Hz and 0.1 Hz. The average value and coefficient of variation (COV) of dynamic modulus E^* , phase angle ϕ and $E^*/\sin\phi$ are included in the tables. Comparing these two tables, the COV values for test results of 0.1 Hz are generally higher than those of 10 Hz. This might be due to the lower value for both dynamic modulus E^* and phase angle ϕ in lower frequency. The same variation in test results measurement and data processing procedure gave the lower test value a higher COV value.

TABLE 5.5 Dynamic Modulus Test Results at Load Frequency of 10 Hz

Agg. Type	NMAAS	Gyrs	E*, MPa		ϕ , degree		E*/sin ϕ , MPa	
			Average	COV,%	Average	COV,%	Average	COV,%
C.GVL	19	100	773.3	4.4	26.8	5.9	1720.1	9.5
C.GVL	12.5	100	834.2	24.4	29.4	2.6	1691.8	22.3
C.GVL	9.5	100	983.3	17.6	27.6	9.4	2147.5	24.4
L.GRN	19	100	894.0	17.6	28.1	7.6	1900.6	17.3
L.GRN	12.5	100	1248.1	10.1	27.4	5.3	2724.1	14.5
L.GRN	9.5	100	1120.0	19.7	30.9	8.7	2189.9	21.6
LMS	19	100	968.7	17.0	29.3	15.9	2038.3	28.8
LMS	12.5	100	1206.6	18.6	30.4	4.1	2384.2	17.3
LMS	9.5	100	1084.5	50.3	28.8	10.6	2339.1	55.2
R.GRN	19	100	865.9	22.4	32.0	5.1	1639.9	23.0
R.GRN	12.5	100	910.3	11.1	31.7	11.0	1732.4	5.5
R.GRN	9.5	100	893.0	31.9	32.9	5.8	1631.1	27.1
TRAP	19	100	820.8	19.7	27.5	3.6	1784.3	21.5
TRAP	12.5	100	900.3	4.1	25.8	1.7	2066.7	4.7
TRAP	9.5	100	1098.7	33.3	27.1	11.3	2492.2	45.3
C.GVL	19	65	615.8	9.7	29.6	16.5	1283.2	26.2
C.GVL	12.5	65	717.8	59.6	31.0	17.8	1498.1	66.9
C.GVL	9.5	65	824.7	10.7	31.6	2.0	1573.4	11.0
L.GRN	19	65	1117.9	25.5	27.5	7.6	2457.6	33.4
L.GRN	12.5	65	1024.9	29.0	30.9	7.8	2022.2	34.9
L.GRN	9.5	65	761.5	31.6	32.5	8.9	1446.5	37.2
LMS	19	65	1112.7	3.7	28.8	2.2	2310.1	4.5
LMS	12.5	65	1009.4	51.5	29.6	21.2	2262.8	72.7
LMS	9.5	65	1214.4	23.1	28.9	9.3	2534.2	27.6
R.GRN	19	65	852.8	22.3	30.3	5.1	1686.7	19.7
R.GRN	12.5	65	785.0	14.0	32.1	6.9	1489.3	19.4
R.GRN	9.5	65	1020.7	20.0	28.4	9.5	2146.0	17.6
TRAP	19	65	573.5	15.5	29.9	13.1	1159.8	16.3
TRAP	12.5	65	976.9	21.4	26.7	10.3	2169.5	15.4
TRAP	9.5	65	656.7	40.1	30.0	11.8	1357.7	46.7
L.GRN	12.5	40	1126.5	9.4	25.9	0.8	2582.6	10.1
R.GRN	12.5	40	1198.8	9.1	22.5	11.4	3167.2	17.8
Overall Average:			943.5	21.8	29.1	8.5	1988.4	25.5

TABLE 5.6 Dynamic Modulus Test Results at Load Frequency of 0.1 Hz

Agg. Type	NMAAS	Gyrs	E*, MPa		ϕ , degree		E*/sin ϕ , MPa	
			Average	COV,%	Average	COV,%	Average	COV,%
C.GVL	19	100	561.0	10.3	11.8	4.1	2757.8	13.2
C.GVL	12.5	100	537.9	30.4	12.6	11.5	2444.2	24.2
C.GVL	9.5	100	647.4	21.1	12.0	5.7	3147.5	26.2
L.GRN	19	100	601.2	28.8	15.6	15.1	2308.0	37.7
L.GRN	12.5	100	893.7	19.0	14.2	13.7	3747.5	30.1
L.GRN	9.5	100	666.2	21.2	16.9	20.5	2352.0	29.4
LMS	19	100	707.7	32.5	14.4	15.6	2940.9	40.9
LMS	12.5	100	683.0	27.9	18.3	21.5	2251.1	34.9
LMS	9.5	100	642.1	58.2	16.2	23.6	2573.1	68.6
R.GRN	19	100	527.4	28.9	17.7	9.1	1759.3	31.8
R.GRN	12.5	100	529.6	4.7	17.2	9.9	1795.4	5.9
R.GRN	9.5	100	596.5	40.0	19.4	16.4	1760.7	26.1
TRAP	19	100	539.2	34.7	14.4	3.4	2161.0	33.0
TRAP	12.5	100	602.3	6.8	13.2	5.5	2656.8	11.5
TRAP	9.5	100	803.1	36.1	13.3	19.5	3782.2	58.2
C.GVL	19	65	422.1	27.1	14.1	43.4	2271.4	82.5
C.GVL	12.5	65	519.8	66.4	12.8	43.9	2932.3	74.4
C.GVL	9.5	65	547.9	7.2	15.4	10.1	2092.5	17.8
L.GRN	19	65	728.0	31.0	14.9	14.5	2964.9	46.9
L.GRN	12.5	65	713.2	29.4	16.5	10.7	2568.7	39.0
L.GRN	9.5	65	401.5	45.7	19.4	3.7	1212.1	45.4
LMS	19	65	717.3	21.2	16.8	4.6	2487.7	21.5
LMS	12.5	65	657.5	71.1	18.0	31.9	2731.6	104.3
LMS	9.5	65	866.9	27.1	14.5	3.1	3481.7	29.8
R.GRN	19	65	558.6	17.1	15.2	9.9	2115.8	8.4
R.GRN	12.5	65	485.6	34.6	20.0	17.3	1507.2	49.9
R.GRN	9.5	65	638.9	27.6	15.7	23.7	2512.8	40.8
TRAP	19	65	321.7	23.0	18.2	14.8	1037.7	22.9
TRAP	12.5	65	716.5	28.8	12.5	7.1	3291.6	25.2
TRAP	9.5	65	406.1	47.4	17.0	24.9	1540.7	59.0
L.GRN	12.5	40	798.7	0.5	13.2	2.1	3496.4	1.8
R.GRN	12.5	40	906.7	12.1	10.5	18.9	5142.3	26.5
Overall Average:			623.3	28.7	15.4	15.0	2557.0	36.5

At 10 Hz load frequency, the average COV for dynamic modulus, phase angle and E*/sin ϕ are 21.8, 8.5 and 25.5 percent, respectively. At 0.1 Hz load frequency, the average COV for dynamic modulus, phase angle and E*/sin ϕ are 28.7, 15.0 and 36.5 percent, respectively.

Some extremely high or low values might adversely affect the analysis of the test results, and are seen as outliers. The outliers were determined based on the $E^*/\sin\phi$ data set with COV higher than 50 percent. This criterion is a round-up value from overall average COV plus one standard deviation of COV values. Within these data sets, the test results that had the biggest difference from the average were considered as potentially erroneous and were excluded from the analysis data set. The average test values for these mixtures were from the average of two remaining individual test results instead of all three replicates.

A total of 6 samples (out of total 96 samples) were determined as outliers following the criteria described above. After removing these outliers, the average COV decreased. The new average and COV values are shown in Tables 5.7 and 5.8. The following data analyses are based on the data set after the removal of the outliers. At 10 Hz load frequency, the average COV for dynamic modulus, phase angle and $E^*/\sin\phi$ are 16.5, 6.4 and 18.6 percent, respectively. At 0.1 Hz load frequency, the average COV for dynamic modulus, phase angle and $E^*/\sin\phi$ are 22.1, 10.5 and 26.1 percent, respectively. The test variability is expected higher for SMA mixture than dense-graded mixture since SMA is a gap-graded mix with high percentage of coarse aggregates. With the same sample size as dense-graded mix, SMA mixture is likely to be more variable because the high potential for segregation. The test precision for dynamic modulus has not yet been developed, however, the COV in this study is similar to that from other studies (84, 86). For load frequency of 10 Hz, Witczak et al (84) and Bonaquist et al (86) reported the average COV values for E^* were 15.2 and 13.0 percent, respectively, and the standard deviation values for phase angle were 2.3 and 1.8 degrees, respectively.

TABLE 5.7 Dynamic Modulus Test Results at Load Frequency of 10 Hz (Without 6 Outlier Samples)

Agg. Type	NMAAS	Gyrs	E*		ϕ		E*/sin ϕ	
			Average	COV,%	Average	COV,%	Average	COV,%
C.GVL	19	100	773.3	4.4	26.8	5.9	1720.1	9.5
C.GVL	12.5	100	834.2	24.4	29.4	2.6	1691.8	22.3
C.GVL	9.5	100	983.3	17.6	27.6	9.4	2147.5	24.4
L.GRN	19	100	894.0	17.6	28.1	7.6	1900.6	17.3
L.GRN	12.5	100	1248.1	10.1	27.4	5.3	2724.1	14.5
L.GRN	9.5	100	1120.0	19.7	30.9	8.7	2189.9	21.6
LMS	19	100	968.7	17.0	29.3	15.9	2038.3	28.8
LMS	12.5	100	1206.6	18.6	30.4	4.1	2384.2	17.3
LMS	9.5	100	1398.1	4.9	27.0	2.3	3079.7	7.0
R.GRN	19	100	865.9	22.4	32.0	5.1	1639.9	23.0
R.GRN	12.5	100	910.3	11.1	31.7	11.0	1732.4	5.5
R.GRN	9.5	100	893.0	31.9	32.9	5.8	1631.1	27.1
TRAP	19	100	820.8	19.7	27.5	3.6	1784.3	21.5
TRAP	12.5	100	900.3	4.1	25.8	1.7	2066.7	4.7
TRAP	9.5	100	889.6	8.5	28.8	2.0	1843.1	6.7
C.GVL	19	65	582.9	4.3	32.3	6.5	1094.7	10.1
C.GVL	12.5	65	939.4	28.5	27.8	1.9	2020.7	30.1
C.GVL	9.5	65	824.7	10.7	31.6	2.0	1573.4	11.0
L.GRN	19	65	1117.9	25.5	27.5	7.6	2457.6	33.4
L.GRN	12.5	65	1024.9	29.0	30.9	7.8	2022.2	34.9
L.GRN	9.5	65	761.5	31.6	32.5	8.9	1446.5	37.2
LMS	19	65	1112.7	3.7	28.8	2.2	2310.1	4.5
LMS	12.5	65	718.6	25.3	33.1	6.9	1327.5	31.1
LMS	9.5	65	1214.4	23.1	28.9	9.3	2534.2	27.6
R.GRN	19	65	852.8	22.3	30.3	5.1	1686.7	19.7
R.GRN	12.5	65	785.0	14.0	32.1	6.9	1489.3	19.4
R.GRN	9.5	65	1020.7	20.0	28.4	9.5	2146.0	17.6
TRAP	19	65	573.5	15.5	29.9	13.1	1159.8	16.3
TRAP	12.5	65	976.9	21.4	26.7	10.3	2169.5	15.4
TRAP	9.5	65	808.0	3.8	28.1	4.1	1720.2	7.6
L.GRN	12.5	40	1126.5	9.4	25.9	0.8	2582.6	10.1
R.GRN	12.5	40	1198.8	9.1	22.5	11.4	3167.2	17.8
Overall Average:			948.3	16.5	29.2	6.4	1983.8	18.6

TABLE 5.8 Dynamic Modulus Test Results at Load Frequency of 0.1 Hz (Without 6 Outlier Samples)

Agg. Type	NMAAS	Gyrs	E*		ϕ		E*/sin ϕ	
			Average	COV,%	Average	COV,%	Average	COV,%
C.GVL	19	100	561.0	10.3	11.8	4.1	2757.8	13.2
C.GVL	12.5	100	537.9	30.4	12.6	11.5	2444.2	24.2
C.GVL	9.5	100	647.4	21.1	12.0	5.7	3147.5	26.2
L.GRN	19	100	601.2	28.8	15.6	15.1	2308.0	37.7
L.GRN	12.5	100	893.7	19.0	14.2	13.7	3747.5	30.1
L.GRN	9.5	100	666.2	21.2	16.9	20.5	2352.0	29.4
LMS	19	100	707.7	32.5	14.4	15.6	2940.9	40.9
LMS	12.5	100	683.0	27.9	18.3	21.5	2251.1	34.9
LMS	9.5	100	856.9	5.3	14.2	14.2	3553.1	19.2
R.GRN	19	100	527.4	28.9	17.7	9.1	1759.3	31.8
R.GRN	12.5	100	529.6	4.7	17.2	9.9	1795.4	5.9
R.GRN	9.5	100	596.5	40.0	19.4	16.4	1760.7	26.1
TRAP	19	100	539.2	34.7	14.4	3.4	2161.0	33.0
TRAP	12.5	100	602.3	6.8	13.2	5.5	2656.8	11.5
TRAP	9.5	100	637.1	7.6	14.7	6.1	2518.9	13.6
C.GVL	19	65	361.0	17.0	17.7	3.4	1193.4	20.2
C.GVL	12.5	65	699.6	30.1	9.6	12.8	4154.6	17.7
C.GVL	9.5	65	547.9	7.2	15.4	10.1	2092.5	17.8
L.GRN	19	65	728.0	31.0	14.9	14.5	2964.9	46.9
L.GRN	12.5	65	713.2	29.4	16.5	10.7	2568.7	39.0
L.GRN	9.5	65	401.5	45.7	19.4	3.7	1212.1	45.4
LMS	19	65	717.3	21.2	16.8	4.6	2487.7	21.5
LMS	12.5	65	392.9	33.7	21.2	5.3	1095.2	38.4
LMS	9.5	65	866.9	27.1	14.5	3.1	3481.7	29.8
R.GRN	19	65	558.6	17.1	15.2	9.9	2115.8	8.4
R.GRN	12.5	65	485.6	34.6	20.0	17.3	1507.2	49.9
R.GRN	9.5	65	638.9	27.6	15.7	23.7	2512.8	40.8
TRAP	19	65	321.7	23.0	18.2	14.8	1037.7	22.9
TRAP	12.5	65	716.5	28.8	12.5	7.1	3291.6	25.2
TRAP	9.5	65	517.0	2.7	14.5	3.3	2063.2	5.9
L.GRN	12.5	40	798.7	0.5	13.2	2.1	3496.4	1.8
R.GRN	12.5	40	906.7	12.1	10.5	18.9	5142.3	26.5
Overall Average:			623.7	22.1	15.4	10.5	2517.9	26.1

The following data analyses are based on the data set after the removal of the outliers. General linear model analysis was used instead of ANOVA since the data set is not balanced after removing the outliers. Since the dynamic modulus E^* or phase angle ϕ alone is not sufficient as an indication of rutting performance, the following analyses on the dynamic modulus test results will focus on the compound index $E^*/\sin\phi$ under load frequencies of 10 Hz and 0.1 Hz.

The test parameter $E^*/\sin\phi$ was recommended as an indication for rutting resistance from the NCHRP study (84). A higher $E^*/\sin\phi$ value indicates a stiffer and more elastic mixture, therefore more rutting resistance. A GLM analysis was conducted to evaluate the effect of the main factors (aggregate type, NMAS, and compaction level) and any interactions between the main factors on 10 Hz $E^*/\sin\phi$ results. The GLM results are shown in Table 5.9.

TABLE 5.9 GLM Results on $E^*/\sin\phi$ at Load Frequency of 10 Hz

Source	DF	Seq SS	Adj SS	Adj MS	F	P
Agg	4	4482858	4397433	1099358	6.27	0.000
NMAS	2	811976	938666	469333	2.68	0.078
Gyrs	1	794780	1060275	1060275	6.05	0.017
Agg*NMAS	8	4001692	4522435	565304	3.22	0.005
Agg*Gyrs	4	648364	716546	179136	1.02	0.405
NMAS*Gyrs	2	311698	246147	123073	0.70	0.500
Agg*NMAS*Gyrs	8	4109750	4109750	513719	2.93	0.009
Error	54	9470151	9470151	175373		
Total	83	24631269				

As shown in Table 5.9, the aggregate type and compaction level are significant factors. The interaction between aggregate type and NMAS, and the interaction among all three main factors are significant.

The average $E^*/\sin\phi$ values for different aggregate types and two compaction levels are shown in Figure 5.11. One standard deviation is shown as error bar. N_1 and N_2 represent the number of samples used for average for each group.

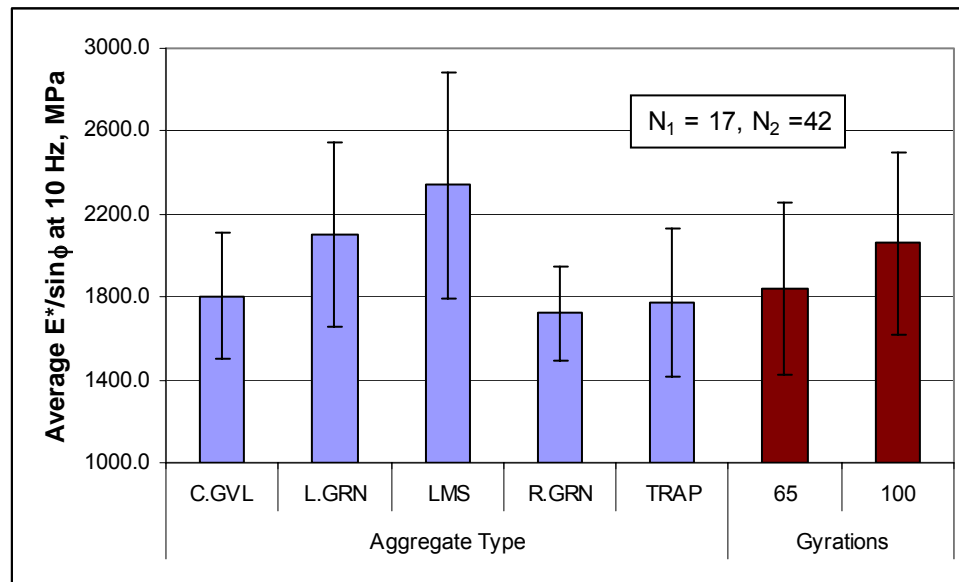


FIGURE 5.11 Average $E^*/\sin\phi$ results at frequency of 10 Hz.

As shown in Figure 5.11, $E^*/\sin\phi$ depends on aggregate type. The limestone had the highest average $E^*/\sin\phi$ value of 2288 MPa, while crushed gravel, ruby granite and traprock had similar average $E^*/\sin\phi$ values of about 1750 MPa in the low end. The limestone and ruby granite had higher $E^*/\sin\phi$ values which may be explained in that these two aggregates had the lowest VMA values (average 17.1 percent versus average 19.5 percent for other three aggregates, with the SSD method) and therefore tighter aggregate structures.

A decrease in compaction level from 100 to 65 gyrations resulted in an increase in $E^*/\sin\phi$ value from 1837 to 2019 MPa (9.9%). A paired t-test was conducted to compare

the mean $E^*/\sin\phi$ value for the mixtures designed with 65 and 100 gyrations, and the results are shown in Table 5.10.

TABLE 5.10 Pair T-Test Results on $E^*/\sin\phi$ Value of Two Compaction Levels

	N	Mean	StDev	SE Mean
100 Gyrs	15	2038.25	420.14	108.48
65 Gyrs	15	1810.56	463.45	119.66
Difference	15	227.69	509.69	131.60

95% CI for mean difference: (-54.570, 509.943)

T-Test of mean difference = 0 (vs not = 0): T-Value = 1.73, P-Value = 0.106

As shown in Table 5.10, there is no significant difference between $E^*/\sin\phi$ values of mixtures designed with these two compaction levels at a significant level of 95 percent. The mean $E^*/\sin\phi$ values shown in Table 5.10 are slightly different from the values shown in Figure 5.11. That is due to mean values shown in Table 5.10 are the mean values of 15 mixtures, and each mixture may have 2 or 3 replicates after removing 6 outliers, while the average values shown in Figure 5.11 are the overall average of individual samples.

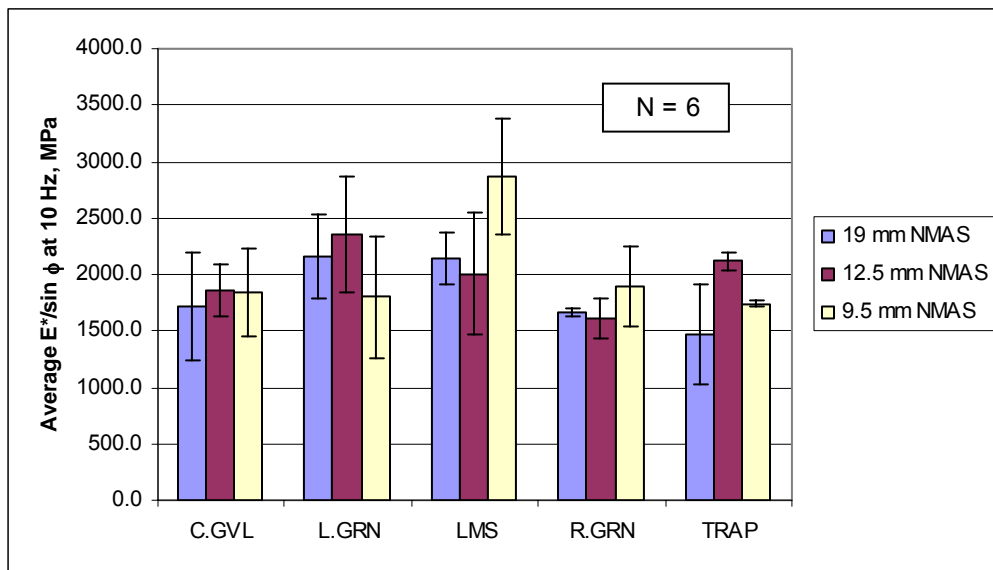


FIGURE 5.12 Interaction between aggregate type and NMA on $E^*/\sin\phi$ results at frequency of 10 Hz.

The interaction between aggregate type and NMAS on $E^*/\sin\phi$ at 10 Hz is shown in Figure 5.12. One standard deviation is shown as error bar. The effect of NMAS varied for different aggregate types. Again, for most aggregate the differences within three NMAS are not large.

A GLM analysis was conducted to evaluate the effect of the main factors (aggregate type, NMAS, and compaction level) and any interactions between the main factors on 0.1 Hz $E^*/\sin\phi$ results. The GLM results are shown in Table 5.11.

TABLE 5.11 GLM Results on $E^*/\sin\phi$ at Load Frequency of 0.1 Hz

Source	DF	Seq SS	Adj SS	Adj MS	F	P
Agg	4	6850333	6488918	1622229	2.98	0.027
NMAS	2	1803832	2222765	1111382	2.04	0.140
Gyrs	1	1252325	1740256	1740256	3.20	0.079
Agg*NMAS	8	20764608	22422769	2802846	5.15	0.000
Agg*Gyrs	4	2029754	2025696	506424	0.93	0.453
NMAS*Gyrs	2	417676	576286	288143	0.53	0.592
Agg*NMAS*Gyrs	8	14399518	14399518	1799940	3.31	0.004
Error	54	29392371	29392371	544303		
Total	83	76910416				

As shown in Table 5.11, only aggregate type is a significant main factor for $E^*/\sin\phi$ at load frequency of 0.1 Hz at a significant level of 95 percent. The interaction between aggregate type and NMAS, and the interaction among three main factors are also significant.

The average $E^*/\sin\phi$ values for different aggregate types are shown in Figure 5.13. One standard deviation is shown as error bar. As shown in Figure 5.13, the ruby granite had the lowest average $E^*/\sin\phi$ value of 1900 MPa, while crushed gravel, lab granite, and limestone had the similar average $E^*/\sin\phi$ values of about 2600 MPa. The low $E^*/\sin\phi$ value for traprock and ruby granite is probably due to the relatively high asphalt content for these two aggregates (average 6.6 percent versus average 6.0 percent for the other

three aggregates). The high asphalt content increased the effect of asphalt binder under high temperature and low load frequency.

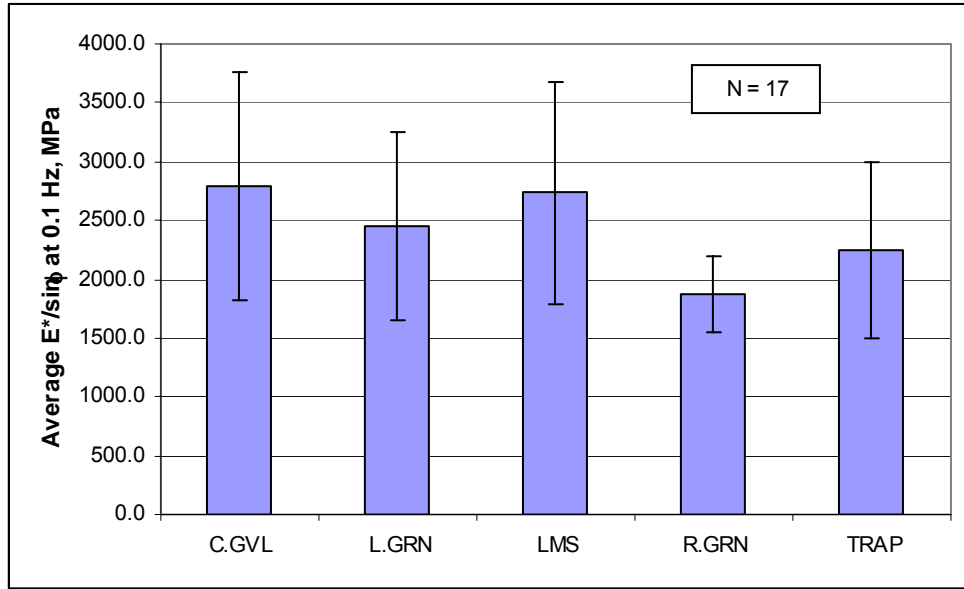


FIGURE 5.13 Average $E^*/\sin\phi$ results at frequency of 0.1 Hz.

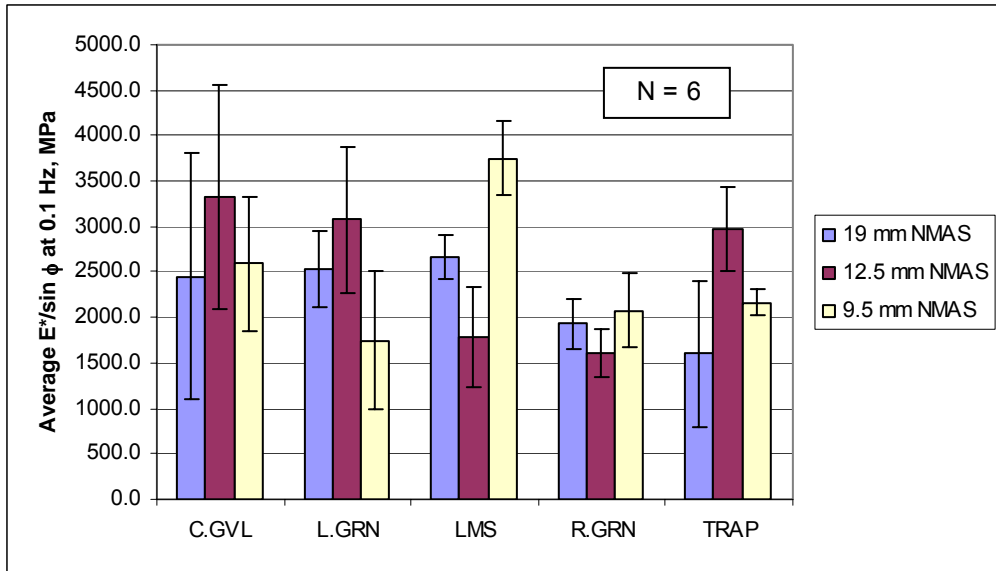


FIGURE 5.14 Interaction between aggregate type and NMAS on $E^*/\sin\phi$ results at frequency of 0.1 Hz.

The interaction between aggregate type and NMAS on $E^*/\sin\phi$ at 0.1 Hz is shown in Figure 5.14. One standard deviation is shown as the error bar. For different aggregate

types, the average $E^*/\sin\phi$ followed the different orders for the three NMAS. 12.5 mm NMAS mixtures for limestone and ruby granite had the lowest $E^*/\sin\phi$ value for the three NMAS mixtures, while for the other three aggregates, 12.5 mm NMAS mixtures had the highest $E^*/\sin\phi$ value for the three NMAS mixtures. There appears to be no scientific reason for the combination effects of aggregate type and NMAS on $E^*/\sin\phi$ value. It is believed that showing that these two properties have an interaction is simply due to normal variation of the test results.

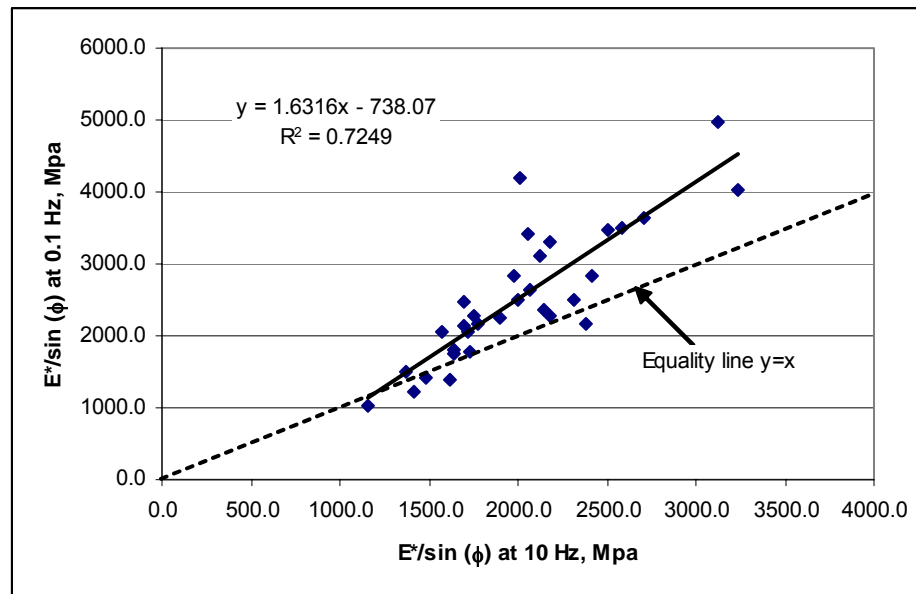
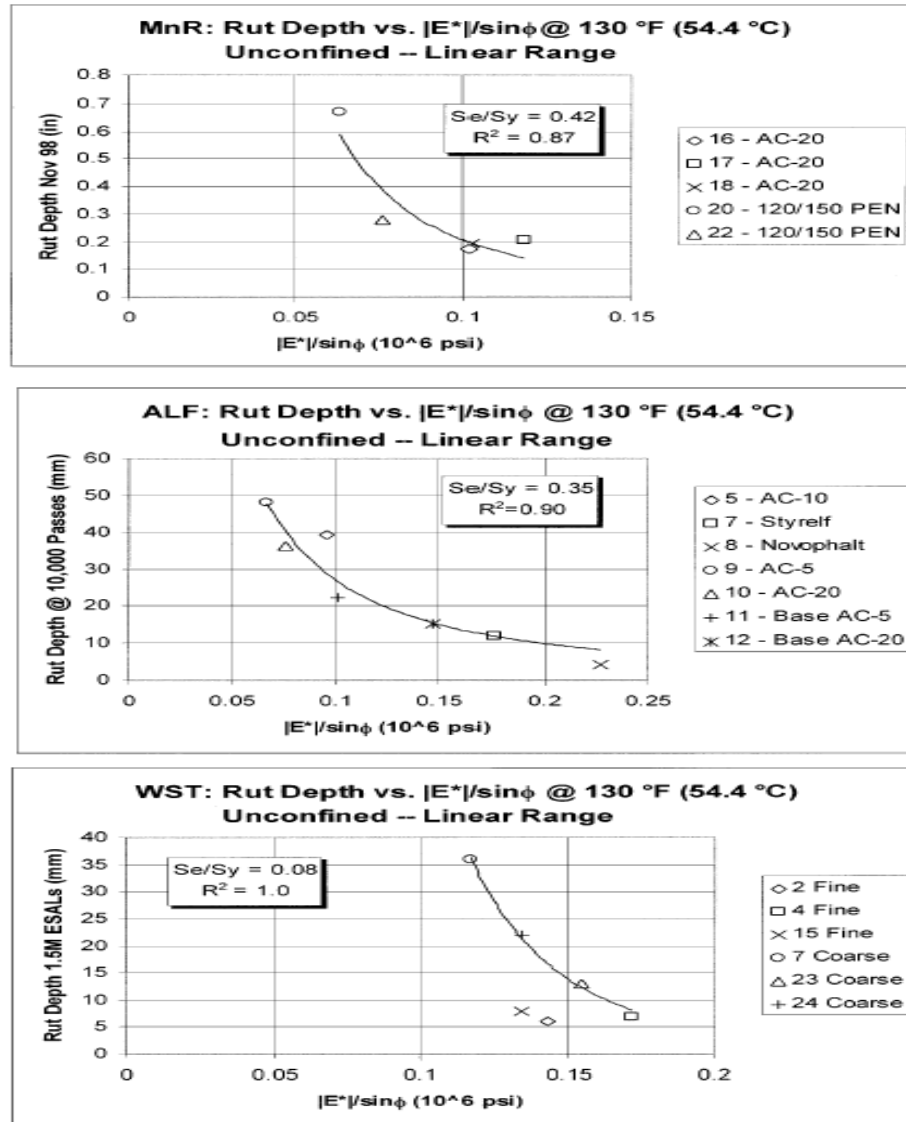


FIGURE 5.15 The comparison of $E^*/\sin\phi$ between 10 Hz and 0.1 Hz.

A comparison on $E^*/\sin\phi$ value between 10 Hz and 0.1 Hz is shown in Figure 5.15. The $E^*/\sin\phi$ value at 0.1 Hz is generally larger than those at 10 Hz. This is due to the combination effects of decreasing E^* and the phase angle ϕ value with the decrease of load frequency. However, this indicates that at the test temperature of 60°C, the $E^*/\sin\phi$ may give an erroneous prediction about the rutting resistance because it is believed that mixture will have lower rutting resistance at lower load frequency.

It is also observed that the difference between two load frequencies increases with the increase of test values. This is likely due to the enlarged effect of phase angle changes when the phase angle is smaller. For example, when the phase angle changes from 10 to 11 degrees, the $E^*/\sin\phi$ value changes about 9 percent, however when the phase angle changes from 30 to 31 degrees, the $E^*/\sin\phi$ value changes only 3 percent if the E^* stays constant.

The theoretical basis of using the $E^*/\sin\phi$ value to predict the rutting resistance relates to the assumption that it gives better protection against rutting at high temperature than the modulus alone by minimizing dissipated energy (87). Dissipated energy can be minimized in two ways: by having a stiffer binder or by having a lower phase angle value in the binder, i.e. more elastic behavior. However, the phase angle decreased with the decrease of load frequency at high temperatures because the elastic response from the aggregate skeleton overpowered the viscous influence of the binder in the mixtures. Thus, the theoretical formulation of minimizing dissipated energy, as it is used for the stiffness factor $G^*/\sin\delta$ in the binder specification, is not valid for the asphalt mixtures throughout the entire range of mixture performance. A study (87) on use of stiffness as a simple performance test concluded that the $E^*/\sin\phi$ value correlated with field rut depth best at high temperature (54.4°C) and relatively high load frequency (5 Hz). When the load frequency goes lower, the correlation between $E^*/\sin\phi$ and permanent deformation decreases.



NOTE: Sections 2 and 15 were treated as outliers and were not included in statistical analysis.

FIGURE 5.16 The correlations between field rut depths and $E^*/\sin\phi$ values (84).

NCHRP project 9-19 (84) presented several correlations between $E^*/\sin\phi$ and field rut depths based on the field data from MnRoad, ALF and Westrack test sections. These correlations are shown in Figure 5.16. It is noteworthy that there are some significant differences in test conditions between the NCHRP 9-19 project and this study. The correlations in Figure 5.16 were developed under unconfined and 130°F test temperature conditions. The unconfined test condition at high temperature is not practical

for SMA mixtures because the test samples with high asphalt content tend to slump and therefore have high test variability. Also, the unconfined test condition does not represent the real situation in the field.

The $E^*/\sin\phi$ results for SMA mixtures designed with 100 and 65 gyrations under confined test conditions of 140°F and 10 Hz are about 2000 MPa (0.29×10^6 psi) and 1800 MPa (0.26×10^6 psi). These values are higher than the maximum value for prediction if we directly put these values in the correlations developed by NCHRP 9-19 researchers. As we discussed above, the lower temperature (130°F versus 140°F) and lower load frequency (5 Hz versus 10 Hz) are likely to get even higher $E^*/\sin\phi$ values based on the results from this study. Therefore the SMA mixtures designed with both 100 and 65 gyrations are likely to be rutting resistant and have less than 10 mm field rut depth if the difference between confined and unconfined test conditions is not considered.

The correlation between $E^*/\sin\phi$ results at the two load frequencies and APA rutting results are shown in Figure 5.17. The regressions shown in Figure 5.17 indicate there is no correlation between $E^*/\sin\phi$ at either load frequency and the APA rut depths. This result is not surprising because as discussed above, the $E^*/\sin\phi$ is not a good indication for rutting resistance at high temperature and low load frequency. The narrow range of data may also contribute to this close to zero correlation. The APA rutting results indicate only 3 out of 32 mixtures showed significant rutting, which is more than 5 mm.

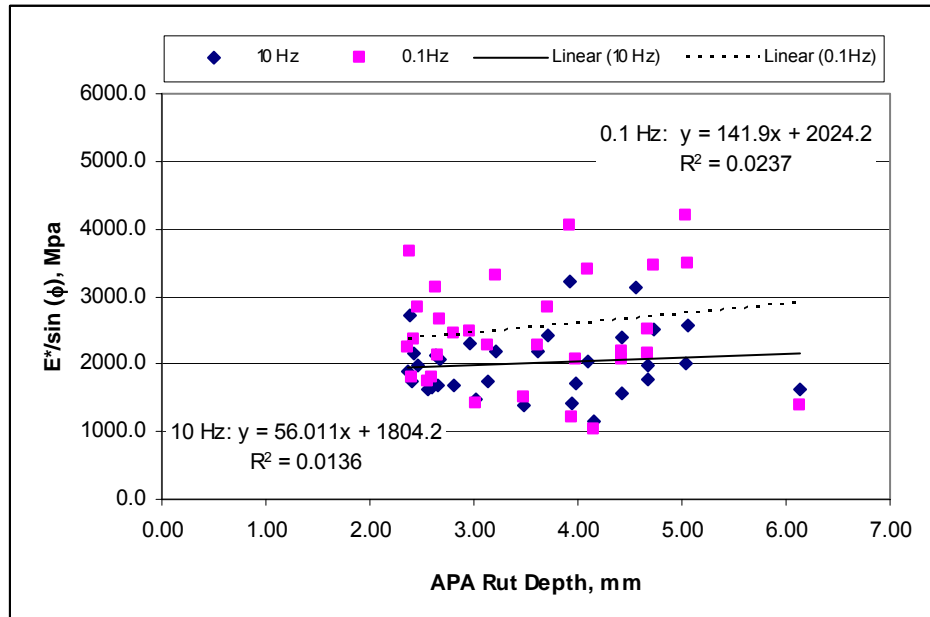


FIGURE 5.17 The relationships between $E^*/\sin\phi$ and APA rut depths.

In summary, compaction level was not shown as a significantly influencing factor for the $E^*/\sin\phi$ value at 10 Hz (Table 5.10) and 0.1 Hz (Table 5.11). The $E^*/\sin\phi$ value seems to depend on VMA values, or the tightness of aggregate structure. If this speculation is true, a dense-graded mixture will likely have a higher dynamic modulus value than a SMA mixture. The effect of stone-on-stone contact and the good resistance to high shearing force within a SMA mixture can't be appropriately evaluated by the relatively low applied stress associated with dynamic modulus test.

The $E^*/\sin\phi$ value at high temperature showed contrary results when the load frequency changed, i.e. had higher value under lower load frequency. The $E^*/\sin\phi$ value appears no longer appropriate as the indication for rutting resistance of SMA mixtures. Therefore, the effectiveness to evaluate rutting potential with the dynamic modulus test is indeed questionable. Many tests (30, 32) in the past have shown that in the laboratory dense-graded mixes have higher dynamic modulus values than SMA mixtures.

5.3 STATIC CREEP

As discussed in the literature review (94-95), the static creep test has been used to evaluate HMA rutting potential for many years. However, it was often conducted under the unconfined test condition. Only a few studies have used confined test conditions and additional work is needed to establish criteria to differentiate a rutting susceptible mix for the confined static creep test. This section will present the static creep test results and examine the influencing factors on the test results. The effect of compaction level on the static creep test results will be evaluated and effectiveness of static creep test for predicting rutting resistance will be discussed.

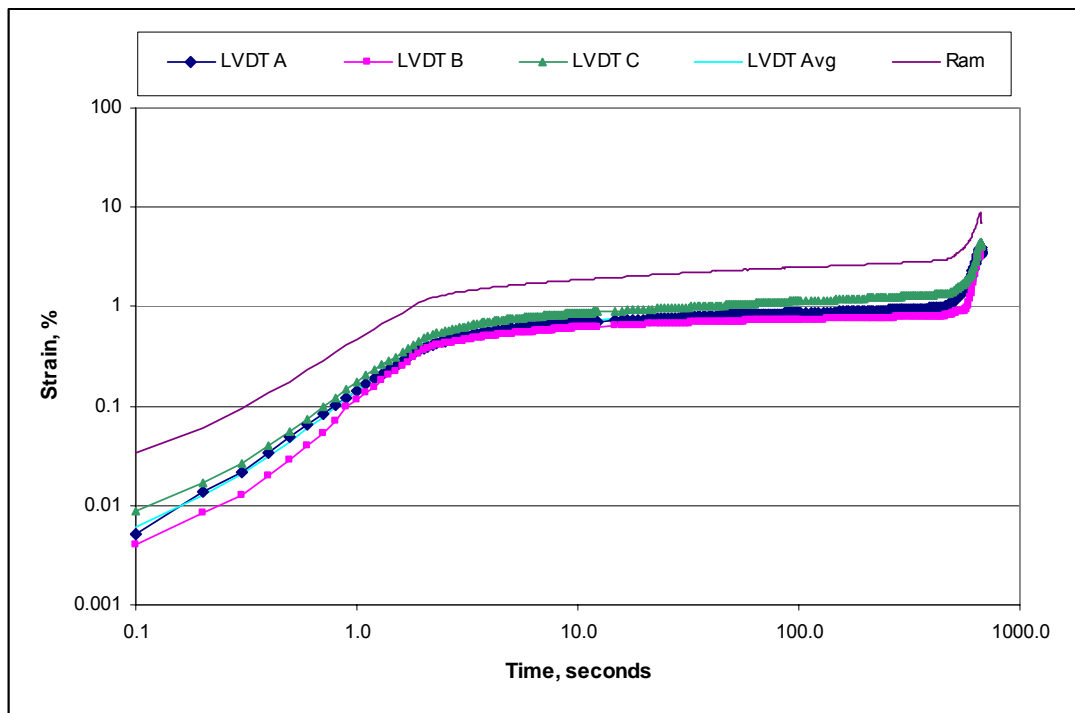


FIGURE 5.18A typical static creep test result with tertiary flow.

The individual static creep test results are shown in Appendix Table D2. Table D2 includes the information about the slope and intercept within the secondary phase, the time to reach 1%, 2%, 3%, and 4% strain level, and the flow time if available. Tertiary

flow was observed for only 7 samples out of 96 samples tested. For most of the samples, no significant increase of strain slope was observed during the test. A typical test result showing tertiary flow is shown in Figure 5.18, and a typical test result showing no tertiary flow is shown in Figure 5.19. Tertiary flow is considered to exist when the displacement of the sample begins to increase quickly as shown on the right side of the curves in Figure 5.18.

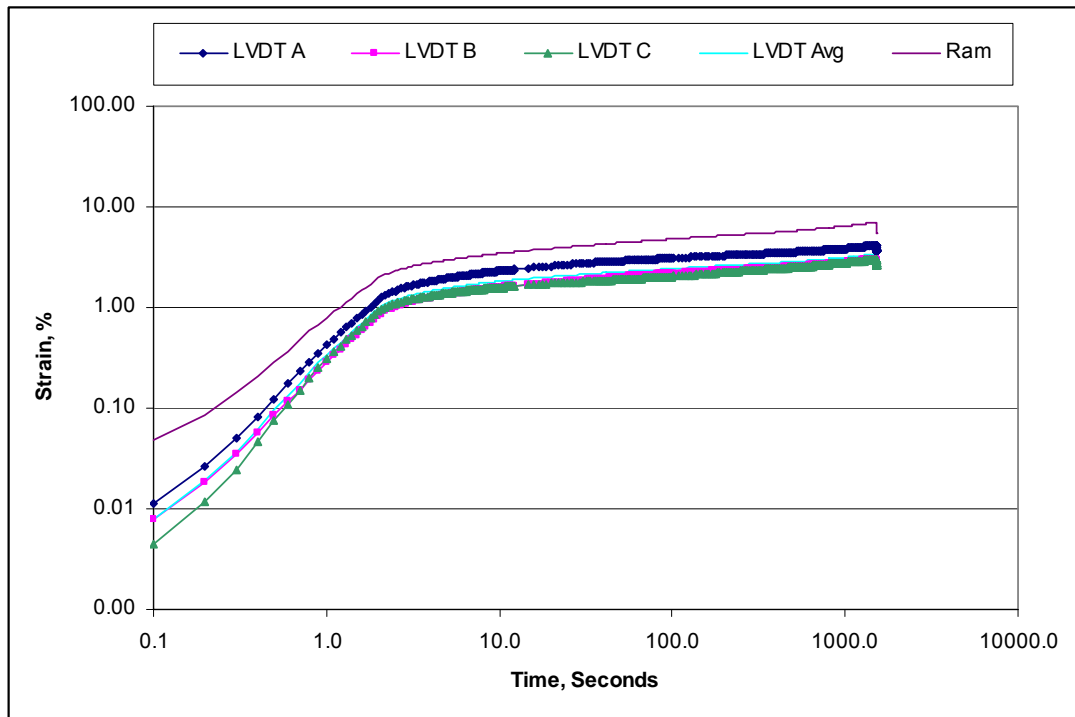


FIGURE 5.19A typical static creep test result without tertiary flow.

The average slope in the secondary phase and the time to reach 4 percent strain are listed in Table 5.12. The time to reach 4 percent strain was converted from seconds to hours for easy reading. The static creep test results showed a very high variability, the overall COV for the time to reach 4 percent strain is 101.8 percent. Within three replicates, one sample reached the LVDT limits in a few seconds and the test was finished, while another sample had less than 4 percent strain and a very flat slope of

strain after more than 4 hours loading and had to be stopped manually. The strain level at a certain time (for example 3600 seconds) and creep modulus at a certain time are not included in the data analysis because high variability in test time makes it very difficult if not impossible to normalize the strain level. For example, if a test reached the LVDT limits in 10 seconds, it is extremely hard to extrapolate and estimate the strain level at 3600 seconds since a linear relationship does not likely exist. Instead of using the strain level at a certain time, the time to reach a specific strain was used.

The high variability of the test time to reach a certain strain still resulted in difficulty in analyzing the test data, and much of the information had to be estimated. Since only a few samples were observed having tertiary flow, all the missing information was extrapolated based on the secondary slope and intercept.

As shown in Table 5.12, the static creep test showed a very high variability as indicated by the overall average COV value of 101.8 percent for test time to reach 4 percent strain. Due to the high COV, no additional analysis was directly conducted on the data for time to 4 percent strain.

The slope of the secondary phase and the logarithmic value of the test time to reach 4 percent strain, however, showed more manageable COV values of 24.2 percent. Therefore, data analysis was conducted on these two properties.

TABLE 5.12 Static Creep Test Results Summary

Agg. Type	Gyrs	NMAAS	Log Slope, 1/log(sec)		Time at 4% strain T _{0.04} , hrs		Log T _{0.04} , log(sec)	
			Average	COV, %	Average	COV, %	Average	COV, %
C.GVL	100	19	0.1314	29.8	126.1	167.7	4.734	26.5
C.GVL	100	12.5	0.1419	12.0	5.8	27.1	4.309	3.0
C.GVL	100	9.5	0.1114	21.7	3454.8	95.9	6.279	26.9
L.GRN	100	19	0.1767	71.3	2142.0	133.4	5.783	34.9
L.GRN	100	12.5	0.0847	23.5	4911.4	72.3	7.141	5.7
L.GRN	100	9.5	0.1208	16.9	15.1	4.3	4.736	0.4
LMS	100	19	0.0856	27.8	10.9	73.8	4.478	9.5
LMS	100	12.5	0.1294	27.0	2.8	58.9	3.918	9.2
LMS	100	9.5	0.1873	81.0	1214.0	173.0	4.399	58.2
R.GRN	100	19	0.0909	5.9	175.7	162.7	4.654	37.2
R.GRN	100	12.5	0.1188	25.2	20.5	23.6	4.860	2.3
R.GRN	100	9.5	0.1191	21.9	415.0	171.4	4.966	29.8
TRAP	100	19	0.2021	95.3	6.2	89.8	3.555	47.0
TRAP	100	12.5	0.1114	19.5	9.4	49.5	4.490	5.2
TRAP	100	9.5	0.1305	12.3	2.9	88.6	3.600	27.9
C.GVL	65	19	0.1358	38.2	56.7	171.2	4.135	35.1
C.GVL	65	12.5	0.3786	101.4	2.4	132.0	2.955	61.9
C.GVL	65	9.5	0.1436	16.8	24.2	118.4	4.729	10.8
L.GRN	65	19	0.1553	23.8	2.2	77.6	3.722	15.7
L.GRN	65	12.5	0.1333	21.9	4.1	32.5	4.152	3.7
L.GRN	65	9.5	0.3245	55.4	1.2	170.2	2.597	50.0
LMS	65	19	0.1070	33.5	309.1	172.6	4.567	37.2
LMS	65	12.5	0.2349	58.6	5.1	172.6	2.760	62.1
LMS	65	9.5	0.0979	19.3	18.6	114.6	4.447	19.4
R.GRN	65	19	0.1097	13.9	10.9	27.3	4.581	2.6
R.GRN	65	12.5	0.1106	37.7	5.2	80.4	4.017	18.2
R.GRN	65	9.5	0.1393	43.1	512.2	170.8	4.775	40.4
TRAP	65	19	0.3704	8.9	0.01	20.6	1.546	6.1
TRAP	65	12.5	0.1104	14.5	9.5	96.2	4.374	11.0
TRAP	65	9.5	0.1918	58.8	0.6	84.5	2.950	34.5
L.GRN	40	12.5	0.2071	5.1	0.08	51.2	2.405	8.6
R.GRN	40	12.5	0.1280	7.8	4545.8	172.9	5.533	34.0
Overall Average:			0.1569	32.8	563.1	101.8	4.255	24.2

Since only two mixtures were designed with 40 gyrations, test results for these two mixtures were not included in the following ANOVA and discussions.

Since most of the tested samples were still in the secondary phase when the tests were finished, the slope of strain at the secondary phase is the most useful information available without the need for extrapolation. An ANOVA was first conducted to evaluate the effect of the main factors (aggregate type, NMAAS, and gyration level) and any interactions between the main factors on slope of strain. The results are shown in Table 5.13. Compaction level and interaction between aggregate type and NMAAS are significant factors at 95 percent significance level.

TABLE 5.13 ANOVA for Slope of Strain in Secondary Phase of Static Creep Test

Source	DF	Seq SS	Adj SS	Adj MS	F	P
Agg	4	0.05882	0.05882	0.0147	1.43	0.235
Gyrs	1	0.06415	0.06415	0.06415	6.24	0.015
NMAAS	2	0.00003	0.00003	0.00001	0.00	0.999
Agg*Gyrs	4	0.02714	0.02714	0.00678	0.66	0.623
Agg*NMAAS	8	0.22856	0.22856	0.02857	2.78	0.011
Gyrs*NMAAS	2	0.00611	0.00611	0.00306	0.30	0.744
Agg*Gyrs*NMAAS	8	0.13341	0.13341	0.01668	1.62	0.138
Error	60	0.61723	0.61723	0.01029		
Total	89	1.13545				

As shown in Figure 5.20, the average slopes of strain for the mixtures designed with 65 and 100 gyrations were 0.183 and 0.129, respectively. One standard deviation is shown as an error bar. The higher slope of mixtures designed with 65 gyrations indicate less deformation resistance than those designed with 100 gyrations, which likely results from the higher optimum asphalt content with the lower compaction level. However, no criteria for the secondary slope in the confined static creep tests using high samples are available at this time to distinguish if the mixtures designed with 65 gyrations can still provide satisfactory rutting resistance. The SMA mixtures designed with 65 and 100

gyrations appear to have good rutting resistance if the criteria of slope with unconfined test conditions (The best and the second best categories for good rutting resistance is less than 0.17 and 0.20, respectively as shown in Table 2.9) are used as references.

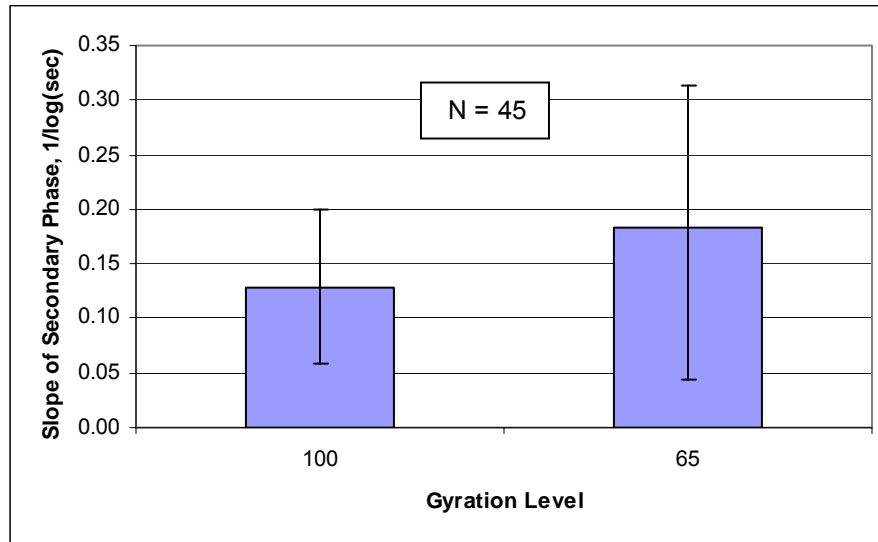


FIGURE 5.20 Average slopes for two gyration levels.

The interaction between aggregate type and NMAS on slope of strain in the secondary phase is shown in Figure 5.21. One standard deviation is shown as error bar. For some combinations of aggregate type and NMAS (e.g. 12.5 mm crushed gravel, 9.5 mm lab granite, and 19 mm traprock), the test variability is significant higher than others. This is likely due to one or two samples of these mixtures should be considered as outliers. These samples reached the limit of LVDTs in very short time and therefore showed a very high slope of the strain without tertiary flow. For different aggregate types, the average slope had no consistent trend with the changes of three NMAS. There appears to be no scientific reason for the combination effects of aggregate type and NMAS on slope results. It is believed that showing that these two properties have an interaction is simply due to high variation of the test results.

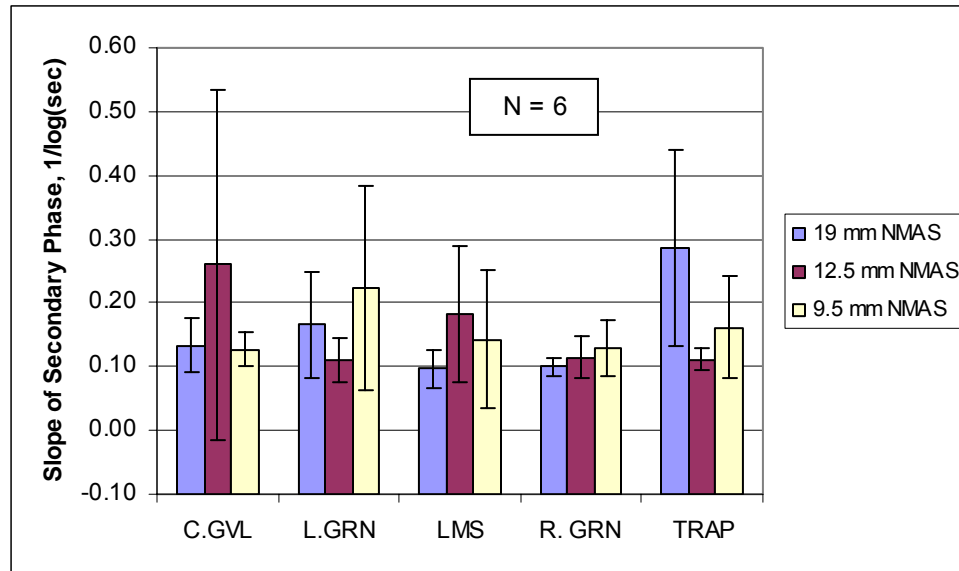


FIGURE 5.21 Interaction between aggregate type and NMA on slope of strain in static creep test.

Since the test times of the static creep test showed high variability, the logarithmic (log) test time was used for the analysis. An ANOVA was conducted to evaluate the effect of the main factors (aggregate type, NMA, and gyration level) and any interactions between the main factors on log test time at 4 percent strain.

TABLE 5.14 ANOVA for Log Test Time when 4 Percent Strain Occurred

Source	DF	Seq SS	Adj SS	Adj MS	F	P
Agg.	4	20.374	20.374	5.094	3.43	0.014
Gyrs	1	24.336	24.336	24.336	16.41	0.000
NMA	2	0.478	0.478	0.239	0.16	0.851
Agg.*Gyrs	4	12.638	12.637	3.159	2.13	0.088
Agg.*NMA	8	38.487	38.487	4.811	3.24	0.004
Gyrs*NMA	2	0.715	0.715	0.357	0.24	0.787
Agg.*Gyrs*NMA	8	5.72	5.72	0.715	0.48	0.864
Error	60	88.976	88.976	1.483		
Total	89	191.725				

The results are shown in Table 5.14. The ANOVA results indicate that aggregate type and gyration level are two significant influencing factors, and the interaction between aggregate type and NMA are also significant. Side by side comparison for the

effects of these significant factors and interactions were shown in the following Figures to better visualize the discussion.

The average log time for five aggregate types and two compaction levels are shown in Figure 5.22. One standard deviation is shown as error bar. N_1 and N_2 represent the number of samples used for the average in each group.

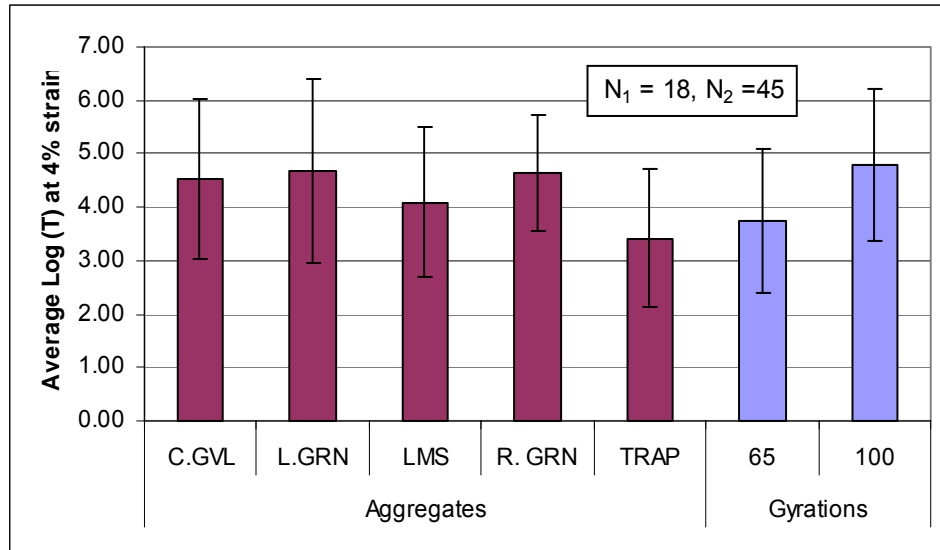


FIGURE 5.22 Average log time to reach 4 percent strain in static creep test.

From Figure 5.22, SMA mixtures designed with 65 gyrations generally required less test time (5674 seconds versus 62166 seconds, or 1.6 hours versus 17.3 hours) to reach 4 percent strain than those designed with 100 gyrations. The higher compaction level will result in less optimum asphalt content and tighter aggregate structure therefore higher rutting resistance. The limestone and traprock aggregates required less time to reach 4 percent strain than the other three aggregates. For traprock, a possible reason is the high optimum asphalt contents (average 6.6 percent). For limestone, it is likely due to its relatively low uncompacted air voids for coarse aggregate (46.6 percent) and fine

aggregate angularity (47.1 percent). The lower angularity and surface texture of the aggregate is likely to produce less rutting resistant mixtures.

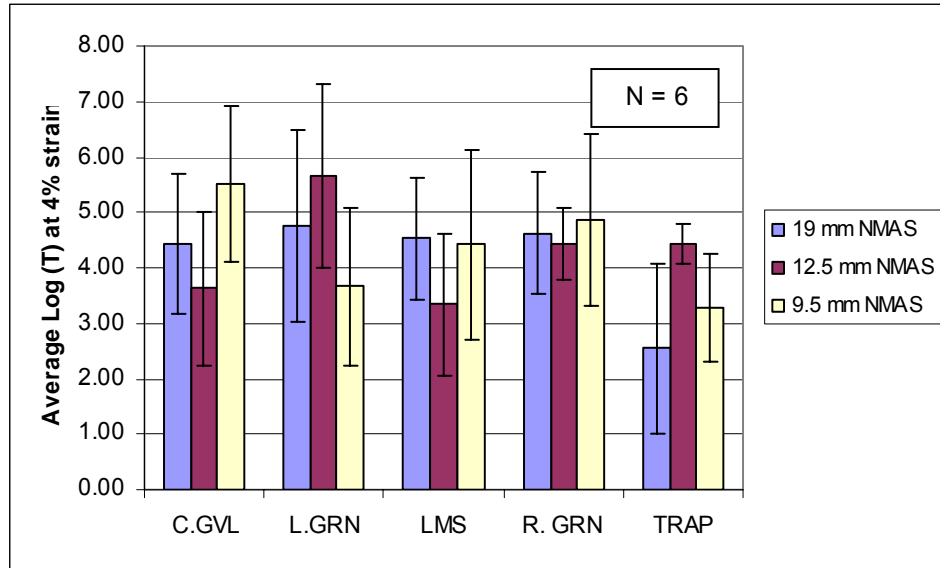


FIGURE 5.23 Interaction between aggregate type and NMAS on average log time to reach 4 percent strain.

The interaction between aggregate type and NMAS is shown in Figure 5.23. One standard deviation is shown as error bar. For lab granite and traprock, 12.5 mm NMAS mixtures required more time to reach 4 percent strain than 19 mm and 9.5 mm NMAS mixtures. However, for the other three aggregates, 12.5 mm NMAS generally required less time to reach 4 percent strain than the 19 mm and 9.5 mm NMAS mixtures. There appears to be no scientific reason for the combination effects of aggregate type and NMAS on average log (T) results. It is believed that showing that these two properties have an interaction is simply due to low precision of the test results.

NCHRP 9-19 project (84) recommended using the flow time as an indicator of rutting resistance, and presented several correlations between flow time and field rut depths based on the field data from MnRoad, ALF and Westrack test sections. These

correlations are shown in Figure 5.24. As expected, the field rut depth show negative trend with the flow time.

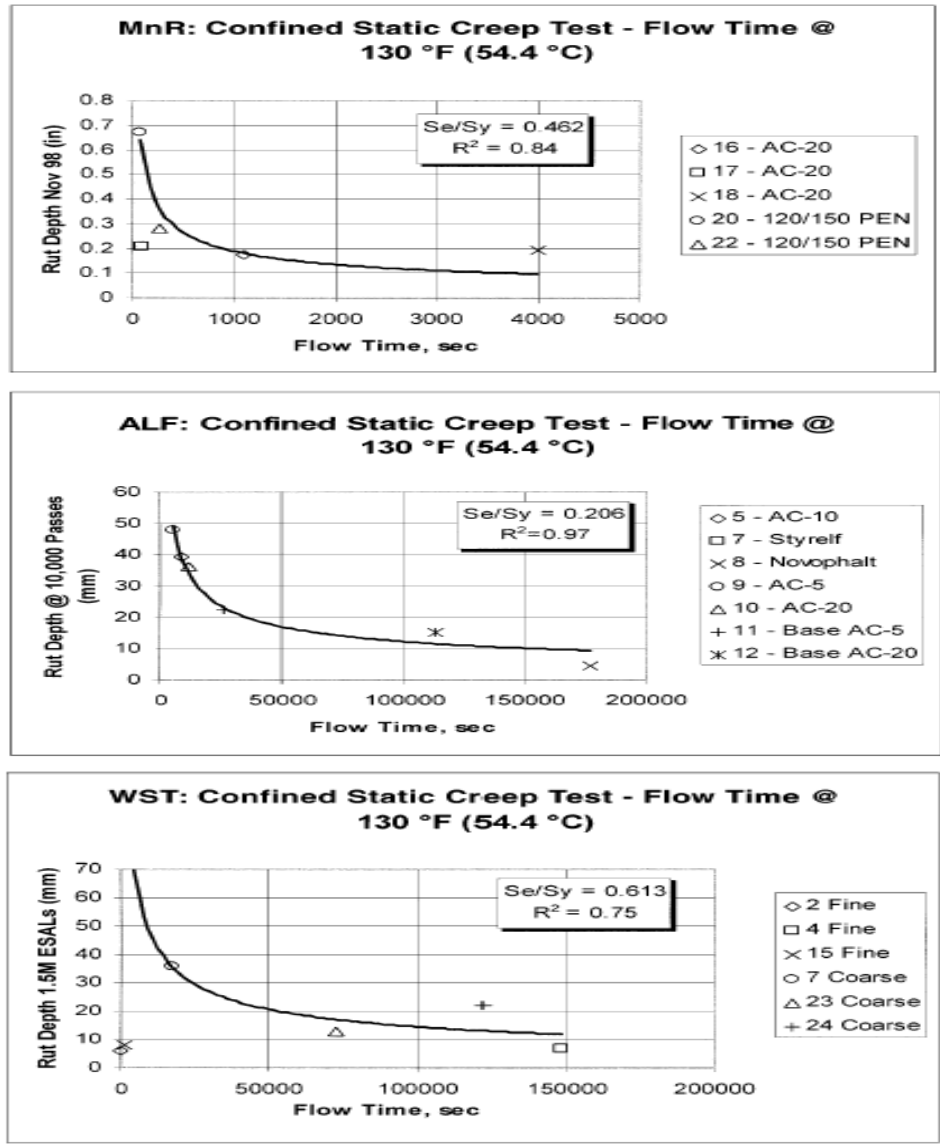


FIGURE 5.24 The Correlations between flow time and field rut depths (84).

There were only 7 out of 96 tested SMA samples that showed tertiary flow even with the higher test temperature (140°F) used in this study. This is partly due to the fact that most tests were manually stopped after 4 hours loading based on the test plan. However, there were a few samples were tested for more than 2 days during the

weekends, which is up to 200,000 seconds. Most of these tests were manually stopped on Monday since it appeared no tertiary flow would happen. Due to the lack of flow time data in this study, it is difficult to make use of these correlations to predict the field rut depth. As shown in Figure 5.24, a 10 mm field rut depth correlates with a flow time of about 150,000 seconds, which is about 2 days testing time for each sample. This long testing time makes static creep test impractical for predicting rutting performance.

In summary, although the data analysis on static creep test results showed a significant difference between 100 and 65 gyrations, the high variability of the static creep test results limited the use of test results for predicting rutting resistance of the SMA mixtures. Also, no criteria of strain level at certain time or time to reach a certain strain level for confined static creep tests are available at this time to distinguish if the SMA mixtures designed with 65 gyrations can still provide a satisfactory rutting resistance. Due to the high variability of results and long testing time for the static creep test, the use of the static creep test for predicting rutting potential is not recommended.

5.4 REPEATED LOAD TEST

5.4.1 Repeated Load Test Results and Analysis

As discussed in the literature review (89, 96-99), the repeated load test has been found to give a better correlation with the field rut depth and more responsive to the presence of modified binder in HMA mixtures than static creep test. The repeated load test has been used for predicting rutting potential of HMA mixtures for many years, and some acceptance criteria has also been established. However, these criteria were often established under unconfined test conditions, using short samples, or using whole sample deformation. Only a few studies used confined test conditions and relatively high (up to 5

inches) samples. Therefore, additional work was needed to establish an acceptance criterion to differentiate a rutting susceptible mix under current test conditions.

This section will present the repeated load test results and examine the influencing factors on the test results. An acceptance criterion for repeated load test under current test conditions will be established. The effect of compaction level on the repeated load test results will be evaluated.

The repeated load confined creep test was conducted for a total of 32 mixtures, in which 15 mixtures were designed with 100 gyrations, 15 mixtures were designed with 65 gyrations, and 2 mixtures were designed with 40 gyrations. Three replicated samples were tested for each mixture.

The repeated load test results for individual samples are shown in Appendix Table D3. Table D3 includes the information on the intercept a and slope b for the linear secondary phase, the microstrain at 100 cycles, 1000 cycles, 5000 cycles, and 10,000 cycles. The average test results of three replicate samples for each mixture are summarized in Table 5.15. Table 5.15 includes information on the slope of the linear secondary phase and the average strain at 10,000 cycles. Since the ideal full range of LVDTs used in this study was limited to 5 percent strain, and there were unequal readings among the three LVDTs, the effective average readings from the three LVDTs were often less than 4 percent. When any LVDT reached the full range of measurement before the 10,000 cycles, the reading at 10,000 cycles was extrapolated from the last point at which all LVDTs were functional using the tangent slope.

TABLE 5.15 Summary of Repeated Load Test Results

Agg. Type	Gyrs	NMAAS, mm	Log Slope b, 1/log(sec)			Strain @ 10, 000 Cycles, %		
			Average	St. Dev	COV, %	Average	St. Dev	COV, %
GVL	100	19	0.130	0.029	22.5	1.2693	0.189	14.9
GVL	100	12.5	0.173	0.082	47.5	1.7506	0.657	37.6
GVL	100	9.5	0.157	0.058	36.7	1.3696	0.630	46.0
L.GRN	100	19	0.120	0.004	3.4	1.1672	0.181	15.5
L.GRN	100	12.5	0.137	0.014	10.5	1.1794	0.178	15.1
L.GRN	100	9.5	0.158	0.017	10.8	1.2706	0.199	15.7
LMS	100	19	0.207	0.011	5.2	2.7016	0.195	7.2
LMS	100	12.5	0.184	0.033	17.9	2.6660	0.081	3.0
LMS	100	9.5	0.236	0.069	29.1	3.4665	0.958	27.6
R.GRN	100	19	0.199	0.058	29.2	2.8104	0.374	13.3
R.GRN	100	12.5	0.197	0.039	19.8	2.0961	0.358	17.1
R.GRN	100	9.5	0.195	0.042	21.6	1.9882	0.334	16.8
TRAP	100	19	0.170	0.070	40.9	3.0269	1.374	45.4
TRAP	100	12.5	0.197	0.034	17.4	2.6278	0.148	5.6
TRAP	100	9.5	0.190	0.049	25.9	3.4426	3.541	102.9
GVL	65	19	0.133	0.024	17.7	2.0486	0.287	14.0
GVL	65	12.5	0.144	0.012	8.1	1.7777	0.500	28.1
GVL	65	9.5	0.143	0.013	8.9	1.3883	0.285	20.5
L.GRN	65	19	0.191	0.033	17.1	2.8100	1.137	40.5
L.GRN	65	12.5	0.255	0.010	4.1	3.4775	0.433	12.5
L.GRN	65	9.5	0.261	0.089	34.2	4.2354	2.374	56.0
LMS	65	19	0.238	0.035	14.5	5.7501	0.306	5.3
LMS	65	12.5	0.221	0.056	25.5	4.3918	1.897	43.2
LMS	65	9.5	0.192	0.014	7.5	3.5698	2.336	65.4
R.GRN	65	19	0.211	0.046	21.6	3.1657	0.399	12.6
R.GRN	65	12.5	0.227	0.028	12.3	3.0269	0.388	12.8
R.GRN	65	9.5	0.218	0.018	8.0	2.6745	0.828	31.0
TRAP	65	19	0.120	0.054	45.3	2.3247	0.269	11.6
TRAP	65	12.5	0.154	0.034	22.1	1.9580	0.177	9.0
TRAP	65	9.5	0.165	0.021	12.6	2.6186	0.850	32.5
L.GRN	40	12.5	0.310	0.067	21.5	5.7059	0.775	13.6
R.GRN	40	12.5	0.259	0.028	11.0	4.8806	1.015	20.8

Tertiary flow was observed for only 4 samples out of 96 tested samples. One of these four samples was designed with 100 gyrations compaction level (traprock 9.5 mm NMAS No.1 sample). The other three were designed with 65 gyrations (limestone 12.5 mm NMAS No.5 sample, limestone 9.5 mm NMAS No.2 sample, and lab granite 9.5 mm NMAS No. 6 sample). A typical repeated load test result that shows tertiary flow is shown in Figure 5.25. For the 92 samples with no tertiary flow, the slope of cumulative strain gradually decreased during the test, and became relatively stable after a certain number of cycles. A typical repeated load test result without tertiary flow is shown in Figure 5.26. The fact that only a few samples have the tertiary flow developed after 10,000 cycles with 120/20 psi loading at 60°C test temperature indicated that most of the designed mixtures had good resistance to deformation.

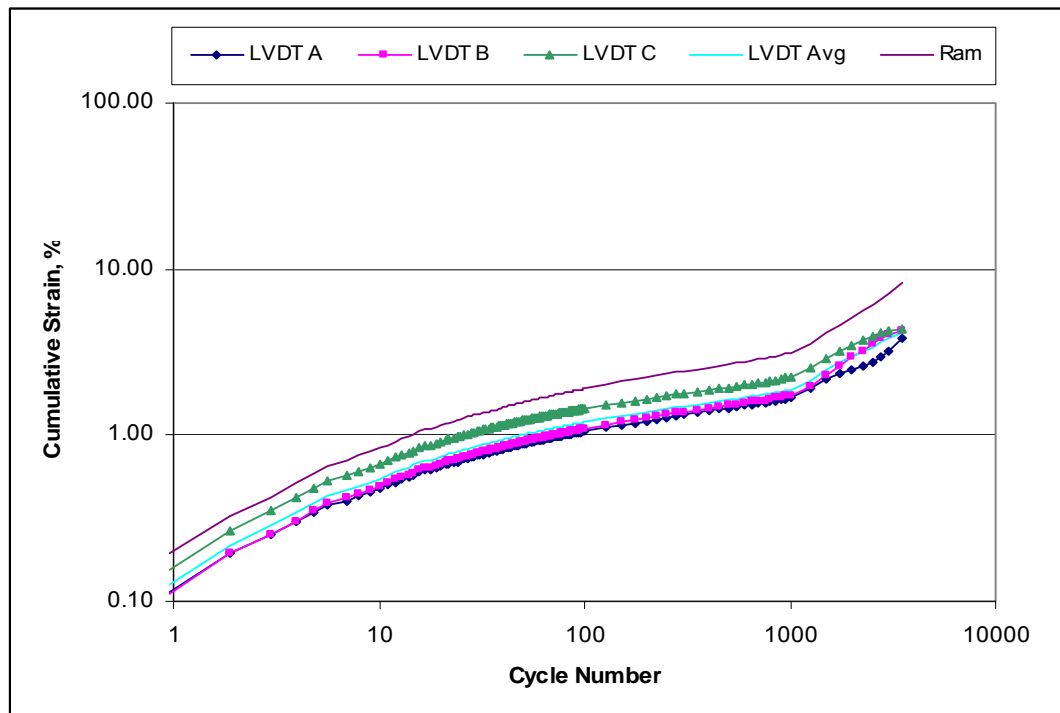


FIGURE 5.25A typical repeated load test result with tertiary flow.

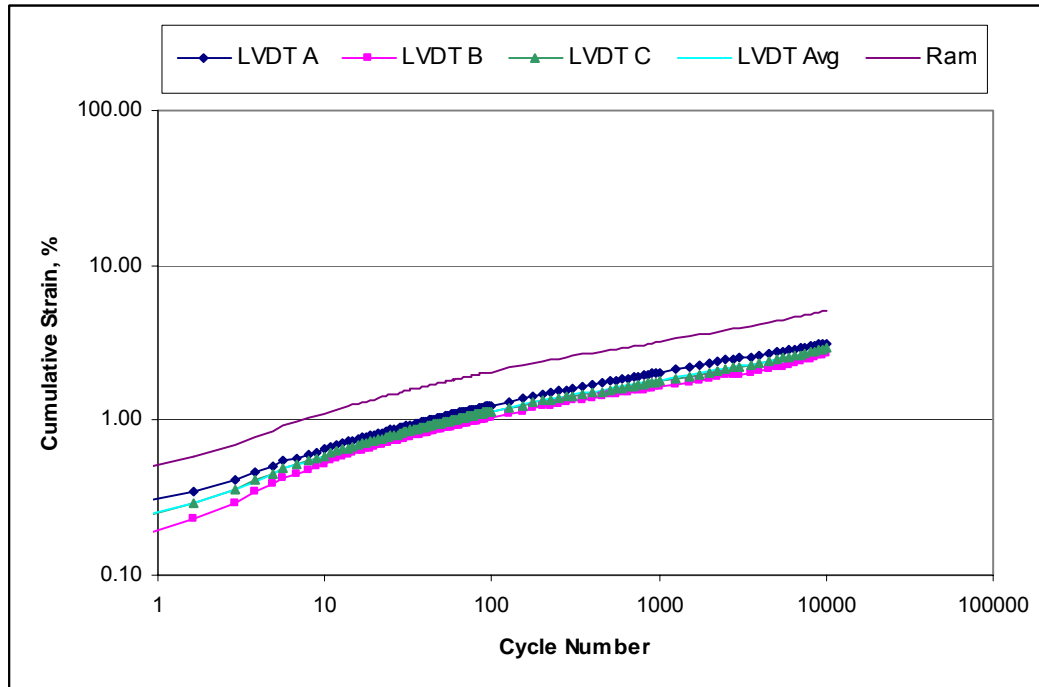


FIGURE 5.26A typical repeated load test result without tertiary flow.

Further statistical analyses were conducted on the accumulated strain at 10,000 cycles and the strain slope during the secondary phase. Since only two mixtures were designed with 40 gyrations, test results for these two mixtures were not included in the following ANOVAs and some of the comparisons.

The cumulative strain levels at 10,000 cycles for all mixtures tested are demonstrated in Figure 5.27. One standard deviation is shown as error bar. All 4 mixtures that had samples showing tertiary flow had higher standard deviations for the results. The pooled standard deviation values are 0.90, 1.11, and 1.06 percent for mixtures designed with 40, 65, and 100 gyrations, respectively. For lab granite and ruby granite 12.5 mm NMAS mixtures with three gyration levels, as expected, the strain level at 10,000 cycles decreased as compaction level increased due to the lower optimum asphalt content. A different trend is shown for traprock. This is likely due to two reasons. One is the

difference between 100 gyrations and 65 gyrations for traprock is smaller than that of the other aggregates due to the smaller changes in asphalt content (average 0.4 percent versus 0.8 percent) and aggregate breakdown (average 1.4 percent versus 6.8 percent changes at critical sieves). The other reason is that one of the 9.5 mm traprock samples showed tertiary flow and had a significantly higher strain level at 10,000 cycles.

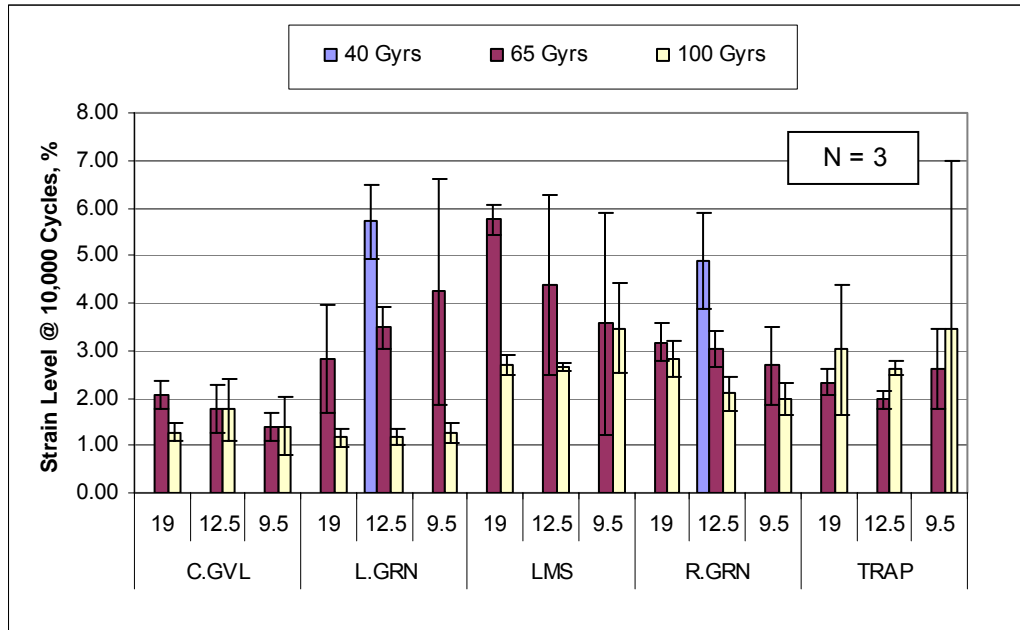


FIGURE 5.27 Strain level at 10,000 cycles for three gyrations levels.

TABLE 5.16 ANOVA for Strain at 10,000 Cycles

Source	DF	Seq SS	Adj SS	Adj MS	F statistics	P value
Agg.	4	43.096	43.096	10.774	9.17	0.000
Gyrs	1	15.273	15.273	15.273	13.00	0.001
NMAS	2	0.676	0.676	0.338	0.29	0.751
Agg.*Gyrs	4	25.142	25.142	6.286	5.35	0.001
Agg.*NMAAS	8	6.464	6.464	0.808	0.69	0.700
Gyrs*NMAAS	2	0.744	0.744	0.372	0.32	0.730
Agg.*Gyrs*NMAAS	8	7.958	7.958	0.995	0.85	0.566
Error	60	70.470	70.470	1.174		
Total	89	169.823				

An ANOVA was conducted to evaluate the effect of the main factors (aggregate type, NMAS, and compaction level) and any interactions between the main factors on cumulative strain at 10,000 cycles. The ANOVA result is shown in Table 5.16. Table 5.16 indicates that aggregate type and compaction level are significant influencing factors, and the interaction between these two factors is also significant. Side by side comparisons for the effects of these significant factors and interactions were shown in Figures 5.28 and 5.29 to better visualize the discussion.

The average strain level at 10,000 cycles for five aggregates and two compaction levels are shown in Figure 5.28. One standard deviation is shown as error bar. N_1 and N_2 represent the number of samples used for the average for each group.

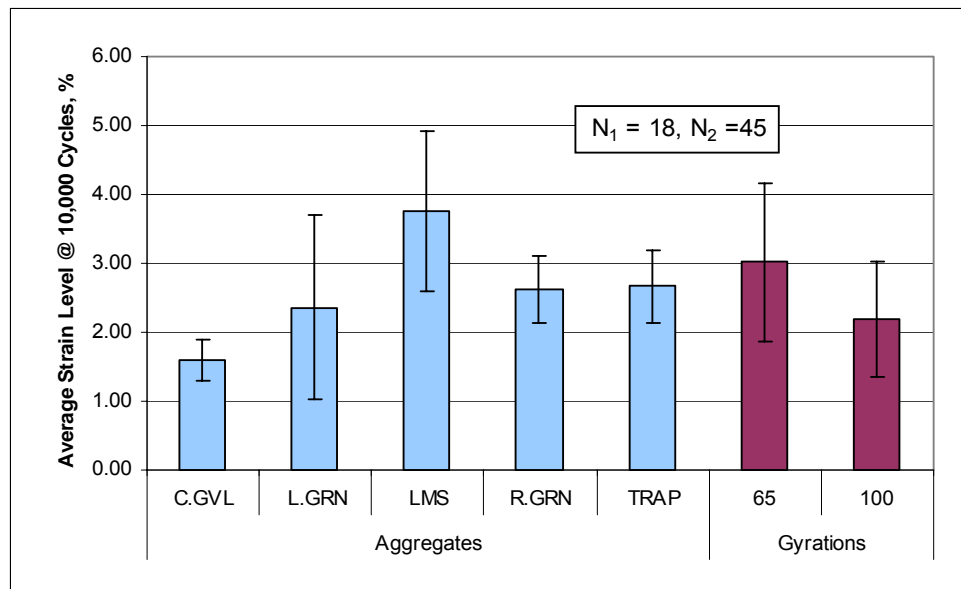


FIGURE 5.28 Average strains at 10,000 cycles for two main factors.

As shown in Figure 5.28, limestone has the highest average strain of about 3.8 percent at 10,000 cycles, while the crushed gravel has the lowest average strain of about 1.6 percent at 10,000 cycles. The high strain results for limestone are consistent with its APA rutting test results, and are likely due to its low angularity and surface texture. The

lowest strain results for crushed gravel are unexpected, because crushed gravel has the highest F&E content (35.2 percent for 3:1 and 9.4 percent for 5:1) and the second highest L.A abrasion value of 30.7 percent in all five aggregates. The high F&E content and L.A abrasion are generally considered undesirable for good performance. However, some recent studies (103) have shown that there did not appear to be a relationship between the F&E content (3:1) - in a range of about 10 to 40 percent- and performance. The good performance of crushed gravel is probably due to its good angularity and surface texture. This is indicated by the high uncompact voids for coarse aggregates (48.4 percent) and high FAA value (50.0 percent). The good repeated load results for crushed gravel indicated that these two aggregate properties (F&E content and L.A abrasion) may not be related to the rutting performance within the range used in this study. Also, the strain results for all aggregate types are considered low based on the literature review (89, 94), therefore the difference between all aggregate types is not practically significant.

The average strain at 10,000 cycles for mixtures designed with 100 gyrations was about 2.2 percent, which is lower than the 3.0 percent for those designed with 65 gyrations. The result is logical because the higher compaction level provides a lower asphalt content and tighter aggregate structure, therefore likely to be more rutting resistant. A paired-t test was employed to compare these two compaction levels on cumulative strain at 10,000 cycles. The result is shown in Table 5.17 and indicates that there is a significant difference between these two compaction levels in terms of strain level at 10,000 cycles.

TABLE 5.17 Paired-T Test Results on Strain at 10,000 Cycles

Gyrs	N	Mean	StDev	SE Mean
65	15	3.0145	1.1474	0.2963
100	15	2.1888	0.8298	0.2143
Difference	15	0.8257	1.2683	0.3275

95% CI for mean difference: (0.1233, 1.5280)

T-Test of mean difference = 0 (vs not = 0): T-Value = 2.52, P-Value = 0.024

The interaction between aggregate types and compaction levels for cumulative strain at 10,000 cycles is shown in Figure 5.29. One standard deviation is shown as error bar.

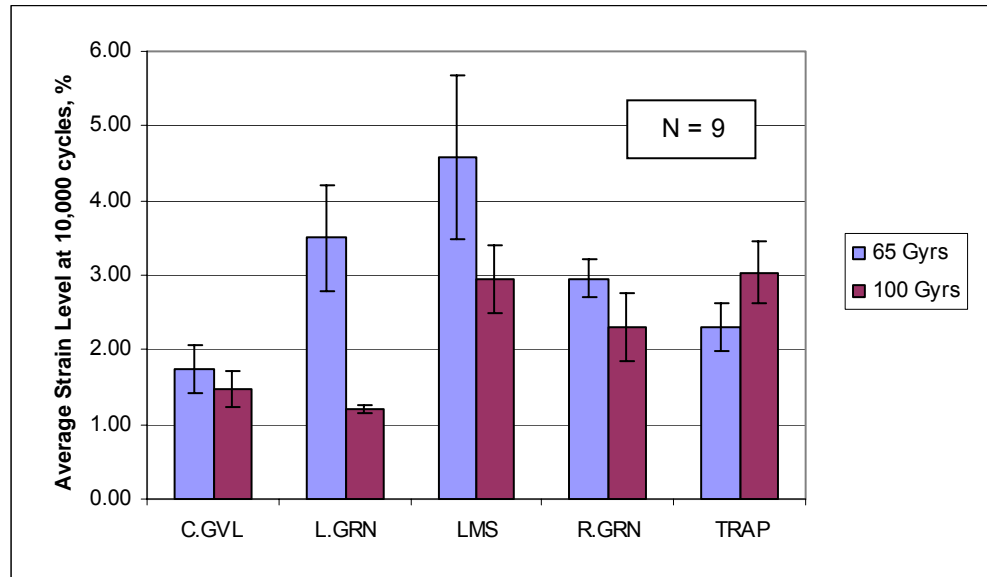


FIGURE 5.29 Interaction between aggregate type and compaction level on strain at 10,000 cycles.

As shown in Figure 5.29, for limestone and lab granite, the changes in design compaction level made a greater difference in strain results than other aggregates. This can be explained in that there was a greater change in optimum asphalt content for these two aggregate types than for the other three aggregate types (1.0 versus 0.5 percent) when compaction level changed from 100 to 65 gyrations. Traprock had a lower average strain at 10,000 cycles for mixtures designed with 65 gyrations than those designed with 100

gyrations. As explained before, this is mainly due to the fact that one traprock sample designed with 100 gyrations had tertiary flow, which resulted in an extremely high strain level at 10,000 cycles. If this traprock sample is seen as an outlier and excluded from the analysis, the average strain at 10,000 cycles for traprock mixtures designed with 100 gyrations will be slightly lower than those designed with 65 gyrations.

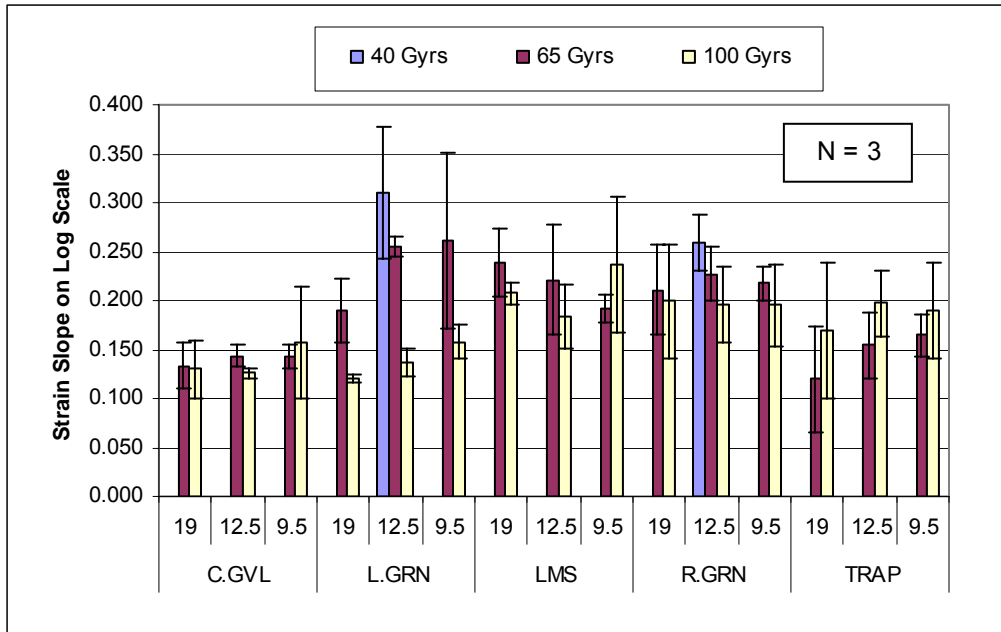


FIGURE 5.30 Strain slope at secondary phase for three compaction levels.

The strain slopes on a log scale for all mixtures tested are demonstrated in Figure 5.30. One standard deviation is shown as error bar. The pooled standard deviation values are 0.051, 0.039, and 0.041 for SMA mixtures designed with 40, 65, and 100 gyrations, respectively. For lab granite and ruby granite 12.5 mm NMAS mixtures with three gyration levels, the strain slope decreased with the increase of compaction level. For a few other mixtures, the trend of strain slope with gyration level is opposite, and this is likely due to the high test variability.

An ANOVA was conducted to evaluate the effect of the main factors (aggregate type, NMAS, and compaction level) and any interactions between the main factors on strain slope at secondary phase. The ANOVA results are shown in Table 5.18. Table 5.18 indicates that aggregate type and the interaction between aggregate type and gyration levels are significant. The compaction level is not a significant influencing factor.

TABLE 5.18 ANOVA for Strain Slope at Secondary Phase of Repeated Load Test

Source	DF	Seq SS	Adj SS	Adj MS	F statistics	P value
Agg.	4	0.056893	0.056893	0.014223	7.79	0.000
Gyrs	1	0.00488	0.00488	0.00488	2.67	0.107
NMAS	2	0.006718	0.006718	0.003359	1.84	0.168
Agg.*Gyrs	4	0.047979	0.047979	0.011995	6.57	0.000
Agg.*NMAS	8	0.010498	0.010498	0.001312	0.72	0.674
Gyrs*NMAS	2	0.000814	0.000814	0.000407	0.22	0.801
Agg.*Gyrs*NMAS	8	0.008794	0.008794	0.001099	0.60	0.772
Error	60	0.109516	0.109516	0.001825		
Total	89	0.246093				

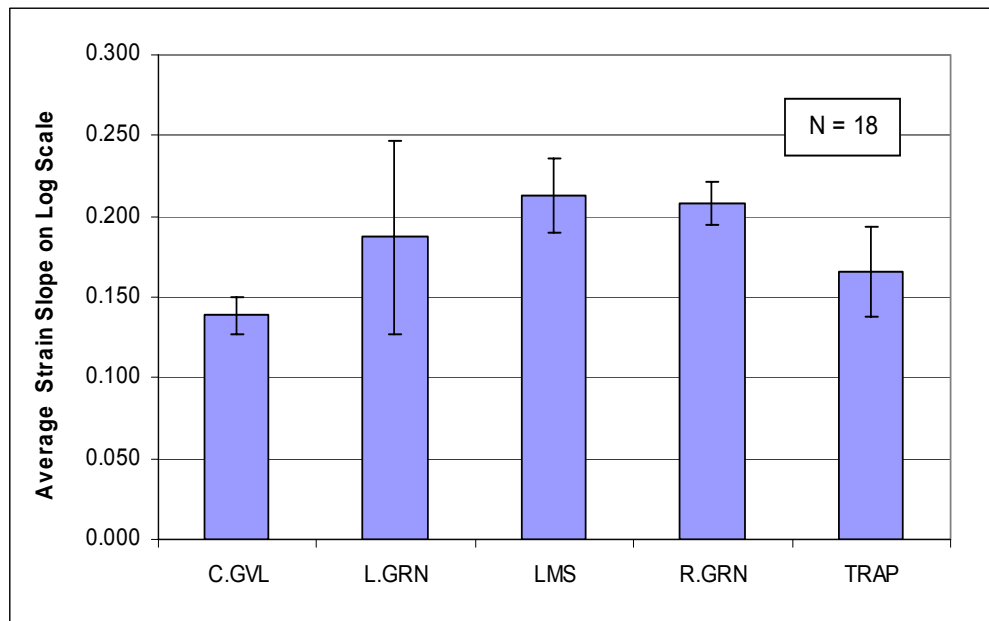


FIGURE 5.31 Average strain slopes for different aggregate types.

The average strain slopes on log scale for five aggregate types are shown in Figure 5.31. One standard deviation is shown as error bar. The lab granite showed

significant higher test variation than other aggregates. This is likely due to the greater difference between two compaction levels for lab granite mixture in terms of strain slope, as shown in Figure 5.33. Combining two sets of data with greater difference will result in higher standard deviation. The limestone had the highest strain slope of 0.213 and the crushed gravel had the lowest strain slope of 0.139. The results are consistent with the accumulated strain results shown in Figure 5.28, i.e. the aggregate that has high accumulated strain also has high strain slope.

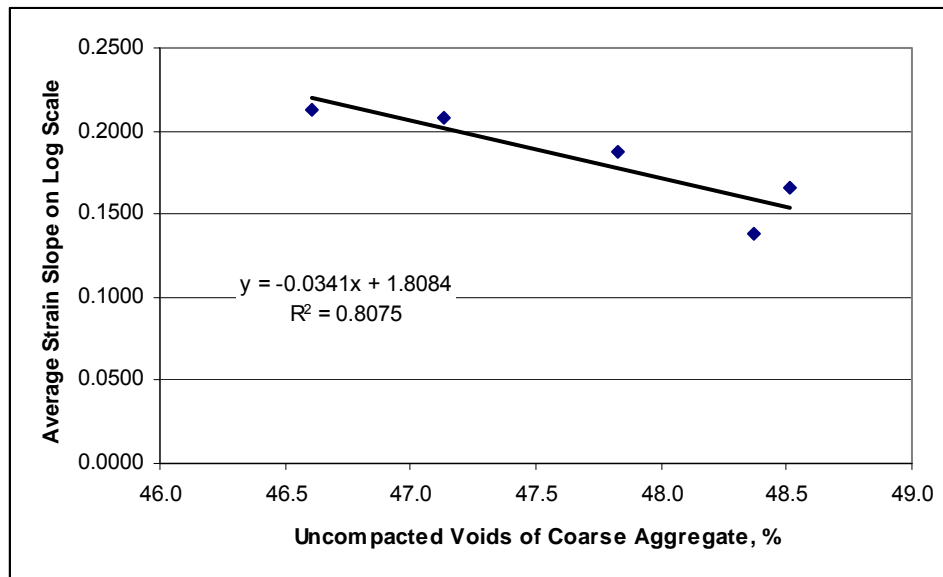


FIGURE 5.32 Relationship between strain slope and uncompacted voids of coarse aggregate.

It is noteworthy that the average strain slope for different aggregate types showed a good correlation with the uncompacted voids of coarse aggregate. As shown in Figure 5.32, the average strain slope decreases with an increase in the uncompacted voids. This trend is as expected because the strong internal friction caused by the increased aggregate angularity and surface texture will increase the rutting resistance. Also, the SMA has a

high coarse aggregate content which makes the coarse aggregate properties more important than fine aggregate properties.

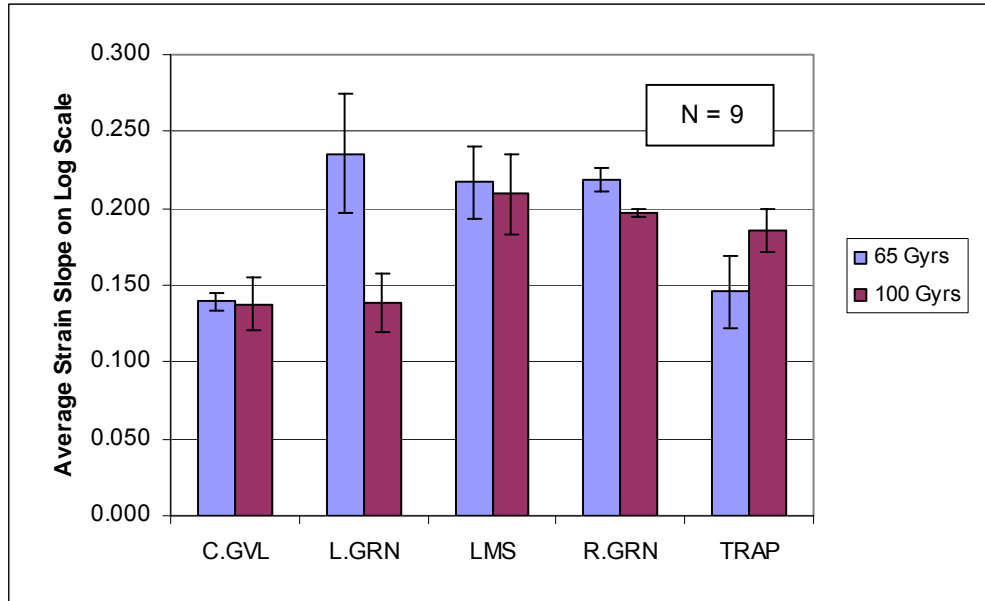


FIGURE 5.33 Interaction between aggregate type and compaction level on strain slope.

The interaction between aggregate types and compaction levels for strain slope is shown in Figure 5.33. One standard deviation is shown as error bar. For lab granite, the changes in design compaction level resulted in a greater difference in slope of strain than any other aggregates. This may be due to the significant change in optimum asphalt content of 1.1 percent between the two compaction levels. Traprock had lower average slope of strain for mixtures designed with 65 gyrations than those designed with 100 gyrations. This is likely due to the lowest change in optimum asphalt content and one outlier sample for traprock designed with 100 gyrations. That sample showed tertiary flow.

5.4.2 Discussion on Cumulative Strain Criteria

At the time this report was written, there was no proven criterion for cumulative strain level at 10,000 cycles to distinguish the acceptable and unacceptable rutting resistance based on the new test procedure. Some studies (71, 89) recommended a critical cumulative strain level range of 10 to 13 percent to determine the good or poor rutting resistance. This range was given based on the correlation between the laboratory repeated load test results and field rutting observations. The sample diameter of 4 inches, test temperature of 60°C, and axial load pressure of 120 psi and confining pressure of 20 psi are the same as used in this study. However, some laboratory test conditions used in that study (89) are different from this study. The laboratory tests were conducted on some short field core samples (The height of samples varied from 1.8 to 5.4 inches), the strain reading was for the whole sample height from the ram transducer, and the cumulative strain used was after 3600 cycles loading.

In order to use the critical strain level for this study, a relationship between ram transducer and LVDT's reading and a relationship between 3600 cycles and 10,000 cycles need to be developed. These two relationships are shown in Figures 5.30 and 5.31 based on the 96 samples tested in this study. Four samples that showed tertiary flow were excluded from the analysis, but are still shown in the Figures using different data symbols. The LVDT strains larger than 5 percent in this study were extrapolated using the secondary phase slope. This extrapolation became invalid once the tertiary flow happened.

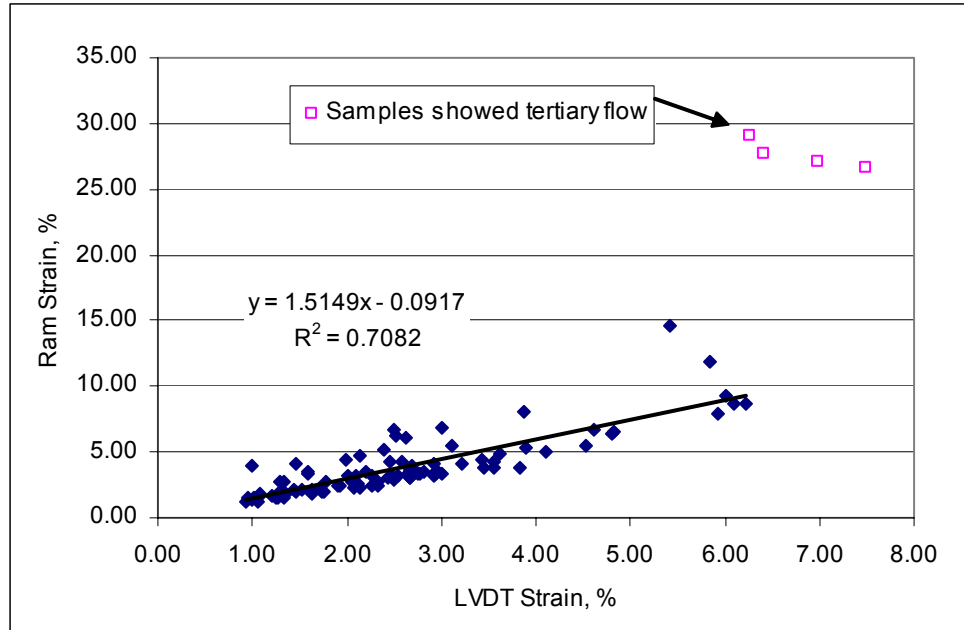


FIGURE 5.34 The relationship between ram strain and LVDT strain reading.

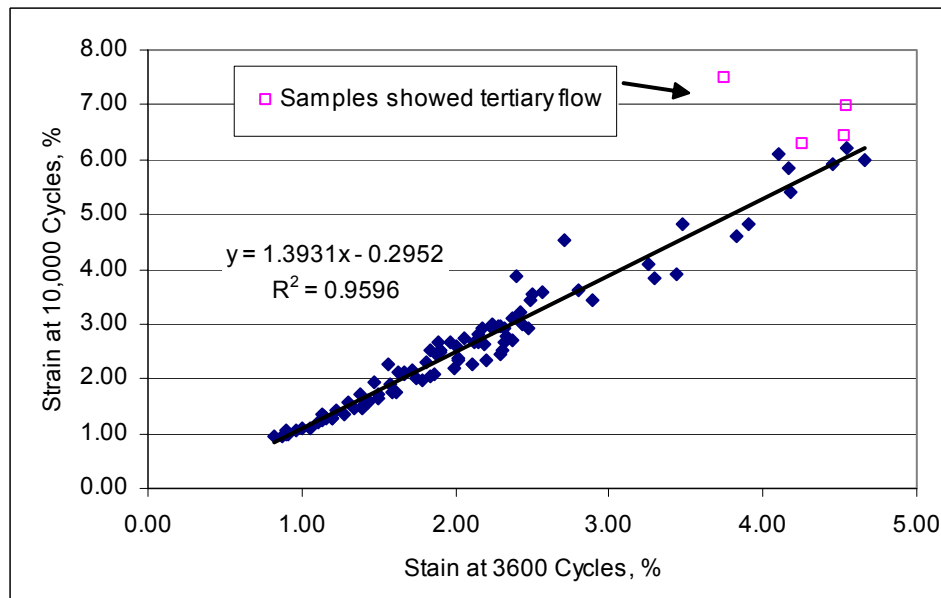


FIGURE 5.35 The relationship between strain at 3600 and 10,000 cycles.

Based on the two relationships shown in Figures 5.34 and 5.35, when 10.0 percent strain is selected as the critical strain level at 3600 cycles with the ram transducer reading, the corresponding critical strain level at 10,000 cycles with LVDT reading will be 9.0

percent. This transformed criteria should be correct only for relatively short samples since the original criteria was developed using short samples (1.5 to 5.4 inches in height). The criterion for the higher samples (6 inches in height) in this study is believed to be lower because of less effect due to end friction and confinement. A study (84) on the effect of ratio of sample height to diameter showed that the failing strain level becomes lower and less variable with the increase of this ratio and is close to a constant level after the ratio exceeds 1.5:1. As shown in Figure 5.34, a cumulative strain of 6 percent seems to be a threshold value when tertiary flow begins. However, as shown in Figure 5.35 a sample showed tertiary flow when the strain was less than 4 percent at 3600 cycles. The corresponding strain level at 10,000 cycles for this result is about 5 percent. All samples showing tertiary flow had cumulative strains higher than 6 percent at 10,000 cycles while all samples having strain levels lower than 5 percent at 10,000 cycles did not show tertiary flow. Therefore a strain level of 5 percent at 10,000 cycles appears to be a criterion for differentiating between good and poor performance mixture. As shown in Figure 5.35, a good linear correlation exists between strain level of 3600 cycles and 10,000 cycles for these mixtures that do not show the tertiary flow. This indicates there is a potential to reduce the test time by more than 60 percent and still get good information. If 5 percent is selected for the criteria at 10,000 cycles, a corresponding criterion for 3600 cycles should be about 3.8 percent.

All the strain results at 10,000 cycles versus gyration levels are shown in Figure 5.36. Since only two mixtures (12.5 mm NMA SMA with lab granite and ruby granite) were designed with three gyrations levels while all the rest of mixtures were designed

with two gyration levels, an overall analysis on the effect of gyration level on the cumulative strain is difficult to conduct.

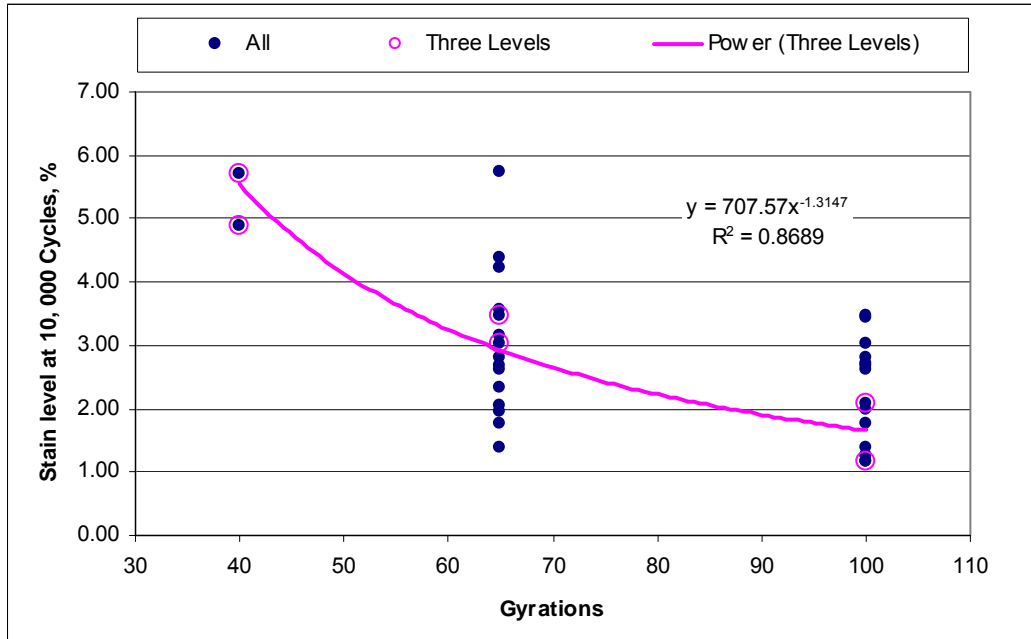


FIGURE 5.36 The relationship between strain level and compaction level.

As shown in Figure 5.36, the cumulative strain results for SMA mixtures designed with 65 gyrations varied over a wider range than those designed with 100 gyrations. This is likely due to the higher variability of mix properties associated with a lower compaction level. The cumulative strain results for all mixtures designed with 100 gyrations and most (14 out of 15) mixtures designed with 65 gyrations are less than the suggested criteria of 5 percent.

The two mixtures with three gyration levels are highlighted using different data symbols. A best fitted regression line for the results of these two mixtures is also included. As shown in Figure 5.36, the cumulative strain of these two mixtures decreases with an increase of gyration level. However, the decrease in cumulative strain is not large when

the compaction level increases from 65 to 100 gyrations. For these two mixtures, the cumulative strain becomes marginal when the gyration level drops to 40 gyrations. In other words, 65 gyrations appear to be the lowest compaction level that still can ensure a rutting resistant mixture based on the suggested repeated load test criteria.

Based on the evaluation of both APA and repeated load test results, the SMA mixtures designed with 65 gyrations have a high probability being rutting resistant. It is interesting to see the correlation between these two tests. The relationship between cumulative strain from repeated load test and APA rut depth results is shown in Figure 5.37.

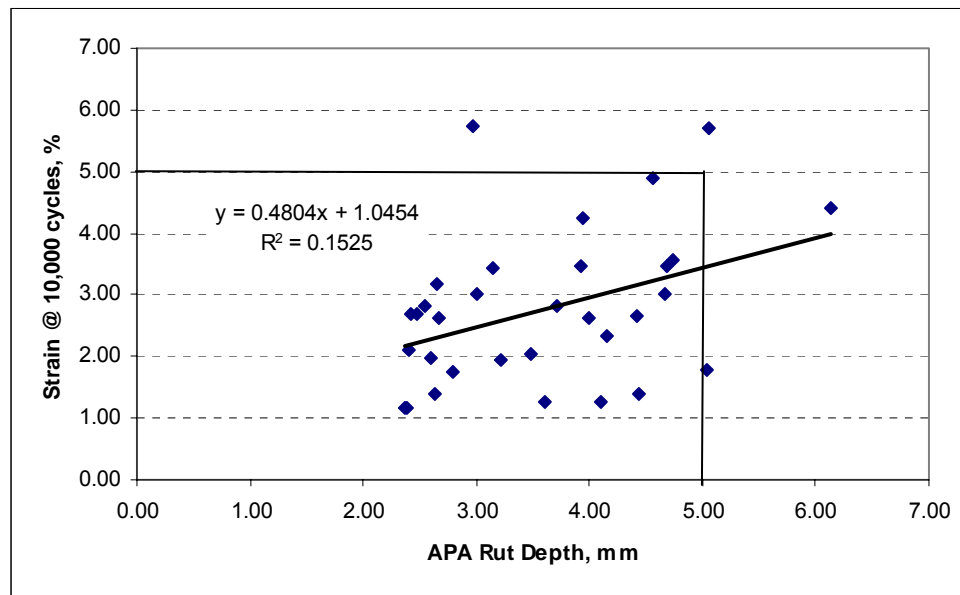


FIGURE 5.37 Relationship between repeated load cumulative strain and APA rut depth.

As shown in Figure 5.37, there is only a poor correlation ($R^2=0.15$) between APA rut depth and strain level at 10,000 cycles of the repeated load test. This poor correlation is not surprising, because most SMA mixtures designed and tested in this study are considered to be resistant to rutting with low APA rut depths and low cumulative strain

values, and these test results are only within a narrow data range. As shown in Figure 5.37, only 4 out of 32 designed SMA mixtures failed either of the two criteria.

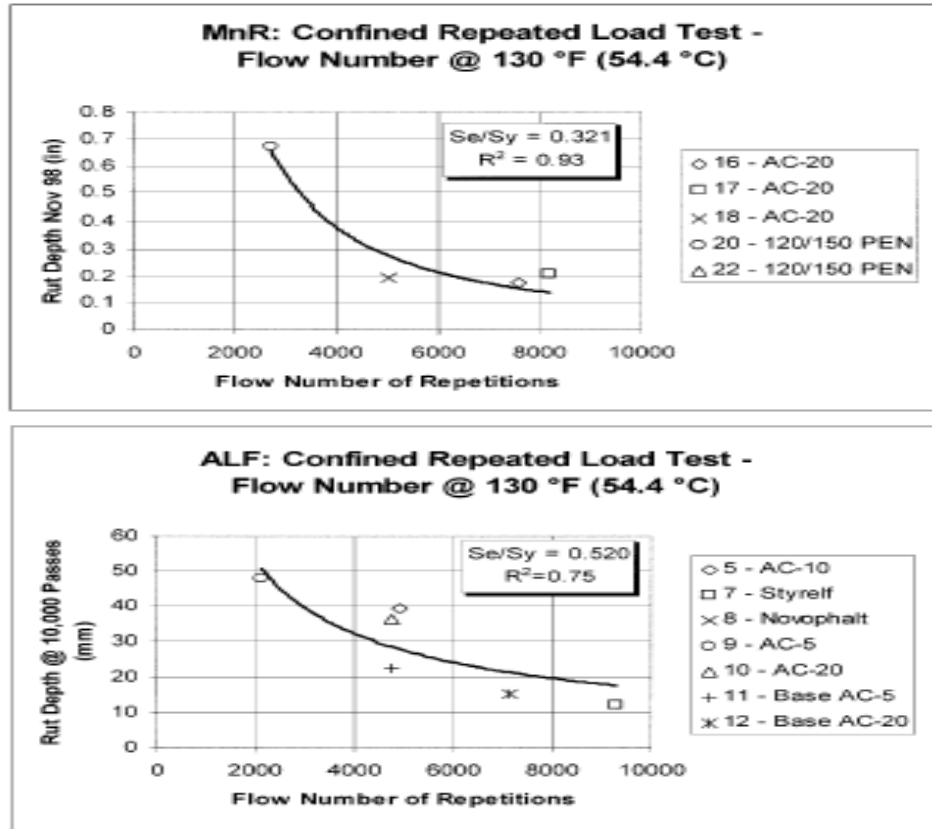


FIGURE 5.38 The Correlations between flow number and field rut depths (84).

NCHRP 9-19 project (84) recommended using the flow number as an indicator of rutting resistance, and presented several correlations between flow number and field rut depths based on the field data from MnRoad, and ALF test sections. These correlations are shown in Figure 5.38.

There were only 4 out of 96 tested SMA samples showed tertiary flow before 10,000 cycles even with higher test temperature (140°F) used in this study. In other words, most of tested samples had flow numbers greater than 10,000 cycles, and therefore should be considered as resistant to rutting. The predicted field rut depths for

most SMA mixtures designed with 65 and 100 gyrations are less than 10 mm if the correlations shown in Figure 5.38 are used.

A national rutting study (96) presented a correlation between field rut depth and cumulative strain from repeated load, as shown in Figure 5.39. The criterion for cumulative strain is about 10 percent if the maximum allowable field rut depth is set as 0.5 inch, or 12.5 mm. However, the lab test conditions were different from this study. The test samples were shorter (1.4 to 5.4 inches in height) and strain results were from ram transducer and recorded at 3600 cycles. As discussed above, a new criterion of 5 percent is recommended based on the data in this study. The predicted field rut depth for SMA mixtures designed with 100 and 65 gyrations are 8.3 and 9.8 mm, respectively, if we assume a linear relationship for the cumulative strain between this SMA study and the national study, and used the correlation shown in Figure 5.39. For SMA mixtures designed with 40 gyrations, the average field rut depth is expected as 12.7 mm, which is marginal if we assume the maximum allowable field rut depth is 12.5 mm.

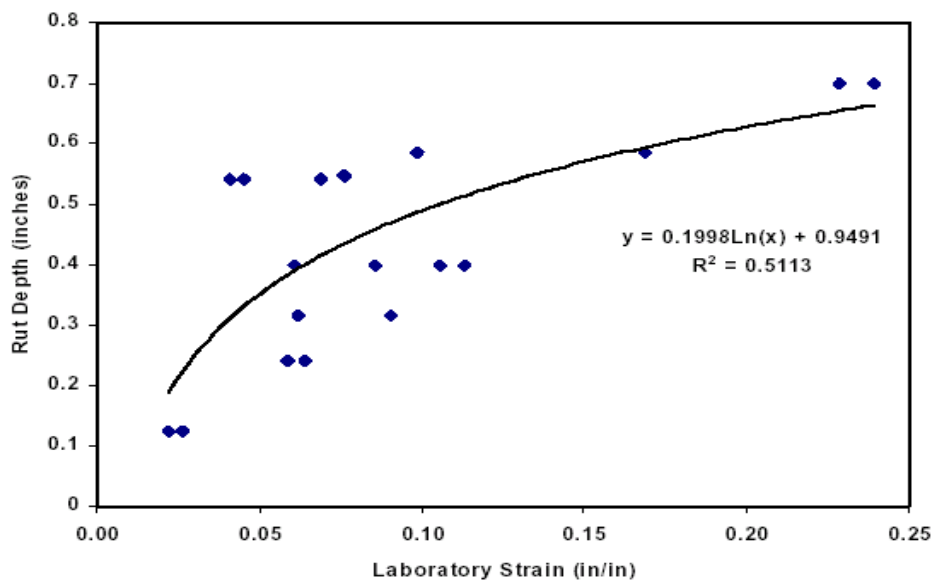


FIGURE 5.39 Field rut depth versus the lab strain from repeated load test (96).

5.5 SUMMARY

The rutting resistance for the SMA mixtures was evaluated by APA rutting test, dynamic modulus, static creep and repeated load tests. The test results for different compaction levels are summarized in Table 5.19.

TABLE 5.19 Average Test Results for Different Compaction Levels

Test	Properties	100 Gyration	65 Gyration	Significant Difference between 100 and 65 gyrations?	40 Gyration ¹	Suggested Criteria
APA Test	Rut depth, mm	3.1	3.9	Yes	4.8	5 max
Dynamic modulus test	E*/sin ϕ at 10 Hz, MPa	2038	1811	No	2875	N/A
	E*/sin ϕ at 0.1 Hz, MPa	2576	2265	No	4236	N/A
Static creep test	Time ² to reach 4% strain, hrs	17.3	1.6	Yes	1.0	N/A
	Slope of Strain in secondary phase, 1/log (sec)	0.129	0.183	Yes	0.168	N/A
Repeated load test	Cumulative strain at 10,000 cycles, %	2.2	3.0	Yes	5.3	5 max
	Slope of Strain in secondary phase, 1/log (sec)	0.174	0.191	No	0.285	N/A

1. Only two mixtures were designed with 40 gyrations.
2. Average value from the antilog of the average logarithmic value.

As shown in Table 5.19, a decrease in compaction level generally resulted in a small decrease in rutting resistance of designed SMA mixtures. However, 13 out of 15 SMA mixtures designed with 65 gyrations were still satisfactory for APA rut depth criterion of 5.0 mm. The rutting resistance for mixtures designed with 40 gyrations becomes marginal, but one of two SMA mixtures designed with 40 gyrations was also able to meet this criterion.

The dynamic modulus test results showed that there is no significant difference between SMA mixtures designed with 65 gyrations and 100 gyrations. The effectiveness of the dynamic modulus test for predicting rutting resistance is questionable because the relatively low stress and strain associated with the test do not reflect the stress-strain situation in the pavement. The $E^*/\sin\phi$ value at high temperature showed contrary results when the load frequency changed, and the dynamic modulus results depended on the tightness of aggregate structure or VMA value, which may not be applicable for SMA mixtures.

The static creep test showed very high variability on test time to reach a certain strain level. The data analysis on slope of strain and log time to reach 4 percent strain indicated that there were significant differences between 65 and 100 gyrations. However, additional work is needed to determine criteria for these static creep results. With the high variability and lack of criteria, the static creep test was not recommended to be used to draw any conclusions for this study.

A cumulative strain criterion of 5 percent after 10,000 cycles for repeated load test was developed based on literature review and test data in this study. Most (14 out of 15) SMA mixtures designed with 65 gyrations were satisfactory for this criterion. One of the two SMA mixtures designed with 40 gyrations marginally met this criterion.

The successful design for SMA mixtures using all aggregate types indicates the requirements for F&E content and L.A abrasion in SMA mixture design guides (43) are too stringent. There appears to be no correlation between these aggregate properties with rutting performance within the range of this study.

In summary, a SMA mixture designed with 65 gyrations level will be resistant to rutting with a good confidence based on the discussion on APA and repeated load test results. The feasibility of dynamic modulus and static creep tests for predicting rutting potential is questionable and need further evaluation.

CHAPTER 6 CONCLUSIONS AND RECOMMENDATIONS

6.1 CONCLUSIONS

Based on the data analysis and discussion presented in chapters 4 and 5, the following general conclusions were drawn for the design and testing of SMA mixtures.

1. The vacuum seal method (CoreLok) appeared to be more accurate than the SSD method at higher air void levels where the SMA mixtures become permeable. The SSD method should only be used when the water absorptions are lower than 0.4 to 0.9 percent depending on NMAAS. The corrected vacuum seal air voids should be used when water absorption higher than these limits.
2. The vacuum seal method overestimated air void content when measuring laboratory compacted samples. The correction factor embedded into the CoregravityTM software program by the manufacturer is appropriate for cored-and-sawn samples, however, is appears not sufficient for laboratory compacted SMA mixtures. An additional correction of 0.5 percent should be used when the software is used. A correction factor of 1.4 percent should be used when the software is not used.
3. SMA mixtures become permeable at higher air void contents for lower NMAAS. If the threshold value for permeable mixtures is set at 125×10^{-5} cm/s, the critical air voids values by the SSD method are approximately 5, 6, and 7 percent for 19, 12.5 and 9.5 mm NMAAS SMA mixtures, respectively.

4. To produce a cored-and-sawn triaxial SMA sample with 4 percent air void content using the SSD method requires that the whole sample be compacted to about 5 percent air void content.
5. Aggregate degradation by laboratory compaction had good correlations with the aggregate L.A. abrasion value and fair correlations with F&E content (3:1).
6. Under the test temperature of 60°C, both dynamic modulus and phase angle results decreased with the decrease of loading frequency. The decrease of phase angle indicated the aggregate structure becomes more dominant with the high temperature and low loading frequency.
7. The successful SMA mix designs with all five aggregates indicate the requirements for aggregate properties, such as L.A abrasion and F&E content, are too stringent. These two aggregate properties within the ranges shown in this study may not be detrimental for the mixture performance.

Based on the data analysis and discussion presented in chapters 4 and 5, the following conclusions were made with respect to the stated project objectives.

1. A lower compaction level of 65 gyrations provides a more durable SMA mixture with increased optimum asphalt content and allows the use of more aggregate types compared to 100 gyrations. SMA mixtures designed with 65 gyrations had an average of 0.7 percent higher optimum asphalt content than those designed with 100 gyrations, and 0.2 percent higher optimum asphalt content than those designed with 50 blows with the Marshall hammer. SMA mixtures designed with 65 gyrations had an average of 1.5 percent higher VMA than those designed with 100 gyrations. All SMA mixtures designed with 65 gyrations met the minimum

optimum asphalt content and VMA requirements for SMA mixture, while only 8 of 15 (53 percent) of mixtures designed with 100 gyrations met these requirements.

2. SMA mixtures designed with 65 gyrations were generally had similar or lower permeability than those designed with 100 gyrations at similar air voids. For 19 mm NMAS mixtures, 65 gyrations resulted in a lower permeability than 100 gyrations at similar air voids. For 12.5 and 9.5 mm NMAS mixtures, the effects of two compaction levels on permeability are not significant.
3. Both 65 gyrations and 100 gyrations resulted in similar aggregate breakdown as in the field construction. Going from 65 to 100 gyrations compaction resulted in an average of 0.6 percent additional aggregate breakdown at the critical sieves. Marshall compacted samples had more fractured aggregates than the SGC compacted samples. The average changes in percent passing the critical sieve for 50 blow Marshall, 100 gyrations and 65 gyrations were 7.3, 5.2, and 4.6 percent, respectively.
4. All designed SMA mixtures with different compaction levels were satisfactory for the draindown requirement. The draindown test results for all mixtures were less than the maximum limit of 0.3 percent with the use of polymer modified asphalt binder and cellulose fiber.
5. The rutting resistance of the SMA mixtures designed with 65 gyrations is generally lower than those designed with 100 gyrations, but is still satisfactory for the APA rut depth and repeated load cumulative strain criteria. Thirteen out of fifteen mixtures compacted with 65 gyrations still performed well when 5.0 mm

was used as the maximum APA rut depth allowed. A cumulative strain criterion of 5 percent for repeated load test was developed based on literature review and the test results in this study. Fourteen out of fifteen SMA mixture designed with 65 gyrations met this criterion. Both APA and repeated load results indicated the SMA mixtures designed with 40 gyrations had marginal rutting resistance, and only one out of two mixtures marginally met these suggested criteria.

6. SMA mixtures designed with 65 gyrations did not show a significant difference with those designed with 100 gyrations in terms of dynamic modulus test results. At high temperature, the $E^*/\sin\phi$ value increased with the decrease of load frequency for SMA mixture. Therefore, the effectiveness of using $E^*/\sin\phi$ to predicting the rutting for SMA is questionable.
7. The data analysis on static creep test results showed a significant difference between 100 and 65 gyrations. However, the high variability of the test results and long testing time limited the use of this test for predicting rutting resistance of the SMA mixtures.
8. The number of gyration should be the same regardless of NMAS. No significant evidence was observed that different compaction levels are necessary for designing SMA mixture with different NMAS. The ANOVA on APA rutting, static creep, and repeated load test results did not show the NMAS was a significant influence factor.

6.2 RECOMMENDATIONS

Based on the data analysis and discussion presented in Chapters 4 and 5, the following recommendations were made:

1. When using the vacuum seal method to determine the air void content, different correction factors are necessary for different combinations of surface conditions, NMAS and air void ranges of tested samples. A sample with a rougher surface, higher NMAS and higher air voids generally requires a higher correlation factor.
2. The correlation factor for vacuum seal method can be calibrated by the difference in air voids between the SSD method and uncorrected calculation for the vacuum seal method. The sample used for calibration should have low air voids and similar surface condition as the sample to be tested.
3. 65 gyrations is recommended as the optimum compaction level in terms of the overall performance in mix durability and rutting resistance.
4. Evaluation of field performance of SMA mixtures designed with 65 gyrations is highly desirable to verify the laboratory test results.

REFERENCES

1. AASHTO, "Report on the 1990 European Asphalt Study Tour", Washington D.C., June 1991.
2. "Guidelines for Materials, Production, and Placement of Stone Matrix Asphalt", National Asphalt Pavement Association, Information Series 118, 8/94, 1994.
3. American Society for Testing Materials (ASTM) Standards on Disc, Volume 04.02, Concrete and Aggregates, 2004.
4. Vavrik, W.R., and S.H. Carpenter. "Calculating Air Voids at Specified Number of Gyration in Superpave Gyratory Compactor". In Transportation Research Record 1630, TRB, National Research Council, Washington, D.C., 1998.
5. Ortolani, L. and H.A. Sandberg, Jr. "The Gyratory-Shear Method of Molding Asphaltic Concrete Test Specimens; Its Development and Correlation with Field Compaction Methods. A Texas Highway Department Standard Procedure", Journal of Association of Asphalt Paving Technologists, Vol: 21, 1952.
6. Consuegra, A., D.H. Little, H.V. Quintus, and J. Burati, "Comparative evaluation of laboratory compaction devices based on their ability to produce mixtures with engineering properties similar to those produced in the field", Transportation Research Record 1228, TRB, National Research Council, Washington, D.C., 1989.
7. Button, J.W., D.N. Little, V. Jagadam, and O.J. Pendleton. "Correlation of Selected Laboratory Compaction Methods with Field Compaction", In Transportation Research Record 1454, TRB, National Research Council, Washington, D.C., 1994.
8. Blankenship, R.B., K.C. Mahboub, and G.A. Huber. "Rational Method for Laboratory Compaction of Hot-Mix Asphalt", In Transportation Research Record 1454, TRB, National Research Council, Washington, D.C., 1994.
9. Harvey, J., C.L. Monismith, and J. Sousa. "A Investigation of Field- and Laboratory-Compacted Asphalt – Rubber, SMA Recycled and Conventional Asphalt – Concrete Mixes Using SHRP A-003A Equipment", Journal of Association of Asphalt Paving Technologists, Vol: 63, 1994.
10. J. Sousa, J. Harvey, L. Painter, J. Deacon and C.L. Monismith. "Evaluation of Laboratory Procedures for Compacting Asphalt-Aggregate Mixtures", SHRP Technical Memorandum No. TM-UCS-A-003A-90-5, University of California, Berkeley, 1991.

11. Cominsky, R., Leahy, R.B., and Harrigan, E.T., "Level One Mix Design: Materials Selection, Compaction, and Conditioning." Strategic Highway Research Program Report No. A-408, National Research Council, Washington D.C., 1994.
12. Sousa, J.B., G. Way, J.T. Harvey and M. Hines. "Comparison of Mix Design Concepts". In Transportation Research Record 1492, TRB, National Research Council, Washington, D.C., 1995.
13. Hafez, I.H. and M.W. Witczak. "Comparison of Marshall and Superpave Level I Mix Design for Asphalt Mixes". In Transportation Research Record 1492, TRB, National Research Council, Washington, D.C., 1995.
14. D'Angelo, J. A., Paugh, C., Harman, T. P., and Bukowski, J., "Comparison of the Superpave Gyratory Compactor to Marshall for Field Quality Control." Journal of the Association of Asphalt Paving Technologists, Volume 64, 1995, pp. 611-635.
15. McGennis, R.B., R.M. Anderson, D. Perdomo and P. Turner. "Issues Pertaining to Use of Superpave Gyratory Compactor". In Transportation Research Record 1543, TRB, National Research Council, Washington, D.C., 1996.
16. Brown, E.R., D.I. Hanson, and R.B. Mallick. "Evaluation of Superpave Gyratory Compaction of Hot-Mix Asphalt". In Transportation Research Record 1543, TRB, National Research Council, Washington, D.C., 1996.
17. Forstie, D. A. and Corum, D. K., "Determination of Key Gyratory Compaction Points for Superpave Mix Design in Arizona." ASTM Special Technical Publication, Volume 1322, September 1997. ASTM, Philadelphia, PA., pp. 201-209.
18. Mallick, R.B., S. Buchanan, E.R. Brown and M. Huner. "An Evaluation of Superpave Gyratory Compaction of Hot Mix Asphalt", NCAT Report No. 98-5, Auburn, AL, 1998.
19. Anderson, R. M., R.B. McGennis, W. on Tam, and T. W. Kennedy, "Sensitivity of Mixture Performance Properties to Changes in Laboratory Compaction Using the Superpave Gyratory Compactor ", Journal of Association of Asphalt Paving Technologists, Vol: 69, 2000.
20. Buchanan, MS and E.R. Brown, "Effect of Superpave Gyratory Compactor Type on Compacted Hot-Mix Asphalt Density" In Transportation Research Record 1761, TRB, National Research Council, Washington, D.C., 2001
21. Brown, E.R., J. Gabrielson, and S. Adettiwar. "Variation in Hot Mix Asphalt Design Properties" Journal of Association of Asphalt Paving Technologists, Vol: 62, 1993.
22. Tashman, L., E. Masad, R. Peterson, and H. Saleg. "Internal Structure Analysis of Asphalt Mixes to Improve the Simulation of Superpave Gyratory Compaction to Field Conditions". Journal of the Association of Asphalt Paving Technologists, Vol. 70, 2001.

23. Harman, T., J.R. Bukowski, F. Moutier, G. Huber, and R. McGennis. "The History and Future Challenges of Gyratory Compaction 1939 to 2001". In Transportation Research Record 1789, TRB, National Research Council, Washington, D.C., 2002.
24. Peterson, R.L., K.C. Mahboub, R.M. Anderson, E. Masad and L. Tashman. "Superpave Laboratory Compaction versus Field Compaction". In Transportation Research Record 1832, TRB, National Research Council, Washington, D.C., 2003.
25. American Association of State Highway and Transportation Officials (AASHTO), Standard Specifications for Transportation Materials and Methods of Sampling and Testing, Part 2A and Part 2B: Tests, 24th Edition, 2004
26. Stuart, K.D. "Stone Mastic Asphalt (SMA) Mixture Design", FHWA-RD-92-006 Federal Highway Administration, March 1992.
27. Kennepohl, G.J., and J.K. Davidson. "Introduction of Stone Mastic Asphalt (SMA) in Ontario", Journal of Association of Asphalt Paving Technologists, Vol: 61, 1992.
28. Brown, E.R. "Evaluation of SMA used in Michigan (1991)", NCAT Report No. 93-3, National Center for Asphalt Technology, Auburn, AL, 1993.
29. Brown, E.R. "Experience with Stone matrix Asphalt in United States", NCAT Report No. 93-4, National Center for Asphalt Technology, Auburn, AL, 1993.
30. Brown, E.R., and H. Manglorkar. "Evaluation of Laboratory Properties of SMA Mixtures", NCAT Report 93-5, National Center for Asphalt Technology, Auburn, AL, 1993.
31. Carpenter, R.H. "Mix Design Considerations for SMA Mixes", Presented in Transportation Research Board Annual Meeting, 1994.
32. Brown, E.R., and R.B. Mallick. "Stone Matrix Asphalt- Properties Related to Mixture Design", NCAT Report No. 94-2, National Center for Asphalt Technology, Auburn, AL, 1994.
33. Mogawer, W.S., and K.D. Stuart. "Evaluation of Stone Matrix Asphalt versus Dense-graded Mixtures", In Transportation Research Record 1454, TRB, National Research Council, Washington, D.C., 1994.
34. Partl, M.N., T.S. Vinison, R.G. Hicks, and K. Younger. "Performance-Related Testing of Stone Mastic Asphalt" Journal of Association of Asphalt Paving Technologists, Vol: 64, 1995.
35. West, R.C. and B.E. Ruth. "Compaction and Shear Strength Testing of Stone Matrix Asphalt Mixtures in the Gyratory Testing Machine", Journal of Association of Asphalt Paving Technologists, Vol: 64, 1995.

36. Brown, E.R., and J.E. Haddock, T.A. Lynn and R.B. Mallick. "Designing SMA Mixtures Volume II- Research Results", NCHRP 9-8/2 Draft Final Report, September 1996.
37. Brown, E.R., R.B. Mallick, J.E. Haddock, and J. Bukowski. Performance of Stone Matrix Asphalt (SMA) Mixtures in the United States. In Journal of the Association of Asphalt Paving Technologists, Volume 66, 1997.
38. Louw, L., C.J. Semmelink, and BMJA. Verhaeghe. "Development of a Stone Mastic Asphalt Design Method for South African Conditions", Eighth International Conference on Asphalt Pavements, Vol. I., Seattle, Washington, August 1997.
39. Brown, E.R., J.E. Haddock, R.B. Mallick, and T.A. Lynn. "Development of a Mixture Design Procedure for Stone Matrix Asphalt (SMA)", Journal of Association of Asphalt Paving Technologists, Vol: 66, 1997.
40. Brown, E.R., and J.E. Haddock. "Method to Ensure Stone-on-Stone Contact in Stone Matrix Asphalt Paving Mixtures", In Transportation Research Record 1583, TRB, National Research Council, Washington, D.C., 1997.
41. Kuennen, T. "Gap-Graded Maryland Mixes Meld SMA, Superpave Designs", HMAT, Vol. 4, No.2, 1999.
42. Brown, E.R. and L.A. Cooley, Jr. NCHRP Report 425. "Designing SMA Mixtures for Rut-Resistant Pavements". Transportation Research Board, Washington, D.C., 1999.
43. NAPA, "Designing and Constructing Stone Matrix Asphalt (SMA) Mixtures - State-of-the-Practice", 1999 (Updated edition is published in 2002).
44. AASHTO, AASHTO Provisional Standards, May 2002 Edition, 2002.
45. Kuennen, T. "Stone Matrix Asphalt is Catching on in the U.S.", in Better Roads, Sep. 2003.
46. Aschenbrener, T. "Results of Survey on Stone Matrix Asphalt", Colorado Department of Transportation, April 2004.
47. American Society for Testing Materials (ASTM) Standards on Disc, Volume 04.03, Road and Paving Materials; Vehicle-Pavement Systems, 2004.
48. Crouch, L.K., et al. Determining Air Void Content of Compacted Hot-mix Asphalt Mixtures. Transportation Research Record 1813, TRB, National Research Council, Washington, D.C., 2002, pp39-46.
49. Cooley, L.A. et al, Bulk Specific Gravity Round-Robin Using the CoreLok Vacuum Sealing Device. NCAT Report No. 02-11. National Center for Asphalt Technology, Auburn, Alabama, 2002.

50. Hall, K.D., F.T. Griffith, and Stacy G. Williams. Examination of Operator Variability for Selected Methods for Measuring Bulk Specific Gravity of Hot-Mix Asphalt Concrete. Transportation Research Record 1761, TRB, National Research Council, Washington, D.C., 2002, pp81-85.
51. Buchanan, M.S. An Evaluation of Selected Methods for Measuring the Bulk Specific Gravity of Compacted Hot Mix Asphalt (HMA) Mixes. Journal of the Association of Asphalt Paving Technologists, Vol. 69. Reno, NV, 2000, pp608-634.
52. Hudson, S.B., and R.L. Davis. "Relationship of Aggregate Voidage to Gradation" In Proceedings of the Association of Asphalt Paving Technologists, Vol. 34, 1965.
53. Lynn, T.A, E.R. Brown, and L.A. Cooley, Jr. "Evaluation of Aggregate Size Characteristics in Stone Matrix Asphalt and Superpave Mixtures", In Transportation Research Record 1681, TRB, National Research Council, Washington, D.C., 1999.
54. L.A. Cooley, Jr. and E.R. Brown. "Potential of Using Stone Matrix Asphalt for Thin Overlays", In Transportation Research Record 1749, TRB, National Research Council, Washington, D.C., 2001.
55. Kanitpong, K, C.H. Benson, and H.U. Bahia. "Hydraulic Conductivity (Permeability) of Laboratory-Compacted Asphalt Mixtures", In Transportation Research Record 1767, TRB, National Research Council, Washington, D.C., 2001.
56. Prowell, B.D, L.A. Cooley, Jr, and R.J. Schreck. "Virginia's Experience with A 9.5-mm Nominal-Maximum-Aggregate-Size Stone Matrix Asphalt", In Transportation Research Record 1813, TRB, National Research Council, Washington, D.C., 2002.
57. Mallick, R.B, L.A. Cooley, Jr., M.R. Teto, R.L. Bradbury, and D. Peabody. "An Evaluation of Factors Affecting Permeability of Superpave Designed Pavements", NCAT Report No. 03-02, National Center for Asphalt Technology, Auburn, AL, 2003.
58. Hainin, MR, and L.A. Cooley, JR. "An Investigation of Factors Influencing Permeability of Superpave Mixes" in International Journal of Pavements, Vol.2, No.2, 2003.
59. Choubane, B., G.C. Page, and J.A. Musselman. "Investigation of Water Permeability of Coarse Graded Superpave Pavements." Journal of the Association of Asphalt Paving Technologists, Vol. 67, 1998.
60. Moavenzadeh, F. and W.H. Geotz. "Aggregate Degradation in Bituminous Mixtures." In Highway Research Record 24, HRB, National Research Council, Washington, D.C., 1963.

61. Subramanyam, B. and M.P. Pratapa. "Degradation of Dense Aggregate Gradings." In Transportation Research Record 1228, TRB, National Research Council, Washington, D.C., 1989.
62. Collins, R., D. Watson, A. Johnson, and Y. Wu. "Effect of Aggregate Degradation on Specimens Compacted by Superpave Gyratory Compactor." In Transportation Research Record 1590, TRB, National Research Council, Washington, D.C., 1997.
63. Aho, B.D., W.R. Vavrik, and S.H. Carpenter. "Effect of Flat and Elongated Coarse Aggregate on Field Compaction of Hot-Mix Asphalt." In Transportation Research Record 1761, TRB, National Research Council, Washington, D.C., 2001.
64. Brown, E.R., L.A. Cooley, Jr., and T.A. Lynn, "Designing Stone Matrix Asphalt Mixtures Volume II (c) – Research Results for Phase II", Final Report for NCHRP 9-8, Transportation Research Board, 1998.
65. Buchanan, M.S. "Evaluation of the Effect of Flat and Elongated Particles on Performance of Hot Mix Asphalt Mixtures." NCAT Report No. 00-03. National Center for Asphalt Technology, Auburn, Alabama, 2000.
66. Vavrik, W.R., R.J. Fries, and S.H. Carpenter. "Effect of Flat and Elongated Coarse Aggregate on Characteristics of Gyratory Compacted Samples". In Transportation Research Record 1681, TRB, National Research Council, Washington, D.C., 1999.
67. Buttlar, W.G. and M. Harrell. "Development of End-Result and Performance-Related Specifications for Asphalt Pavement Construction in Illinois" Crossroads 2000 Transportation Conference Proceedings, Ames, Iowa, 1998.
68. Georgia Department of Transportation (GDOT), Standard Specification for Construction of Transportation Systems, 2001 Edition with Special Provisions, State of Georgia, 2001.
69. Alabama Department of Transportation (ALDOT), Alabama Standard Specifications for Highway Construction, 2002 Edition with Special Provisions, Alabama, 2002
70. Zhang, J; L.A.Cooley, Jr, and P.S. Kandhal, "Comparison of Fundamental and Simulative Test Methods for Evaluating Permanent Deformation of Hot-Mix Asphalt", in Journal of Transportation Research Record 1789, TRB, National Research Council, Washington D.C., 2002.
71. Brown, E.R., P.S. Kandhal, and J. Zhang. "Performance Testing for Hot Mix Asphalt", NCAT Report No.01-05, Auburn, AL 2001.
72. Lai, J.S. "Development of a Simplified Test Method to Predict Rutting Characteristics of Asphalt Mixtures" Final Report, Research Project No.8503, Georgia DOT, 1986.

73. West, R.C, G.C. Page, and K.H. Murphy. "Evaluation of the Loaded Wheel Tester" Research Report FL/DOT/SMO/91-391, 1991.
74. Miller, T., K. Ksaibati, and M. Farrar. "Using Georgia Loaded-Wheel Tester to Predict Rutting" In Transportation Research Record 1454, TRB, National Research Council, Washington D.C., 1994.
75. Choubane, B., G.C. Page, and J.A. Musselman, "Suitability of Asphalt Pavement Analyzer for Predicting Pavement Rutting", in Journal of Transportation Research Record 1723, TRB, Washington D.C., 2000.
76. Mohammad, L.N, Z. Wu, L. Wang, and C. Abadie, "A Rut Susceptibility Study of Superpave Asphalt Mixtures" in International Journal of Pavements, IJP 2002, Vol. 1, No.2, 2002.
77. WesTrack Forensic Team. "Performance of Coarse-Graded Mixes at WesTrack-Premature Rutting." Final Report, 1998.
78. West, R.C. "A Ruggedness Study of the Asphalt Pavement Analyzer Rutting Test." Memorandum to the Asphalt Pavement Analyzer User Group and New APA Owners, 1999.
79. Bennert, T., A. Maher, and I. Marukic. "Characterization of NJ HMA", Final Report, FHWA-NJ-2002-027, 2003.
80. Kandhal P.S., and L.A. Cooley, Jr. "Accelerated Laboratory Rutting Tests: Evaluation of the Asphalt Pavement Analyzer", NCHRP Report 508, TRB, Washington DC, 2003.
81. Willims, C.R. and B.R. Prowell. "Comparision of Laboratory Wheel-Tracking Test Results to WesTrack Performance" In Transportation Research Record 1681, TRB, National Research Council, Washington DC, 1999.
82. Buchanan, M.S., T.D. White, and B.J. Smith "Use of the Asphalt Pavement Analyzer to Study In-Service Asphalt Mixture Performance" FHWA/MS-DOT-RD-04-155, Final Report, Mississippi State, MS, 2004.
83. Khosla, N.P., and M.S. Omer. "Characterization of Asphaltic Mixtures for Prediction of Permanent Deformation" in Journal of Transportation Research Record 1034, TRB, Washington DC, 1985.
84. Witczak, M.W., K. Kaloush, T. Pellinen, M.E. Basyouny, and H.V. Quintus. "Simple Performance Test for Superpave Mix Design" NCHRP Report 465. TRB, Washington DC, 2002.
85. Sousa, J.B. and S.L. Weissman. "Modeling Permanent Deformation of Asphalt Aggregate Mixes" in Journal of the Association of Asphalt Paving Technologist, Vol. 63, St. Paul, Minnesota, 1994.

86. Bonaquist, R.F., D.W. Christensen, and W. Stump, III. "Simple Performance Tester for Superpave Mix Design: First-Article Development and Evaluation" NCHRP report 513, TRB, Washington DC, 2003.
87. Pellinen, T.K., and M.W. Witzczak. "Use of Stiffness of Hot-Mix Asphalt as A Simple Performance Test". In Transportation Research Record 1789, TRB, Washington DC, 2002.
88. Brown, S.F. and J.M. Gibb. "Validation Experiments for Permanent Deformation Testing of Bituminous Mixtures", in Journal of the Association of Asphalt Paving Technologists, Vol. 65, St. Paul, Minnesota, 1996.
89. Gabrielson, J. R. "Evaluation of Hot Mix Asphalt (HMA) Static Creep and Repeated Load Tests" Ph.D. Dissertation, Auburn University, 1992.
90. Foo, K.Y. "Predicting Rutting in Hot Mix Asphalt" Ph.D. Dissertation, Auburn University, 1994.
91. Kaloush, K.E and M.W. Witzczak, "Tertiary Flow Characteristics of Asphalt Mixtures (With Discussion and Closure)" in Journal of the Association of Asphalt Paving Technologists, Vol. 71, Colorado Springs, Colorado, 2002.
92. Bhasin, A, J.W. Button, and A. Chowdhury. "Evaluation of Simple Performance Tests on Hot-Mix Asphalt Mixtures from South Central United States" in Transportation Research Record 1891, TRB, Washington D.C. 2004.
93. Birgisson, B, R. Roque, J. Kim, L.V. Pham. "The Use of Complex Modulus to Characterize the Performance of Asphalt Mixtures and Pavements in Florida", UF Project 4910-4504-784-12, University of Florida, Gainesville, FL, 2004.
94. Sousa, J.B., J. Craus, and C.L. Monismith. "Summary Report on Permanent Deformation in Asphalt Concrete" Strategic Highway Research Program, Report No. SHRP-A/IR-91-104, Washington DC, 1991.
95. Little, D. N., J.W. Button, and H. Youssef. "Development of Criteria to Evaluate Uniaxial Creep Data and Asphalt Concrete Permanent Deformation potential". in Transportation Research Record 1417, TRB, Washington D.C. 1993.
96. Brown, E.R., and S.A. Cross. "A National Study of Rutting in Hot Mix Asphalt (HMA) Pavements", In Journal of the Association of Asphalt Paving Technologists, Vol. 61, 1992.
97. Harvey, J, S. Weissman, F.Long, and C. Monismith, "Tests to Evaluate the Stiffness and Permanent Deformation Characteristics of Asphalt/Binder-Aggregate Mixes, and Their Use in Mix Design and Analysis (With Discussion)" in Journal of the Association of Asphalt Paving Technologists, Vol. 70, Clearwater Beach, Florida, 2001.
98. Valkering, C.P., J.L. Lancon, E. de Hiltseter, and D.A. Stoker. "Rutting Resistance of Asphalt Mixes Containing Non-Conventional and Polymer-

- Modified Binders” In Journal of the Association of Asphalt Paving Technologists, Vol. 59, 1990.
99. Tanco, A.J. “Permanent Deformation Response of Conventional and Modified Asphalt-Aggregate Mixes under Simple and Compound Shear Loading Conditions”, Ph.D. Dissertation, University of California, Berkeley, 1992.
 100. Brown, S.F. and M.S. Snaith. “The Permanent Deformation Characteristics of a Dense Bitumen Macadem Subjected to Repeated Loading” in Journal of the Association of Asphalt Paving Technologist, Vol. 43, St. Paul, Minnesota, 1974.
 101. Pell, P.S. and S.F. Brown. “The Characteristics of Materials for the Design of Flexible Pavements Structures” Proceedings, Third International Conference on the Structural Design of Asphalt Pavements, London, U.K. 1977.
 102. Hofastra, A. and A.J. Klomp. “Permanent Deformation of Flexible Pavements Under Simulated Road Traffic Conditions” Proceedings, Third International Conference on the Structural Design of Asphalt Pavements, London, U.K. 1977.
 103. Prowell, B.D., J. Zhang, and E.R. Brown. “Aggregate Properties and Their Relationship to the Performance of Superpave-Designed HMA: A Critical Review”, NCHRP 9-35 Final Report, TRB, 2004.
 104. Roberts, F.L., P.S. Kandhal, E.R. Brown, D-Y, Lee, and T.W. Kennedy. “Hot Mix Asphalt Materials, Mixture Design, and Construction”. Second Edition. National Asphalt Pavement Association, Research and Education Foundation. Lanham, Maryland, 1996.
 105. ASTM, ASTM Provisional Specifications, 2001
 106. AASHTO, AASHTO Provisional Standards, June 2004 Edition, 2004.
 107. Ferry, J. D., “Viscoelastic Properties of Polymers”, 2nd edition, Wiley, New York, 1970.
 108. Harvey, J., J.B. Sousa, J.A. Deacon, C.L Monismith. “Effects of Sample Preparation and Air-Void Measurement on Asphalt Concrete Properties”. In Transportation Research Record 1317, TRB, National Research Council, Washington, D.C., 1991.
 109. Anderson, D.A. “Guidelines on Use of Baghouse Fines”. NAPA, Information Services 101, 1987.
 110. InstroTek, Incorporated. “CoreLok Operator’s Guide”, Raleigh, NC, 2003.
 111. Florida DOT, “Section 334-Superpave Asphalt Concrete”, Standard Specifications for Road and Bridge Construction, State of Florida, 2004.
 112. Clyne, T.R., X. Li, M.O. Marasteanu, and E.L. Skok. “Dynamic and Resilient Modulus of MN/DOT Asphalt Mixtures”. MN/DOT Final Report, St. Paul, Minnesota, 2003.

113. Kandhal, P.S., and F. Parker, Jr. NCHRP Report 405: Aggregate Tests Related to Asphalt Concrete Performance in Pavements, Transportation Research Board, National Research Council, Washington, DC, 1998.
114. Rismantojo, E. "Permanent Deformation and Moisture Susceptibility Related aggregate Tests for Use in Hot-Mix Asphalt Pavements," Doctoral Thesis, Purdue University, West Lafayette, IN, 2002.
115. Mallick, R.B., M.R. Teto, and J.E. Haddock. "Use of the Concept of Pore Pressure in Unsaturated Soils for Evaluation of Rutting Potential of Asphalt Paving Mixtures". In Proceeding of Ninth International Conference on Asphalt Pavements, ISAP, Copenhagen, Denmark 2002.

**APPENDIX A AIR VOID CONTENT AND PERMEABILITY TEST
RESULTS**

TABLE A1 Air Voids and Permeability Test Results

Agg. Type	NMAS, mm	Grad.	Gyrs	AC, %	ID	Air Voids (SSD), %	Air Voids (Corelok)%	Water Absorp. in SSD, %	CORR. K_{20} , 1×10^{-5} cm/s
C.GVL	19	N	100	5.5	1	4.13	5.58	0.41	119.1
C.GVL	19	N	100	5.5	2	4.09	5.94	0.35	68.4
C.GVL	19	N	100	5.5	3	3.90	5.47	0.33	109.6
C.GVL	19	N	100	6.0	1	3.53	5.58	0.45	318.2
C.GVL	19	N	100	6.0	2	3.78	5.15	0.37	99.2
C.GVL	19	N	100	6.0	3	3.75	5.34	0.43	2.27
C.GVL	19	N	100	6.5	1	3.57	4.87	0.28	11.4
C.GVL	19	N	100	6.5	2	3.12	4.35	0.20	0.00
C.GVL	19	N	100	6.5	3	2.87	3.79	0.21	62.5
C.GVL	19	N	100	7.0	1	1.99	3.20	0.14	0.00
C.GVL	19	N	100	7.0	2	2.37	3.60	0.23	0.00
C.GVL	19	N	100	7.0	3	2.00	2.76	0.11	0.00
C.GVL	12.5	N	100	6.0	1	4.74	5.63	0.34	1.63
C.GVL	12.5	N	100	6.0	2	4.89	6.36	0.64	52.5
C.GVL	12.5	N	100	6.0	3	4.54	5.89	0.51	21.12
C.GVL	12.5	N	100	6.5	1	4.12	5.16	0.30	0.00
C.GVL	12.5	N	100	6.5	2	4.16	5.51	0.30	54.8
C.GVL	12.5	N	100	6.5	3	4.08	5.12	0.32	10.3
C.GVL	12.5	N	100	7.0	1	2.81	3.37	0.15	0.00
C.GVL	12.5	N	100	7.0	2	2.73	3.43	0.21	0.00
C.GVL	12.5	N	100	7.0	3	2.64	3.53	0.17	3.6
C.GVL	9.5	N	100	6.0	1	4.51	5.34	0.35	22.6
C.GVL	9.5	N	100	6.0	2	4.50	5.16	0.43	3.48
C.GVL	9.5	N	100	6.0	3	4.55	5.44	0.49	1.27
C.GVL	9.5	N	100	6.5	1	3.50	4.25	0.24	0.67
C.GVL	9.5	N	100	6.5	2	3.73	4.12	0.18	0.29
C.GVL	9.5	N	100	6.5	3	3.85	4.59	0.18	3.3
C.GVL	9.5	N	100	7.0	1	2.05	2.95	0.12	0.00
C.GVL	9.5	N	100	7.0	2	2.30	2.84	0.14	0.00
C.GVL	9.5	N	100	7.0	3	2.01	3.47	0.11	0.39
L.GRN	19	N	100	4.5	1	4.63	6.27	0.57	503.4
L.GRN	19	N	100	4.5	2	4.06	5.57	0.42	447.4
L.GRN	19	N	100	4.5	3	4.5	6.31	0.64	203.2
L.GRN	19	N	100	5.0	1	2.9	4.27	0.24	2.6
L.GRN	19	N	100	5.0	2	3.08	4.69	0.30	45.3
L.GRN	19	N	100	5.0	3	3.09	4.3	0.31	5.0
L.GRN	19	N	100	5.5	1	4.1	5.88	0.51	30.6
L.GRN	19	N	100	5.5	2	2.85	4.33	0.22	28.4
L.GRN	19	N	100	5.5	3	3.14	4.32	0.33	8.8
L.GRN	19	N	100	6.0	1	2.41	3.32	0.17	6.2
L.GRN	19	N	100	6.0	2	2.32	3.06	0.17	13.8
L.GRN	19	N	100	6.0	3	1.98	2.98	0.16	3.6
L.GRN	12.5	N	100	5.0	1	4.31	5.46	0.43	55.4
L.GRN	12.5	N	100	5.0	2	4.39	5.45	0.48	42.2

Agg. Type	NMAS, mm	Grad.	Gyrs	AC, %	ID	Air Voids (SSD), %	Air Voids (Corelok)%	Water Absorp. in SSD, %	CORR. $K_{20}, 1 \times 10^{-5}$ cm/s
L.GRN	12.5	N	100	5.0	3	4.83	6.17	0.54	51.6
L.GRN	12.5	N	100	5.5	1	3.86	5.08	0.36	48.1
L.GRN	12.5	N	100	5.5	2	3.76	4.97	0.43	18.4
L.GRN	12.5	N	100	5.5	3	3.67	4.81	0.27	21.2
L.GRN	12.5	N	100	6.0	1	3.05	3.87	0.23	1.8
L.GRN	12.5	N	100	6.0	2	3.21	4.28	0.23	17.2
L.GRN	12.5	N	100	6.0	3	3.18	4.25	0.29	15.9
L.GRN	12.5	N	100	6.5	1	1.81	2.58	0.10	0.00
L.GRN	12.5	N	100	6.5	2	1.14	1.64	0.06	0.19
L.GRN	12.5	N	100	6.5	3	1.53	2.14	0.07	0.19
L.GRN	9.5	N	100	5.5	1	4.09	5.22	0.30	5.7
L.GRN	9.5	N	100	5.5	2	4.41	5.08	0.31	13.3
L.GRN	9.5	N	100	5.5	3	4.47	5.21	0.21	18.4
L.GRN	9.5	N	100	6.0	1	3.12	3.88	0.20	1.9
L.GRN	9.5	N	100	6.0	2	3.46	3.94	0.23	0.68
L.GRN	9.5	N	100	6.0	3	3.27	3.82	0.16	1.3
LMS	19	N	100	5.0	1	4.76	6.22	0.54	544.4
LMS	19	N	100	5.0	2	4.39	5.52	0.40	33.1
LMS	19	N	100	5.0	3	3.93	5.13	0.34	31.1
LMS	19	N	100	5.5	1	3.09	4.15	0.23	0.28
LMS	19	N	100	5.5	2	2.71	3.83	0.21	1.3
LMS	19	N	100	5.5	3	3.06	4.06	0.25	44.0
LMS	19	N	100	6.0	1	2.16	3.17	0.12	0.27
LMS	19	N	100	6.0	2	2.14	3.14	0.13	0.00
LMS	19	N	100	6.0	3	2.25	2.8	0.11	0.00
LMS	12.5	N	100	5.0	1	4.92	5.79	0.37	53.8
LMS	12.5	N	100	5.0	2	5.48	6.52	0.54	83.7
LMS	12.5	N	100	5.0	3	5.12	5.91	0.47	114.8
LMS	12.5	N	100	5.5	1	3.8	4.63	0.25	5.4
LMS	12.5	N	100	5.5	2	3.8	4.52	0.25	0.00
LMS	12.5	N	100	5.5	3	4.05	4.79	0.27	17.3
LMS	12.5	N	100	6.0	1	3.17	4	0.17	0.29
LMS	12.5	N	100	6.0	2	2.92	4.72	0.16	0.39
LMS	12.5	N	100	6.0	3	2.88	3.62	0.13	8.4
LMS	12.5	N	100	6.5	1	2.51	3.1	0.17	0.67
LMS	12.5	N	100	6.5	2	2.69	3.88	0.26	0.1
LMS	12.5	N	100	6.5	3	2.11	2.8	0.15	0.57
LMS	9.5	N	100	5.0	1	4.98	5.83	0.37	17.9
LMS	9.5	N	100	5.0	2	5.11	5.79	0.43	5.9
LMS	9.5	N	100	5.0	3	4.71	5.32	0.23	0.5
LMS	9.5	N	100	5.5	1	3.62	4.22	0.14	7.5
LMS	9.5	N	100	5.5	2	3.48	3.9	0.21	0.00
LMS	9.5	N	100	5.5	3	3.64	4.28	0.18	1.7
LMS	9.5	N	100	6.0	1	2.41	2.97	0.10	0.00
LMS	9.5	N	100	6.0	2	2.14	2.57	0.09	0.00

Agg. Type	NMAS, mm	Grad.	Gyrs	AC, %	ID	Air Voids (SSD), %	Air Voids (Corelok)%	Water Absorp. in SSD, %	CORR. $K_{20}, 1 \times 10^{-5}$ cm/s
LMS	9.5	N	100	6.0	3	2.46	3.08	0.10	1.8
R.GRN	19	N	100	6.0	1	5.75	8.32	0.66	644.0
R.GRN	19	N	100	6.0	2	5.53	7.56	0.55	85.5
R.GRN	19	N	100	6.0	3	5.37	8.02	0.65	360.7
R.GRN	19	N	100	6.5	1	4.57	6.97	0.44	285.7
R.GRN	19	N	100	6.5	2	3.51	5.46	0.33	1.6
R.GRN	19	N	100	6.5	3	3.12	4.85	0.27	5.2
R.GRN	19	N	100	7.0	1	2.14	3.17	0.20	1.6
R.GRN	19	N	100	7.0	2	2.57	4.04	0.23	160.6
R.GRN	19	N	100	7.0	3	2.24	3.9	0.19	68.4
R.GRN	12.5	N	100	6.0	1	6.05	8.22	0.56	494.5
R.GRN	12.5	N	100	6.0	2	6.25	7.8	0.44	319.1
R.GRN	12.5	N	100	6.0	3	5.92	7.67	0.46	193.7
R.GRN	12.5	N	100	6.5	1	4.71	6.05	0.38	76.3
R.GRN	12.5	N	100	6.5	2	4.97	6.16	0.39	8.3
R.GRN	12.5	N	100	6.5	3	4.14	5.53	0.34	67.2
R.GRN	12.5	N	100	7.0	1	4.08	5.16	0.30	2.1
R.GRN	12.5	N	100	7.0	2	3.54	4.78	0.25	0.1
R.GRN	12.5	N	100	7.0	3	3.7	4.99	0.32	104.6
R.GRN	12.5	N	100	7.5	1	3.19	3.84	0.19	34.1
R.GRN	12.5	N	100	7.5	2	2.95	4.00	0.28	19.9
R.GRN	12.5	N	100	7.5	3	2.58	3.74	0.21	1.1
R.GRN	9.5	N	100	6.0	1	4.99	5.99	0.44	159.2
R.GRN	9.5	N	100	6.0	2	5.03	5.87	0.34	35.2
R.GRN	9.5	N	100	6.0	3	5.37	6.63	0.55	85.6
R.GRN	9.5	N	100	6.5	1	4.41	5.45	0.38	6.0
R.GRN	9.5	N	100	6.5	2	4.19	5.13	0.32	17.0
R.GRN	9.5	N	100	6.5	3	4.55	5.44	0.34	32.9
R.GRN	9.5	N	100	7.0	1	3.45	4.49	0.28	26.3
R.GRN	9.5	N	100	7.0	2	3.51	4.24	0.21	0.00
R.GRN	9.5	N	100	7.0	3	3.22	4.11	0.19	0.5
R.GRN	9.5	N	100	7.5	1	2.59	3.62	0.19	3.9
R.GRN	9.5	N	100	7.5	2	2.9	3.55	0.24	0.7
R.GRN	9.5	N	100	7.5	3	2.6	3.58	0.23	4.4
TRAP	19	N	100	6.0	1	6.15	9.41	0.77	2181.7
TRAP	19	N	100	6.0	2	6.26	10.86	0.86	6343.9
TRAP	19	N	100	6.0	3	5.77	9.28	0.86	4569.4
TRAP	19	N	100	6.5	1	5.61	7.94	0.66	20.0
TRAP	19	N	100	6.5	2	5.92	8.31	0.44	535.1
TRAP	19	N	100	6.5	3	5.38	7.88	0.39	432.2
TRAP	19	N	100	7.0	1	4.97	7.3	0.41	266.1
TRAP	19	N	100	7.0	2	5.19	7.89	0.51	1333.6
TRAP	19	N	100	7.0	3	5.47	7.2	0.34	6.8
TRAP	19	N	100	7.5	1	3.77	5.95	0.24	41.08
TRAP	19	N	100	7.5	2	4.73	6.57	0.22	179.84

Agg. Type	NMAS, mm	Grad.	Gyrs	AC, %	ID	Air Voids (SSD), %	Air Voids (Corelok)%	Water Absorp. in SSD, %	CORR. $K_{20}, 1 \times 10^{-5}$ cm/s
TRAP	19	N	100	7.5	3	4.1	6.35	0.39	1243.73
TRAP	12.5	N	100	6.0	1	7.02	9.68	0.81	836.2
TRAP	12.5	N	100	6.0	2	6.35	8.76	0.85	469.3
TRAP	12.5	N	100	6.0	3	7.13	9.43	0.77	983.8
TRAP	12.5	N	100	6.5	1	5.98	7.99	0.62	987.3
TRAP	12.5	N	100	6.5	2	6.1	7.7	0.34	107.4
TRAP	12.5	N	100	6.5	3	5.68	7.48	0.48	407.4
TRAP	12.5	N	100	7.0	1	5.55	6.57	0.26	130.9
TRAP	12.5	N	100	7.0	2	6.06	7.44	0.40	196.8
TRAP	12.5	N	100	7.0	3	5.46	6.67	0.27	75.2
TRAP	12.5	N	100	7.5	1	3.59	4.72	0.23	53.13
TRAP	12.5	N	100	7.5	2	3.92	5.65	0.33	0.28
TRAP	12.5	N	100	7.5	3	4.27	5.09	0.18	32.39
TRAP	9.5	N	100	6.0	1	6.46	7.74	0.57	128.0
TRAP	9.5	N	100	6.0	2	6.5	8.31	0.72	271.2
TRAP	9.5	N	100	6.0	3	6.34	7.69	0.52	133.5
TRAP	9.5	N	100	6.5	1	4.82	5.95	0.21	32.4
TRAP	9.5	N	100	6.5	2	4.65	5.63	0.20	9.8
TRAP	9.5	N	100	6.5	3	4.45	5.4	0.19	16.1
TRAP	9.5	N	100	7.0	1	4.52	5.37	0.19	0.3
TRAP	9.5	N	100	7.0	2	4.18	5.07	0.22	3.6
TRAP	9.5	N	100	7.0	3	4.76	5.66	0.22	47.3
TRAP	9.5	N	100	7.5	1	2.41	2.97	0.16	2.7
TRAP	9.5	N	100	7.5	2	3.32	3.78	0.13	3.3
TRAP	9.5	N	100	7.5	3	3.17	3.83	0.16	1.3
R.GRN	19	F	100	5.5	1	5.25	7.18	0.63	133.2
R.GRN	19	F	100	5.5	2	5.31	6.69	0.69	226.3
R.GRN	19	F	100	5.5	3	5.70	6.95	0.52	165.1
R.GRN	19	F	100	6.0	1	4.48	5.89	0.45	3.9
R.GRN	19	F	100	6.0	2	4.09	5.42	0.53	0.0
R.GRN	19	F	100	6.0	3	4.55	5.74	0.44	0.0
R.GRN	19	F	100	6.5	1	3.36	4.43	0.16	0.0
R.GRN	19	F	100	6.5	2	3.87	4.81	0.24	0.2
R.GRN	19	F	100	6.5	3	3.09	4.23	0.21	0.0
R.GRN	12.5	F	100	5.5	1	5.46	6.35	0.49	131.0
R.GRN	12.5	F	100	5.5	2	4.96	6.25	0.54	80.2
R.GRN	12.5	F	100	5.5	3	5.09	6.10	0.54	61.2
R.GRN	12.5	F	100	6.0	1	3.84	4.72	0.25	1.7
R.GRN	12.5	F	100	6.0	2	3.85	4.74	0.30	0.89
R.GRN	12.5	F	100	6.0	3	3.84	4.54	0.35	7.6
R.GRN	12.5	F	100	6.5	1	3.20	3.95	0.19	0.0
R.GRN	12.5	F	100	6.5	2	3.24	3.96	0.17	0.6
R.GRN	12.5	F	100	6.5	3	3.52	4.24	0.22	0.0
R.GRN	9.5	F	100	5.5	1	6.59	7.79	0.84	187.3
R.GRN	9.5	F	100	5.5	2	6.81	7.68	0.71	132.7

Agg. Type	NMAS, mm	Grad.	Gyrs	AC, %	ID	Air Voids (SSD), %	Air Voids (Corelok)%	Water Absorp. in SSD, %	CORR. $K_{20}, 1 \times 10^{-5}$ cm/s
R.GRN	9.5	F	100	5.5	3	6.56	7.68	0.77	267.2
R.GRN	9.5	F	100	6.0	1	4.93	5.64	0.27	6.6
R.GRN	9.5	F	100	6.0	2	5.50	6.13	0.34	34.1
R.GRN	9.5	F	100	6.0	3	4.99	5.85	0.30	18.9
R.GRN	9.5	F	100	6.5	1	4.93	5.72	0.27	18.2
R.GRN	9.5	F	100	6.5	2	4.28	5.26	0.30	9.60
R.GRN	9.5	F	100	6.5	3	4.62	5.66	0.30	1.0
R.GRN	9.5	F	100	7.0	1	3.05	4.30	0.15	0.0
R.GRN	9.5	F	100	7.0	2	3.39	4.10	0.14	0.0
R.GRN	9.5	F	100	7.0	3	3.34	4.01	0.19	16.2
TRAP	19	F	100	6.0	1	5.21	6.93	0.31	38.5
TRAP	19	F	100	6.0	2	4.59	6.40	0.40	51.4
TRAP	19	F	100	6.0	3	5.12	6.55	0.46	47.0
TRAP	19	F	100	6.5	1	4.63	6.22	0.51	83.0
TRAP	19	F	100	6.5	2	4.34	5.77	0.46	9.1
TRAP	19	F	100	6.5	3	3.83	4.95	0.32	34.2
TRAP	19	F	100	7.0	1	3.35	4.69	0.33	44.5
TRAP	19	F	100	7.0	2	3.43	4.74	0.31	53.6
TRAP	19	F	100	7.0	3	3.40	4.13	0.19	1.0
TRAP	12.5	F	100	6.0	1	4.38	5.59	0.28	1.8
TRAP	12.5	F	100	6.0	2	4.04	5.16	0.35	3.1
TRAP	12.5	F	100	6.0	3	4.28	5.49	0.31	30.1
TRAP	12.5	F	100	6.5	1	3.18	4.10	0.23	0.00
TRAP	12.5	F	100	6.5	2	3.78	4.87	0.32	0.38
TRAP	12.5	F	100	6.5	3	3.34	4.77	0.30	0.00
TRAP	9.5	F	100	6.0	1	4.76	5.73	0.30	17.5
TRAP	9.5	F	100	6.0	2	4.63	5.60	0.35	35.6
TRAP	9.5	F	100	6.0	3	4.67	5.45	0.31	29.8
TRAP	9.5	F	100	6.5	1	4.06	5.02	0.28	0.59
TRAP	9.5	F	100	6.5	2	3.57	4.44	0.21	1.3
TRAP	9.5	F	100	6.5	3	3.94	4.79	0.22	1.4
C.GVL	19	N	65	6.0	1	5.29	6.97	0.54	159.8
C.GVL	19	N	65	6.0	2	4.48	6.35	0.36	60.7
C.GVL	19	N	65	6.0	3	5.29	7.04	0.62	212.4
C.GVL	19	N	65	6.5	1	4.53	5.91	0.36	222.5
C.GVL	19	N	65	6.5	2	4.47	6.20	0.42	1.45
C.GVL	19	N	65	6.5	3	4.01	5.22	0.42	142.7
C.GVL	19	N	65	7.0	4	3.52	4.79	0.41	0.00
C.GVL	19	N	65	7.0	5	3.42	4.73	0.22	0.38
C.GVL	19	N	65	7.0	6	2.74	4.13	0.23	0.00
C.GVL	12.5	N	65	6.0	1	5.59	7.00	0.58	83.7
C.GVL	12.5	N	65	6.0	2	6.03	7.19	0.59	350.5
C.GVL	12.5	N	65	6.0	3	5.78	6.97	0.72	175.3
C.GVL	12.5	N	65	6.5	1	4.87	6.18	0.56	45.0
C.GVL	12.5	N	65	6.5	2	4.82	5.74	0.48	118.4

Agg. Type	NMAS, mm	Grad.	Gyrs	AC, %	ID	Air Voids (SSD), %	Air Voids (Corelok)%	Water Absorp. in SSD, %	CORR. $K_{20}, 1 \times 10^{-5}$ cm/s
C.GVL	12.5	N	65	6.5	3	4.69	6.21	0.52	29.5
C.GVL	12.5	N	65	7.0	1	4.03	4.83	0.36	10.3
C.GVL	12.5	N	65	7.0	2	4.17	4.91	0.42	87.5
C.GVL	12.5	N	65	7.0	3	4.43	5.21	0.35	17.9
C.GVL	9.5	N	65	6.0	1	5.47	6.40	0.40	9.3
C.GVL	9.5	N	65	6.0	2	5.39	6.09	0.34	11.7
C.GVL	9.5	N	65	6.0	3	5.43	6.18	0.51	13.1
C.GVL	9.5	N	65	6.5	1	4.15	4.93	0.34	1.89
C.GVL	9.5	N	65	6.5	2	4.08	4.67	0.30	4.90
C.GVL	9.5	N	65	6.5	3	4.15	4.85	0.29	1.34
C.GVL	9.5	N	65	7.0	1	3.58	3.98	0.23	2.22
C.GVL	9.5	N	65	7.0	2	3.02	3.60	0.22	1.24
C.GVL	9.5	N	65	7.0	3	2.91	3.88	0.18	0.00
L.GRN	19	N	65	5.5	1	4.34	5.05	0.18	0.00
L.GRN	19	N	65	5.5	2	4.80	6.25	0.66	54.2
L.GRN	19	N	65	5.5	3	4.79	6.95	0.76	58.3
L.GRN	19	N	65	6.0	1	4.02	4.96	0.44	150.6
L.GRN	19	N	65	6.0	2	4.10	5.26	0.48	18.7
L.GRN	19	N	65	6.0	3	3.49	4.16	0.32	7.2
L.GRN	19	N	65	6.5	1	2.80	3.82	0.24	8.3
L.GRN	19	N	65	6.5	2	3.17	4.03	0.22	0.00
L.GRN	19	N	65	6.5	3	3.12	4.19	0.27	10.8
L.GRN	12.5	N	65	5.5	1	7.95	10.48	1.66	1741.7
L.GRN	12.5	N	65	5.5	2	6.48	8.58	0.95	286.7
L.GRN	12.5	N	65	5.5	3	5.99	7.48	0.86	394.0
L.GRN	12.5	N	65	6.0	1	5.17	6.01	0.55	9.8
L.GRN	12.5	N	65	6.0	2	4.68	5.96	0.50	99.8
L.GRN	12.5	N	65	6.0	3	4.99	6.06	0.54	2.6
L.GRN	12.5	N	65	6.5	1	4.22	4.94	0.36	10.4
L.GRN	12.5	N	65	6.5	2	3.87	4.48	0.35	2.3
L.GRN	12.5	N	65	6.5	3	4.01	4.94	0.41	1.6
L.GRN	9.5	N	65	6.0	1	5.60	6.41	0.43	37.2
L.GRN	9.5	N	65	6.0	2	5.56	6.52	0.50	87.7
L.GRN	9.5	N	65	6.0	3	5.25	5.95	0.51	33.1
L.GRN	9.5	N	65	6.5	1	4.34	4.97	0.36	4.2
L.GRN	9.5	N	65	6.5	2	3.94	4.43	0.35	0.09
L.GRN	9.5	N	65	6.5	3	4.26	4.94	0.38	4.6
L.GRN	9.5	N	65	7.0	1	2.66	3.16	0.18	0.19
L.GRN	9.5	N	65	7.0	2	2.77	3.35	0.17	0.00
L.GRN	9.5	N	65	7.0	3	2.84	3.32	0.25	0.09
LMS	19	N	65	5.5	1	4.81	6.10	0.38	132.7
LMS	19	N	65	5.5	2	5.71	6.90	0.54	159.6
LMS	19	N	65	5.5	3	5.08	6.16	0.51	134.7
LMS	19	N	65	6.0	1	3.99	4.84	0.30	0.00
LMS	19	N	65	6.0	2	4.31	5.39	0.36	26.5

Agg. Type	NMAS, mm	Grad.	Gyrs	AC, %	ID	Air Voids (SSD), %	Air Voids (Corelok)%	Water Absorp. in SSD, %	CORR. $K_{20}, 1 \times 10^{-5}$ cm/s
LMS	19	N	65	6.0	3	3.72	4.83	0.31	27.3
LMS	19	N	65	6.5	1	2.88	3.64	0.21	4.06
LMS	19	N	65	6.5	2	3.10	3.89	0.21	11.9
LMS	19	N	65	6.5	3	3.05	3.95	0.17	0.00
LMS	12.5	N	65	6.0	1	4.64	5.32	0.35	26.1
LMS	12.5	N	65	6.0	2	4.75	5.62	0.31	23.2
LMS	12.5	N	65	6.0	3	5.10	5.92	0.36	0.87
LMS	12.5	N	65	6.5	1	4.26	4.67	0.22	0.29
LMS	12.5	N	65	6.5	2	3.66	4.19	0.24	0.00
LMS	12.5	N	65	6.5	3	3.73	4.53	0.26	0.19
LMS	12.5	N	65	7.0	1	2.79	3.81	0.23	0.00
LMS	12.5	N	65	7.0	2	2.95	3.86	0.19	0.00
LMS	12.5	N	65	7.0	3	2.58	3.44	0.22	0.00
LMS	9.5	N	65	6.0	1	4.29	5.23	0.19	3.8
LMS	9.5	N	65	6.0	2	4.28	5.34	0.18	6.7
LMS	9.5	N	65	6.0	3	4.37	5.34	0.25	1.4
LMS	9.5	N	65	6.5	1	3.33	4.13	0.14	0.00
LMS	9.5	N	65	6.5	2	3.26	4.08	0.16	0.00
LMS	9.5	N	65	6.5	3	3.19	3.77	0.13	0.09
LMS	9.5	N	65	7.0	1	2.23	2.68	0.10	0.00
LMS	9.5	N	65	7.0	2	2.09	2.54	0.08	0.00
LMS	9.5	N	65	7.0	3	2.30	2.74	0.10	0.00
R.GRN	19	N	65	6.5	1	5.66	7.93	0.63	22.9
R.GRN	19	N	65	6.5	2	4.65	7.27	0.70	251.1
R.GRN	19	N	65	6.5	3	5.37	7.87	0.73	113.4
R.GRN	19	N	65	7.0	1	4.93	7.58	0.63	417.6
R.GRN	19	N	65	7.0	2	4.13	5.89	0.49	8.0
R.GRN	19	N	65	7.0	3	3.65	5.07	0.39	0.55
R.GRN	19	N	65	7.5	1	4.03	6.39	0.41	29.0
R.GRN	19	N	65	7.5	2	2.72	3.88	0.25	8.2
R.GRN	19	N	65	7.5	3	4.17	6.52	0.43	192.8
R.GRN	12.5	N	65	6.5	1	7.08	9.39	0.73	391.4
R.GRN	12.5	N	65	6.5	2	6.39	8.78	0.75	981.6
R.GRN	12.5	N	65	6.5	3	7.17	9.14	0.70	1174.2
R.GRN	12.5	N	65	7.0	1	5.98	7.95	0.69	165.0
R.GRN	12.5	N	65	7.0	2	5.71	8.06	0.68	132.8
R.GRN	12.5	N	65	7.0	3	5.40	7.10	0.49	5.7
R.GRN	12.5	N	65	7.5	1	5.25	7.71	0.45	22.6
R.GRN	12.5	N	65	7.5	2	4.99	6.37	0.41	216.4
R.GRN	12.5	N	65	7.5	3	4.74	6.06	0.39	51.7
R.GRN	9.5	N	65	6.5	1	6.56	8.33	0.75	134.5
R.GRN	9.5	N	65	6.5	2	6.66	8.16	0.80	34.0
R.GRN	9.5	N	65	6.5	3	6.63	8.48	0.82	232.3
R.GRN	9.5	N	65	7.0	1	5.61	6.67	0.62	102.6
R.GRN	9.5	N	65	7.0	2	6.00	6.84	0.64	46.2

Agg. Type	NMAS, mm	Grad.	Gyrs	AC, %	ID	Air Voids (SSD), %	Air Voids (Corelok)%	Water Absorp. in SSD, %	CORR. K_{20} , 1×10^{-5} cm/s
R.GRN	9.5	N	65	7.0	3	5.21	6.11	0.59	35.4
R.GRN	9.5	N	65	7.5	1	4.41	5.06	0.37	7.0
R.GRN	9.5	N	65	7.5	2	4.22	5.31	0.23	9.7
R.GRN	9.5	N	65	7.5	3	4.16	5.20	0.46	116.4
R.GRN	19	F	65	6.0	1	5.83	6.86	0.44	48.0
R.GRN	19	F	65	6.0	2	5.77	6.85	0.61	304.0
R.GRN	19	F	65	6.0	3	5.27	6.72	0.59	397.2
R.GRN	19	F	65	6.5	1	4.48	6.06	0.40	17.1
R.GRN	19	F	65	6.5	2	4.03	5.40	0.40	21.4
R.GRN	19	F	65	6.5	3	3.98	5.07	0.34	3.10
R.GRN	19	F	65	7.0	1	3.62	4.78	0.26	0.00
R.GRN	19	F	65	7.0	2	3.36	4.19	0.17	11.9
R.GRN	19	F	65	7.0	3	3.09	4.00	0.19	5.40
R.GRN	12.5	F	65	6.0	1	6.46	7.71	0.67	97.5
R.GRN	12.5	F	65	6.0	2	5.54	6.82	0.57	104.1
R.GRN	12.5	F	65	6.0	3	6.02	7.33	0.56	315.5
R.GRN	12.5	F	65	6.5	1	4.24	5.46	0.35	55.5
R.GRN	12.5	F	65	6.5	2	4.27	5.13	0.27	10.9
R.GRN	12.5	F	65	6.5	3	4.66	5.56	0.36	39.7
R.GRN	12.5	F	65	7.0	1	3.36	4.07	0.14	16.6
R.GRN	12.5	F	65	7.0	2	3.61	4.62	0.24	0.00
R.GRN	12.5	F	65	7.0	3	2.70	3.66	0.17	0.00
R.GRN	9.5	F	65	6.5	1	6.39	8.03	0.94	330.6
R.GRN	9.5	F	65	6.5	2	5.83	6.97	0.82	18.4
R.GRN	9.5	F	65	6.5	3	5.44	6.57	0.69	53.2
R.GRN	9.5	F	65	7.0	1	4.17	4.94	0.35	11.2
R.GRN	9.5	F	65	7.0	2	4.52	5.22	0.44	7.90
R.GRN	9.5	F	65	7.0	3	4.52	5.06	0.37	82.1
R.GRN	9.5	F	65	7.5	1	3.08	4.10	0.18	0.00
R.GRN	9.5	F	65	7.5	2	3.43	4.01	0.23	0.19
R.GRN	9.5	F	65	7.5	3	3.01	3.63	0.14	0.00
TRAP	19	F	65	6.5	1	5.02	7.26	0.55	362.4
TRAP	19	F	65	6.5	2	5.01	6.65	0.54	447.7
TRAP	19	F	65	6.5	3	4.94	6.66	0.52	446.5
TRAP	19	F	65	7.0	1	3.72	4.88	0.41	56.4
TRAP	19	F	65	7.0	2	4.34	5.60	0.47	2.51
TRAP	19	F	65	7.0	3	3.62	4.62	0.38	8.52
TRAP	19	F	65	7.5	1	2.95	4.07	0.22	34.1
TRAP	19	F	65	7.5	2	3.05	3.91	0.25	0.00
TRAP	19	F	65	7.5	3	2.78	3.71	0.20	0.00
TRAP	12.5	F	65	6.0	1	5.36	7.44	0.60	347.0
TRAP	12.5	F	65	6.0	2	5.72	7.43	0.51	541.3
TRAP	12.5	F	65	6.0	3	5.10	6.51	0.37	396.9
TRAP	12.5	F	65	6.5	1	3.88	5.34	0.35	242.3
TRAP	12.5	F	65	6.5	2	4.00	5.69	0.30	25.4

Agg. Type	NMAS, mm	Grad.	Gyrs	AC, %	ID	Air Voids (SSD), %	Air Voids (Corelok)%	Water Absorp. in SSD, %	CORR. $K_{20}, 1 \times 10^{-5}$ cm/s
TRAP	12.5	F	65	6.5	3	4.51	5.77	0.38	93.5
TRAP	12.5	F	65	7.0	1	3.43	4.43	0.20	0.00
TRAP	12.5	F	65	7.0	2	2.91	3.59	0.14	0.00
TRAP	12.5	F	65	7.0	3	2.64	3.83	0.15	0.00
TRAP	9.5	F	65	6.5	1	5.44	6.92	0.56	217.0
TRAP	9.5	F	65	6.5	2	5.75	7.00	0.49	168.9
TRAP	9.5	F	65	6.5	3	5.52	6.55	0.49	155.3
TRAP	9.5	F	65	7.0	1	3.87	5.01	0.35	68.2
TRAP	9.5	F	65	7.0	2	4.18	4.95	0.32	0.00
TRAP	9.5	F	65	7.0	3	4.17	5.03	0.37	11.2
TRAP	9.5	F	65	7.5	1	2.96	3.43	0.12	0.00
TRAP	9.5	F	65	7.5	2	3.19	3.81	0.22	0.39
TRAP	9.5	F	65	7.5	3	3.13	3.74	0.19	3.20

APPENDIX B COREGRAVITY™ PROGRAM CORRECTION FACTOR

TABLE B1 CoreGravity™ Program Correction Factors (110)

R= Ratio M _c /M _b	Correction Factor, CF		
	Small Bag	Large Bag	Double Bags
	CF=-0.000566*R+0.8121	CF=-0.00166*R+0.8596	CF=-0.0022448*R+0.81518
10	0.806	0.843	0.793
20	0.801	0.826	0.770
30	0.795	0.810	0.748
40	0.789	0.793	0.725
50	0.784	0.777	0.703
60	0.778	0.760	0.680
70	0.772	0.743	0.658
80	0.767	0.727	0.636
90	0.761	0.710	0.613
100	0.756	0.694	0.591
110	0.750	0.677	0.568
120	0.744	0.660	0.546
130	0.739	0.644	0.523
140	0.733	0.627	0.501
150	0.727	0.611	0.478
160	0.722	0.594	0.456
170	0.716	0.577	0.434
180	0.710	0.561	0.411
190	0.705	0.544	0.389
200	0.699	0.528	0.366
210	0.693	0.511	0.344
220	0.688	0.494	0.321
230	0.682	0.478	0.299
240	0.676	0.461	0.276
250	0.671	0.445	0.254
260	0.665	0.428	0.232
270	0.659	0.411	0.209
280	0.654	0.395	0.187
290	0.648	0.378	0.164
300	0.642	0.362	0.142

Note: M_c is mass of dry sample, M_b is mass of bag

**APPENDIX C AGGREGATE BREAKDOWN FOR DIFFERENT
COMPACTION EFFORTS**

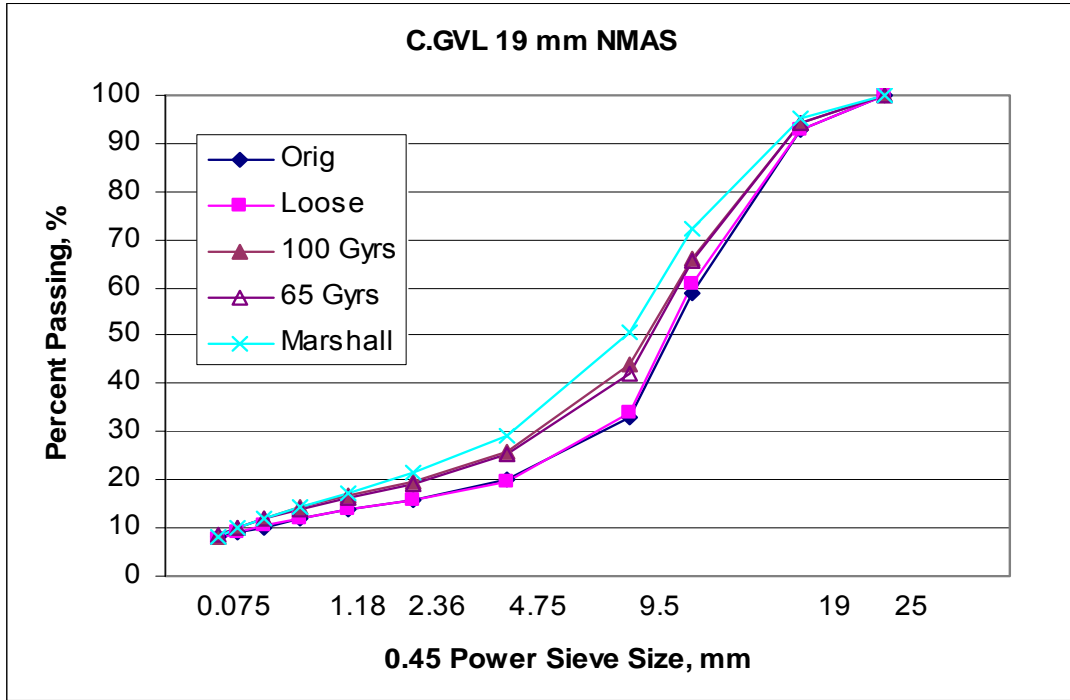


FIGURE C1 Aggregate breakdown for crushed gravel 19 mm NMAS mixture.

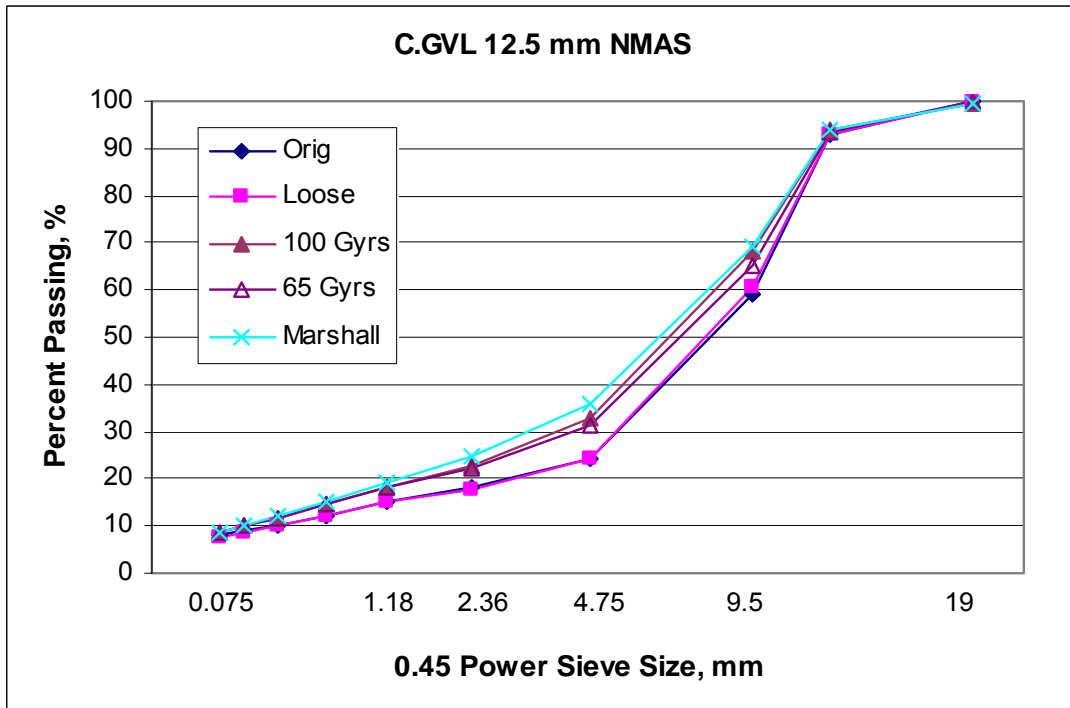


FIGURE C2 Aggregate breakdown for crushed gravel 12.5 mm NMAS mixture.

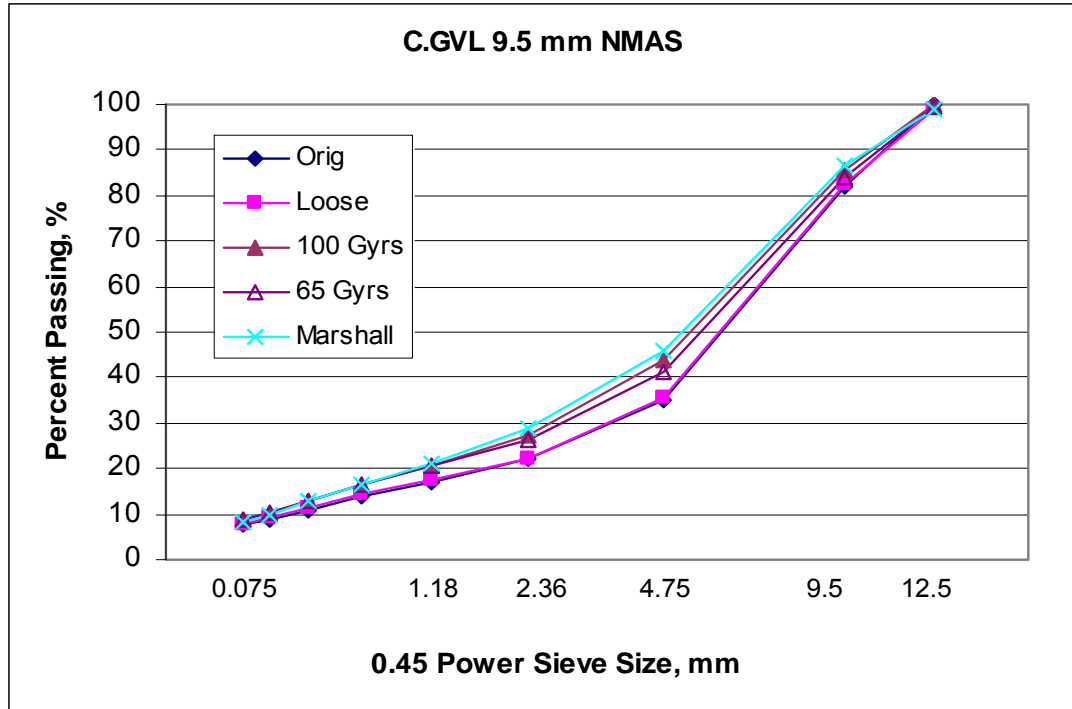


FIGURE C3 Aggregate breakdown for crushed gravel 9.5 mm NMAS mixture.

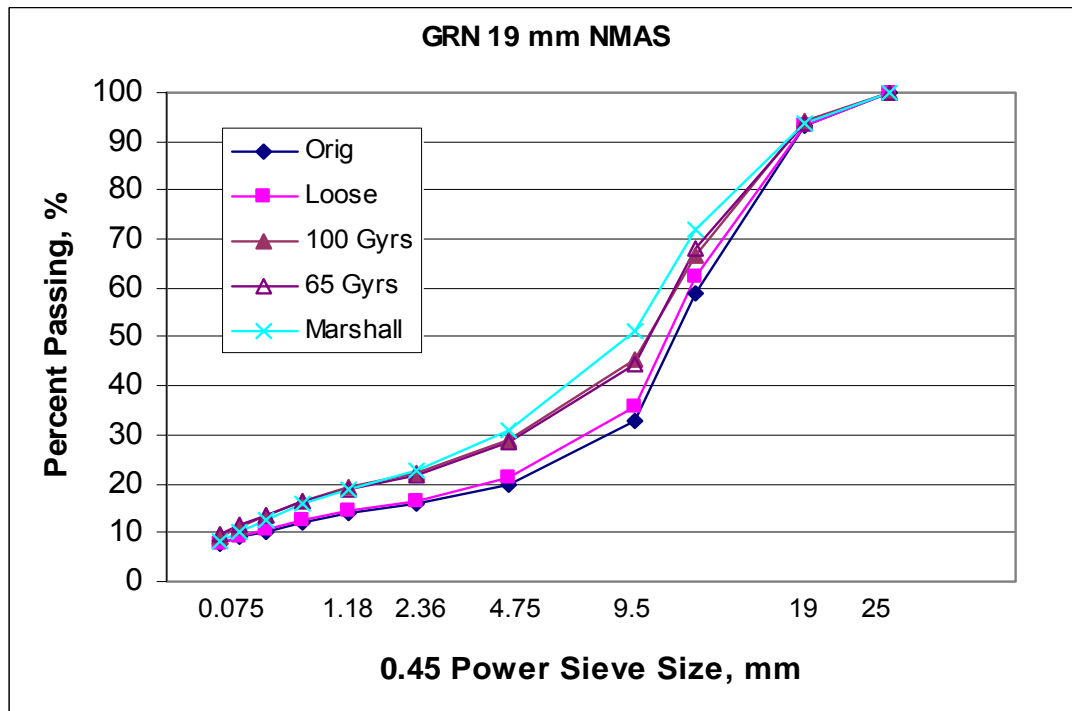


FIGURE C4 Aggregate breakdown for lab granite 19 mm NMAS mixture.

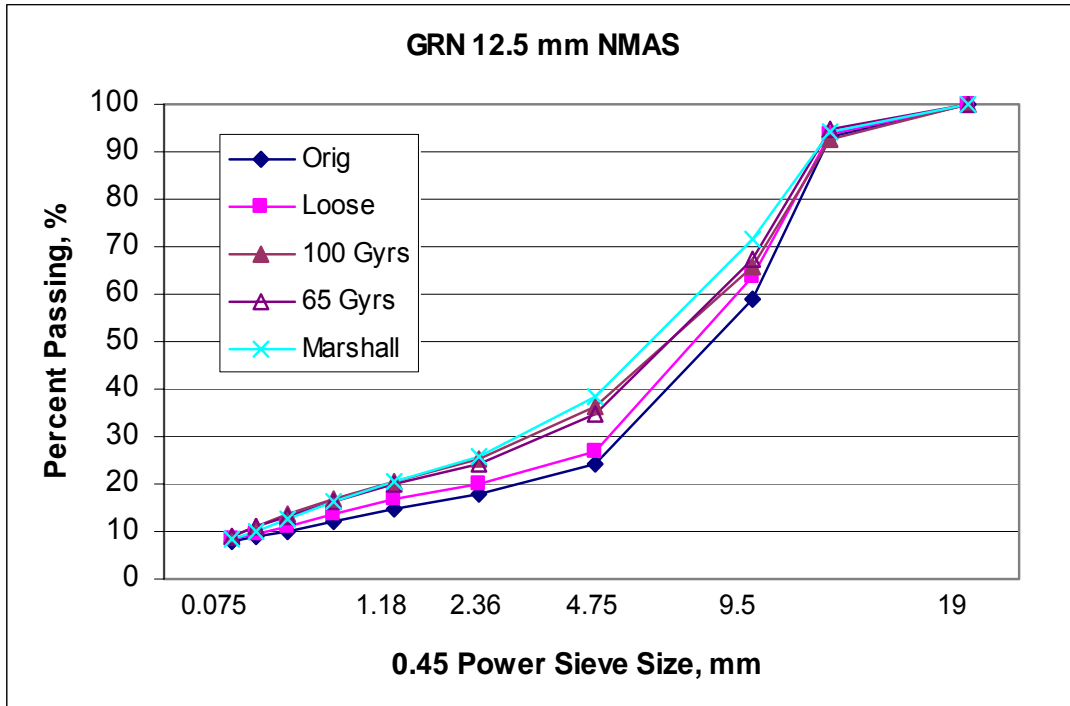


FIGURE C5 Aggregate breakdown for lab granite 12.5 mm NMAS mixture.

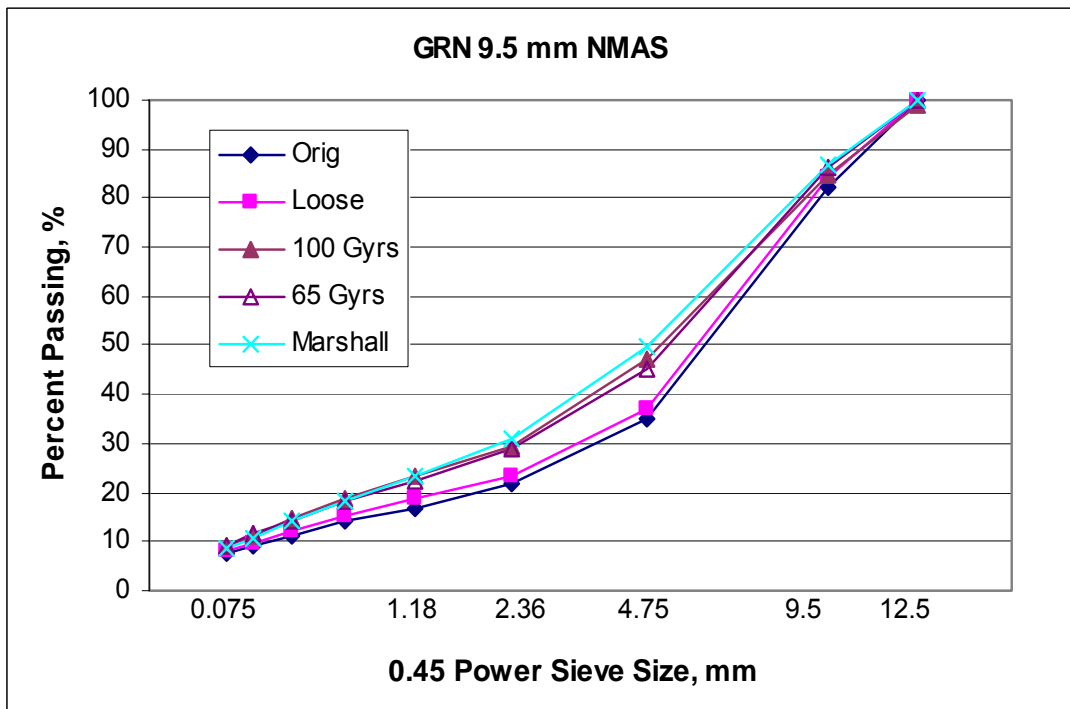


FIGURE C6 Aggregate breakdown for lab granite 9.5 mm NMAS mixture.

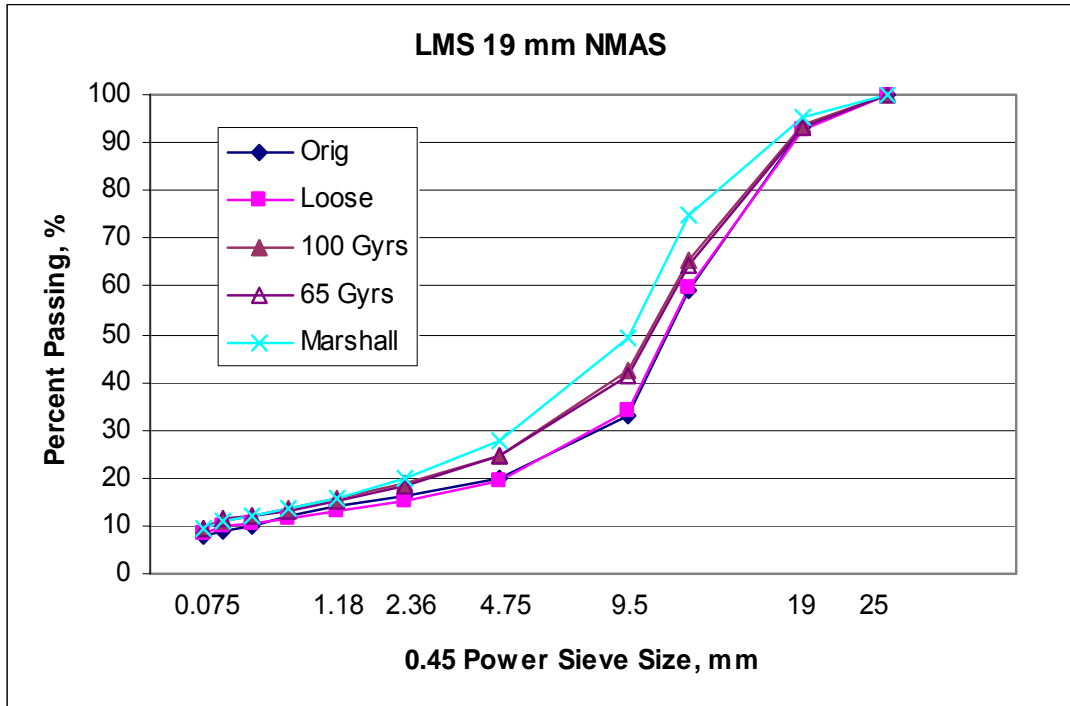


FIGURE C7 Aggregate breakdown for limestone 19 mm NMAS mixture.

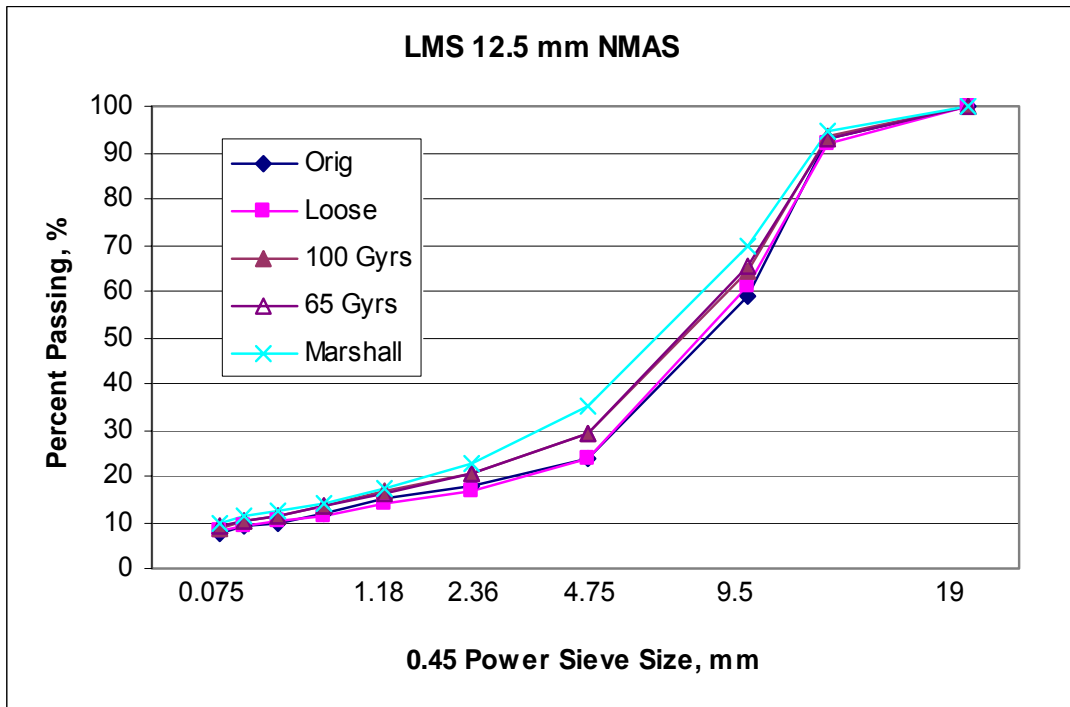


FIGURE C8 Aggregate breakdown for limestone 12.5 mm NMAS mixture.

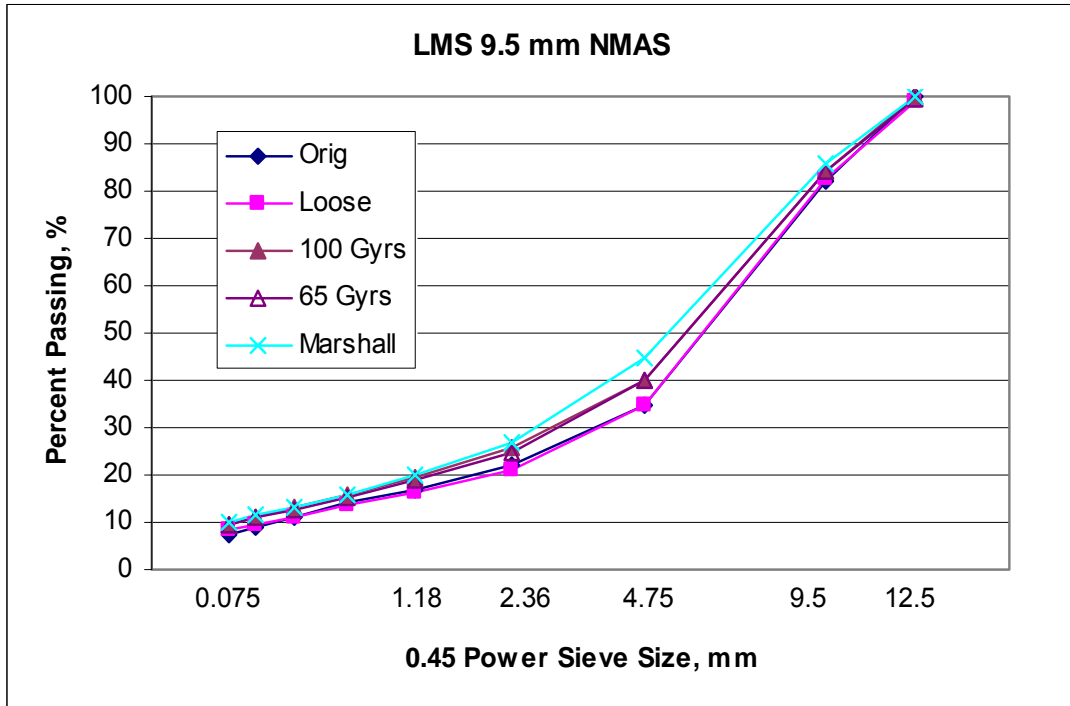


FIGURE C9 Aggregate breakdown for limestone 9.5 mm NMAS mixture.

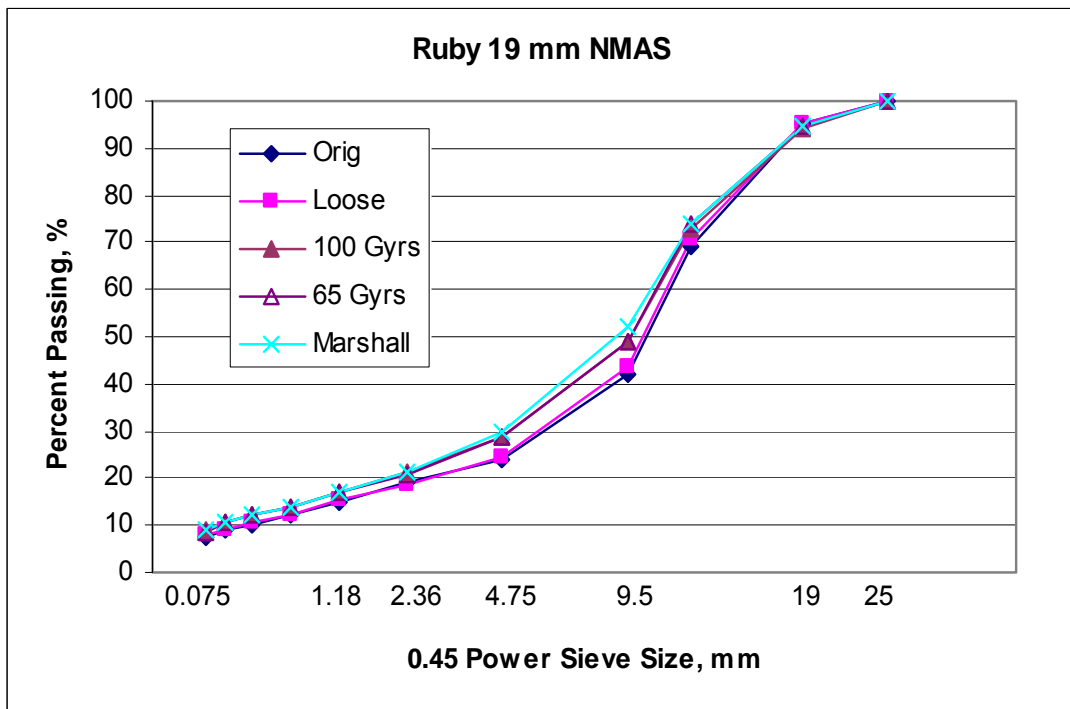


FIGURE C10 Aggregate breakdown for ruby granite 19 mm NMAS mixture.

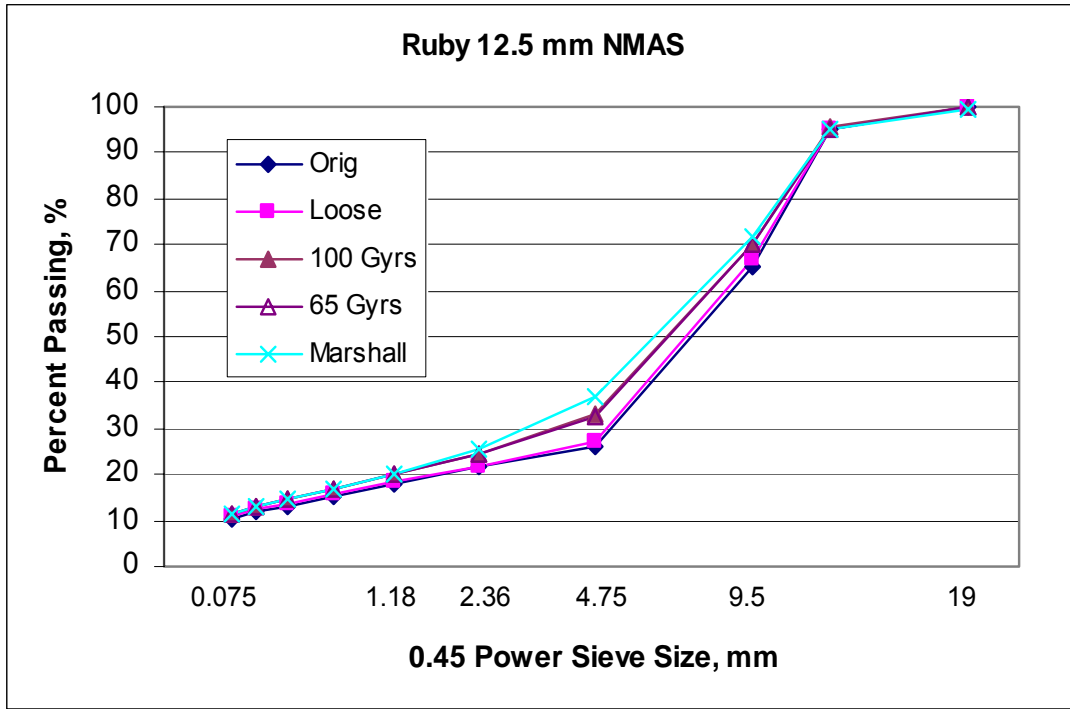


FIGURE C11 Aggregate breakdown for ruby granite 12.5 mm NMAS mixture.

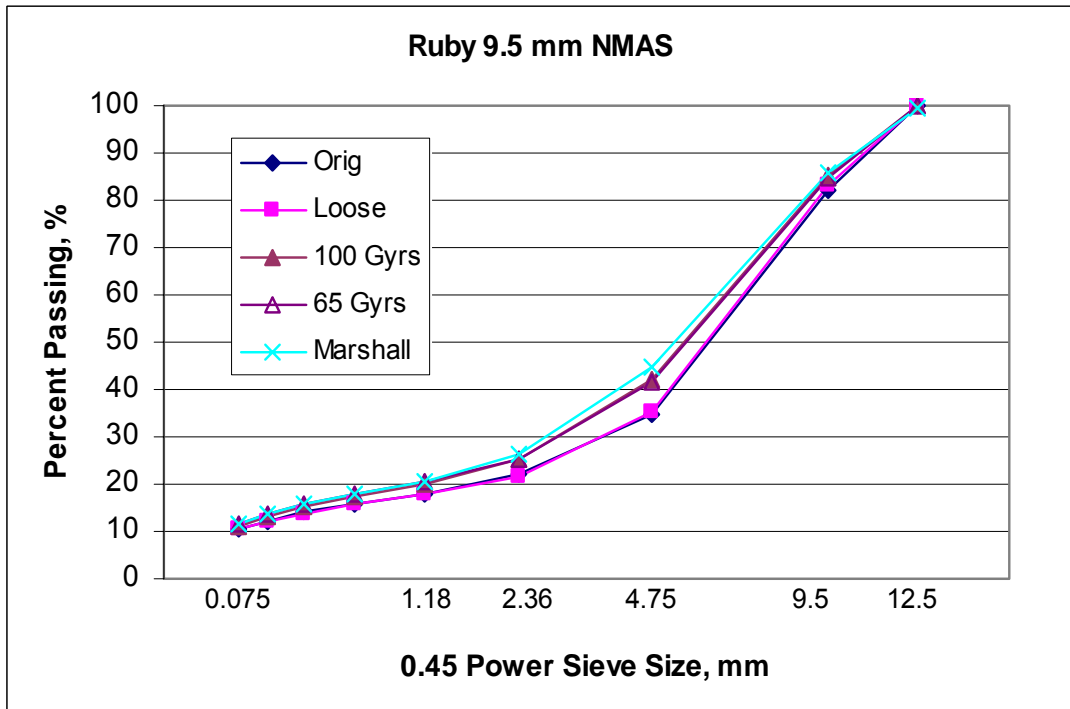


FIGURE C12 Aggregate breakdown for ruby granite 9.5 mm NMAS mixture.

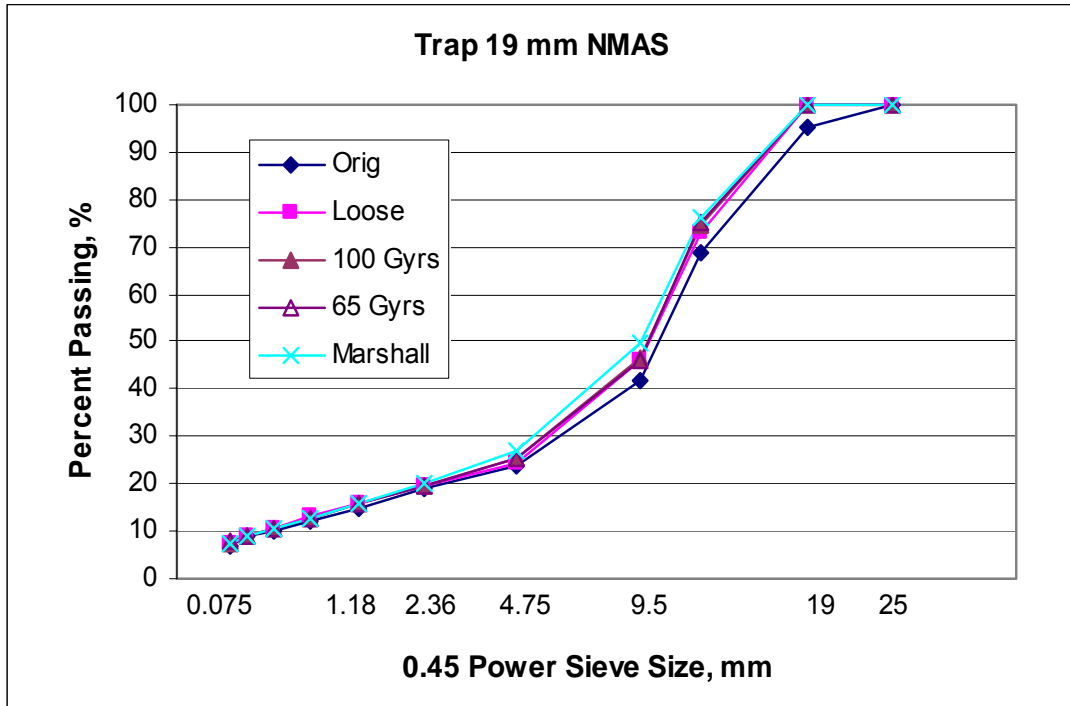


FIGURE C13 Aggregate breakdown for traprock 19 mm NMAS mixture.

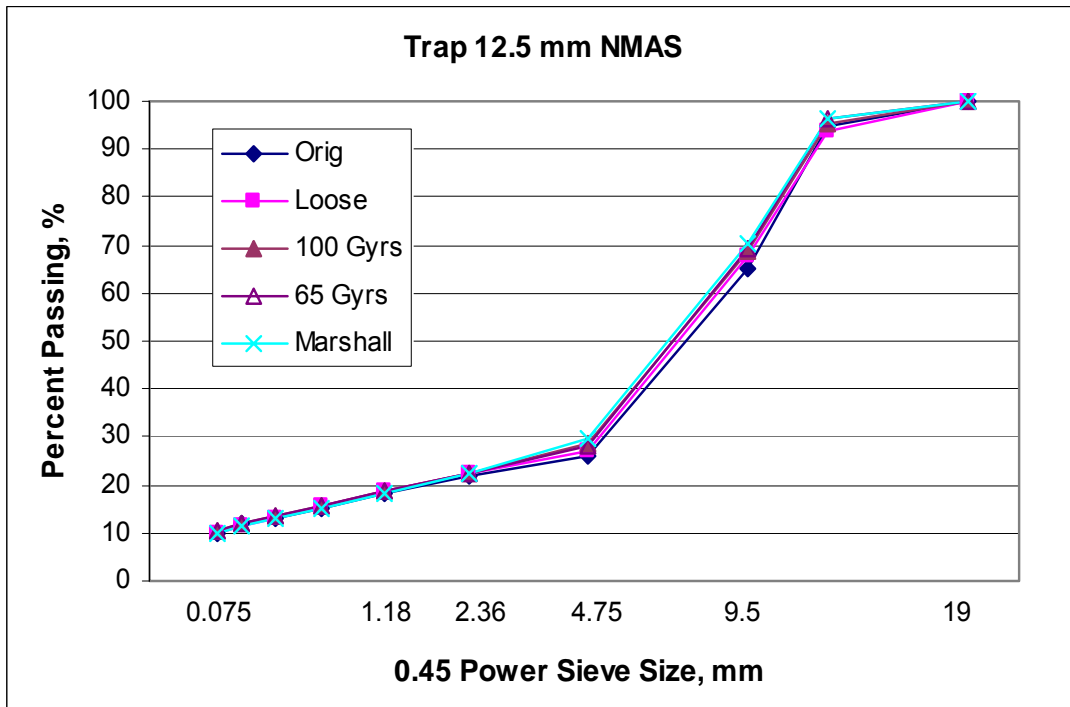


FIGURE C14 Aggregate breakdown for traprock 12.5 mm NMAS mixture.

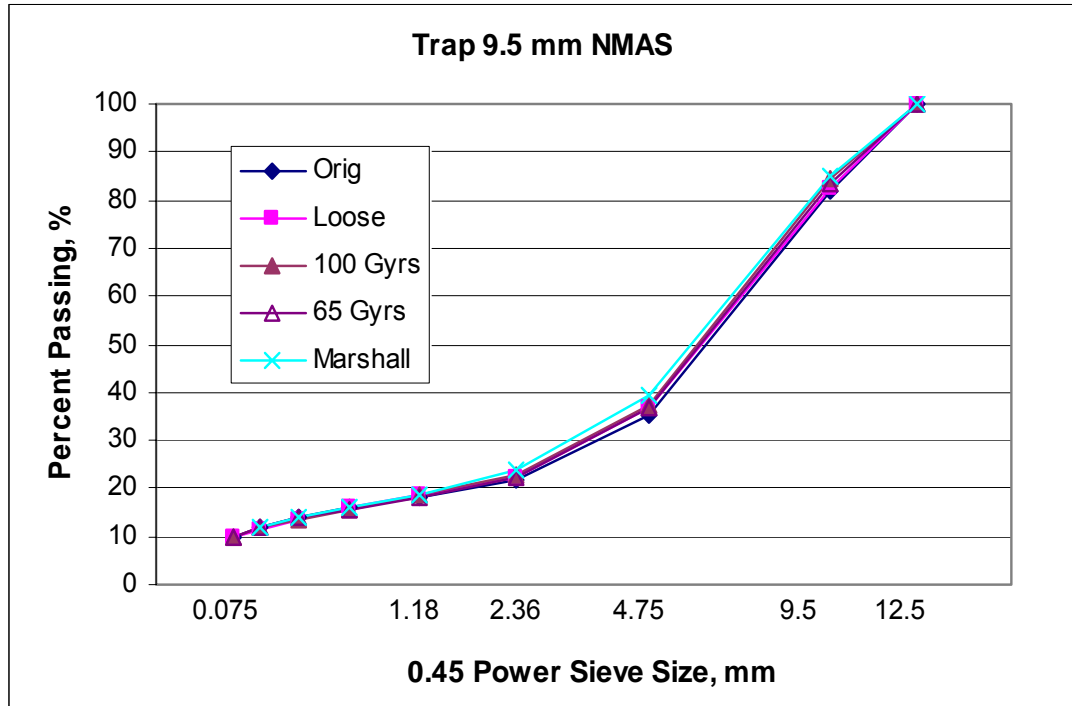


FIGURE C15 Aggregate breakdown for traprock 9.5 mm NMAS mixture.

APPENDIX D TRIAXIAL PERFORMANCE TEST RESULTS

TABLE D1 Dynamic Modulus Test Results

Agg. Type	Gyrs	NMAAS	ID	25Hz		10Hz		5Hz		1Hz		0.5Hz		0.1Hz	
				E*	ϕ	E*	ϕ	E*	ϕ	E*	ϕ	E*	ϕ	E*	ϕ
C.GVL	65	19	7	693.8	34.4	600.5	30.8	518.6	28.9	403.9	23.4	365.2	20.4	317.6	18.1
C.GVL	65	19	8	774.7	39.0	681.8	24.2	630.4	19.9	574.7	12.9	564.5	10.0	544.3	7.1
C.GVL	65	19	9	697.9	41.8	565.2	33.8	507.0	29.5	424.5	21.4	409.7	19.8	404.4	17.2
C.GVL	65	12.5	1	1297.7	35.1	1128.6	27.4	1049.7	21.0	931.6	15.3	885.9	13.2	848.4	10.5
C.GVL	65	12.5	8	825.1	36.1	750.2	28.2	682.7	20.9	598.4	14.2	572.9	12.2	550.7	8.7
C.GVL	65	12.5	10	347.7	49.8	274.5	37.3	248.3	32.9	194.2	26.8	176.8	24.9	160.2	19.2
C.GVL	65	9.5	6	1069.6	40.5	921.4	31.8	804.4	25.3	653.4	19.0	624.3	17.1	593.3	13.6
C.GVL	65	9.5	8	991.2	44.6	804.4	30.9	694.9	27.6	573.5	20.6	543.1	19.1	526.5	15.9
C.GVL	65	9.5	9	872.4	40.7	748.4	32.2	673.0	27.5	560.0	20.8	539.0	19.2	523.9	16.6
C.GVL	100	19	7	891.6	36.8	790.2	26.9	726.1	22.5	636.9	16.8	625.4	15.0	612.0	11.7
C.GVL	100	19	9	870.4	39.2	734.3	28.4	658.6	23.6	553.7	17.0	528.1	15.8	498.3	12.3
C.GVL	100	19	10	826.7	30.7	795.4	25.2	718.6	21.0	617.3	15.8	592.3	13.7	572.8	11.3
C.GVL	100	12.5	2	1015.0	41.8	827.4	29.1	714.0	24.9	580.8	18.1	552.2	16.5	507.6	13.7
C.GVL	100	12.5	3	774.7	41.4	634.2	29.0	558.3	24.3	449.7	17.4	426.8	15.0	391.8	11.0
C.GVL	100	12.5	7	1217.2	39.6	1041.0	30.3	917.8	25.0	766.6	18.9	742.7	16.9	714.5	13.2
C.GVL	100	9.5	5	1330.8	38.0	1056.3	29.1	926.2	23.7	765.9	17.2	723.4	15.3	668.3	12.3
C.GVL	100	9.5	6	1273.1	34.8	1107.7	24.6	997.1	20.8	846.7	15.5	812.8	14.1	772.3	11.2
C.GVL	100	9.5	7	940.5	42.2	785.8	29.2	691.7	24.9	566.9	18.1	534.2	16.0	501.6	12.4
L.GRN	65	19	R2	1712.5	34.4	1441.9	25.1	1286.9	20.5	1131.2	15.4	1054.5	14.9	975.2	12.4
L.GRN	65	19	R3	1085.4	38.2	908.0	28.9	769.0	26.3	634.3	20.2	590.6	19.0	533.3	16.1
L.GRN	65	19	W	1114.2	38.8	1003.7	28.6	911.2	24.4	752.2	19.2	702.4	18.8	675.6	16.1
L.GRN	65	12.5	R2	1544.6	36.5	1310.9	28.2	1165.5	23.5	1005.7	17.8	963.1	16.0	917.1	14.5
L.GRN	65	12.5	R3	1215.5	39.3	1045.3	32.9	962.3	27.1	796.9	21.9	744.4	21.2	723.7	17.9
L.GRN	65	12.5	R4	818.8	40.2	718.3	31.6	643.5	25.6	545.8	19.6	526.5	17.4	498.7	17.2
L.GRN	65	9.5	R1	1145.5	37.5	916.2	30.3	758.2	27.5	548.6	23.6	498.0	21.6	430.6	18.6
L.GRN	65	9.5	R3	609.1	41.2	484.7	35.8	409.3	29.8	295.0	24.1	251.4	23.3	205.0	19.8

Agg. Type	Gyrs	NMA5	ID	25Hz		10Hz		5Hz		1Hz		0.5Hz		0.1Hz	
				E*	ϕ	E*	ϕ	E*	ϕ	E*	ϕ	E*	ϕ	E*	ϕ
L.GRN	65	9.5	7	1096.0	39.1	883.6	31.4	795.8	28.4	656.8	22.3	606.0	21.2	568.9	19.8
L.GRN	100	19	6	1197.6	42.4	979.2	30.5	865.8	26.4	739.7	20.7	699.1	20.0	704.5	17.2
L.GRN	100	19	7	818.6	36.9	712.7	27.2	637.0	23.7	511.1	18.6	463.7	18.3	401.2	16.7
L.GRN	100	19	10	1180.9	35.5	990.0	26.6	890.1	22.2	757.6	16.4	714.6	15.3	697.8	12.9
L.GRN	100	12.5	8	1336.1	39.7	1116.2	29.1	1002.9	25.4	818.9	19.7	778.0	18.1	734.8	16.4
L.GRN	100	12.5	9	1505.6	36.3	1261.2	26.7	1130.6	22.5	965.9	16.9	925.4	15.7	873.9	13.4
L.GRN	100	12.5	10	1371.4	30.5	1366.9	26.4	1275.6	21.5	1103.2	16.8	1087.1	16.2	1072.4	12.7
L.GRN	100	9.5	9	1596.8	38.9	1325.3	29.2	1165.4	25.1	926.2	20.2	877.8	18.9	824.3	15.4
L.GRN	100	9.5	11	1408.8	41.5	1148.6	34.0	965.2	30.7	760.6	23.5	703.3	22.8	622.0	20.9
L.GRN	100	9.5	12	1037.9	40.7	886.3	29.5	788.1	24.3	641.7	18.7	602.0	17.5	552.3	14.5
LMS	65	19	6	1420.5	38.1	1150.5	29.1	1038.3	26.4	896.4	20.9	862.5	19.8	855.4	16.3
LMS	65	19	7	1366.5	37.6	1119.6	28.1	953.7	24.4	727.7	19.9	625.5	19.2	554.7	16.3
LMS	65	19	9	1212.8	40.2	1068.1	29.2	953.4	26.2	836.4	20.3	769.4	19.2	741.7	17.7
LMS	65	12.5	3	997.3	39.0	847.0	31.5	713.5	29.2	613.4	24.5	576.8	22.5	486.6	20.5
LMS	65	12.5	6	1807.8	37.6	1590.9	22.6	1465.9	19.3	1259.8	15.0	1224.5	14.5	1186.7	11.4
LMS	65	12.5	8	744.1	41.4	590.3	34.8	500.9	31.2	382.7	26.7	344.8	25.9	299.2	22.0
LMS	65	9.5	4	1720.7	33.4	1422.2	26.1	1285.1	23.1	1129.9	17.4	1089.8	16.5	1073.7	14.1
LMS	65	9.5	6	1016.4	37.6	895.1	29.2	807.7	25.4	665.9	19.5	636.6	17.4	611.3	15.0
LMS	65	9.5	7	1599.1	40.3	1325.8	31.5	1193.2	25.8	987.7	19.7	938.4	18.3	915.8	14.5
LMS	100	19	10	1055.7	46.8	829.5	34.6	703.2	30.2	551.1	22.0	528.3	20.2	503.1	17.0
LMS	100	19	11	1248.8	39.0	1150.5	25.9	1089.7	22.4	977.8	17.5	969.4	16.0	957.1	13.4
LMS	100	19	13	1098.8	36.8	926.0	27.3	838.8	23.2	729.2	16.0	696.7	15.4	663.0	12.9
LMS	100	12.5	5	1640.4	38.3	1308.8	31.8	1116.6	29.0	805.1	25.4	704.8	24.7	583.0	22.7
LMS	100	12.5	6	1571.7	33.4	1361.5	29.8	1226.7	26.2	1011.0	20.8	958.1	19.8	902.9	17.1
LMS	100	12.5	7	1132.7	38.6	949.5	29.4	839.9	26.0	675.4	19.9	618.4	18.1	563.0	15.1
LMS	100	9.5	3	1728.6	35.1	1446.4	26.6	1312.6	22.7	1074.8	17.3	988.2	16.9	889.1	12.7

Agg. Type	Gyrs	NMA5	ID	25Hz		10Hz		5Hz		1Hz		0.5Hz		0.1Hz	
				E*	ϕ	E*	ϕ	E*	ϕ	E*	ϕ	E*	ϕ	E*	ϕ
LMS	100	9.5	5	577.3	42.7	457.4	32.2	384.8	31.5	294.5	24.9	252.1	23.9	212.6	20.3
LMS	100	9.5	8	1626.6	37.7	1349.7	27.5	1204.9	24.2	1002.8	19.2	924.4	17.2	824.6	15.6
R.GRN	65	19	7	1260.9	41.0	1050.3	30.8	933.8	25.6	769.2	20.5	719.2	19.2	636.6	16.1
R.GRN	65	19	8	799.6	39.9	670.1	28.5	596.1	20.9	503.7	17.3	477.3	15.9	452.2	13.5
R.GRN	65	19	10	961.4	42.1	837.9	31.5	766.2	27.1	630.4	21.0	596.8	19.5	587.1	16.1
R.GRN	65	12.5	7	844.9	41.8	663.8	33.5	551.8	32.0	397.8	27.0	358.9	25.7	303.4	23.0
R.GRN	65	12.5	9	983.8	40.7	877.1	29.5	802.4	24.8	675.8	18.8	662.3	17.1	635.0	16.2
R.GRN	65	12.5	10	985.0	44.1	814.2	33.2	735.9	29.1	601.3	25.0	550.3	24.5	518.4	20.7
R.GRN	65	9.5	6	1037.9	40.2	840.0	29.2	741.5	27.9	585.4	23.1	515.8	21.0	446.3	19.3
R.GRN	65	9.5	7	1520.9	40.4	1242.5	30.7	1097.8	27.4	873.2	21.7	832.1	19.2	792.0	15.9
R.GRN	65	9.5	9	1154.2	31.9	979.4	25.4	885.3	20.6	775.7	14.9	732.4	13.2	678.4	11.9
R.GRN	100	19	3	1057.7	39.4	837.0	30.2	715.4	24.7	597.1	18.5	565.9	17.2	540.9	15.9
R.GRN	100	19	6	886.5	42.6	687.7	33.3	579.3	30.4	449.6	23.2	410.1	21.9	368.7	19.1
R.GRN	100	19	7	1327.3	42.8	1072.9	32.4	967.7	29.0	790.8	23.5	735.2	20.8	672.5	17.9
R.GRN	100	12.5	4	1224.0	38.8	975.8	32.0	835.3	25.8	647.2	22.8	601.2	20.5	542.4	18.9
R.GRN	100	12.5	10	1167.1	44.3	961.6	35.1	831.2	31.1	645.6	24.1	599.7	22.7	545.5	17.3
R.GRN	100	12.5	11	990.7	39.4	793.6	28.1	697.1	25.2	577.0	18.6	549.4	17.3	501.0	15.5
R.GRN	100	9.5	6	786.4	42.9	630.4	30.9	548.8	25.8	459.7	19.0	423.0	17.8	389.9	15.9
R.GRN	100	9.5	7	1329.2	44.6	1195.8	34.6	1078.4	31.7	923.6	26.8	865.3	25.1	857.6	22.1
R.GRN	100	9.5	9	1058.3	43.0	852.9	33.1	780.7	29.6	622.8	24.0	589.4	22.5	542.0	20.2
TRAP	65	19	8	538.9	41.9	473.8	29.0	415.9	25.5	322.3	22.4	285.1	21.8	242.9	18.2
TRAP	65	19	9	626.0	38.2	602.4	26.4	540.9	22.2	440.6	17.2	402.7	16.9	332.1	15.5
TRAP	65	19	10	655.7	47.3	644.3	34.1	584.4	30.6	479.7	25.0	434.6	25.3	390.0	20.9
TRAP	65	12.5	6	953.7	36.0	835.6	27.2	749.5	22.4	636.5	16.3	595.9	14.7	577.2	13.0
TRAP	65	12.5	9	1364.3	38.6	1216.5	29.2	1098.9	22.8	956.3	18.7	943.3	17.2	953.7	13.1
TRAP	65	12.5	10	1013.9	34.8	878.7	23.7	797.0	19.8	697.1	14.8	663.8	13.4	618.5	11.5

Agg. Type	Gyrs	NMA5	ID	25Hz		10Hz		5Hz		1Hz		0.5Hz		0.1Hz	
				E*	ϕ	E*	ϕ	E*	ϕ	E*	ϕ	E*	ϕ	E*	ϕ
TRAP	65	9.5	7	952.4	37.2	829.8	27.3	745.4	23.3	621.9	18.4	579.0	17.5	526.8	14.2
TRAP	65	9.5	8	942.5	38.5	786.2	28.9	706.1	24.9	588.7	18.8	547.6	17.3	507.2	14.9
TRAP	65	9.5	9	438.5	44.6	354.0	34.0	299.4	30.9	227.5	24.9	202.4	23.3	184.1	21.8
TRAP	100	19	3	766.1	36.7	637.2	27.8	564.4	22.9	437.7	17.4	387.2	16.9	331.7	13.9
TRAP	100	19	7	1070.0	40.3	885.6	28.3	788.7	23.5	674.0	17.6	632.7	16.9	591.4	14.8
TRAP	100	19	8	1048.9	34.9	939.8	26.4	851.4	22.4	749.1	16.6	713.8	15.6	694.3	14.4
TRAP	100	12.5	1	974.8	31.0	879.5	26.3	796.0	23.0	656.7	18.0	648.5	15.6	615.3	13.6
TRAP	100	12.5	6	1100.3	35.6	943.3	25.7	846.0	20.9	718.2	16.1	688.3	14.8	635.4	12.3
TRAP	100	12.5	7	1023.0	30.3	878.0	25.5	786.6	22.5	647.0	17.1	609.9	16.2	556.2	13.6
TRAP	100	9.5	6	942.5	36.5	836.0	28.4	752.0	24.1	649.9	18.7	619.7	18.0	602.8	15.3
TRAP	100	9.5	7	1717.1	33.3	1517.0	23.6	1376.7	19.2	1204.6	14.0	1182.3	12.5	1135.1	10.4
TRAP	100	9.5	8	1100.8	38.3	943.1	29.2	846.9	24.7	732.5	19.2	686.5	18.0	671.5	14.1
L.GRN	40	12.5	6	1183.6	36.0	1054.9	26.1	960.4	22.0	845.1	16.5	816.6	15.0	803.2	13.4
L.GRN	40	12.5	7	1183.9	35.4	1076.2	25.8	991.6	22.1	871.0	16.5	839.0	13.6	797.2	12.9
L.GRN	40	12.5	9	1447.9	35.1	1248.4	25.7	1116.2	22.5	949.3	16.7	872.1	15.0	795.7	13.3
R.GRN	40	12.5	6	1290.2	34.3	1101.0	25.5	1016.9	20.7	885.0	15.2	864.2	13.6	798.1	12.8
R.GRN	40	12.5	8	1321.4	31.2	1178.3	21.0	1114.3	17.1	981.6	12.1	951.7	10.8	905.1	9.3
R.GRN	40	12.5	10	1521.5	32.2	1317.1	21.1	1219.0	16.9	1099.9	11.9	1063.6	10.9	1016.8	9.4

Note: The shady rows were determined as outliers and were excluded from the statistical analysis.

TABLE D2 Static Creep Test Results

Agg.Type	Gyrs	NMAS	ID	Secondary		Max time, sec	Flow time, sec	Time at strain level, sec				Log (T _{0.04})
				Slope	Intercept			1%	2%	3%	4%	
C.GVL	65	19	7	0.17042	12741.2	598		2.4	12.3	134.5	1133.0	3.05
C.GVL	65	19	8	0.07611	15150.0	17974		2.2	18.6	5153.8	608000.0	5.78
C.GVL	65	19	9	0.16100	11749.0	1195		2.7	18.4	159.6	3682.0	3.57
C.GVL	65	12.5	1	0.15473	6449.5	14500		15.5	1864.7	6574.8	21840.0	4.34
C.GVL	65	12.5	8	0.15924	10957.8	2013		2.9	25.4	319.3	4404.0	3.64
C.GVL	65	12.5	10	0.82184	7869.5	6.5		1.6	2.7	4.9	7.6	0.88
C.GVL	65	9.5	6	0.16627	6533.8	18734		11.7	819.2	11214.3	23813.0	4.38
C.GVL	65	9.5	8	0.14623	7438.9	22500		8.2	848.9	9694.0	31400.0	4.50
C.GVL	65	9.5	9	0.11817	8550.0	20404		5.9	1493.4	90400.0	206000.0	5.31
C.GVL	100	19	8	0.10951	6284.7	61565		42.6	269000.0	801000.0	1333000.0	6.12
C.GVL	100	19	9	0.17656	9442.3	1797		3.3	35.5	624.2	4939.0	3.69
C.GVL	100	19	10	0.10817	7917.3	22555	5500	9.2	9404.7	20434.9	24229.0	4.38
C.GVL	100	12.5	2	0.12498	7699.6	18875		8.8	2564.3	13874.6	25326.0	4.40
C.GVL	100	12.5	3	0.14161	7220.5	20105	7150	9.9	1544.6	14144.9	22955.0	4.36
C.GVL	100	12.5	7	0.15898	7215.7	13174		8.5	544.2	4104.1	14533.0	4.16
C.GVL	100	9.5	5	0.11625	4872.1	101006		359.4	6314000.0	15060000.0	23810000.0	7.38
C.GVL	100	9.5	6	0.08520	4777.8	53436		352000.0	4726000.0	9100000.0	13480000.0	7.13
C.GVL	100	9.5	7	0.13287	6611.9	17604		16.6	4635.1	12755.2	21398.0	4.33
L.GRN	65	19	R2	0.18522	9588.7	1114		3.4	34.8	443.9	1126.0	3.05
L.GRN	65	19	R3	0.11389	11473.7	789		2.9	78.7	4169.0	9793.0	3.99
L.GRN	65	19	W	0.16686	8654.4	13209		4.8	78.4	2924.4	13284.6	4.12
L.GRN	65	12.5	R2	0.16523	6904.9	9914	2900	9.6	594.7	5704.4	9584.4	3.98
L.GRN	65	12.5	R3	0.12635	6786.0	18505		17.4	4094.6	11684.8	19080.0	4.28
L.GRN	65	12.5	R4	0.10823	10361.8	14770		3.4	329.3	8824.2	15670.0	4.20
L.GRN	65	9.5	7	0.11746	10531.6	13671		3.2	139.8	6144.6	12414.7	4.09

Agg.Type	Gyrs	NMA5	ID	Secondary		Max time, sec	Flow time, sec	Time at strain level, sec				Log (T _{0.04})
				Slope	Intercept			1%	2%	3%	4%	
L.GRN	65	9.5	R1	0.41597	6282.2	95		3.3	15.2	38.2	83.2	1.92
L.GRN	65	9.5	R3	0.43997	6639.2	38		2.9	11.5	30.3	60.0	1.78
L.GRN	100	19	6	0.11553	7280.6	50436		12.7	1894000.0	10643000.0	19390000.0	7.29
L.GRN	100	19	7	0.32162	3883.9	3129		12.9	42.3	229.6	3084.4	3.49
L.GRN	100	19	10	0.09307	5633.4	16765		215.0	1121000.0	2433000.0	3740000.0	6.57
L.GRN	100	12.5	8	0.10711	5515.2	101007		145.2	8170000.0	19420000.0	30470000.0	7.48
L.GRN	100	12.5	9	0.07791	4765.7	47875		799000.0	6423000.0	12048000.0	17670000.0	7.25
L.GRN	100	12.5	10	0.06906	5184.7	16795		178600.0	1753000.0	3328000.0	4903000.0	6.69
L.GRN	100	9.5	9	0.10112	3099.9	52826		11444.9	30855.6	45696.2	53998.0	4.73
L.GRN	100	9.5	11	0.14190	5063.5	64587	9500	78.1	20434.9	43005.8	56976.3	4.76
L.GRN	100	9.5	12	0.11926	7057.6	52696		12.3	7704.3	32675.2	52416.0	4.72
LMS	65	19	6	0.06804	20637.8	15564		1.9	5.2	53.3	3330000.0	6.52
LMS	65	19	7	0.13867	11116.8	3894		3.0	40.3	1284.7	2964.8	3.47
LMS	65	19	9	0.11416	14794.7	7955		2.5	11.3	199.8	5095.1	3.71
LMS	65	12.5	3	0.33223	10985.9	34		2.2	5.6	17.4	54.0	1.73
LMS	65	12.5	6	0.07743	10531.1	19275		4.3	5924.6	25066.0	54700.0	4.74
LMS	65	12.5	8	0.29495	12100.2	88		1.9	5.3	17.4	64.4	1.81
LMS	65	9.5	4	0.08482	7942.9	19635		12.3	30935.0	88600.0	152000.0	5.18
LMS	65	9.5	6	0.08930	13307.5	70912		2.5	36.1	15434.3	45604.9	4.66
LMS	65	9.5	7	0.11955	11171.0	2841		3.2	92.3	1445.5	3159.0	3.50
LMS	100	19	10	0.11309	13547.5	4164		2.6	16.3	1294.3	10078.0	4.00
LMS	100	19	11	0.07028	15917.7	51816		2.4	13.0	16145.5	39726.0	4.60
LMS	100	19	13	0.07356	15698.4	18155		2.2	13.1	17615.1	68035.0	4.83
LMS	100	12.5	5	0.15825	9818.8	2845		2.9	45.3	1165.2	3191.0	3.50
LMS	100	12.5	6	0.13941	8496.1	7675		5.9	184.8	6214.7	13640.0	4.13
LMS	100	12.5	7	0.09063	14202.8	11824		2.4	21.2	4124.2	13038.0	4.12

Agg.Type	Gyrs	NMA5	ID	Secondary		Max time, sec	Flow time, sec	Time at strain level, sec				Log (T _{0.04})
				Slope	Intercept			1%	2%	3%	4%	
LMS	100	9.5	3	0.10430	10494.6	9504		3.5	494.5	4664.6	11036.0	4.04
LMS	100	9.5	5	0.36228	7337.8	125		2.9	14.7	45.7	109.1	2.04
LMS	100	9.5	8	0.09523	12057.5	40815		2.8	75.4	5227000.0	13100000.0	7.12
R.GRN	65	19	7	0.11278	10496.1	29390		3.3	229.3	24943.9	29536.0	4.47
R.GRN	65	19	8	0.12312	11295.8	18745		2.7	60.5	24400.0	50600.0	4.70
R.GRN	65	19	10	0.09312	11486.2	32893		3.1	194.6	18045.0	37084.0	4.57
R.GRN	65	12.5	7	0.15867	12584.3	2955		2.1	15.3	189.6	1484.7	3.17
R.GRN	65	12.5	9	0.08395	10864.3	20235		3.3	2014.4	20234.8	29406.0	4.47
R.GRN	65	12.5	10	0.08916	14309.6	37769		2.1	25.4	6244.6	25795.1	4.41
R.GRN	65	9.5	6	0.20762	10399.4	1094		2.8	17.6	95.6	764.0	2.88
R.GRN	65	9.5	7	0.09487	9742.3	20205		4.6	3214.8	24258.0	50500.0	4.70
R.GRN	65	9.5	9	0.11548	11538.7	14523		1.6	561000.0	3020000.0	5480000.0	6.74
R.GRN	100	19	3	0.09692	5852.0	662	390	258.6	608.6	638.6	658.6	2.82
R.GRN	100	19	6	0.08660	17145.9	16000		1.9	8.0	258.9	76700.0	4.88
R.GRN	100	19	7	0.08921	8767.5	49805		6.9	195166.0	1007000.0	1820000.0	6.26
R.GRN	100	12.5	4	0.13148	7172.6	47336		11.5	6224.8	52593.0	80700.0	4.91
R.GRN	100	12.5	10	0.14027	7728.4	21325		7.2	864.5	30611.0	87000.0	4.94
R.GRN	100	12.5	11	0.08454	9010.8	53804	45500	6.4	11154.6	47815.4	54129.0	4.73
R.GRN	100	9.5	6	0.13455	10316.9	26082		3.1	78.9	8233.5	24523.8	4.39
R.GRN	100	9.5	7	0.13370	8815.3	8383		4.3	429.0	3523.7	7263.8	3.86
R.GRN	100	9.5	9	0.08901	9303.4	17164		5.4	515000.0	2483000.0	4450000.0	6.65
TRAP	65	19	8	0.34132	11225.1	36.4		1.9	5.4	16.4	42.0	1.62
TRAP	65	19	9	0.40609	9427.2	35.1		2.0	6.1	15.1	37.5	1.57
TRAP	65	19	10	0.36366	11120.2	9.3		1.8	5.0	13.3	27.6	1.44
TRAP	65	12.5	6	0.10406	13237.9	22679		2.3	30.0	3724.1	23975.0	4.38
TRAP	65	12.5	9	0.09856	10213.9	4374		3.9	799.1	35600.0	71400.0	4.85

Agg.Type	Gyrs	NMAS	ID	Secondary		Max time, sec	Flow time, sec	Time at strain level, sec				Log (T _{0.04})
				Slope	Intercept			1%	2%	3%	4%	
TRAP	65	12.5	10	0.12854	11409.1	5186		2.6	70.8	2644.3	7744.0	3.89
TRAP	65	9.5	7	0.13443	13305.0	4739		2.2	15.0	319.4	3374.4	3.53
TRAP	65	9.5	8	0.11923	14017.4	1495		2.0	15.8	654.2	3534.0	3.55
TRAP	65	9.5	9	0.32169	10970.8	57.5		1.9	6.2	18.5	59.5	1.77
TRAP	100	19	3	0.42441	7720.1	11.7		2.6	9.3	25.8	42.6	1.63
TRAP	100	19	7	0.09236	13945.9	10660		2.0	27.6	6604.0	27947.0	4.45
TRAP	100	19	8	0.08947	10287.2	38305		3.5	1594.6	22425.0	38880.0	4.59
TRAP	100	12.5	1	0.13483	8137.6	20945		6.1	654.6	17055.2	33449.0	4.52
TRAP	100	12.5	6	0.10729	10813.3	32237		3.5	124.1	20744.2	50843.0	4.71
TRAP	100	12.5	7	0.09203	9503.2	13064		4.5	2204.1	11004.3	17330.0	4.24
TRAP	100	9.5	6	0.11202	11271.8	19130		2.8	88.2	6165.3	18195.5	4.26
TRAP	100	9.5	7	0.14086	5149.3	274	60	101.8	224.0	259.0	277.0	2.44
TRAP	100	9.5	8	0.13866	8337.0	12648		5.5	479.3	6074.7	12524.9	4.10
L.GRN	40	12.5	6	0.21417	12649.0	285		2.1	8.6	44.1	209.8	2.32
L.GRN	40	12.5	7	0.21221	9787.9	199		2.8	27.6	211.0	437.0	2.64
L.GRN	40	12.5	9	0.19496	14394.1	289		2.0	6.9	28.6	179.2	2.25
R.GRN	40	12.5	6	0.13520	9549.2	23175		5.3	56.6	8283.9	16754.2	4.22
R.GRN	40	12.5	8	0.13234	12899.7	20845		2.5	19.2	469.4	48345.0	4.68
R.GRN	40	12.5	10	0.11655	9248.0	101009		5.5	114.9	22780000.0	49030000.0	7.69

Note: The shady cells are filled with estimated value.

TABLE D3 Repeated Load Confining Creep Test Results

Agg. Type	Gyrs	NMA5	ID	log intercept, a	log slope, b	Microstrain at Cycles			
						100	1000	5000	10,000
GVL	65	19	1	7830	0.1240	13858	19420	22511	23381
GVL	65	19	3	4265	0.1597	8897	13670	16616	17645
GVL	65	19	5	7144	0.1152	12145	16498	19064	20431
GVL	65	12.5	3	4061	0.1564	8346	12700	15391	16356
GVL	65	12.5	4	4171	0.1342	7736	11133	13076	13638
GVL	65	12.5	5	6456	0.1399	12296	17596	21256	23337
GVL	65	9.5	1	2820	0.1478	5569	8312	9927	10606
GVL	65	9.5	3	4082	0.1518	8214	12144	14876	15796
GVL	65	9.5	4	4874	0.1282	8795	12283	14521	15246
GVL	100	19	2	4264	0.1207	7435	10718	11925	12673
GVL	100	19	3	3469	0.1621	7318	11379	13797	14592
GVL	100	19	5	4314	0.1059	7027	9801	10636	10814
GVL	100	12.5	1	5051	0.1217	8847	12387	14241	14646
GVL	100	12.5	4	4053	0.1296	7360	10664	12218	12845
GVL	100	12.5	5	2125	0.2678	8053	14178	20787	25026
GVL	100	9.5	1	3556	0.1255	6338	9052	10358	10886
GVL	100	9.5	3	2906	0.2236	8136	13689	19510	20972
GVL	100	9.5	4	3330	0.1219	5837	7916	9403	10029
L.GRN	65	19	6	3578	0.1604	7487	11315	14028	15866
L.GRN	65	19	7	7293	0.1866	17221	27576	35754	38350
L.GRN	65	19	8	3913	0.2251	11035	20140	26622	30084
L.GRN	65	12.5	2	2854	0.2665	9738	17323	27621	38626
L.GRN	65	12.5	6	3100	0.2467	9890	17046	25356	30085
L.GRN	65	12.5	8	3374	0.2505	10693	18368	28511	35614
L.GRN	65	9.5	1	4590	0.1930	11163	17177	23769	28106
L.GRN	65	9.5	2	3478	0.2289	9980	16705	24456	29198

Agg. Type	Gyrs	NMA5	ID	log intercept, a	log slope, b	Microstrain at Cycles			
						100	1000	5000	10,000
L.GRN	65	9.5	6	2474	0.3625	12876	29011	54256	69757
L.GRN	100	19	1	4375	0.1157	7455	10120	11724	12553
L.GRN	100	19	2	3201	0.1215	5603	7565	9014	9595
L.GRN	100	19	3	4279	0.1236	7561	10457	12262	12868
L.GRN	100	12.5	1	2895	0.1363	5424	7730	9247	9873
L.GRN	100	12.5	4	3292	0.1509	6598	9483	11909	13381
L.GRN	100	12.5	5	4000	0.1223	7025	9709	11334	12128
L.GRN	100	9.5	5	2341	0.1662	5033	7765	9649	10486
L.GRN	100	9.5	6	2891	0.1696	6312	9906	12263	13294
L.GRN	100	9.5	8	3990	0.1385	7549	10704	12983	14337
LMS	65	19	1	7801	0.2216	21643	37613	51497	60046
LMS	65	19	4	7480	0.2148	21451	33032	46616	54101
LMS	65	19	5	4517	0.2778	16236	29684	48134	58355
LMS	65	12.5	1	5971	0.1670	12885	20320	24781	26539
LMS	65	12.5	2	5755	0.2169	15627	25062	36534	41054
LMS	65	12.5	5	4886	0.2796	17705	31202	52857	64160
LMS	65	9.5	1	4380	0.1752	9813	15376	19484	22984
LMS	65	9.5	2	4887	0.1979	12157	19194	45728	62660
LMS	65	9.5	3	3387	0.2020	8569	13971	18938	21451
LMS	100	19	1	3204	0.2183	8755	14313	20579	25258
LMS	100	19	2	4678	0.1966	11545	17766	24978	29120
LMS	100	19	4	3970	0.2075	10321	17354	23255	26671
LMS	100	12.5	1	5487	0.1697	11988	18153	23297	26577
LMS	100	12.5	3	5572	0.1599	11618	16760	21766	25898
LMS	100	12.5	4	3542	0.2210	9800	15659	23277	27506
LMS	100	9.5	1	5684	0.1809	13076	19775	26553	32127

Agg. Type	Gyrs	NMA5	ID	log intercept, a	log slope, b	Microstrain at Cycles			
						100	1000	5000	10,000
LMS	100	9.5	2	3513	0.2150	9455	15367	21940	26611
LMS	100	9.5	4	2273	0.3134	9594	16511	32827	45256
R.GRN	65	19	2	6353	0.1599	13224	19359	24810	29453
R.GRN	65	19	3	3784	0.2470	11803	22365	31047	36262
R.GRN	65	19	5	3739	0.2264	10055	18508	25741	29257
R.GRN	65	12.5	2	2517	0.2512	8005	14095	21404	26731
R.GRN	65	12.5	4	4688	0.1966	11572	18514	25041	29660
R.GRN	65	12.5	6	3803	0.2340	11174	19278	27937	34416
R.GRN	65	9.5	2	2938	0.2005	7397	11822	16219	19273
R.GRN	65	9.5	3	3341	0.2174	9091	14792	21293	25311
R.GRN	65	9.5	5	3895	0.2355	11522	19667	28973	35651
R.GRN	100	19	1	2947	0.2626	9877	16562	27619	31035
R.GRN	100	19	2	6148	0.1480	12046	17431	21704	23896
R.GRN	100	19	4	5458	0.1878	12961	20510	27038	29380
R.GRN	100	12.5	1	2827	0.2175	7697	13050	18036	21321
R.GRN	100	12.5	2	4393	0.1519	8803	13063	16032	17211
R.GRN	100	12.5	9	3174	0.2210	8782	14654	20862	24351
R.GRN	100	9.5	1	4292	0.1488	8514	12431	15245	16208
R.GRN	100	9.5	2	2438	0.2311	7065	12074	17462	22730
R.GRN	100	9.5	3	3199	0.2051	8226	13342	18361	20707
TRAP	65	19	1	12049	0.0788	17322	21738	23584	24529
TRAP	65	19	2	4021	0.1813	9266	14861	18841	20161
TRAP	65	19	3	9906	0.0991	15634	23042	23042	25052
TRAP	65	12.5	2	5537	0.1296	10060	14329	16712	17702
TRAP	65	12.5	3	3524	0.1931	8572	13817	18253	21219
TRAP	65	12.5	5	5709	0.1398	10871	15976	18795	19820

Agg. Type	Gyrs	NMA5	ID	log intercept, a	log slope, b	Microstrain at Cycles			
						100	1000	5000	10,000
TRAP	65	9.5	2	3228	0.1802	7401	11546	14983	17345
TRAP	65	9.5	4	7595	0.1410	20747	20747	25252	26915
TRAP	65	9.5	5	7279	0.1724	23753	23753	31621	34298
TRAP	100	19	2	7138	0.1319	13104	19573	21954	22582
TRAP	100	19	4	7061	0.1279	12723	17779	20980	22094
TRAP	100	19	5	5130	0.2505	16256	28925	43340	46130
TRAP	100	12.5	2	2894	0.2348	8533	14479	21377	24820
TRAP	100	12.5	3	6041	0.1676	13070	19875	25176	27788
TRAP	100	12.5	4	4910	0.1889	11721	16979	24542	26226
TRAP	100	9.5	1	2205	0.2470	6878	12653	43867	74934
TRAP	100	9.5	2	4255	0.1624	8989	13642	16969	18990
TRAP	100	9.5	5	2213	0.1611	4647	7172	8729	9355
L.GRN	40	12.5	3	1724	0.3870	10242	24969	46547	60868
L.GRN	40	12.5	4	5420	0.2649	18356	33782	51742	62171
L.GRN	40	12.5	5	3682	0.2791	13314	25696	39672	48139
R.GRN	40	12.5	3	6303	0.2432	19321	34239	50038	59227
R.GRN	40	12.5	4	3629	0.2917	13901	30759	43509	48236
R.GRN	40	12.5	5	4715	0.2416	14345	29664	36914	38954

Note: The shady cells are filled with estimated value.